

**MICROSTRUCTURAL CHARACTERIZATION & ANTI-BACTERIAL
ACTIVITY OF Cu₂O NANOSTRUCTURES**

**Project work submitted to St. Mary's College (Autonomous), Thoothukudi, affiliated
to Manonmaniam Sundaranar University, Tirunelveli in partial fulfillment of
requirement for the award of**

BACHELOR'S DEGREE IN PHYSICS

BY

A. Anto Agnes Virgin	-18AUPH04
A. Chandia	-18AUPH11
R. Kalishree Dharani	-18AUPH23
J. Nivetha	-18AUPH33
K. Priyanka Dishni	-18AUPH35
P. Subalakshmi	-18AUPH44

UNDER THE GUIDANCE AND SUPERVISION OF

Mrs. P . DHANALAKSHMI M.Sc,B.Ed,SET.



DEPARTMENT OF PHYSICS

St. Mary's College (Autonomous), Thoothukudi-1

(Re-Accredited with 'A+' grade by NAAC-5th Cycle) 2020-

2021

CERTIFICATE

This is to certify that the project work entitled "MICROSTRUCTURAL CHARACTERIZATION & ANTI-BACTERIAL ACTIVITY OF Cu_2O NANOSTRUCTURES" is submitted to ST. MARY'S COLLEGE (AUTONOMOUS), THOOTHUKUDI in partial fulfillment for the award of Bachelor's Degree in Physics and is a record work done during the year 2020-2021 by the following students

A. Anto Agnes Virgin	-18AUPH04
A. Chandia	-18AUPH11
R. Kalishree Dharani	-18AUPH23
J. Nivetha	-18AUPH33
K. Priyanka Dishni	-18AUPH35
P. Subalakshmi	-18AUPH44

Dhanalakshmi P.
GUIDE

Devi S do
HEAD OF THE DEPARTMENT
HEAD
Department of Physics,
St. Mary's College (Autonomous),
Thoothukudi - 628 001.

S. Lakshmi Chinnappa
EXAMINER
9/4/21

Lucia Rose
PRINCIPAL
St. Mary's College (Autonomous),
Thoothukudi - 628 001.

ACKNOWLEDGEMENT

First and foremost, we ascribe all praise and thanks to the Lord Almighty for guiding us to complete our project work successfully.

We express our deepest sense of gratitude to our Respected Principal, **Dr.Sr. A.S.J.Lucia Rose, M.Sc., M.Phil.,Ph.D., PGDCA.** St. Mary's College (Autonomous), Thoothukudi for providing a wonderful opportunity to execute this project work.

We wish to record our hearty and sincere thanks to **Dr.Sr.Jessie Fernando, M.Sc., M.Phil.,Ph.D.,** Head of the Department of Physics for her encouragement and support to perform this project.

We are grateful to our guide **Mrs. P. Dhanlakshmi, M.Sc., B.Ed., SET.,** for her useful ideas and guidance in bringing out this project successfully.

We sincerely acknowledge the financial assistance funded by the **DBT**, New Delhi for the successful completion of the project work.

We would like to extend our gratitude to the Department of Physics, Manonmaniam Sundaranar University, Tirunelveli and Department of Chemistry, V. O. C. College, Thoothukudi for their timely help in completing our project.

We wish to extend our sincere gratitude to our non-teaching staff for their cooperation and assistance. We would also like to thank our parents and friends for their constant support and encouragement throughout the project.

	CONTENTS	PAGE NO
CHAPTER I	INTRODUCTION	1
1.1	Nanoscience & Nanotechnology	2
1.2	Importance of Nanomaterials	3
1.2.1	Types of Nanomaterials	4
1.2.2	Classification of Nanomaterials	5
1.2.3	Applications of Nanomaterials	6
1.3	Cuprous Oxide	7
1.3.1	Properties of Cuprous Oxide	7
1.3.2	Structure of Cuprous Oxide	8
1.3.3	Applications of Cuprous Oxide	9
1.4	Literature Review	9
1.5	Objectives	11

CHAPTER II	EXPERIMENT	12
2.1	Synthesis of Nanoparticles	13
2.1.1	Top down approach	13
2.1.2	Bottom up approach	14
2.2	Chemical Precipitation Method	14
2.3	Preparation of Cuprous Oxide Nanoparticles	15
2.4	Flow Chart	16
CHAPTER III	MATERIALS AND METHODS	17
3.1	Chemicals	18
3.2	Experimental Section	18
3.2.1	Synthesis of SDBS capped Cu₂O nanostructures	18
3.3	Characterization Techniques	19
3.3.1	X-ray Diffraction	19
3.3.2	Scanning Electron Microscopy	19
3.3.3	Disk diffusion Assay	20

CHAPTER IV	RESULTS AND DISCUSSIONS	21
4.1	Structural Characterization	22
4.2	Microstructural Charaterization	23
4.2.1	SEM Characterization	23
4.3	Anti-Bacterial Assay	25
CHAPTER V	CONCLUSION	26
5.1	Summary	27
5.2	References	28

CHAPTER-I

CHAPTER-I

INTRODUCTION

1.1 Nanoscience and Nanotechnology

The word nanoscience refers to the study, manipulation and engineering of matter, particles and structures on the nanometer scale (one millionth of a millimeter, the scale of atoms and molecules). Important properties of materials, such as the electrical, optical, thermal and mechanical properties, are determined by the way molecules and atoms assemble on the nanoscale into larger structures. Moreover, in nanometer size structures these properties are often different than on macroscale, because quantum mechanical effects become important.

Nanotechnology is the application of nanoscience leading to the use of new Nanomaterials and nanosize components in useful products. Nanotechnology will eventually provide us with the ability to design custom made materials and products with new enhanced properties, new nanoelectronics components, new types of “smart” medicines and sensors and even interfaces between electronics and biological systems.

Nanosciences and nanotechnologies are leading to a major turning point in our understanding of nature. Such a force has its consequences or in the words of a famous fictional character: every force has its dark side. Our future depends on how we use new discoveries and what risks they bring upon humanity and our natural environment. The nanoworld is the intermediary between the atom and the solid, from the large molecule or the small solid object to the strong relationship between surface and volume. Strictly speaking, the nanoworld has existed for a long time and it is up to chemists to study the structures and properties of molecules.

These newborn scientific disciplines are situated at the interface between Physics, Chemistry, Materials science, Microelectronics, Biochemistry and Biotechnology. Control of these disciplines therefore requires an academic and multidisciplinary scientific education.

1.2 Importance of Nanomaterials

Nanomaterials are special for several reasons, but for one in particular is their size. Nanomaterials are up to 10000 times smaller than the width of a human hair. And this tiny size makes them very valuable for all kinds of practical uses. Nanomaterials also exhibit shape dependent properties that are useful for applications such as

- catalysis,
- data storage,
- optics.

Reduction of size affects various properties such as,

- melting point,
- band gap,
- reactivity,
- mechanical properties,
- optical properties,
- magnetic properties,
- electrical and electronic properties.

Nanoengineered materials can be designed to have greater structural strength, chemical sensitivity, conductivity, or optical properties. All of these have great potential in the field of engineering.

One of the most well-known and exciting development that is emerging thanks to the study of nanomaterial is the application of carbon nanotubes. Carbon nanotubes are also extremely light, making them the perfect material for the construction of next- generation aircraft, cutting the weight of a commercial jet by around 20 %. The huge surface area of carbon nanotubes allows them to be used as the electrodes in batteries

and capacitors, providing better electrical and mechanical stability than other materials which have previously been used.

Nanomaterials can be used as lubricant additives, having the ability to reduce friction in moving parts, worn parts can even be repaired with self-assembling nanoparticles.

Developments like this give us more control over the materials we work with, unlocking new potential and new functions that can change the way we approach engineering problems.

1.2.1 Types of Nanomaterials

Nanomaterials could be organised into four types

- Carbon Based Materials
- Metal Based Materials
- Dendrimers
- Composites_

Carbon Based Materials

These nanomaterials are composed of mostly of carbon, most commonly taking the form of hollow spheres, ellipsoids,tubes.Spherical and ellipsoidal carbon nanomaterials are referred to as fullerenes,while cylindrical ones are called nanotubes.

Metal Based Materials

These nanomaterials include quantum dots ,nanogold,nanosilver and metal oxides, such as titanium dioxide. A quantum dots is a closely packed semiconductor crystal.

Dendrimers

These nanomaterials are nanosized polymers built from branched units. The surface of a dendrimer has numerous chain ends, which can be tailored to perform specific chemical functions.

Composites

Composites combine nanomaterials with other nanoparticles or with larger, bulk type materials.

1.2.2 Classification of Nanomaterials

According to the structure, nanomaterials are classified into two major groups as Consolidated materials and Nanodispersions. Consolidated nanomaterials are further classified into several groups.

For the nanomaterials, the size is an important physical attribute. Nanomaterials are often classified depending upon the number of their dimensions fall under nanoscale.

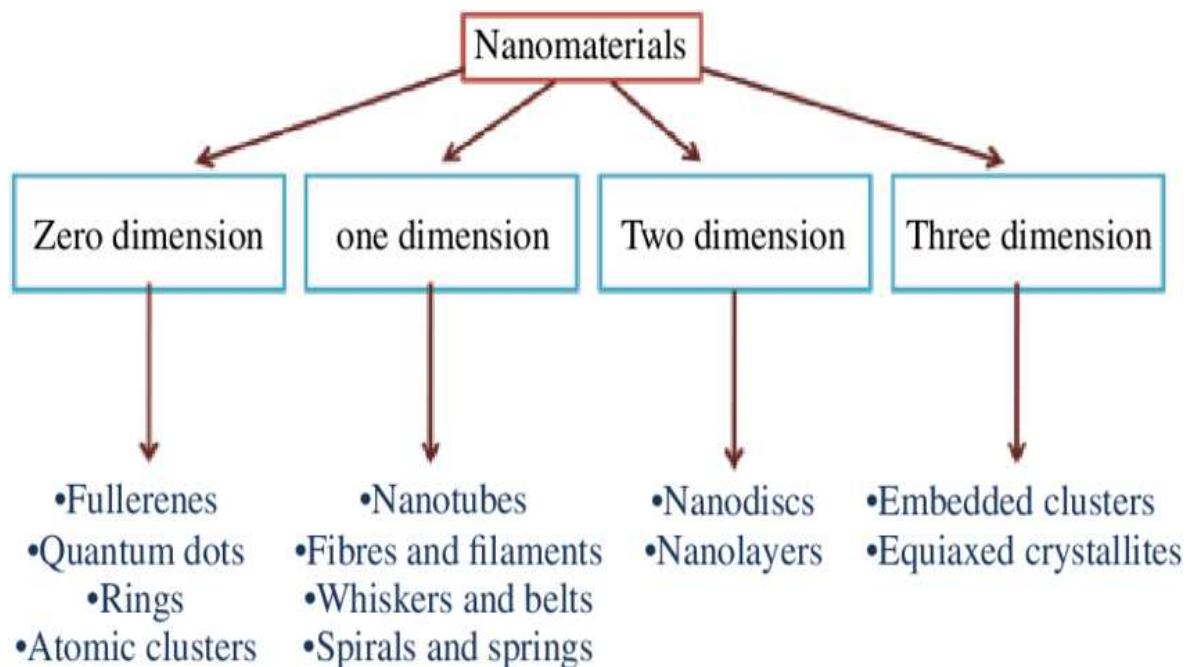


Fig 1.1 Classification of naomaterials

1.2.3 Applications of Nanomaterials

After more than 20 years of basic nanoscience research, applications of nanotechnology are delivering in both expected and unexpected ways on nanotechnology's promise to benefit society.

Nanotechnology is helping to considerably improve, even revolutionize, many technology and industry sectors: information technology, homeland security, medicine, transportation, energy, food safety, and environmental science, among many others. Described below is a sampling of the rapidly growing list of benefits and applications of nanotechnology.

Using nanotechnology, materials can effectively be made stronger, lighter, more durable, more reactive, more sieve-like, or better electrical conductors, among many other traits. Many everyday commercial products are currently on the market and in daily use that rely on nanoscale materials and processes:

- Nanoscale additives or surface treatments of fabrics can provide lightweight ballistic energy deflection in personal body armor, or can help them resist wrinkling, staining, and bacterial growth.
- Clear nanoscale films on eyeglasses, computer and camera displays and other surfaces can make them water- and residue-repellent, self-cleaning, resistant to ultraviolet or infrared light, antifog, antimicrobial.
- Nanoscale materials are beginning to enable washable, durable “smart fabrics” equipped with flexible nanoscale sensors and electronics with capabilities for health monitoring.
- Lightweighting of cars, trucks, airplanes, boats, and space craft could lead to significant fuel savings.
- Nanoscale additives in polymer composite materials are being used in baseball bats, tennis rackets, bicycles, motorcycle helmets, automobile parts, luggage, and power tool housings, making them lightweight, stiff, durable, and resilient.

- Carbon nanotube sheets are now being produced for use in next-generation air vehicles. For example, the combination of light weight and conductivity makes them ideal for applications such as electromagnetic shielding and thermal management.

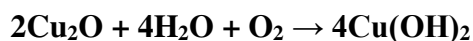
1.3 Cuprous Oxide

Copper(I) Oxide is also called as cuprous oxide an inorganic compound with the chemical formula Cu_2O . It is covalent in nature. Copper(I) oxide crystallizes in a cubic structure. It is easily reduced by hydrogen, when heated It undergoes disproportionation in acid solutions producing copper(II) ions and copper. When the cupric oxide is gently heated with metallic copper, it is converted into cuprous oxide. It acts as a good corrosion resistance, due to reactions at the surface between the copper and the oxygen in air to give a thin protective oxide layer

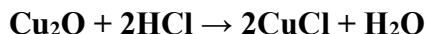
1.3.1 Properties of Cuprous Oxide

Chemical Properties

Copper(I) oxide reacts with water in the presence of oxygen forms copper(II) hydroxide. The chemical equation is given below.



Copper(I) oxide reacts with hydrogen chloride forms Copper(I) chloride and water. The chemical equation is given below.



Physical Properties

- No odour
- Red coloured solid
- Insoluble in water
- Covalent bond unit-3

- Molar mass-143.09g/mol
- Density-6g/cm³

1.3.2 Structure of Cuprous Oxide

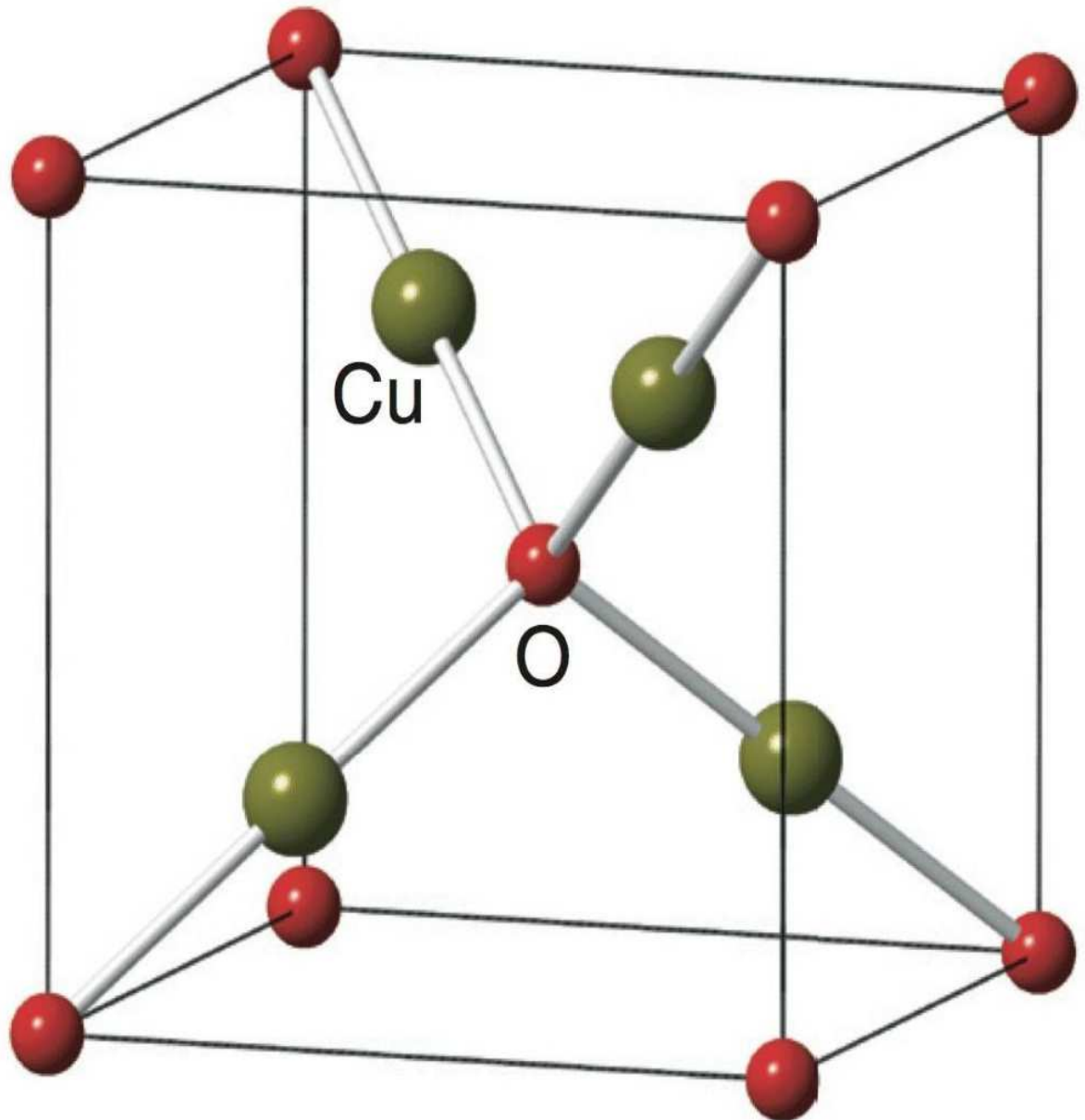


Fig 1.2 Structure of Cuprous Oxide

1.3.3 Applications of Cuprous Oxide

Copper compounds are crucial for major areas of application, basically due to the biological impact of small amounts of copper. The key applications of cuprous oxide are as follows:

- Copper is used in the form of cuprous oxide as a coating for the hulls of ships to prevent algae growth
- It is indispensable as a trace element in animal foodstuffs.
- Used as a p-type semiconductor material that was used to make photocells for light meters and fabricate rectifiers.
- Also used as a fungicide and seed dressing.
- Other applications (e.g., the manufacture of catalysts or pigments) are presently quantitatively small.

1.4 Literature Review

1. A. Erroh, A. M. Ferraria (2015), grew Cu_2O nanoparticles bound to cotton fibres
The method is based on a mild surface oxidation of cellulose fibres to generate in a controlled way carboxylic groups acting as a binding site for the adsorption of Cu^{2+} via electrostatic coordination. Then, the adsorbed Cu^{2+} ions were readily converted into Cu_2O by dipping the treated cotton fibres into an aqueous solution of a reducing agent. The morphology of the ensuing Cu_2O nanoparticles was shown to be dependent on the reducing agent used. The hybrid cotton- Cu_2O was shown to exhibit good antibacterial properties.
2. Ling-I Hung, Peidong Yang (2010), produced hollow Cu_2O nanoparticles at room temperature. Monodisperse Cu_2O nanoparticles (NPs) are synthesized using tetradecylphosphonic acid as a capping agent. Dispersing the NPs in chloroform and hexane at room temperature results in the formation of hollow Cu_2O NPs. The monodisperse Cu_2O NPs are used to fabricate hybrid solar cells with efficiency of 0.14% under AM 1.5 and 1 Sun illumination
3. Chao Yin Kuo, Chueh-Ying Pai (2012), synthesized cuprous oxide from copper-containing waste liquid to treat aqueous reactive dye. A microwave hydrothermal

method was applied in the synthesis. The highest recovery rate of Cu from wastewater was 87% and was obtained when the synthesis was performed at a power of 200 W for 15 min. An RB19 decolorization efficiency of 99.9% was achieved when the Fenton-like reaction was conducted with 50 mmol/L H_2O_2 and 0.9 g/L of Cu_2O .

4. Haijun Huang,Zhigang Zang (2017)Prepared cubic Cu_2O nanoparticles wrapped by reduced graphene oxide for the efficient removal of rhodamine B Cu_2O nanoparticles evenly distributed on reduced graphene oxide (rGO) to form $\text{Cu}_2\text{O}/\text{rGO}$ nanocomposites were fabricated by a facile in-situ wet-reduced method. $\text{Cu}_2\text{O}/\text{rGO}$ nanocomposites exhibited an excellent photocatalytic activity under visible light irradiation.
5. Manoj Devaraj,Santhalakshmi Jeyadevan(2016)Fabricated novel shape Cu_2O nanoparticles modified electrode for the determination of dopamine and paracetamol they demonstrated and compared the synthesis of Cu_2O nanoparticles *via* thermal decomposition method using a combination of oleic acid and oleylamine and oleic acid alone. The Cu_2O nanoparticles stabilized by oleic acid alone exhibit excellent electrochemical enhancement in the peak current response. Cu_2O on MWCNTs modified electrode shows excellent electrochemical sensor.
6. Mohammad Aslam,W.Vogel(2001)Formed Cu_2O Nanoparticles by Variation of the Surface Ligand The optical absorption spectrum ($\lambda_{\text{max}}=289$ nm) is found to be invariant with the nature of the capping molecule while the particle shape and distribution are found to depend strongly on it. Despite the variation in particle size and relative stability, nanoparticles have been found to form oxides after a few days
7. Manab Mallik,Himadri Roy(2019),synthesized Cuprous Oxide by aqueous precipitation method for the production of low-cost conductive ink, which is suitable for a printed, electronic application. The major drawback of copper ink,is rapid oxidation The Cu_2O nanoparticles show an absorption band at 650 nm with a bandgap of 2 eV. The contact angle measurement suggests that the as-prepared ethanol-based Cu_2O ink has excellent wettability on a glass substrate.

8. Jinxia Shu, Wei Zhang (2014), prepared Polyhedral cuprous oxide nanoparticles (Cu_2O NPs) with rough surfaces by a one-pot sonochemical precipitation method. The prepared Cu_2O NPs exhibited remarkable adsorption properties toward Congo Red (CR). CR adsorption onto Cu_2O is a spontaneous, endothermic and chemisorption process. The Cu_2O NPs show unprecedented adsorption capability toward Congo red.

1.5 Objectives

- To give an overview of the preparation of Cu_2O Nanoparticles.
- To synthesize the pure cuprous oxide nanoparticles by chemical precipitation method.
- To realise the potential applications at nanoscale.
- To review on some unique properties and applications of Cu_2O nanostructures.
- To provide a critical discussion of the synthesis of Cu_2O nanostructures..
- To analyse the purity level of the synthesized Cu_2O nanoparticles.

CHAPTER II

CHAPTER II

EXPERIMENT

2.1 Synthesis of Nanoparticles

Nanoparticles are typically synthesized from a

- top-down or
- bottom-up approach

2.1.1 Top down approach

In Top-down method, a bulk material is physically broken down to make smaller molecules

The method include

- milling,
- laser ablation,
- spark ablation.
- chemical etching
- electro-explosion

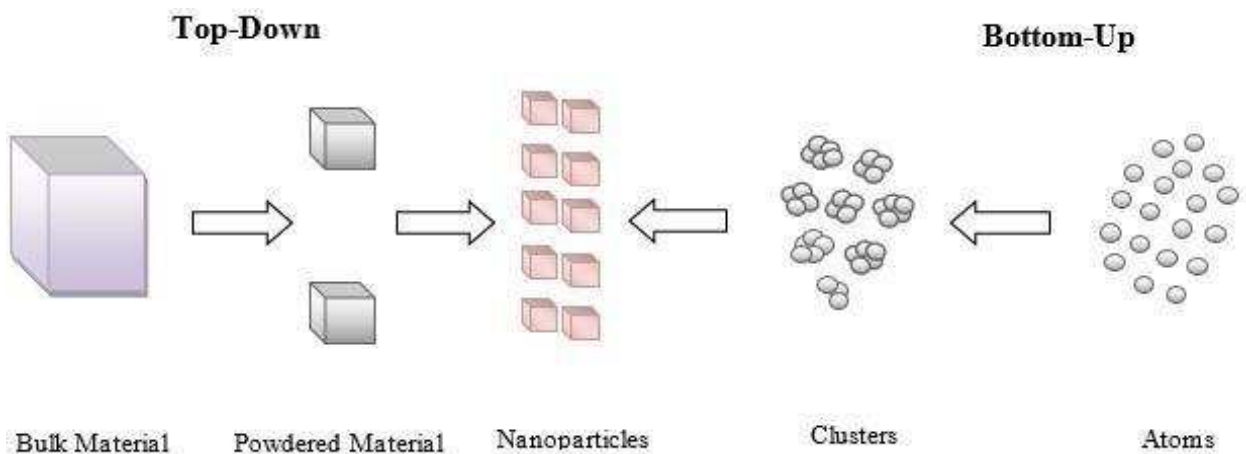


Fig 2.1 Top down & Bottom up approach

2.1.2 Bottom up approach.

A bottom-up approach relies on nucleating atomic-sized materials into the eventual nanoparticles

Some common methods include the

- Turkevich method (citrate reduction),
- gas phase synthesis,
- block copolymer synthesis,
- microbial synthesis

In many of these methods, the main objective is to reduce the cost of chemical synthesis and to produce materials for technological applications. We have synthesized Cu₂O nanoparticles by chemical precipitation process which is a simple cost- effective method since the starting materials are few and inexpensive.

2.2 Chemical Precipitation Method

In precipitation method, the ionic metals are converted to an insoluble form (particle) by the chemical reaction between the soluble metal compounds and the precipitating reagent. The particles formed by this reaction are removed from the solution by settling and filtration.

The unit operations typically required in this technology include neutralization, precipitation, coagulation/flocculation, solids/liquid separation, and dewatering. The effectiveness of a chemical precipitation process is dependent on several factors including the type and concentration of ionic metals present in solution, the precipitant used, the reaction conditions (especially the pH of the solution), and the presence of other constituents that may inhibit the precipitation reaction.

The most widely used chemical precipitation process is hydroxide precipitation, in which metal hydroxides are formed by using Calcium hydroxide or Sodium hydroxide as the precipitant.

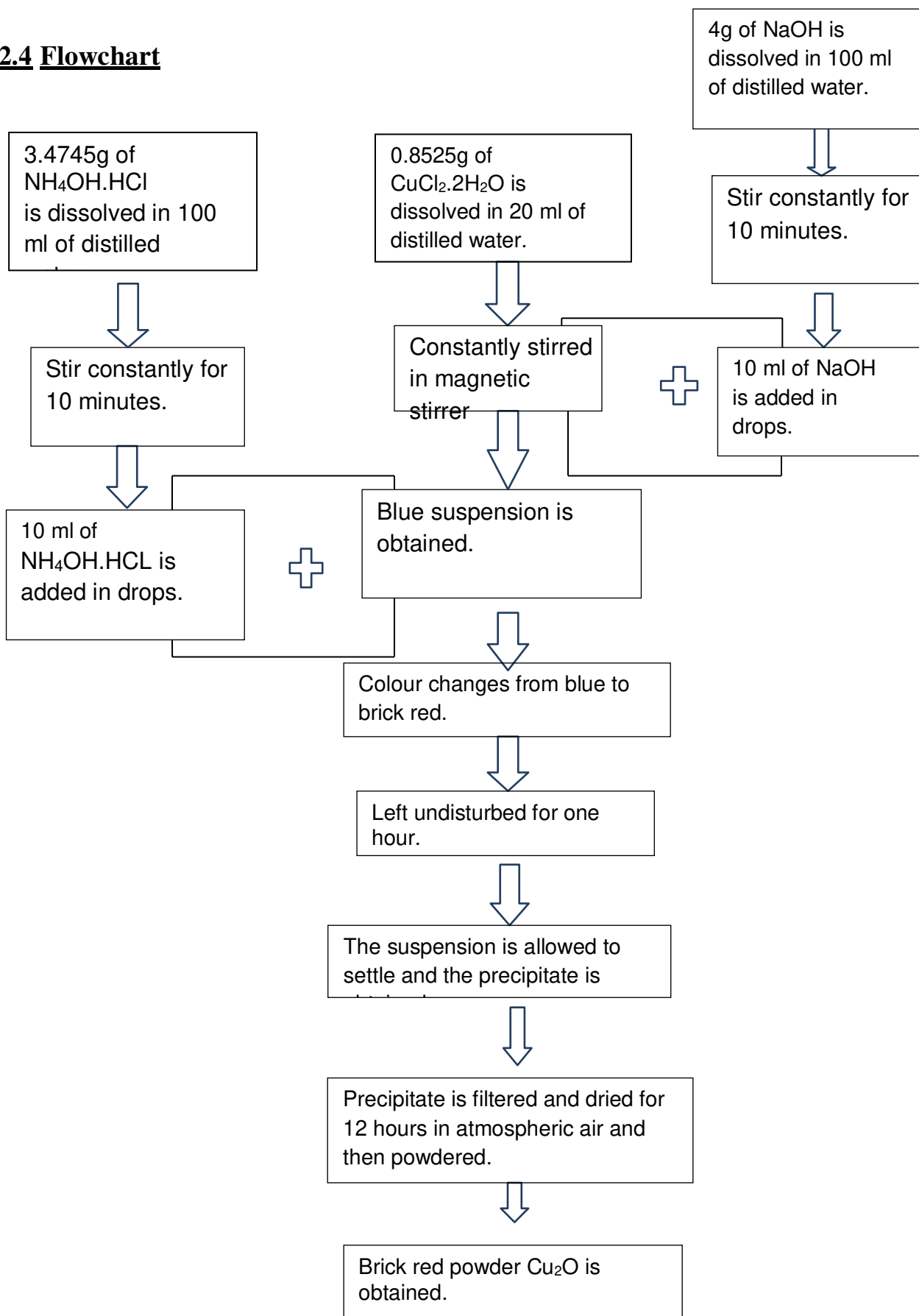
2.3 Preparation of Cuprous Oxide Nanoparticles

The experiment was done with 0.8525g of cupric chloride dihydrate along with 4g of NaOH and 3.4745g of hydroxyl amine hydrochloride. Each of the substances were dissolved separately in distilled water and solutions of 200 ml separately and 20 ml separately were prepared. NaOH solution was taken in a burette and was allowed to drip into the cupric chloride dihydrate solution that was at constant stirring. On completion of the dripping process, the solution mixture NaOH and cupric chloride dihydrate was kept at constant stirring for 15 minutes, blue suspension was obtained. Now the burette again was filled with hydroxyl amine hydrochloride solution and was now allowed to drip into the blue suspension obtained from the previous stirring. On completion of the dripping process, the solution was kept at constant stirring for 15 minutes. And finally brick red suspension was produced. It was left undisturbed for one hour. The suspended particles was filtered and dried for 12 hours in atmospheric air and then powdered using mortar and pestle.



Fig 2.2 Pure Cu₂O Nanoparticles

2.4 Flowchart



CHAPTER III

CHAPTER III

MATERIALS AND METHODS

3.1 Chemicals

All the chemicals and reagents used in the present study were of analytical grade and were used as received without further purification. Cupric chloride dihydrate ($\text{CuCl}_2 \cdot 2\text{H}_2\text{O}$, 99.9%, Sigma-Aldrich), Hydroxylamine hydrochloride ($\text{NH}_2\text{OH} \cdot \text{HCl}$, 98.0%, Loba Chemie), Sodium hydroxide (NaOH , 98%, Loba Chemie), Methanol (CH_3OH , 99%, Merck) and Ethanol ($\text{C}_2\text{H}_5\text{OH}$, 99%, Merck). Double distilled water was used in all the experiments.

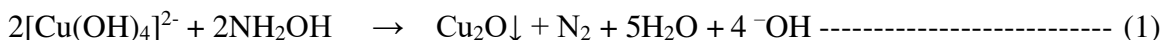
3.2 Experimental Section

3.2.1 Synthesis of SDBS capped Cu_2O nanostructures:

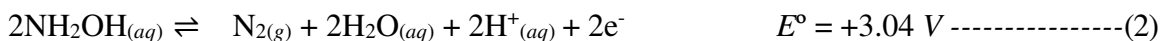
In a typical synthesis, 0.8525g (0.5 M) of cupric chloride dihydrate ($\text{CuCl}_2 \cdot 2\text{H}_2\text{O}$) was dissolved in 10 mL of deionized water at room temperature and subjected to gentle stirring for 30 minutes to ensure complete dissolution. After obtaining a homogenous solution, 10 mL of 1 M NaOH solution was added dropwise under constant stirring to the mixture placed in a water bath set at 305 K (32 °C) while a blue precipitate of $\text{Cu}(\text{OH})_2$ was produced. The resulting solution was stirred for 1 h and then 10 mL of 0.5 M solution of the reducing agent hydroxylamine hydrochloride, was added drop-by-drop as the solution is being stirred vigorously. The colour of the solution turning ochre or brick red gradually after the addition of reducing agent indicates the formation of Cu_2O . The obtained precipitate was left undisturbed for 1 h and then centrifuged at 3000 rpm, washed several times with ethanol and redispersed in methanol for further analysis.

Hydroxylamine as the reducing agent:

The reducing agent hydroxylamine is environmentally benign and involves the formation of by-product nitrogen gas, which liberates during the course of the reaction as shown below,



The redox reactions involved in the above synthesis at alkaline medium are given below



3.3 Characterization Techniques

3.3.1 X-ray Diffraction

The powder X-ray diffraction patterns were acquired at room temperature on a PANalytical X'Pert Pro X-ray diffractometer using Cu K α radiation equipped with an X'Celerator detector in the continuous scanning mode. The samples were scanned over the angular range of $2\theta = 10^\circ$ - 80° with a step size of 0.02° and acquisition time of 0.5s per step.

The peak width varies inversely with crystallite size and microstrain and is more pronounced at higher 2θ angles. Therefore, the average crystallite size (L) of the nanostructures can be calculated from the extent of line broadening in the high intense peak using Scherrer equation, [2]

$$L = 0.94 \lambda / \beta_{2\theta} \cos \theta$$

where $\beta_{2\theta}$ is the full width at half maximum (FWHM) of the peak after correcting for instrumental line broadening, θ is the angle of incidence or Bragg Angle, λ ($= 1.5406 \text{ \AA}$) is the wavelength of the X-ray used.

3.3.2 Scanning Electron Microscopy

Scanning electron microscopy (SEM) images of the samples were obtained using field emission scanning electron microscope (FE-SEM) Quanta FEG 250 operated at an accelerating voltage of 20 kV equipped with energy dispersive X-ray spectrometric (EDS) detector. Samples were prepared by placing 2 or 3 drops of the dilute dispersion of the nanostructures in ethanol on the conductive carbon tape and left to drying at room temperature in vacuum.

3.3.3 Disk diffusion Assay

The anti-bacterial activity of the samples were evaluated against gram positive (*Staphylococcus aureus* and *Bacillus subtilis*) as well as gram negative bacterial strains (*Escherichia coli* and *Pseudomonas aeruginosa*) by agar diffusion method adhering to the recommendations of the Clinical and Laboratory Standards Institute (CLSI). In a typical assay, the stock cultures of bacteria were revived by inoculating in broth media and grown at 360 K for 18h. The agar plates of the above media were prepared and wells were made in the plate. Each plate was inoculated with 18h old cultures (100 μ L, 10^{-4} CFU) and spread evenly on the plate. And now the diluted dispersion of the nanostructures at a single concentration and the antibiotic ciprofloxacin were filled on the wells after 20 minutes of inoculation. Subsequently, the plates were incubated at 360 K for 24 h and the diameter of inhibition zone (mm) was measured.

CHAPTER IV

CHAPTER IV

RESULTS AND DISCUSSIONS

4.1 Structural Characterization

The phase purity and crystal structure of the as-synthesized samples were analysed from the powder X-ray diffraction patterns recorded between the 2θ range 20° - 80° and is shown in Fig. 4.1 & 4.2. All the diffraction peaks (Fig. 4.1) can be readily indexed to the cuprite crystal structure (space group:) of Cu_2O having lattice constants $a = b = c = 4.267 \text{ \AA}$ and are in accordance with those reported in literature (JCPDS Card No. 05-0667).

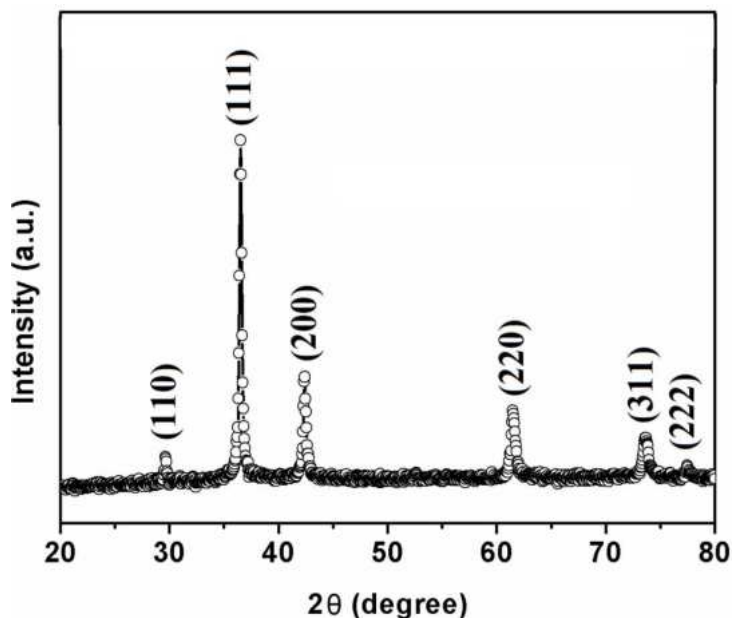


Fig. 4.1 Powder X-ray diffractogram of the as-synthesized Cu_2O nanocrystals.

The diffraction peaks with 2θ values 29.6° , 36.5° , 42.4° , 61.4° , 73.6° and 77.5° correspond to the crystal planes (110), (111), (200), (220), (311) and (222) of the cubic phase⁴³ of Cu_2O respectively. Moreover, no distinct peaks of any impurities such as copper or other copper oxides were detected in the diffraction pattern implying the high purity of the sample. The broadening of diffraction peaks could be ascribed to the small crystallite size and the resulting strain in the crystal lattice.

Table 1. Crystallographic parameters of prepared Cu₂O nanostructures prepared with the reducing agents (a) Hydroxylamine (b) L-Ascorbic acid (c) D-Glucose.

	Crystal plane	<i>d</i> -spacing (Å)	Relative Intensity (%)
29.66°	(110)	3.0113	7.41
36.52°	(111)	2.4601	100.0
			0
42.40°	(200)	2.1318	30.70
61.47°	(220)	1.5082	19.85
73.61°	(311)	1.2867	11.56
77.53°	(222)	1.2312	2.48

4.2 Microstructural Characterization

4.2.1 SEM Characterization:

The morphology and surface topography of the Cu₂O nanostructures was examined by performing scanning electron microscopy. Figure 4.2 presents the panoramic view of the as-obtained nanostructures and the morphology of the sample is observed to be rhombic dodecahedral in nature all through the sample. The magnified view of a selected area of the sample, in figure 4.2(b) and 4.2(c), shows that the morphology of the nanostructures is found to be uniform with the grain size ranging between 200-250 nm. The elemental composition of the sample was investigated employing energy dispersive X-ray spectroscopy analysis, which confirms the presence of copper and oxygen with slight oxygen deficiency.

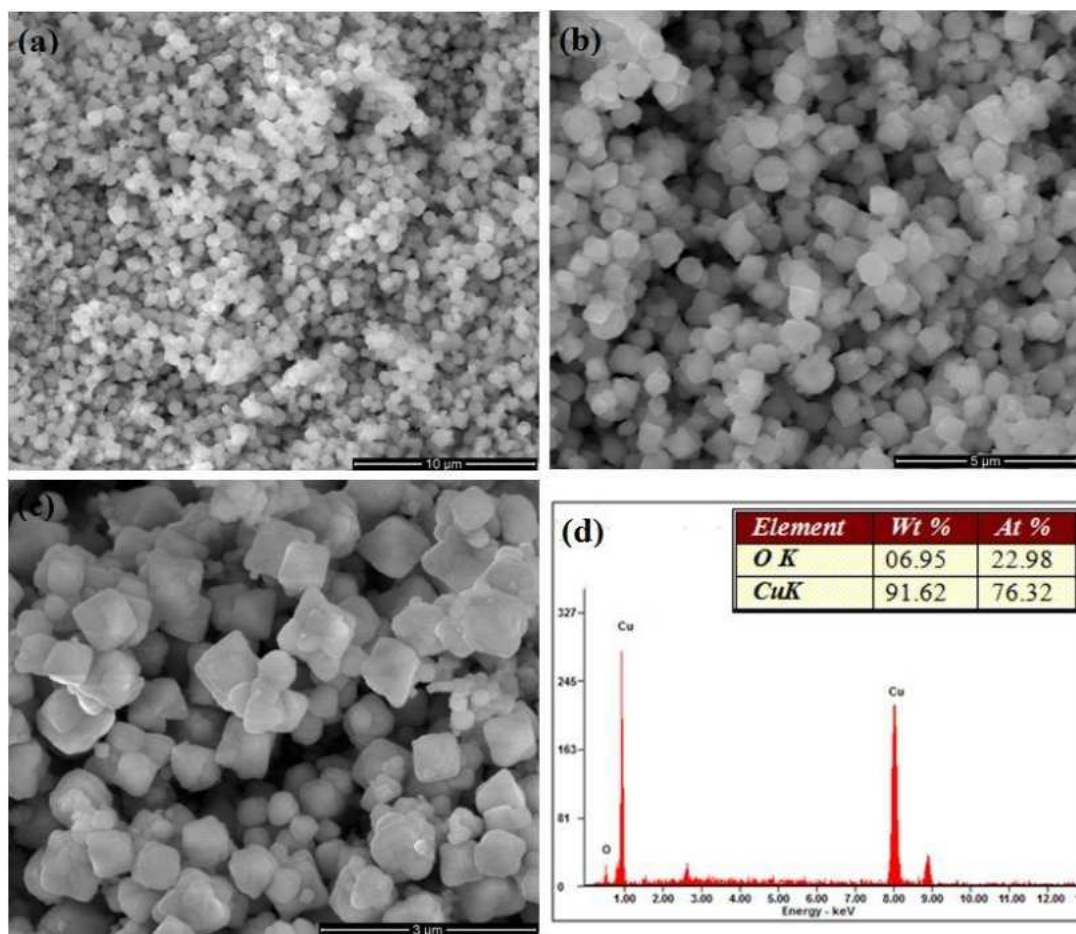


Fig. 4.2(a), (b) and (c) Representative scanning electron micrographs of Cu₂O nanostructures prepared using NH₂OH at different magnifications (d) EDX Spectrum of Cu₂O nanostructures.

The elemental composition of the sample (Fig. 4.2 (d)) was investigated employing energy dispersive X-ray spectroscopy analysis, which confirms the presence of copper and oxygen with slight oxygen deficiency (Table 1).

Table 2: Elemental composition of Cu₂O and Ag-CuO from EDAX spectra

NPs	Elements	Wt %	At %
Cu ₂ O	O	06.95	22.98
	Cu	91.62	76.32

4.3 Anti-Bacterial Assay

The anti-bacterial activity of Cu₂O nanostructures were tested against four bacterial strains namely *Staphylococcus aureus*, *Bacillus subtilis*, *Escherichia coli* and *Pseudomonas aeruginosa*, where the former two microorganisms are gram positive and the rest of them two are gram negative ones. The control employed in our experiments is the well-known fluoroquinolone antibiotic, ciprofloxacin, owing to its broad spectrum of activity against both gram-negative and gram-positive bacteria.

Nature of Sample	Diameter of the inhibition zone (mm)			
	Gram positive bacteria		Gram negative bacteria	
	<i>Staphylococcus aureus</i>	<i>Bacillus subtilis</i>	<i>Escherichia coli</i>	<i>Pseudomonas aeruginosa</i>
Cuprous Oxide nanostructures	6	7	6	11

Table 3. Diameter of inhibition zone observed for Cu₂O heteronanostructures

The diameter of the inhibition zone in case of the control for the bacterial species *S.aureus*, *B.subtilis*, *E. coli* and *P.aeruginosa* are 37, 38, 40 and 33 mm respectively. It is quite clear from the table that Cu₂O nanostructures have shown appreciable growth inhibiting effects for *P.aeruginosa* compared to other bacterial strains.

CHAPTER V

CHAPTER V

CONCLUSION

5.1 Summary

The cuprous oxide nanoparticles were successfully synthesized by chemical precipitation method.

The crystal structure and phase purity of the synthesized sample were analyzed from X-ray Diffraction patterns.

No distinct peaks of impurities were detected, implying the high purity of the sample.

Moreover it is found that the peaks width varies inversely with the crystallite size.

The morphology and surface topography of the Cu₂O nanostructure were examined by scanning electron microscope.

The morphology of the sample is found to be rhombic dodecahedral in nature

Using X-ray spectroscopy analysis the presence of copper and oxygen with slight oxygen deficiency was determined.

Cu₂O nanostructure has shown appreciable growth inhibiting effects in bacterial strains.

The synthesis of cuprous oxide wasn't a complex process. The knowledge we gained through it has widen our minds.

Numerous prospective benefits for health and the environment are being offered by nanotechnology.

We hope and wish to explore more about it in the future.

5.2 References

1. A. Erroh, A.M. Ferrari (2015), had grown Cu₂O nanoparticles bound to cotton fibers.
2. Ling-I Hung, Peidong Yang (2010), formed hollow Cu₂O nanoparticles at room temperature.
3. Chao-Yin Kuo, Cheuh-Ying Pai (2012), synthesized cuprous oxide from copper containing waste liquid to treat aqueous reactive dye.
4. Haijun Huang, Zhigang Zang (2017), prepared cubic Cu₂O nanoparticles wrapped by reduced graphene oxide for the efficient removal of rhodamine B.
5. Manoj Devaraj, Santhanalakshmi Jayadevan (2016), fabricated novel shape of Cu₂O nanoparticles modified electrode for the determination of dopamine and paracetamol.
6. Mohammed Aslam, W. Vogel (2001), formed Cu₂O nanoparticles by variation of surface ligand.
7. Manab Mallik, Himadri Roy (2019), synthesized and characterized Cu₂O nanoparticles.
8. Jinxes Shu, Wei Zhang (2014), Adsorption removal of Congo red from aqueous solution using polyhedral Cu₂O nanoparticles.

A STUDY OF CLASSIFICATION OF LANDS OF THOOTHUKUDI

Project report submitted to the Department of Physics

ST. MARY'S COLLEGE (AUTONOMOUS)

THOOTHUKUDI

Affiliated to MANONMANIUM SUNDARANAR UNIVERSITY, TIRUNELVELI

In partial fulfillment of the requirement for the award of

BACHELOR'S DEGREE IN PHYSICS

BY

A. BAVANI LAKSHMI - 18AUPH07

S. DEENA LIYONIKA - 18AUPH14

M.ISHWARYAA - 18AUPH19

J. LINGA DHARSHINI - 18AUPH25

V. MUTHU ANUSHIYA - 18AUPH31

M. SNEKHA - 18AUPH42

Under the Guidance of

Ms. Lucas Rexline M.Sc., M.Ed., M.Phil.



Department of Physics

ST. MARY'S COLLEGE (AUTONOMOUS)

Reaccredited with "A+" Grade by NAAC

Thoothukudi

2020 – 2021.

CERTIFICATE

This is the certify that this project work entitled, "A STUDY OF CLASSIFICATION OF LANDS OF THOOTHUKUDI " is submitted to ST. MARY'S COLLEGE (AUTONOMOUS), THOOTHUKUDI in partial fulfillment for the award of Bachelor's degree in Physics and is a record of work done during the year 2020-2021 by the following students.

A.BAVANI LAKSHMI	- 18AUPH07
S.DEENA LIYONIKA	- 18AUPH14
M.ISHWARYAA	- 18AUPH19
J.LINGA DHARSHINI	- 18AUPH25
V.MUTHU ANUSHIYA	- 18AUPH31
M.SNEKHA	- 18AUPH42

A. Lucas Rexelme
GUIDE
9/4/21

Pessie J do

HEAD OF THE
DEPARTMENT HEAD

Department of Physics,
St. Mary's College (Autonomous),
Thoothukudi - 628 001.

S. Kuchukemmanur
EXAMINER
9/4/21

Lucia Rose
PRINCIPAL
St. Mary's College (Autonomous)
Thoothukudi - 628 001.

ACKNOWLEDGEMENT

First of all, I would like to thank the supreme power the Almighty god who is obviously the one has always guided us to work on the right path of life

Then we express our sincere gratitude and thanks to our principal Dr. Sr. A. S. J. Lucia Rose M.Sc., M.Phil., Ph.D., PGDCA, for providing as an opportunity to do this project work we are much grateful to our head of the department Dr. Sr. Jessie Fernando M.Sc., M.Phil., Ph.D., for her encouragement to complete this project.

We thank our guide Ms. Lucas Rexceline M.Sc., M.Ed., M.Phil, Associate Professor of physics for motivating us and having given us valuable idea that has been helped us patch this project and make it full proof success.

We would like to express my whole hearted indebtedness to my family members and friends to their immense help to do this project work. I have no valuable words to express by thanks, but my heart is still full of favours received from every person

CONTENT

Certificate

Acknowledgement

Abstract

1. Introduction

2. Literature Review

3. Study Area

4. Materials and methods

4.1 Classification of land

4.1.1 Salt pan

4.1.2 Settlement

4.1.3 Urban area

4.1.4 Vegetation

4.1.5 Shrubs

4.1.6 Water bodies

4.1.7 Barren

4.1.8 Forest

4.2 Image Visualization

4.2.1 Pixel Values

4.2.2 Colour composite

4.3 Image enhancement

4.3.1 Contrast enhancement

4.3.2 Histogram

4.3.3 Linear Stretching

4.4 Spatial Enhancement

4.4.1 Low Pass Filtering

4.4.2 High Pass Filtering

4.5 Band Ratioing

4.5.1 Normalized Differential Vegetation Index

4.6 Principal Components Analysis

4.7 Unsupervised Classification

4.8 Supervised Classification

4.8.1 Sample Statistics

4.8.2 Feature space

5. Result and discussion

5.1 Area table

5.2 Accuracy Assessment Table-2020

5.3 Overall Accuracy

5.4 User Accuracy

5.5 Producer Accuracy

5.6 Kappa Coefficient

6. Conclusion

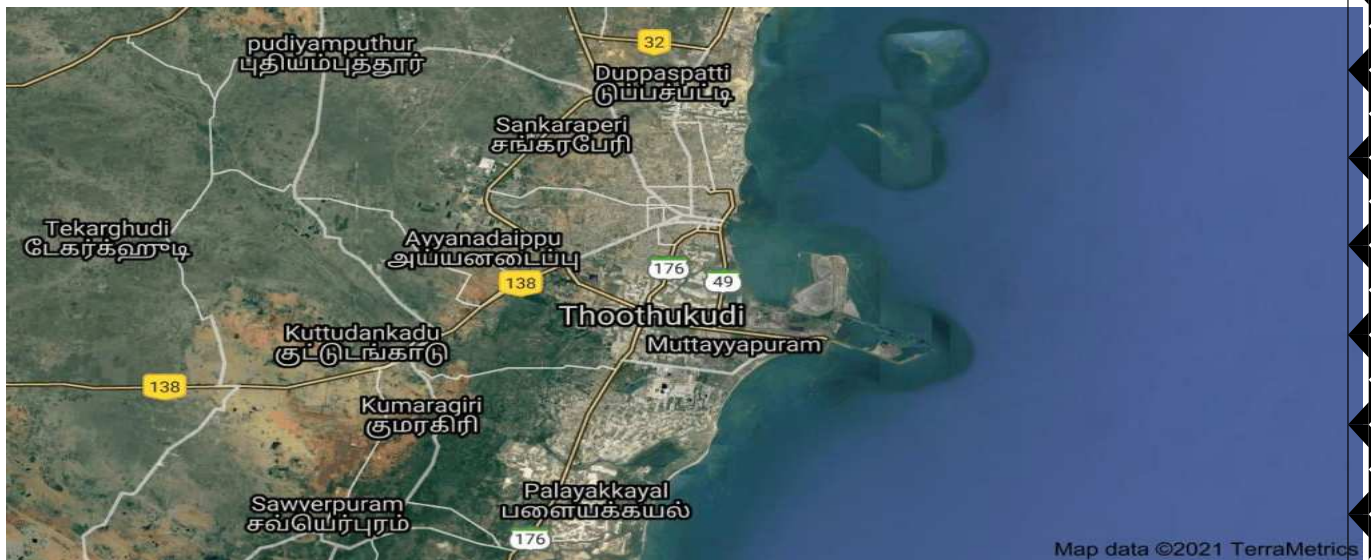
7. Reference

ABSTRACT

Mapping of water bodies, soil and vegetation region from satellite imagery has been widely explored in the recent past. Remote sensing images have wide application. One of the most important applications is classification of lands. Land use and land cover is an important parameter for development planning. Major problem with the study area which are identified as are (i) Rapid Growth of Population and (ii) Unplanned growth of the city both horizontally in all direction and vertically also. These problems can be solved with the study of Remote Sensing and GIS. Six major land use classes identified and mapped for the study area are cultivated land, Salt pans, Barren land, Shrubs, Settlement area and Water bodies. This study observed that cultivated land is dominant in Thoothukudi and its surroundings followed by salt pans. The study recommends the use of satellite imageries for future environmental monitoring studies and it is profitable for the urban planning authorities of Thoothukudi. It is reported that, this study is very valuable in mapping and computing the extent of urban area in different time periods.

1. Introduction:

The coast is a unique environment where land, sea and atmosphere interact and interplay continuously influencing a strip of spatial zone defined as coastal zone. coastal zones are the areas having the influence of both marine and terrestrial processes. Coastal zones are the most fragile, dynamic and productive ecosystem and are quite often under pressure from both anthropogenic activities and natural processes. It supports a large amount of floral and faunal biodiversity. Coastal Zone is endowed with a very wide range of habitats such as coral reefs, mangroves, sea grasses, sand dunes, vegetated stungle, mudflats, salt marshes, estuaries, lagoons etc., which are characterized by distinct biotic and abiotic processes. Thoothukudi is one of the most famous coastal area. Thoothukudi is traditionally known for pearl fishing and shipping activities, production of salt and other related business. This is a port city in the southern region of Tamilnadu.



Thoothukudi experience remarkable changes in land use and land cover features due to impacts of marine and terrestrial factors and human activities. Due to anthropogenic activities, the earth surface is being significantly altered and man's presence on the earth and his use of land has had a profound effect on the natural environment. Land is becoming a scarce resource due to immense agricultural and demographic pressure. The changes in land use and land cover due to various physical, climatic and socio-economic factors are directly influencing the socio-economic status of local people along the coastal area in space and time. Rapid growth of population, urbanization and tourism developmental activities are altering the existing state of land use and land cover features. The land use changes without considering environmental sustainability is increasing the demand for land resources like agriculture, minerals, soil and water. Increasing of population and climatic variability produces pressure on the land use and land cover (LULC) causing the greatest environmental impact on vegetative cover, shoreline change, landform degradation, loss of biodiversity, seawater intrusion and groundwater pollution, deterioration of soils and air along the coastal regions. Nowadays, the rate of demand is

exceeding than the rate of earth causes more serious long-term sustainability issues along the coastal regions in worldwide. Thus, maintaining the capacity of the land to sustain that demand will remain of fundamental importance

Hence, information on land use and land cover and possibilities of their optimal use is essential for the selection, planning and implementation of land use schemes to meet the increasing demands for basic human needs and welfare. This information could assist in monitoring the dynamics of land use resulting out of changing demands of increasing population. Remote Sensing plays a key role in providing the land coverage mappings and classification of land cover features which mainly includes vegetation, roads, water bodies etc.

The LULC change analysis provides a primary information for sustainable coastal zone management therefore, it is very essential for obtaining the reliable information in order to support proper coastal resource management planning in national or regional scale under immense population pressure. The integrated remote sensing and GIS techniques provide a successful platform for mapping the LULC features of Thoothukudi. A chief use of remotely sensed data is to produce a classification map of the features and classes of land cover types in Thoothukudi. Water, Soil and Vegetation are essential component of ecosystems for the sustainability of life on earth. They balance ecosystem and maintain climate variation, carbon cycling, etc. It is equally important to humans and other forms of life. The identification can be useful in various ways, such as estimation of water areas, demarcation of flooded regions, wetland inventories, change detection, and so on. The availability of water helps in the estimation of agricultural land irrigation, productivity, hydropower energy and many others.

Soil surveys are the main information source for sustainable agriculture and land use management. Soil survey mapping units are defined by the soil properties that affect management practices, such as drainage, erosion control, tillage and nutrition, and they involve the whole soil profile. Vegetation survey defines vegetation types and helps to understand differences among them, which is essential for both basic ecological research and applications in biodiversity conservation and environmental monitoring. Landsat satellite sensors have been used for land use classification and water body identification. It is necessary to explore the inputs based on the UGCS Landsat images. By using reflectance bands from Landsat 8 OLI imagery it is easy to analyse the water and soil regions from the Landsat images

This project therefore examines the relevance of some land use and land cover classification in Thoothukudi derived from multi-temporal remotely sensed data (Landsat images , UGCS satellite images) and their contributions to the emerging patterns in global land cover and land use studies and to map dynamically and monitor the land use/cover change and to analyse the changes

2. Literature review:

C. P. Lo, D. A. Quattroci & J. C. Luvall (2010) have studied day and night airborne thermal infrared image data at 5 m spatial resolution acquired with the 15-channel Advanced Thermal and Land Applications Sensor (ATLAS) over Alabama, Huntsville. These images were used to study changes in the thermal signatures of urban land cover types between day and night. This research also examined the relation between land cover irradiance and vegetation amount, using the Normalized Difference Vegetation Index (NDVI), obtained by rationing the difference and the sum of the red and reflected infrared ATLAS data. The high-resolution thermal infrared images match the complexity of the urban environment, and are capable of characterizing accurately the urban land cover types for the spatial modeling of the urban heat island effect using a GIS approach.

NorsalizaUsali & Mohd Hasmadi Ismail (2010) have studied the application of remote sensing and GIS specifically in monitoring water quality parameter such as suspended matter, phytoplankton, turbidity, and dissolved organic matter. Potential application and management was identified in promoting concept of sustainable water resource management. Remote sensing and GIS technologies coupled with computer modelling are useful tools in providing a solution for future water resources planning and management to government especially in formulating policy related to water quality.

M. Palaniyandi (2014) has used Remote Sensing and GIS for spatial prediction of vector-borne diseases transmission. The nature of the presence and the abundance of vectors and vector-borne diseases, disease infection and the disease transmission are not ubiquitous and are confined with geographical, environmental and climatic factors, and are localized. The presence of vectors and vector-borne diseases is confined and fuelled by the geographical, climatic and environmental factors including man-made factors. They gave the detailed information on the classical studies of the past and present, and the future role of remote sensing and GIS for the vector-borne diseases control.

Savita P. Sabale ,Chhaya R. Jadhav (2015) have studied about the hyperspectral image classification methods in remote sensing. They given a current approach for classifying hyper spectral images based on supervised, unsupervised and semi supervised classification methods. They have also discusses, issues and prospect to conduct hyper spectral image classification to acquire good classification results.

ShakhislamUzakbaevichLaishanov(2016) have studied about the dynamics of soil salinity in irrigation areas. Based on computer analysis of LANDSAT images they determined that soil salinity has increased due to significant decrease of the area of non-saline soil by 41.5% and increase of the areas of low and moderately saline soils by 34.9%, also regions with heavily saline soils at 6.6%.

ImasSukaesih, SitanggangNalar and others (2016) have determined the sequential 21 patterns of hotspot occurrences and classified satellite image data and identified the fire spots. Their study showed that, about 72.62% and 87.50% hotspots sequentially occurred in Pulang Pisau and Palangkaraya, respectively.

Those hotspots are considered as fire spots that become strong indicator for peatland fires.

Han Liu, Lin He, Jun Li(2017) have studied about the classifications based on convolutional neural networks with two-fold sparse regularization. They introduced a new two-fold sparse regularization method for remote sensing image classification. Their experimental results are conducted with three types of remote sensing data: hyperspectral images, multispectral images and synthetic aperture radar (SAR), suggesting that the proposed framework achieves excellent classification performance in all cases

Ying Li, Haokui Zhang and the others (2018) have reported that the earth observation technology using RS data having been widely exploited in both military and civil fields. They have briefly introduced a number of typical DL models that may be used to perform RS image classification, including: CNNs, SAEs and DBNs. They have systematically reviewed the state-of-the-art DL approaches for RS image classification.

Mercedes.EPaoletti, Juan.H, and the others(2018) have studied about the Deep and Dense conventional Neural Network for hyper spectral image classification. They newly proposed framework which introduced shortcut connections between layers, in which the feature maps of inferior layers are used as inputs of the current layer, feeding its own output to the rest of the upper layers. Their experimental results with four well-known HIS datasets reveal that the proposed deep and dense CNN model is able to provide competitive advantages in terms of classification accuracy when compared to other state-of –the-methods for HIS classification

Mario Benincasa, Federincofalcinini and others (2019) have studied about the synergy of satellite in remote sensing. They focused on mesoscale and sub-mesoscale processes, such as coastal currents and river plumes. They computed the divergence of this flux. The divergence field thus obtained shows how the aforementioned mesoscale processes distribute the sediments.

Ajay Singh(2019) has used remote sensing and GIS techniques for managing the environmental problems of waste disposal. An indication of the waste disposal problems and its management alongside the ramifications of the analysis is discussed. The background and rationale of the waste disposal problems are detailed. The applications of remote sensing and GIS in waste management modeling are presented and applications of these techniques in diverse case studies worldwide are described. The study reveals that the efficiency of waste management system can be maximized by the proper use of remote sensing and GIS techniques. The study also revealed that these techniques are most commonly used for siting the landfill and waste bin for waste disposal and evaluation of environmental impact of buried waste.

S. Meivel& S. Maheswari(2020) have made the analysis of drone remote sensing using NDVI and NIR sensor in a multispectral view of agricultural land. Irrigation techniques followed the treatment of the plant within continuous data per second. The implemented view focused only on growth controlling of plant in-depth irrigation between 30 and 90 cm in 60% deviation. NDVI, green normalized difference vegetation index (GNDVI), soil brightness index (SBI),

green vegetation index (GVI), degree of yellow vegetation index (YVI), nitrogen sufficiency index (NSI), perpendicular vegetation index (PVI), transformed vegetation index (TVI), soil adjusted vegetation index (SAVI) and vegetation condition index (VCI) vegetation indices are used to the correlation of plant growth control with managing leaf strength and import python packages display the Vegetation various Real-time value in QGIS. They have provided a drone survey analysis of compost percentage and vegetation indices of agricultural land

Dylan& S. Davis(2020) have studied about the geographic disparity in Machine Intelligence for Archaeological Remote Sensing Research. Computational methods have expedited the rate of archaeological survey and discovery via remote sensing instruments. They investigated the degree of disparity and some potential reasons for geographical imbalance. Analyses from Web of Science and Microsoft Academic searches have revealed that there is a substantial difference between the Global North and South in the output of machine intelligence remote sensing archaeology literature. They have also studied about the regional imbalances.

AbhilashPerisetty,SaiTejaBodempudi and others(2020) have classified hyperspectral images using Edge Preserving Filter and Nonlinear Support Vector Machine. They have given a methodology to extract rich information from the hyperspectral images. This research work was tested on the standard dataset Indian Pines. The performance of the proposed method on this dataset has been assessed through various accuracy measures. The accuracies are 96%, 92.6%, and 95.4%. over the other methods. This methodology can be applied to forestry applications to extract the various metrics in the real world

GerritHuunemna and Lucas Broekema(2020) have studied about the classification of multi-sensor Data using a combination of Image Analysis Techniques. They have classified an area with optical and microwave data as input. The optical data has been acquired by the SPOT satellite in multi-spectral mode and the microwave data has been acquired by the ERS-1 and ERS-2 satellites in single look complex mode. The coherence map has created based on the correlation of two complex SAR data sets. Indication the level of correlation, this map provides information about the relation between groundcover and temporal changes.

3. Study area:

Thoothukudi is located strategically close to the East-West international sea routes on the South Eastern coast of India. It is a coastal town with a sea port and has been recently upgraded as Corporation. The study area spreads over a geographical area of 358 km² and lies between 8°39'–8°51'N and 78°57'–78°12'E ... The city lies on the Gulf of Mannar of the Indian Ocean, about 25 miles (40 km) east of Tirunelveli, to which it is connected by road and rail.



[Corner Upper Left Lat DMS](#)

9°43'27.70"N

[Corner Upper Left CLong DMS](#)

76°51'57.28"E

[Corner Upper Right Lat DMS](#)

9°42'24.66"N

[Corner Upper Right Long DMS](#)

78°55'50.88"E

[Corner Lower Left Lat DMS](#)

7°37'59.92"N

[Corner Lower Left Long DMS](#)

76°51'20.20"E

[Corner Lower Right Lat DMS](#)

7°37'10.60"N

[Corner Lower Right Long DMS](#)

78°54'32.94"E

In general the study area is an undulating topography with general slope towards east. The drainage network in the district is constituted by the rivers originating in Western Ghats and Tamilnadu uplands and flowing towards the Bay of Bengal. Few streams originate in the hillocks within the district and confluences directly with the sea. Vaippar(VilathikulamTakuk) and Karamaniyar(Sathankulam Taluk) are the major rivers draining the area which are ephemeral in nature., Tamiraparani is the major and perennial river in the district with a mature stage of development Rich deposits of garnet and ilmenite sand occurs along the coast part of Thiruchendur Taluk, in Thoothukudi district. Kayalpatnam, Manappadu, Vaippar, Madhavankurichi, Vembar, Periyasampuram and Padukkapathu areas show notable garnet and ilmenite sands occurrences. The district is divided into twelve revenue blocks for rural and urban development. The twelve revenue blocks are Thoothukudi, Tiruchendur, Udangudi, Sathankulam, Thiruvaikundam, Alwarthirunagari, Karunkulam, Ottapidaram,

Kovilpatti, Kayathar, Vilathikulam, and Pudur. The district has one municipal corporation, Thoothukudi, two municipalities, Kayalpattinam and Kovilpatti, nineteen town panchayats, and 403 panchayat villages

4. Material and methods:

On-screen visual interpretation was used in the current exercise wherein the GIS LULC vector layer created during the first cycle was overlaid on to the terrain corrected Resourcesat 2 LISS III imagery acquired during 2019-2020. The methodology essentially is based on editing the above vector layer for the changed areas thereby creating the new LULC vector layer for 2019-2020.

4.1 Classifications of land:

4.1.1 Salt pan:

Thoothukudi constitutes 70 percent of the total salt production of Tamil Nadu and 30 per cent of that of India. Tamil Nadu is the second largest producer of Salt in India next to Gujarat. Salt not only plays an incredibly important role in sustaining our daily lives but it has done much to shape the landscape around us – and continues to do so today. A salt pan is created when pools of seawater evaporate at a rate faster than it is replenished by rainfall. As the water evaporates, it leaves behind the minerals precipitated from the salt ions dissolved in the water. Salt is typically the most abundant of these minerals, accumulating over many thousands of years, giving the surface its hard white crust. Salt marshes are areas of vegetation often found in sheltered water areas, such as estuaries or behind land-spits. An estuary creates perfect conditions for salt marshes – a wide, shallow area of water where a river meets the sea. It contains both fresh water entering from a river, and salt water replenished twice daily as a result of flooding by the tidal actions. Salt pans are highly dynamic environments that are difficult to study by in situ methods because of their harsh climatic conditions and large spatial areas. Remote sensing can help to elucidate their environmental dynamics and provide important constraints regarding their sedimentological, mineralogical, and hydrological evolution. This study utilizes spaceborne multitemporal multispectral optical data combined with spectral endmembers to document spatial distribution of surface salt in Thoothukudi. Salt pan evaporite surfaces are common features in arid regions where closed drainage basins and high evaporation rates favor the development of crusted surfaces mainly composed of evaporate.

4.1.2 Settlement:

A settlement is a colony or any small community of people. A settlement is also the resolution of something such as a lawsuit. One kind of settlement is a place where people live. There are 5 types of settlement classified according to their pattern, these are, isolated, dispersed, nucleated, and linear. An isolated settlement consists of a single farm or house very remote from any other one, usually found in farming or hunting rural communities. Dispersed settlements are ones where the houses are spread out over a wide area. They are often the homes of farmers and can be found in rural areas. Rural areas are the

lands used for human settlement of size comparatively less than the urban settlements of which the majority of population is involved in the primary activity of agriculture. These are the built-up areas, smaller in size, mainly associated with agriculture and allied sectors and non-commercial activities. They can be seen in clusters non- contiguous or scattered. Nucleated settlements are towns where buildings are close together, often clustered around a central point.

4.1.3 Urban area:

An urban area, or built-up area, is a human settlement with a high population density and infrastructure of built environment. Urban areas are created through urbanization and are categorized by urban morphology as cities, towns, conurbations or suburbs. In urbanism, the term contrasts to rural areas such as villages and hamlets; in urban sociology or urban anthropology it contrasts with natural environment..Urban areas are non-linear built up areas covered by impervious structures adjacent to or connected by streets. This cover is related to centres of population. This class usually occurs in combination with, vegetated areas that are connected to buildings that show a regular pattern, such as vegetated areas, gardens etc. and industrial and/or other areas. (FAO, 2005).It includes residential areas, mixed built-up, recreational places, public/ semi-public utilities, communications, public utilizes/facility, commercial areas, reclaimed areas, vegetated areas, transportation, industrial areas and their dumps, and ash/cooling ponds.

4.1.4 Vegetation:

Vegetation is an assemblage of plant species and the ground cover they provide. It is a general term, without specific reference to particular taxa, life forms, structure, spatial extent, or any other specific botanical or geographic characteristics. These are the areas with standing crop as on the date of Satellite overpass. Cropped areas appear in bright red to red in color with varying shape and size in a contiguous to non- contiguous pattern. They are widely distributed indifferent terrains; prominently appear in the irrigated areas irrespective of the source of irrigation. It includes kharif, rabi and zaid crop lands along with areas under double or triple crops. These are the areas under agricultural tree crops planted adopting agricultural management techniques. Depending on the location, they exhibit a dispersed or contiguous pattern. Use of multi-season data will enable their separation in a better way. It includes agricultural vegetation (like tea, coffee, rubber etc.) horticultural vegetation (like coconut, arecanut, citrus fruits, orchards, fruits, ornamental shrubs and trees, vegetable gardens etc.) and agro-horticultural vegetation.

4.1.5 Shrubs:

A shrub or bush is a small- to medium-sized perennial woody plant. Unlike herbaceous plants, shrubs have persistent woody stems above the ground. Shrubs

can be deciduous or evergreen. Shrubs are seen at the fringes of dense forest cover and settlements, where there is biotic and abiotic interference. Most times they are located closer to habitations. Forest blanks which are the openings amidst forest areas, devoid of tree cover, observed as openings of assorted size and shapes as manifested on the imagery are also included in this category. Shrub areas possess shallow and skeletal soils, at times chemically degraded extremes of slopes, severely eroded or subjected to excessive aridity with scrubs dominating the landscape.

4.1.6 Water bodies:

Water covers almost 70% of our Earth. The largest body of water is the ocean, while the remaining bodies of water can be subdivided into categories like glaciers and ice caps, groundwater, freshwater and atmospheric water. About 97% of our water resources are saltwater. This category comprises areas with surface water in the form of ponds, lakes, tanks and reservoirs. Inland water bodies are the areas that include ox-bow lakes, cut-off meanders, playas, marsh, etc. which are seasonal as well as permanent in nature. It also includes manmade wetlands like waterlogged areas. Coastal waterbodies include estuaries, lagoons, creek, backwater, bay, tidal flat/mud flat, sand/beach, rocky coast, mangrove, salt marsh/marsh vegetation and other hydrophytic vegetation and saltpans. Rivers/streams are natural course of water flowing on the land surface along a definite channel/slope regularly or intermittently towards a sea in most cases or in to a lake or an inland basin in desert areas or a marsh or another river. Canals are artificial water course constructed for irrigation, navigation or to drain out excess water from agricultural lands.

4.1.7 Barren:

A barren landscape is dry and bare, and has very few plants and no trees. Barren land consists of soil that is so poor that plants cannot grow in it. Barren vegetation describes an area of land where plant growth may be sparse, stunted, and/or contain limited biodiversity. Environmental conditions such as toxic or infertile soil, high winds, coastal salt-spray, and climatic conditions are often key factors in poor plant growth and development. Barren vegetation can be categorized depending on the climate, geology, and geographic location of a specific area. These are rock exposures of varying lithology often barren and devoid of soil and vegetation cover.

4.1.8 Forest:

The term forest is used to refer to land with a tree canopy cover of more than 10 percent and area of more than 0.5 ha. Forests are determined both by the presence of trees and the absence of other predominant land uses. The trees should be able to reach a minimum height of 5 m. The forest is a complex ecosystem consisting mainly of trees that buffer the earth and support a myriad of life forms. The trees help create a special environment which, in turn, affects the kinds of animals and plants that can exist in the forest. Trees are an important component of the environment. Forests are the dominant terrestrial ecosystem of Earth, and are distributed around the globe. Forest the areas of tree

species of forestry importance, raised and managed especially in notified forest areas. The species mainly constitute teak, Sal, eucalyptus. Mangrove forest are tropical and subtropical vegetation species that are densely colonized on coastal tidal flats, estuaries salt marshes etc. This category includes all the areas where the canopy cover/density is above 10%.

4.2 Image visualization

For satellite images and scanned black and white aerial photographs the image domain is used. Pixels in a satellite image or scanned aerial photograph usually have values ranging from 0-255. The values of the pixels represent the reflectance of the surface object. The image domain is in fact a special case of a value domain. Raster maps using the image domain are stored using the '1 byte' per pixel storage format. A single band image can be visualized in terms of its gray shades, ranging from black (0) to white (255). The values of the pixels represent the reflectance of the surface object. The image domain is in fact a special case of a *value domain*. Raster maps using the image domain are stored using the '1 byte' per pixel storage format. The pixel location in an image (rows and columns), can be linked to a georeferenced which in turn is linked to a coordinate system which can have a defined map projection.

The objectives of the exercises in this section are to understand the relationship between the digital numbers of satellite images and the display, and to be able to display several images, scroll through and zoom in/out on the images and retrieve the digital numbers of the displayed images. Satellite or airborne digital image data is composed of a two-dimensional array of discrete picture elements or pixels. The intensity of each pixel corresponds to the average brightness, or radiance, measured electronically over the ground area corresponding to each pixel. Pixels with a weak spectral response are dark toned (black) and pixels representing a strong spectral response are bright toned (white). The digital numbers are thus represented by intensities from black to white. To compare bands and understand the relationship between the digital numbers of satellite images and the display, and to be able to display several images, you can scroll through and zoom in/out on the images and retrieve the DNs of the displayed images.



Image visualization map

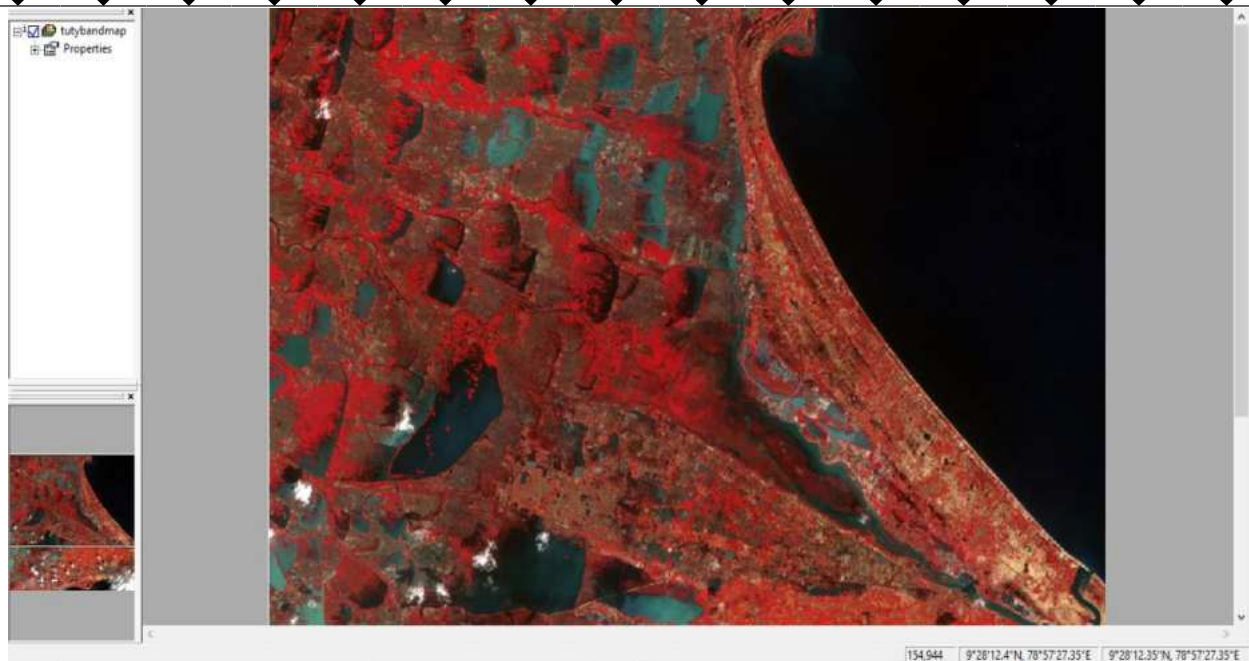
4.2.1 Pixel values:

The spectral responses of the earth's surface in specific wavelengths, recorded by the spectrometers on board of a satellite, are assigned to picture elements (pixels). Pixels with a strong spectral response have high digital numbers. The digital numbers are thus represented by intensities on a black to white scale.

Coordinate	9°02'48.48"N, 78°22'55.14"E
tuty_band2	924,608
tuty_band2	50

4.2.2 Colour composite:

A natural or true colour composite is an image displaying a combination of the visible red, green and blue bands to the corresponding red, green and blue channels on the computer display. Colour composite image of Tuticorin port is displayed.



Colour composite

4.3 Image enhancement:

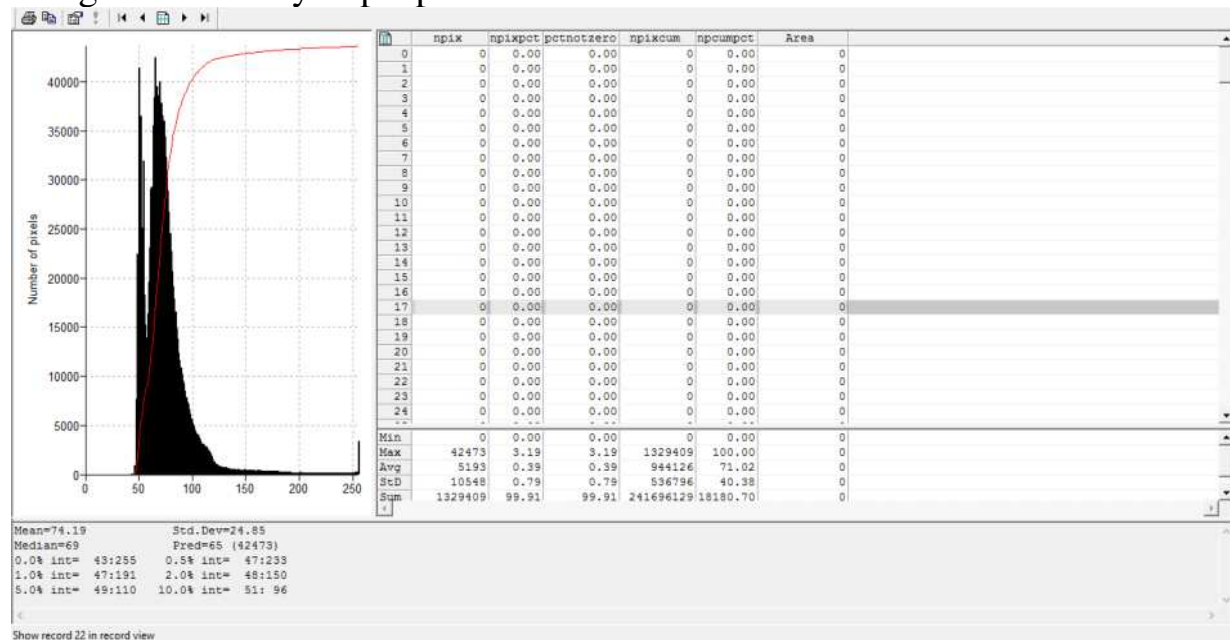
Image enhancement deals with the procedures of making a raw image better interpretable for a particular application. Image enhancement techniques can be classified in many ways. Contrast enhancement, also called global enhancement, transforms the raw data using the statistics computed over the whole data set. Examples are: linear contrast stretch, histogram equalized stretch and piece-wise contrast stretch. Contrary to this, spatial or local enhancement only takes local conditions into consideration and these can vary considerably over an image. Examples are image smoothing and sharpening.

4.3.1 Contrast enhancement

The objective of this section is to understand the concept of contrast enhancement and to be able to apply commonly used contrast enhancement techniques to improve the visual interpretation of an image. The goal of contrast enhancement is to improve the visual interpretability of an image, by increasing the apparent distinction between the features in the scene. By using contrast enhancement techniques, these slight differences are amplified to make them readily observable. Contrast stretch is also used to minimize the effect of haze. Scattered light that reaches the sensor directly from the atmosphere, without having interacted with objects at the earth's surface, is called haze or path radiance. Haze results in overall higher DN values and this additive effect results in a reduction of the contrast in an image. The haze effect is different for the spectral ranges recorded; highest in the blue, and lowest in the infrared range of the electromagnetic spectrum. Techniques used for contrast enhancement are: the linear stretching technique and the histogram equalization. To enhance specific data ranges showing certain land cover types, the piece-wise linear contrast stretch can be applied.

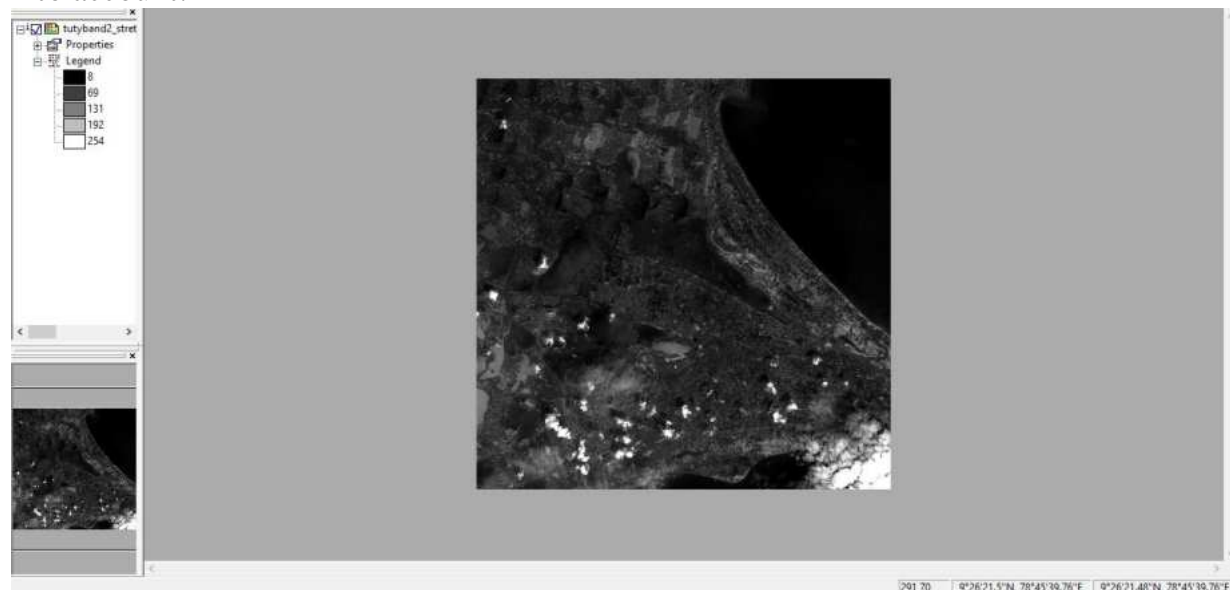
4.3.2 Histogram:

A histogram is a dependent table which stores frequency information on values, classes or IDs in a raster, polygon, segment or point map. A raster histogram is automatically calculated when displaying a value raster map which is stored using one or two bytes per pixel.



4.3.3 Linear stretching:

After a histogram has been calculated for a certain image, the image can be stretched. A linear stretch is used here. Only the pixel values in the 1 to 99% interval will be used as input; pixel values below the 1% boundary and above the 99% boundary will not be taken into account.



Linear stretch map

4.4 SPATIAL ENHANCEMENT:

Spatial Enhancement procedures result in modification of an image pixel value, based on the pixel values in its immediate vicinity. Spatial frequency filters, also often simply called spatial filters, may emphasize or suppress image data of various spatial frequencies.

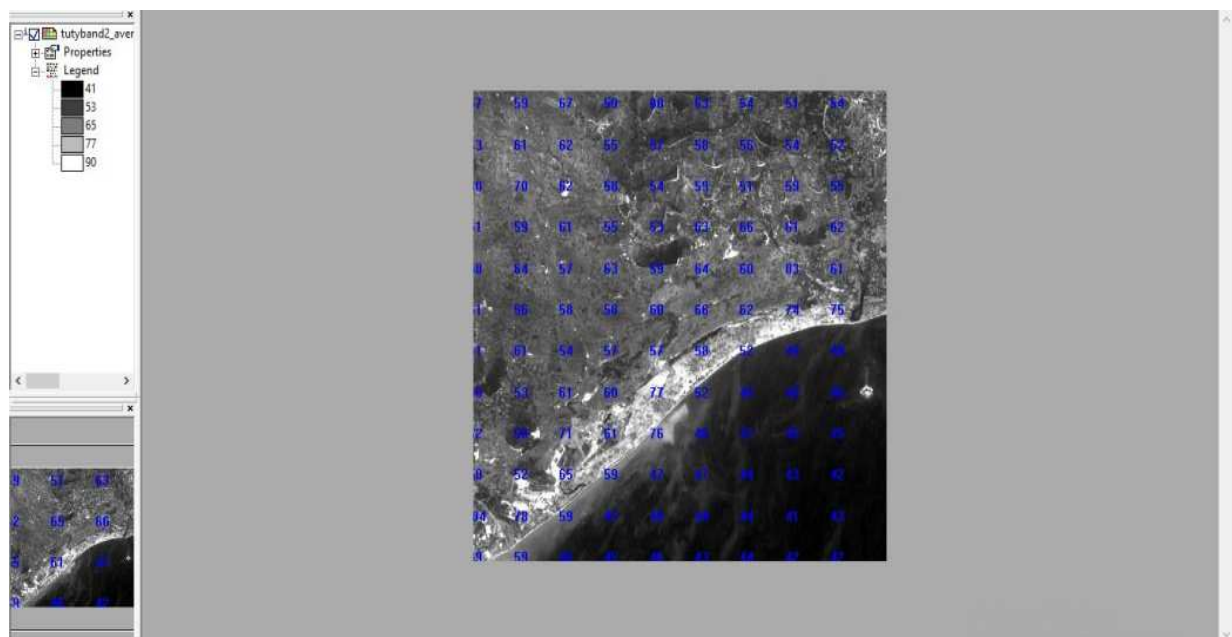
Spatial frequency refers to the roughness of the variations in DN values occurring in an image. In high spatial frequency areas, the DN values may change abruptly over a relatively small number of pixels (e.g. across roads, field boundaries, shorelines). Smooth image areas are characterized by a low spatial frequency, where DN values only change gradually over a large number of pixels (e.g. large homogeneous agricultural fields, water bodies). Like all image enhancement procedures, the objective is to create new images from the original image data, in order to increase the amount of information that can be visually interpreted.

Filters are commonly used to:

- 1) Correct and restore images affected by system malfunctioning,
- 2) Enhance the images for visual interpretation and
- 3) Extract features.

4.4.1 LOW PASS FILTERING:

Applying a low pass filter has the effect of filtering out the high and medium frequencies and the result is an image, which has smooth appearance. Hence, this procedure is sometimes called image smoothing and the low pass filter is called a smoothing filter. It is easy to smooth an image. The basic problem is to do this without losing interesting features. For this reason much emphasis in smoothing is on edge-preserving smoothing. The filter can be considered as a window that moves across an image and that looks at all DN values falling within the window. Each pixel value is multiplied by the corresponding coefficient in the filter. For a 3x3 filter. The 9 resulting values are summed and the resulting value replaces the original value of the central pixel. This operation is called convolution

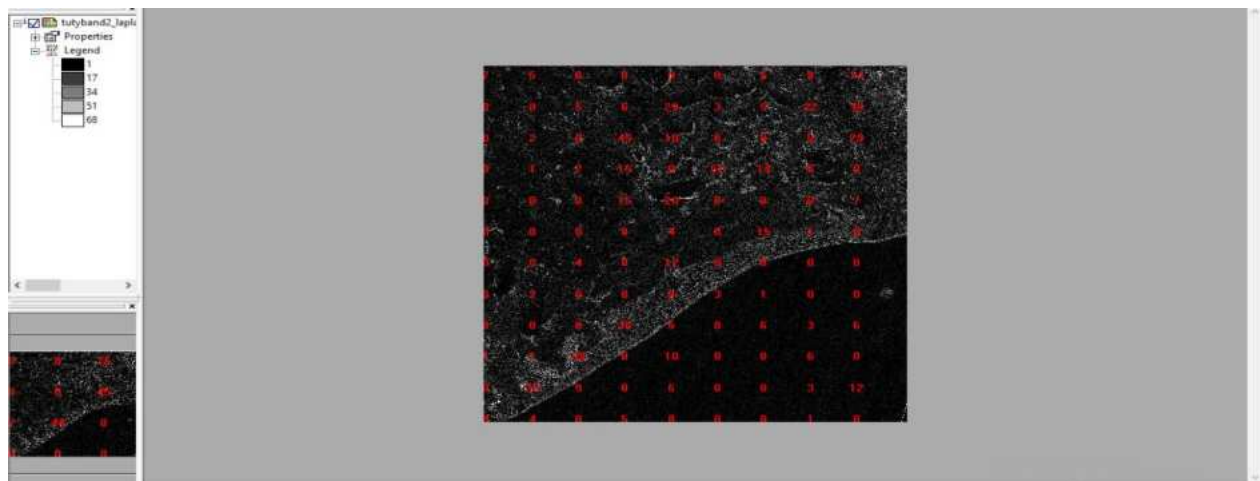


LOW PASS FILTER MAP

4.4.2 HIGH PASS FILTERING:

Sometimes abrupt changes from an area of uniform DN's to an area with other DN's can be observed. This is represented by a steep gradient in DN

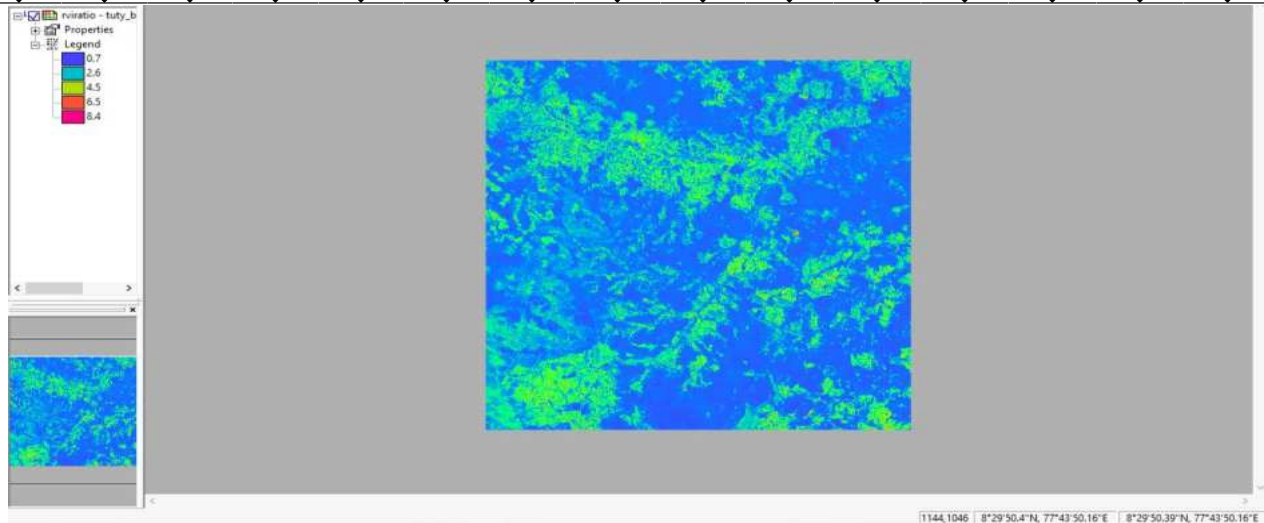
values. Boundaries of this kind are known as edges. They occupy only a small area and are thus high-frequency features. High pass filters are designed to emphasize high frequencies and to suppress low-frequencies. Applying a high pass filter has the effect of enhancing edges. Hence, the high pass filter has the effect of enhancing edges. Hence, the high pass filter is also called an edge enhancement filter. Two classes of high-pass filters can be distinguished: gradient (or directional) filters and Laplacian (or non-directional) filters. Gradient filters are directional filters and are used to enhance specific linear trends. They are designed in such a way that edges running in a certain direction (e.g. horizontal, vertical or diagonal) are enhanced. In their simplest form, they look at the difference between the DN of a pixel to its neighbour and they can be seen as the result of taking the first derivative (i.e. the gradient). Laplacian filters are non-directional filters because they enhance linear features in any direction in an image. They do not look at the gradient itself, but at the changes in gradient.



HIGH PASS FILTER MAP

4.5 Band Ratioing:

Band rationing means dividing the pixels in one band by the corresponding pixels in a second band. Sometimes differences in brightness values from identical surface materials are caused by topographic slope and aspect, shadows, or seasonal changes in sunlight illumination angle and intensity. Rationed images are created in order to minimize the effects of difference in illumination. Various mathematical combination of satellite bands, have been found to be sensitive indicators of the presence and condition of green vegetation. These band combinations are thus referred to as vegetation indices. Two such indices are the simple vegetation index (VI) and the Normalized Difference Index (NDVI). Both are based on the reflectance properties of vegetated areas as compared to clouds, water and snow on the one hand, and rocks and bare soil on the other. Vegetated areas have a relatively high reflection in the near-infrared and a low reflection in the visible range of the spectrum. Clouds, water and snow have larger visual than near-infrared reflectance. Rock and bare soil have similar reflectance in both spectral regions. To show the effect of band ratio for suppressing topographic effects on illumination, LISS IV Infrared and Red bands are used



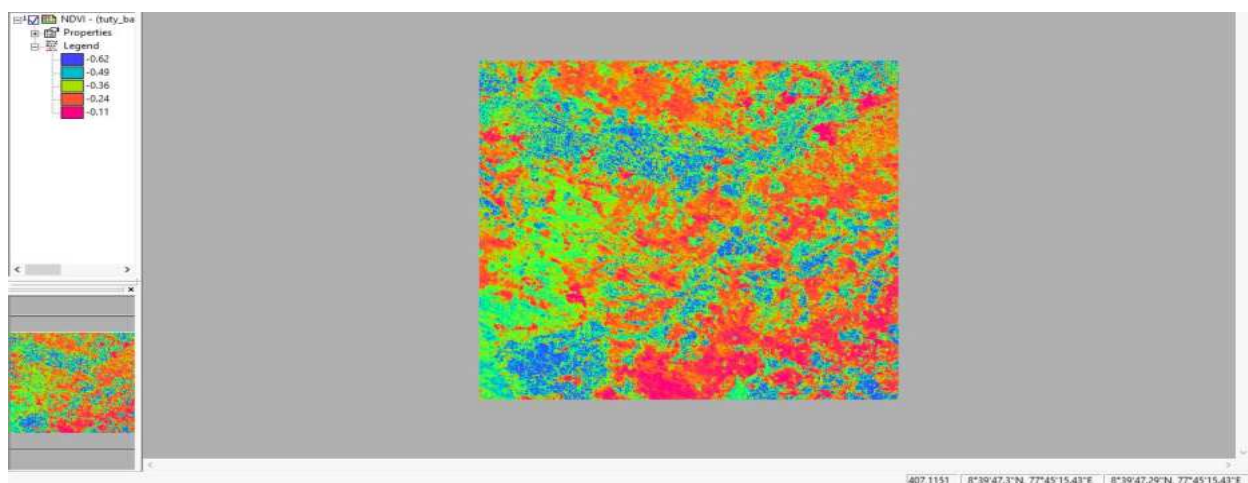
4.5.1 Normalized Differential Vegetation Index (NDVI):

The normalized difference vegetation index (NDVI) is a simple graphical indicator that can be used to analyze remote sensing measurements, often from a space platform, assessing whether or not the target being observed contains live green vegetation.

- $NDVI = (Infrared\ band - Red\ Band) / (Infrared\ band + Red\ Band)$
- Double - click the Map Calculation operations in the operation - list.

The Map Calculation dialog box is opened.

- In the Expression text box type the following map calculation formula: $(tuty_band5 - tuty_band4) / (tuty_band5 + tuty_band4)$.
- Enter NDVI for Output Raster map , select system Domain value, change.
- The Value Range to -1 and +1, and the precision to 0.01. Click show.



4.6 Principal Component Analysis:

Principal components Analysis(PCA), can be applied to compact the redundant data into few layer .Principal components analysis can be used to transform a set of image bands, as that the new layer also called components are not correlated with one another. The first two or three components will carry most of the real information of

the original data set. Therefore, only by keeping the first few components most of the information is kept. Through this type of image transformation the relationship with the raw image data is lost. It should be noted that the covariance values computed are strongly depending on the actual data set or subset used.

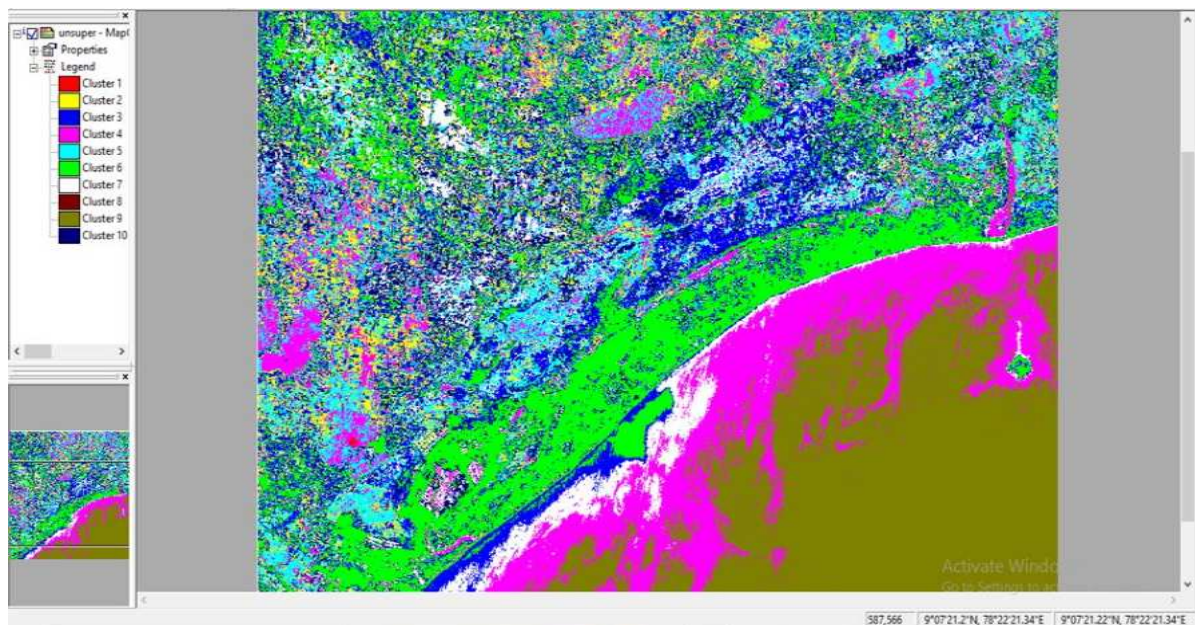
Variance per band:			
140.02	37.96	6.79	
Variance percentages per band:			
75.78	20.54	3.67	
<			
	lis4sul	lis4sul	lis4sul
PC 1	0.558	0.820	0.129
PC 2	0.039	0.130	-0.991
PC 3	-0.829	0.558	0.041

4.7 UNSUPERVISED CLASSIFICATION:

Unsupervised classification is where the outcomes (groupings of pixels with common characteristics) are based on the software analysis of an image without the user providing sample classes. The computer uses techniques to determine which pixels are related and groups them into classes. Unsupervised classification is a form of pixel based classification and is essentially computer automated classification. Unsupervised image classification is the process by which each image in a dataset is identified to be a member of one of the inherent categories present in the image collection without the use of labelled training samples.

Three types of unsupervised classification methods were used in the imagery analysis:

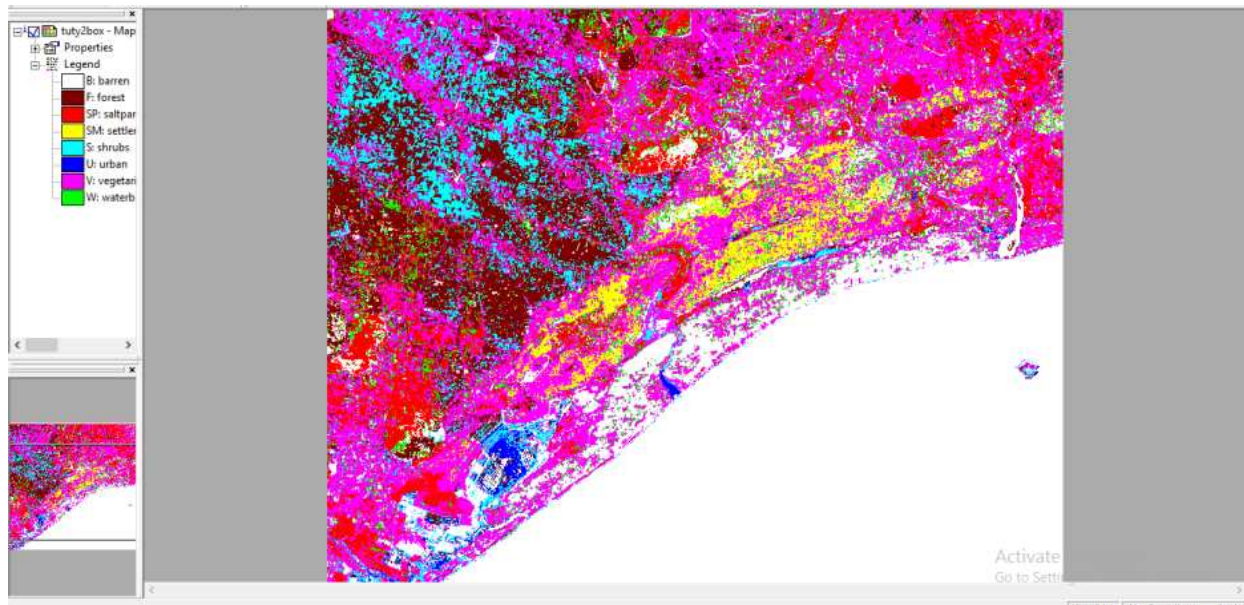
- ISO Cluster
- Fuzzy K-Means
- K-Means, which each resulted in spectral classes representing clusters of similar image values.



UNSUPERVISED CLASSIFICATION

4.8 SUPERVISED CLASSIFICATION:

In supervised classification the user or image analyst “supervises” the pixel classification process. The user specifies the various pixels values or spectral signatures that should be associated with each class. This is done by selecting representative sample sites of a known cover type called Training Sites or Areas. Supervised classification method are divided into two phases: a training phase, where the user ‘trains’ the computer, by assigning for a limited number of pixels to what classes they belong in the particular image, followed by the decision making phase, where the computer assigns a class label to all image pixels, by looking for each pixel to which of the trained classes this pixel is most similar

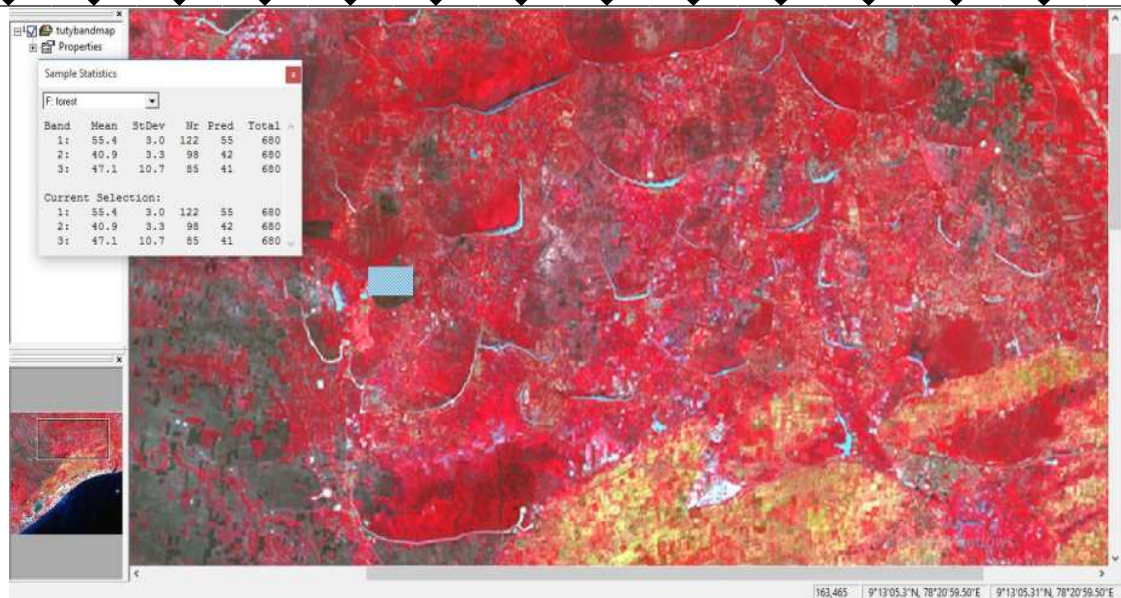


Supervised classification map

4.8.1 Sample statistics:

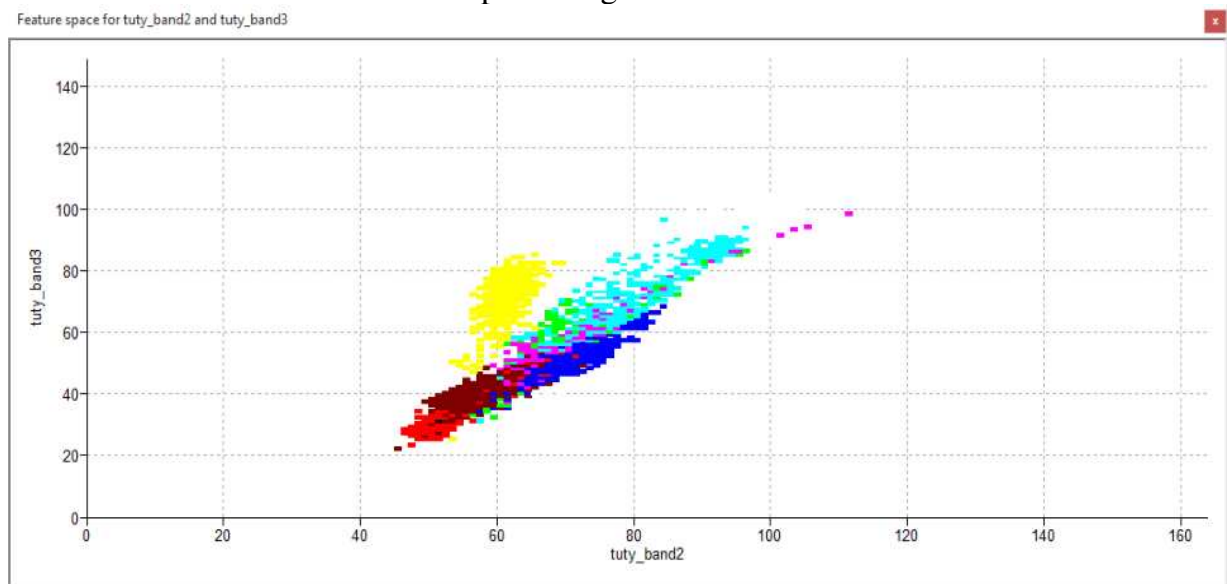
The Sample Statistics window contains the code and name of the selected class as well as the number of bands. The following statistics are shown for a selected class:

- Mean value of pixels (Mean).
- Standard deviation of pixels (StDev).
- The number of pixels having the predominant value (Nr).
- The predominant pixel value (Pred.).
- The total number of the selected pixels (Total).



4.8.2 Feature space:

One way to perform a classification is to plot all pixels of the image in a feature space, and then to analyze the feature space and to group the feature vectors into clusters. The classes can be plotted in distinct colors in the *feature space*, which enables a judgement of whether the classes can really be spectrally distinguished and whether each class corresponds to only one spectral cluster. The number of training samples should be between 30 and some hundreds of samples per class, depending on the number of features and on the decision making that is going to be applied. The feature space is a graph in which DN values of one band are plotted against the values of another.



5. Result and discussion

With the help of satellite images from USGS we worked on different bands to classify lands in Thoothukudi. From the metadata from USGS and from the Thoothukudi District analysis report using ArcGIS 10.8Max likelihood classifier software we got the area for different classification of lands.

5.1Area table:

Classification of lands	Sum of Area	Land in %
Barren Land	476.8178149	10
Cultivate Land	1335.278276	28
Salt Pan	92.72056748	2
Settlement Area	1306.413854	28
Shrub	1501.456695	32
Water Bodies	8.326142074	0
Grand Total	4721.013349	100



5.2 Accuracy Assessment Table-2020:

	Water Bodies	Shrub Area	Cultivated Land	Settlement Area	Barren	Salt Pan	User
Water Bodies	16	0	0	0	0	0	16
Shrubs Area	0	21	1	0	3	0	25
Cultivate Area	0	2	19	0	1	0	22
Settlement Area	0	1	3	21	2	0	27
Barren and Uncultivated Land		2	1		17		20
Salt Pan	0	0	0	0	0	23	23
Producers	16	26	24	21	23	23	133

5.3 Overall Accuracy:

Overall Accuracy = (Total Number of Correctly Classified Pixels (Diagonal)) / (Total Number of Reference Pixels) $\times 100$

$$= 16 + 21 + 19 + 21 + 17 + 23 = 117$$

$$= 117 / 133 \times 100 = 87.96 \%$$

5.4 User Accuracy:

Users Accuracy = (Number of Correctly Classified Pixels in each Category) / (Total number of Classified Pixels in that Category (The Row Total)) $\times 100$

$$\text{Water Bodies} = 16 / 16 \times 100 = 100 \%$$

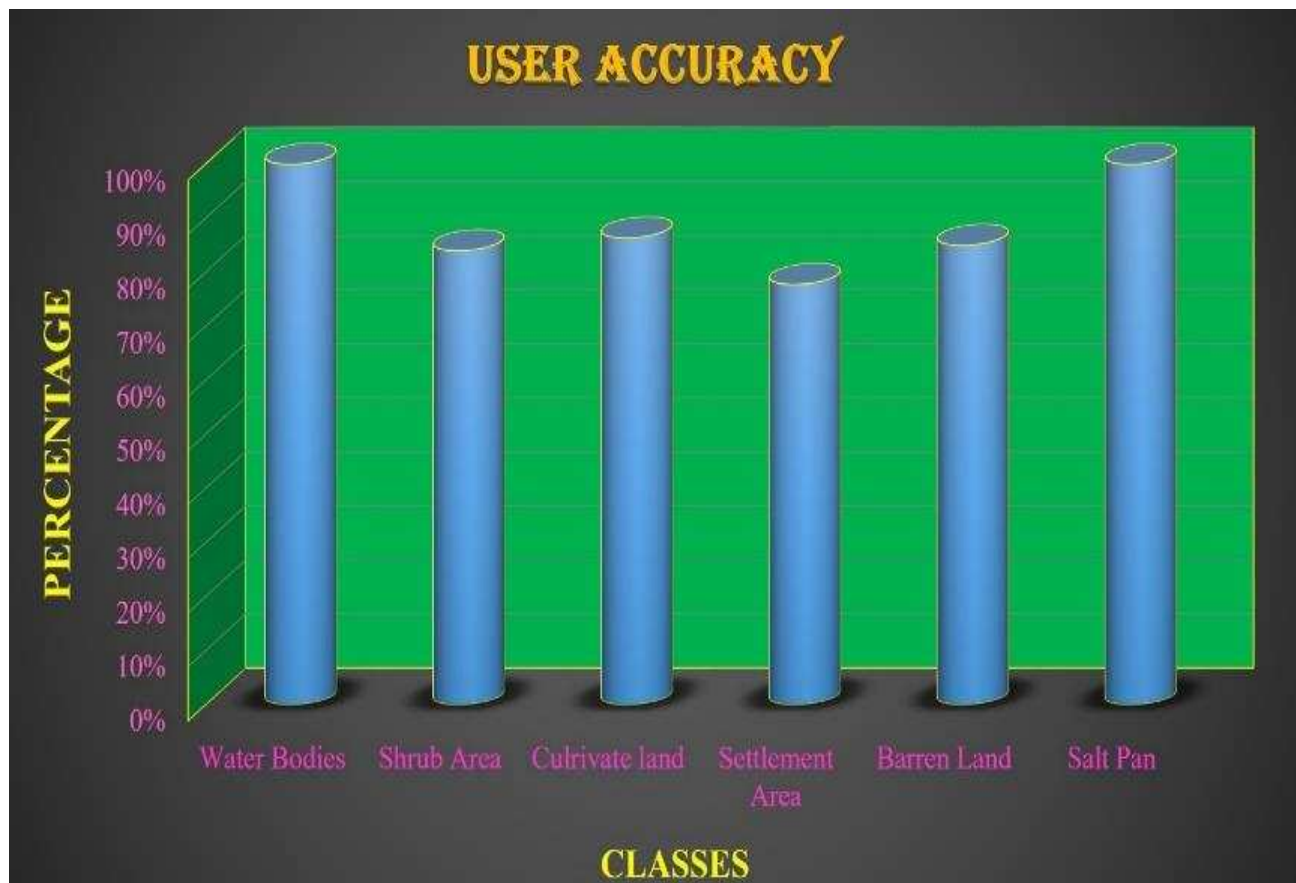
$$\text{Shrub Area} = 21 / 25 \times 100 = 84 \%$$

$$\text{Cultivated Land} = 19 / 22 \times 100 = 86.36 \%$$

$$\text{Settlement Area} = 21 / 27 \times 100 = 77.77 \%$$

$$\text{Barren \& Uncultivated Land} = 17 / 20 \times 100 = 85 \%$$

$$\text{Salt Pan} = 23 / 23 \times 100 = 100 \%$$



5.5 Producer Accuracy:

Producer Accuracy=(Number of Correctly Classified Pixels in each Category)/(Total Number of Reference Pixels in that Category (The Column Total)) \times 100

Water Bodies = $16/16 \times 100 = 100\%$

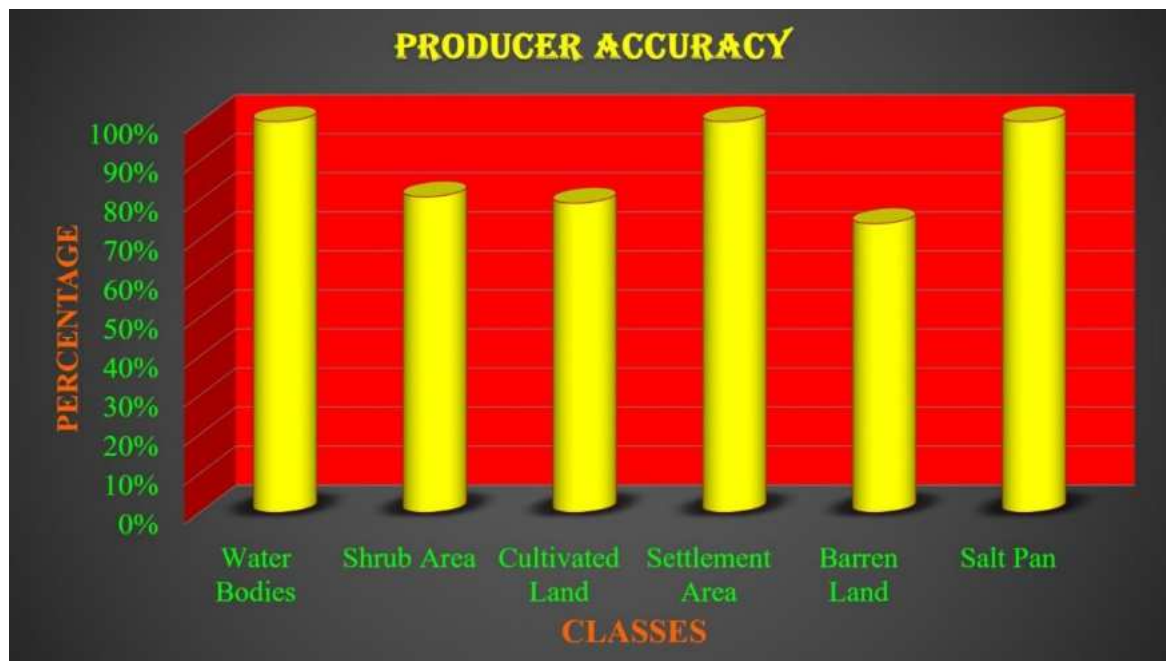
Shrub Area = $21/26 \times 100 = 80.76\%$

Cultivated Land = $19/24 \times 100 = 79.16\%$

Settlement Area = $21/21 \times 100 = 100\%$

Barren & Uncultivated Land = $17/23 \times 100 = 73.91\%$

Salt Pan = $23/23 \times 100 = 100\%$



5.6 Kappa Coefficient:

Kappa Coefficient (T) = $\frac{(TS \times TCS) - \sum (\text{Column Total} \times \text{Row Total})}{(TS^2 - \sum (\text{Column Total} \times \text{Row Total}))} \times 100$

$$= \frac{(117 \times 133) - ((19 \times 16) + (25 \times 26) + (22 \times 24) + (27 \times 21) + (20 \times 23) + (23 \times 23))}{(117^2 - ((19 \times 16) + (25 \times 26) + (22 \times 24) + (27 \times 21) + (20 \times 23) + (23 \times 23))} \times 100$$

$$= \frac{15561 - 3038}{17689 - 3038}$$

$$= \frac{12523}{14651}$$

$$= 0.84 \%$$

Thus the total Kappa statistics chance result of classification of 0.84 measured values obtained in this application it can be considered as 84 % better.

6. Conclusion:

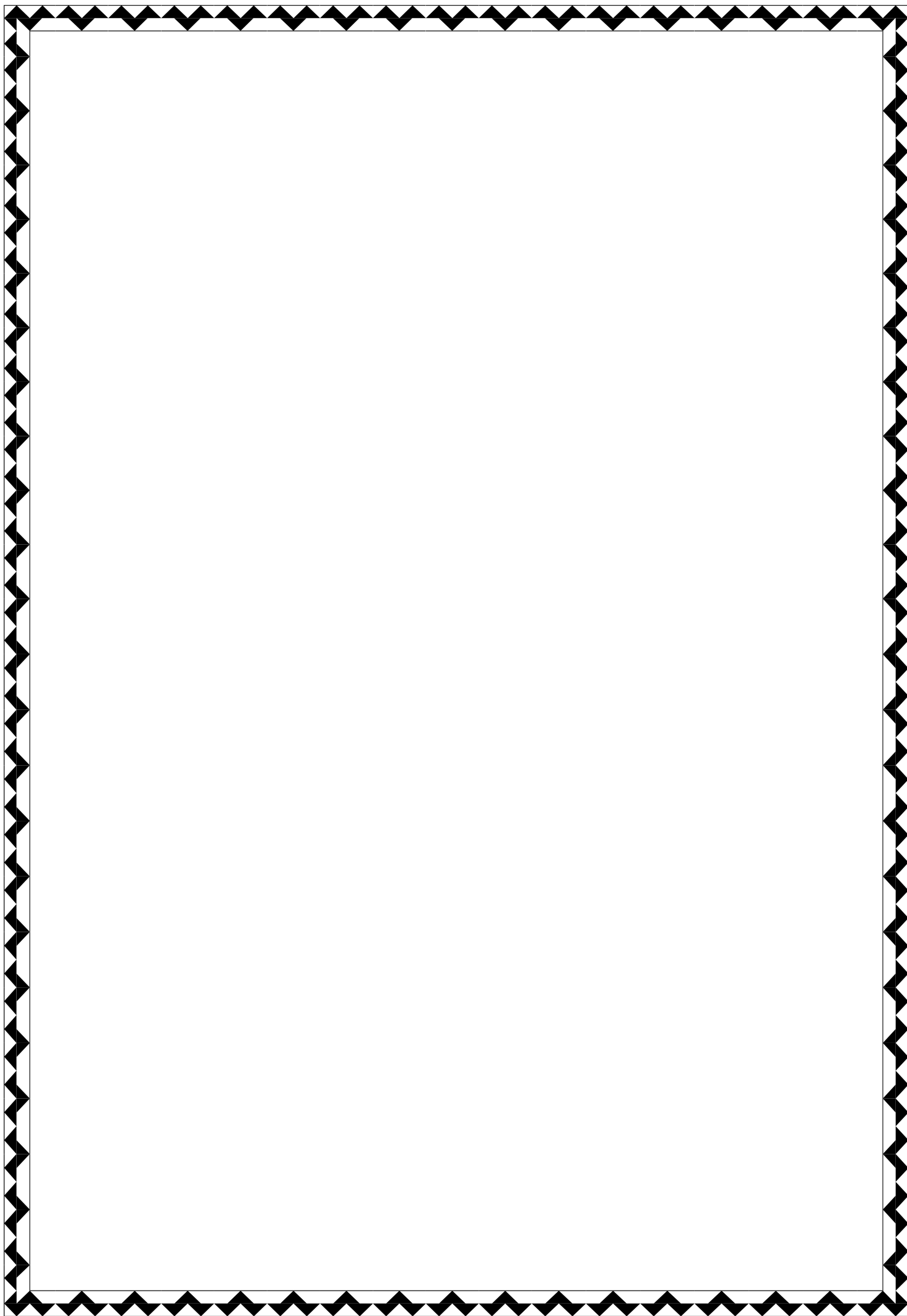
Remote Sensing and GIS techniques are a powerful tool for mapping and evaluating the classification of lands. We classified various lands of Thoothukudi such as cultivate land, barren, saltpan, settelement, water bodies and shrubs using Land Sat-8 images from bhuvan ISRO. This study classify Land Use and Land Cover area of Thoothukudi using Image Classification through ILWIS 3.3 software and ArcGIS 10.8 software. This map clearly shows that Thoothukudi land forms increased in cultivatable land, salt pan and shrubs, Water bodies are decreased. This study warrants proper urban planning for Thoothukudi for sustainable use of resource and environment. So, based on these results, the city could be categorized as one of the fastest growing city in spatial and temporal

terms. As a result, an integrated estimation of land use and land cover change mapping and spatial and temporal modelling works should be done in regular prise. The study has to integrate remote sensing and GIS to deal with urban growth and expanding impermeable surfaces. This study may help the Government to increase the Vegetation and Industrialization in Thoothukudi.

7. Reference:

1. C. P. Lo, D. A. Quattrochi & J. C. Luvall (2010), "Application of high-resolution thermal infrared remote sensing and GIS to assess the urban heat island effect", E-Journal.
2. Gerrit Huunemna and Lucas Broekema (2020), "Classification of multi-sensor data using a combination of image analysis techniques", International Journal of Aerospace Survey and Earth Sciences.
3. Abhilash Perisetty, Sai Teja Bodempudi and others (2020), "Classification of Hyperspectral Images using Edge Preserving Filter and Nonlinear Support Vector Machine (SVM)", Journal of computer and geographical science.
4. Dylan & S. Davis (2020), "Geographic Disparity in Machine Intelligence Approaches for Archaeological Remote Sensing Research", Journal of Remote sensing.
5. S. Meivel & S. Maheswari (2020), "Optimization of Agricultural Smart System using Remote Sensible NDVI and NIR Thermal Image Analysis Techniques", Remote Sensing of UA.
6. Ying Li, Haokui Zhang and the others (2018), "Deep Learning for Remote Sensing Image Classification", International Journal of Remote Sensing.
7. Mercedes E. Paoletti, Juan H. and the others (2018), "Deep and Dense convolutional Neural Network for hyper spectral image classification", International Journal of Physics.
8. Amina Ben Hamida, Alexandre Benoit and others (2018), "3-D deep learning research for remote sensing image classification", International of Remote sensing.
9. Xin Pan and Jian Zhao (2018), "High-Resolution Remote Sensing Image Classification Method", International journal of Remote Sensing.
10. Mario Benincasa, Federico Falcini, Claudia Adduce, Rosalia Santoleri (Nov 2019), "Synergy of satellite remote sensing and numerical ocean modelling for coastal geomorphology diagnosis", CNR ISMAR Institute of Marine sciences, Italy.
11. Ajay Singh (May 2019), "Remote Sensing and GIS Applications for municipal waste management", Indian Institute of Technology, Kharagpur.

12. N Usali, MH Ismail (2010), "Use of remote sensing and GIS in monitoring water quality", *Journal of Sustainable Development*.
13. Han Liu, Lin He, Jun Li (2017), "Remote sensing image classification based on convolutional neural networks", *Journal of Remote Sensing*.
14. Shaohua Gao, Yunqiang Zhu & Chenyan Ma (2019), "A survey of remote sensing image classification based on CNNs", *E Journal*.
15. B. Yang, Z. J. Liu, Y. Xing, and C. F. Luo (2017), "Remote sensing image classification based on improved BP neural network", *E Journal*.
16. L. Gómez-Chova and others (2010), "Urban monitoring using multitemporal SAR and multispectral data", *Journal of Remote Sensing*.
17. D. Tuia, N. Courty and R. Flamary (2012), "Multiclass feature learning for hyperspectral image classification", *Journal of Remote Sensing*.
18. Casey Cleve (2008), "Classification of the wildland-urban interface", *Journal of Remote Sensing*.
19. Adrian Werner, Christopher D Storie (2014), "Evaluating SAR-Optical Image Fusions for Urban LULC Classification in Vancouver Canada", *Canadian Journal of Remote Sensing*.
20. Shi Liang Zhang, Ting Cheng Chan, (2016), "A Study of Image Classification of Remote Sensing Based on Back-Propagation Neural Network with Extended Delta Bar Delta", *Journal of Mathematical Problems in remote sensing*.
21. Mahyat Shafapour Tehrani, Biswajeet Pradhan (2013), "A comparative assessment between object and pixel-based classification approaches for land use/land cover mapping using SPOT 5 imagery", *Journal of Geocarto International*.
22. Savita P. Sabale, Chhaya R. Jadhav (2015), "Hyperspectral Image Classification methods in remote sensing", *Journal of Remote Sensing*.
23. Wenjuan Yu (2016), "A new approach for land cover classification and change analysis", *Journal of Remote Sensing*.
24. Brian A. Johnson (2016), "Integrating OpenStreetMap crowdsourced data and Landsat time-series imagery for rapid land use/land cover (LULC) mapping", *Journal of Applied Geography*.
25. Sophia S. Rwanga (2017), "Accuracy Assessment of Land Use/Land Cover Classification Using Remote Sensing and GIS", *Journal of Geosciences*.



STRUCTURAL AND OPTICAL CHARACTERIZATION OF CUPROUS OXIDE NANOPARTICLES

Project work submitted to **St. Mary's College (Autonomous), Thoothukudi**,
affiliated to Manonmaniam Sundaranar University, Tirunelveli in partial
fulfillment of the requirement for the award of the

BACHELOR'S DEGREE IN PHYSICS

BY

C. ANTONY CLERISHA DEMEL -18AUPH05

A. GNANA BRINTHA -18AUPH18

M. MOHAMED SHIFANA -18AUPH30

G. MYSTICA GOMEZ -18AUPH32

J. SNEHA -18AUPH41

P. TERANCY -18AUPH46

GUIDE AND SUPERVISOR

Mrs. P . DHANALAKSHMI, M.Sc., B.Ed., SET.,



DEPARTMENT OF PHYSICS

ST. MARY'S COLLEGE (AUTONOMOUS)

(Re-Accredited with 'A+' grade by NAAC-5th Cycle)

2020-2021

THOOTHUKUDI-628001

CERTIFICATE

This is to certify that the project work entitled, "STRUCTURAL AND OPTICAL CHARACTERIZATION OF CUPROUS OXIDE NANOPARTICLES" is submitted to ST. MARY'S COLLEGE (AUTONOMOUS), THOOTHUKUDI in partial fulfillment for the award of Bachelor's Degree in Physics and it is a record work done during the year 2020-2021 by the following students,

C. ANTONY CLERISHA DEMEL	-18AUPH05
A. GNANA BRINTHA	-18AUPH18
M. MOHAMED SHIFANA	-18AUPH30
G. MYSTICA GOMEZ	-18AUPH32
J. SNEHA	-18AUPH41
P. TERANCY	-18AUPH46

Dhanalakshmi P
GUIDE

Ressie J do
HEAD OF THE DEPARTMENT
HEAD

Department of Physics,
St. Mary's College (Autonomous),
Thoothukudi - 628 001.

S. Eusebia Annamalai
EXAMINER 5/4/21

Lucia Rose
PRINCIPAL
St. Mary's College (Autonomous)
Thoothukudi - 628 001.

ACKNOWLEDGEMENT

First and foremost, We ascribe all praise and thanks to the Lord Almighty for guiding us to complete our project work successfully.

We express our deepest sense of gratitude to our Respected Principal, Dr.Sr.A.S.J.Lucia Rose, M.SC., M.Phil., Ph.D., PGDCA., St. Mary's College (Autonomous), Thoothukudi for providing a wonderful opportunity to execute this project work.

We wish to record our hearty and sincere thanks to Dr.Sr.Jessie Fernando, M.Sc.,M.Phil.,Ph.D Head of the Department of Physics, for her encouragement and support to perform this project.

We are grateful to our guide Mrs.P.Dhanalakshmi, M.Sc., B.Ed., SET., for her useful ideas and guidance in bringing out this project successfully.

We sincerely acknowledge the financial assistance funded by the DBT, New Delhi for the successful completion of the project work.

We would like to extend our gratitude to the Department of Physics, Manonmaniam Sundaranar University, Tirunelveli and Department of Chemistry, V.O.C. College, Thoothukudi for their timely help in completing our project.

We wish to extend our sincere gratitude to our non-teaching staff for their cooperation and assistance. We would also like to thank our parents and friends for their constant support and encouragement throughout the project.

CHAPTER	CONTENTS	PAGE NO
I	INTRODUCTION	1
1.1	Background	2
1.2	Cornerstone	2
1.3	Domain areas of Nanotechnology	3
1.4	The future of Nanotechnology	5
1.5	Cuprous Oxide	5
1.6	Structure of Cuprous Oxide	6
1.7	Aim and scope of the thesis (Cu₂O)	7
1.8	Antimicrobial potential of Cu₂O	7
1.9	Literature Review	7
1.10	Properties	11
1.11	Applications of Cuprous Oxide	11
1.12	Objectives	12
II	EXPERIMENT	13
2.1	Synthesis of Nanoparticles	14
2.2	Chemical Precipitation Method	15
2.3	Preparation of Cu₂O nanoparticles	16

2.4	Flowchart	18
III	MATERIALS AND METHODS	19
3.1	Chemicals	20
3.2	Experimental Section	20
3.3	Characterization Techniques	21
3.4	X-ray Diffraction	21
3.5	Optical Absorbance	22
3.6	FTIR spectroscopy	23
IV	RESULTS AND DISCUSSION	25
4.1	Structural Characterization	26
4.2	Optical Characterization	27
V	CONCLUSION	29
5.1	Summary	30
5.2	References	31

CHAPTER I

CHAPTER I

INTRODUCTION

1.1 Background

The field of nanotechnology is one of the most active research areas in modern material science. Nanoparticles exhibit new or improved properties based on specific characteristics such as size, distribution and morphology. There have been impressive developments in the field of nanotechnology in the recent past years, with numerous methodologies developed to synthesize nanoparticles of particular shape and size depending on specific requirements. New applications of nanoparticles and nanomaterials are increasing rapidly. Nanotechnology can be termed as the synthesis, characterization, exploration and application of nanosized (1-100nm) materials for the development of science. It deals with the materials whose structures exhibit significantly novel and improved physical, chemical and biological properties, phenomena and functionality due to their nano scaled size. Because of their size, nanoparticles have a larger surface area than macro-sized materials. The intrinsic properties of metal nanoparticles are mainly determined by size, shape, composition, crystallinity and morphology. Nanoparticles, because of their small size, have distinct properties compared to the bulk form of the same material, thus offering many new developments in the fields of biosensors, biomedicine, and bio nanotechnology. Nanotechnology is also being utilized in medicine for therapeutic drug delivery and for the development of treatments for many diseases and disorders. Nanotechnology is an enormously powerful technology, which holds a huge promise for the design and development of many types of novel products with its potential and medical applications on early disease detection, treatment and prevention.

1.2 Cornerstone

Nanotechnology is the manipulation of matter at a molecular or atomic level which produces novel materials and devices with new extraordinary properties. However, nanotechnology is not a new discipline. It is rather the merging of multiple scientific

disciplines (Biology, Physics, Chemistry, Medicine and Engineering) and the combination of knowledge to tailor materials at the nanoscale. Nanotechnology is closely related to Nanoscience, the basic theoretical and experimental study of matter at the nanoscale before applying the acquired knowledge for device manufacturing. But the question is why nanotechnology is so innovative and revolutionary? The answer lies in quantum mechanics. The behaviour of matter changes significantly when the surface area to volume ratio increases so dramatically. Classical physics no longer control the behaviour of the material which is now under the control of quantum laws. This fact gives the nano-structured material new abilities and properties that may be more favourable than the ones of the bulk material version. A good example is that some polymers, although being insulators in the bulk form, they become semiconductors at the nanoscale.

1.3 Domain areas of Nanotechnology

Energy: Nanotechnology can improve the existing technology of fuel cells in order to increase their life cycle and reduce the cost of catalysts. Solar cells will also increase their energy conversion efficiency by reducing cost. The production of fuel could also become more effective by making extraction and processing more economical.

Medicine: Nanoparticles can be developed in order to deliver drugs to diseased cells. New bio-compatible materials are produced that can be used to make medical implants. Stents are also developed to prevent artery blockage.



Fig 1.1 DNA Manipulation using nanotechnology

Industry: Vehicle manufacturers can use the new light and extremely strong materials (eg. carbon nanotubes) to build faster and safer cars. The same technology applies in aerospace as well. The textile industry can benefit from the development of nanofibers. Clothing made of nanofibers is stain-repellent and can be washed at very low temperature. Another great application has to do with the embedded wearable electronics. Nanotechnology could also revolutionize the food industry by improving the conservation, processing, and packaging procedures. Other applications include bacteria identification and nanoencapsulation of bioactive food compounds in order to keep them in a safe anti-microbial environment.

Communication and Electronics: The advances in nanotechnology will reduce the weight and power consumption of electronic devices. Data processing speed will increase, and new portable devices will be available soon. This will revolutionize the world of communication and data transfer.

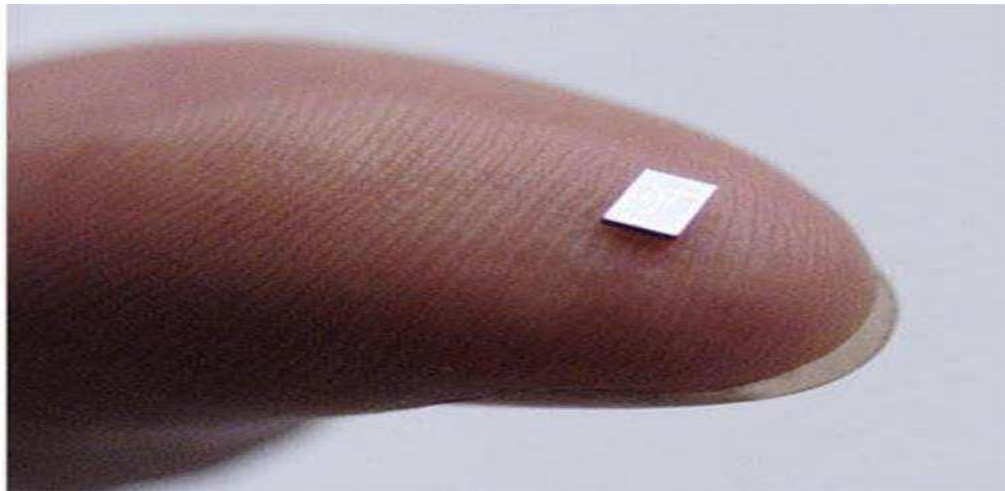


Fig 1.2 Light weight micro chips using nanotechnology

Consumer Goods: Other goods of every-day use that could be developed include anti-reflective sunglasses, new generation cosmetics, easy-to-use ceramics and glasses, etc.

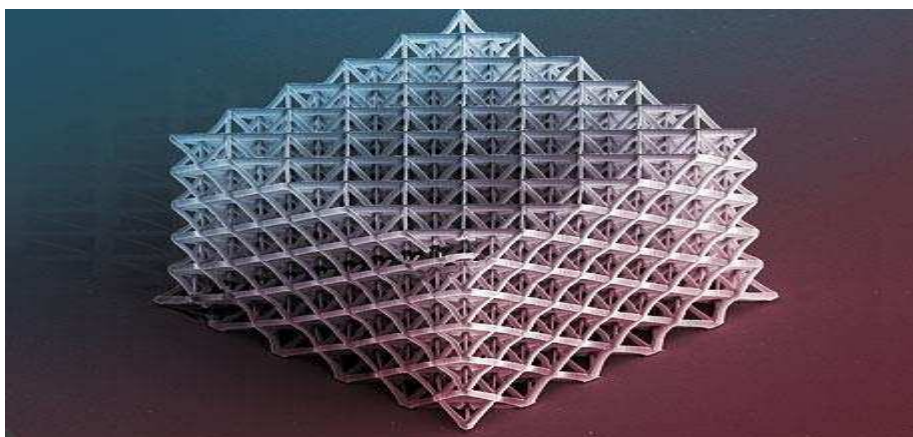


Fig 1.3 Feather Weight Nano-Ceramics

1.4 The future of Nanotechnology

Nanotechnology is often referred to as "the future technology" that can solve many problems. Some even talk about a nanotechnology revolution. Nanotechnology definitely brings tremendous benefits and potential, but the fact that even the youngest technology has its dangers, and much less explored, should be well known to everyone. It is claimed that environmental problems such as pollution and climate change could also be solved. However, there are also negative properties that nanotechnology entails. For example, the development of usable nanoparticles requires enormous energy and water consumption as well as the use of toxic solvents and chemicals. In addition, the use of nano packaging promotes longer shelf life of food, which in turn means that the food continues to be transported over long distances. Everyone knows that global transport is a major environmental burden. For humans, dangers arise when such nano-pesticides are ingested via food, as research cannot yet foresee how the human body absorbs and degrades these substances.

1.5 Cuprous Oxide

Copper(I) oxide or cuprous oxide is the inorganic compound with the formula Cu_2O . It is one of the principal oxides of copper, the other being copper (II) oxide or cupric oxide (CuO). This red-coloured solid is a component of some antifouling paints. The compound can appear either yellow or red, depending on the size of the particles. Copper(I) oxide is found as the reddish mineral cuprite.

- Molecular formula: Cu_2O
- Molar mass: 143.091
- Appearance: Copper(I) oxide, 99.9% (metals basis); Copper(I) oxide, 97% (Cu + Cu_2O Assay); red-brown powder
- Melting point: 1232 °C
- Boiling point: 1800 °C
- Net Charge : 0
- Monoisotopic Mass: 141.85411

1.6 Structure of Cuprous Oxide

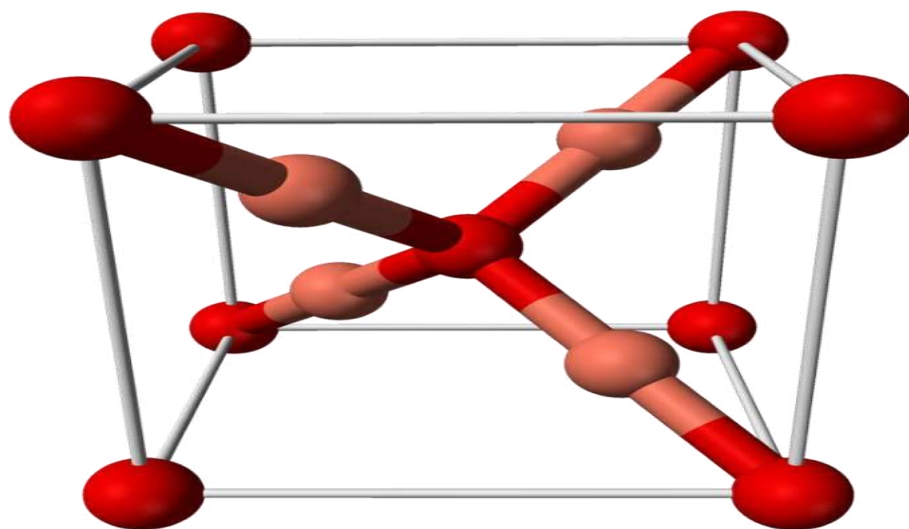


Fig 1.4 Structure of Cuprous Oxide

<u>Structure</u>	
<u>Crystal structure</u>	<u>cubic</u>
<u>Space group</u>	<u>Pn3m, #224</u>
<u>Lattice constant</u>	<u>$a = 4.2696$</u>

1.7 Aim and scope of the thesis (Cu₂O)

This thesis will focus on strategies for synthesizing, characterizing and applications of cuprous oxide nanoparticles with morphology and size control. There are five main chapters in this thesis. A brief introduction has been given in chapter 1. In chapter 2, literature review related to cuprous oxide is demonstrated, in which the synthesis approaches, growth mechanisms and applications are introduced. Chapter 3-4 are going to emphasize on the research work and results on cuprous oxide nanoparticles. Finally, the conclusion is summarized in the last chapter 5.

1.8 Antimicrobial potential of Cu₂O

The fast emergence of antibiotic and antifungal resistant bacteria and fungi is occurring on a world scale. The overuse and misuse of these medications, as well as a lack of new antibacterial and antimycotic materials have been the cause of this antibiotic and antifungal resistance crisis. The most notable of the diseases present in the oral cavity in humans is a common fungal infection known as oral candidiasis. This is an opportunistic infection which may reflect immunological changes and a possible association with potentially malignant disorders of the oral mucosa. *Candida* species, like *C. tropicalis*, *C. krusei* and *C. parapsilosis* have increased significantly the number of infections in the last decade, especially *C. tropicalis* which is has become the most common non-albicans *Candida* species in Asia. The use of nanotechnology is a viable prospective that can be employed in order to address this issue effectively.

Copper I oxide nanoparticles (Cu₂O NPs) stand out by possessing very well-known antibacterial properties, being active against a varied range of pathogenic bacteria. The administration of Cu₂ONPs as an antimicrobial treatment needs a vehicle, being the polymer films the most widely used materials in this area. The integration of metal oxide nanoparticles improves its antimicrobial as well as its physical, chemical and mechanical properties.

1.9 Literature Review

[1] Hui Wang and Hong-Yuan Chen(2002), successfully prepared Cu₂O nanoparticles using microwave irradiation method. Cu₂O nanoparticles with an average size of ca.4 nm were prepared using copper (I) acetate and sodium hydroxide as starting materials

and ethanol as the solvent. The prepared Cu₂O nanoparticles had regular shape, narrow size distribution and high purity.

[2] Suresh Sahadevan ,Kaushik Pal and Zaira Zaman Chowdhury(2017),synthesised Cu₂O nanoparticles using chemical precipitation method. The grain size was determined using XRD investigations. The SAED pattern was determined for Cu₂O nanoparticles and its polycrystalline nature was confirmed.

[3] V.D.Rajput and A.Fedorenko (2018), determined the effects of Cu₂O nanoparticles on crop plants. This article clearly denoted the toxic effects of Cu₂O nanoparticles on cultivated crop plants by inhibiting seed germination, decreases in the shoot and root length, reduction in photosynthesis and respiration rate as well as enzymatic changes.

[4] Amin Asadi and Loke Kok Foong(2020),characterised the stability and dynamic viscosity of Cu₂O water hybrid nanofluids. The chemical, atomic, surface structures of the Cu₂O nanoparticles were examined using X-Ray diffraction. The final results of dynamic viscosity measurements indicated the solid concentration of 1vol% and the temperature of 25°C.

[5] Ali Nazari and Shadi Riahi (2011) determined the effects of Cu₂O nanoparticles on compressive strength of self-compacting concrete. Cu₂O nanoparticles with an average particle size of 15 nm were added to self-compacting concrete and various properties of the specimens were measured. The results indicate that Cu₂O nanoparticles are able to improve the compressive strength of self-compacting concrete and reverse the negative effects of superplasticizer on compressive strength of the specimens.

[6] Paniz Esfandfar and Aliakbar Saboury (2015) made a spectroscopic study on interaction between Cu₂O nanoparticles and bovine serum albumin. The zeta potential value for BSA and Cu₂O nanoparticles with average diameter of around 50 nm at concentration of 10 µM in the deionized (DI) water were -5.8 and -22.5 mV, respectively. Circular dichroism studies did not show any changes in the content of secondary structure of the protein after Cu₂O nanoparticles interaction. This study provides important insight into the interaction of Cu₂O nanoparticles with proteins, which may be of importance for further application of these nanoparticles in biomedical application.

[7] Fang wang and Heng deng (2016) synthesized Cu_2O via sol-gel method. In this paper, Cu_2O nanoparticles were synthesized *via* a sol-gel method and their corresponding gas sensor was achieved simultaneously. Cu_2O nanoparticle samples were characterized by X-ray diffraction, Raman spectroscopy, X-ray photoelectron spectroscopy and field emission scanning electron microscopy, respectively. The results show that the sample we have synthesized was Cu_2O and the morphology of the sample was nanoparticles with an average diameter of ~ 100 nm.

[8] Zhigang Zang and Jiro Temmyo (2013) synthesized cuprous oxide films by radical oxidation at low temperature for PV application. Cuprous oxide (Cu_2O) films synthesis by radical oxidation with nitrogen (N_2) plasma treatment and different RF power at low temperature (500°C) are studied in this paper. X-ray diffraction measurements show that synthesized Cu_2O thin films grow on c-sapphire substrate with preferred (111) orientation. With nitrogen (N_2) plasma treatment, the optical bandgap energy is increased from 1.69 to 2.42 eV, when N_2 plasma treatment time is increased from 0 min to 40 min. Although the hole density is increased from 10^{14} to 10^{15} cm^{-3} and the resistivity is decreased from 1879 to $780 \Omega\text{cm}$ after N_2 plasma treatment, the performance of Cu_2O films is poorer compared to that of Cu_2O using RF power of 0. The fabricated $\text{ZnO}/\text{Cu}_2\text{O}$ solar cells based on Cu_2O films with RF power of 0 W show a good rectifying behavior with a efficiency of 0.02%, an open-circuit voltage of 0.1 V, and a fill factor of 24%.

[9] Ye feng wang and jing hui zeng (2008) determined the hydrothermal synthesis of cuprous oxide microcrystals with controlled morphology. Cuprous oxide (Cu_2O) with controlled morphology was synthesized via a hydrothermal method by reducing copper nitrate with formic acid. Reactant concentration, reaction temperature, and time show strong effects on the phase formation and morphology of the products. The products were characterized by X-ray powder diffraction (XRD), scanning electron microscope (SEM), and UV-vis diffuse reflectance spectroscopy. The possible crystal growth processes have been proposed. The band gap versus different morphology was also studied.

[10] HuamingYanga and JingOuyanga(2006) electrochemically synthesized the property of cuprous oxide nanoparticles. Cuprous oxide (Cu_2O) nanoparticles of 35 nm in crystal size have been successfully synthesized via electrochemical method in alkali

NaCl solutions with copper as electrodes and $\text{K}_2\text{Cr}_2\text{O}_7$ as additive. Photocatalytic degradation of methyl orange in aqueous Cu_2O solution was investigated under either ultraviolet (UV) light or sunlight. X-ray diffraction (XRD), transmission electron microscopy (TEM), Fourier transformation infrared spectroscopy (FT-IR), ultraviolet–visible spectroscopy (UV–vis) and X-ray photoelectron spectroscopy (XPS) were introduced to characterize the samples. The results indicate that electric current shows no obvious effect on the growth of Cu_2O nanocrystals and that 97% of MeO can be decolorized under UV irradiation for 2 h or under sunlight for 3 h when amount of Cu_2O is 2 g/L. Recycling use of the catalyst revealed that Cu_2O still has a high photocatalytic efficiency when repeatedly used for four times. Cu_2O nanoparticles still kept its cubic crystal phase, but fractionally oxidized to be Cu_2O after the photocatalysis. Compared with the original Cu_2O nanoparticles, there has 1 eV shift of Cu 2p electron and 1.6 eV shift of Cu Auger signals for the Cu_2O powders after four times photocatalysis. Some new peaks can also be observed at 401.1, 237.4 and 170.2 eV in the Cu_2O powders after photocatalysis.

[11] FenXu and Xiaohui (2003) synthesized shape controlled sub-micro cuprous oxide octahedra. Monodisperse submicro-sized cuprous oxide (Cu_2O) octahedra are successfully prepared in large quantities assisted by the capping reagent poly(vinyl pyrrolidone) (PVP-K30, MW=58 000) and the formation mechanism of Cu_2O octahedra is analysed.

[12] KOUTI. Mand MATOURI L. (2010) determined the fabrication of nanosized cuprous oxide using feshling's solution. This paper describes a facile method for the synthesis of Cu_2O nanoparticles by reduction of Fehling's solution, using glucose as reducing agent. Copper sulphate is used as a precursor with potassium sodium tartarate in an alkaline media to produce Fehling's solution. The precipitation of Cu_2O nanoparticles from this solution in the presence of glucose was controlled by addition of SLES or Triton-X 100 as surfactants. The reactions have been carried out at 60°C with high repeatability. The purification process of the Cu_2O product does not require expensive methods, since a solid product is obtained from a reaction in liquid phase. The resulting Cu_2O nanoparticles were characterized by X-Ray Diffraction (XRD), Scanning Electron Microscopy (SEM), Energy-Dispersive X-ray

spectroscopy(EDX),Transmission Electron Microscopy (TEM) and Fourier-transform infrared (FTIR) spectroscopy.

1.10 Properties

The solid is diamagnetic. In terms of their coordination spheres, copper centres are coordinated and the oxides are tetrahedral. The structure thus resembles in some sense the main polymorphs of SiO_2 , and both structures feature interpenetrated lattices. Copper(I) oxide dissolves in concentrated ammonia solution to form the colourless complex $[\text{Cu}(\text{NH}_3)_2]^+$, which is easily oxidized in air to the blue $[\text{Cu}(\text{NH}_3)_4(\text{H}_2\text{O})_2]^{2+}$. It dissolves in hydrochloric acid to give solutions of CuCl_2 . Dilute sulfuric acid and nitric acid produce copper(II) sulphate and copper(II) nitrate, respectively. Cu_2O degrades to copper(II) oxide in moist air.

1.10.1 Semiconducting Properties: The lowest excitons in Cu_2O are extremely long lived; absorption line shapes have been demonstrated with neV linewidths, which is the narrowest bulk exciton resonance ever observed. The associated quadrupole polaritons have low group velocity approaching the speed of sound. Thus, light moves almost as slowly as sound in this medium, which results in high polariton densities. Another unusual feature of the ground state excitons is that all primary scattering mechanisms are known quantitatively. Cu_2O was the first substance where an entirely parameter-free model of absorption linewidth broadening by temperature could be established, allowing the corresponding absorption coefficient to be deduced. It can be shown using Cu_2O that the Kramers–Kronig relations do not apply to polaritons.

1.11 Applications of Cuprous Oxide

Cuprous oxide is commonly used as

1. pigments,
2. fungicides,
3. antifouling agents for marine paints.

Rectifier diodes based on this material have been used industrially as early as 1924, long before silicon became the standard. Copper(I) oxide is also responsible for the pink colour in a positive Benedict's test.

1.12 Objectives

- ✓ To give an overview of the preparation of Cu_2O Nanoparticles.
- ✓ To synthesize pure cuprous oxide nanoparticles by chemical precipitation method.
- ✓ To realise the potential applications at nanoscale.
- ✓ To review on some unique properties and applications of Cu_2O nanostructures.
- ✓ To provide a critical discussion of the synthesis of Cu_2O nanostructures.
- ✓ To provide evidence for the cubic structure of cuprous oxide nanoparticles using XRD studies.
- ✓ To obtain the peak using FTIR spectrum to confirm the presence of Cu(I)-O bond.
- ✓ To estimate the UV absorption onset for cuprous oxide nanoparticles.

CHAPTER II

Chapter II

Experiment

2.1 Synthesis of Nanoparticles

Several methods have been used and developed to synthesize crystalline oxide powders in nanoscale dimensions. These methods are broadly classified into two ways:

- (i) Top down approaches
- (ii) Bottom up approaches

2.1.1 Top down approach

In this approach, the bulk materials are broken down into nanosized particles.

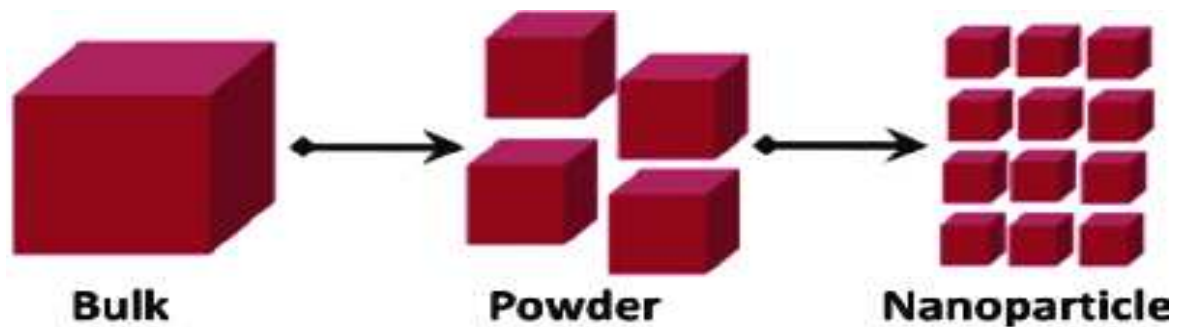


Fig 2.1 Top down approach

These approaches include methods like

- Ball milling method
- Mechanical grinding
- Chemical etching
- Thermal/Laser ablation
- Electro-explosion

2.1.2 Bottom up approach

In this approach, nanomaterials are produced by building atom by atom.

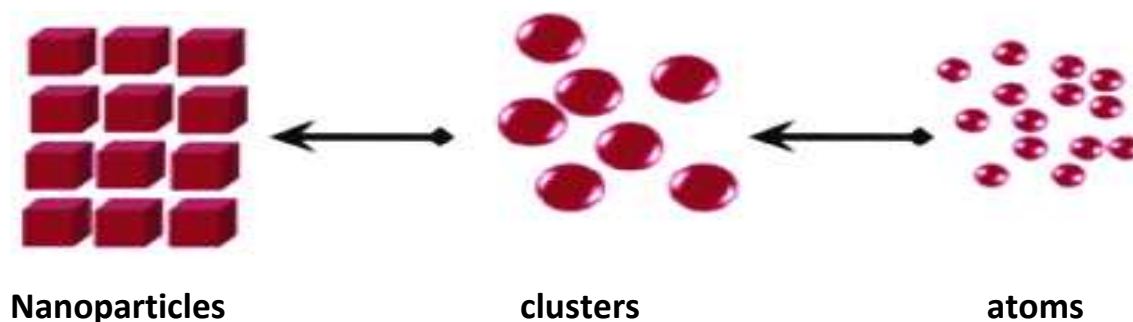


Fig 2.2 Bottom up approach

These approaches include methods like:

- Chemical precipitation method
- Sol-gel method
- Vapour deposition method
- Spray pyrolysis
- Aerosol process
- Bio-reduction method
- Electrochemical precipitation method

In many of these methods, the main objective is to reduce the cost of chemical synthesis and to produce materials for technological applications. We have synthesized Cu_2O nanoparticles by chemical precipitation process which is a simple cost-effective method since the starting materials are few and inexpensive.

2.2 Chemical Precipitation Method

In precipitation method, the ionic metals are converted to an insoluble form (particle) by the chemical reaction between the soluble metal compounds and the precipitating reagent. The particles formed by this reaction are removed from the solution by settling and filtration.

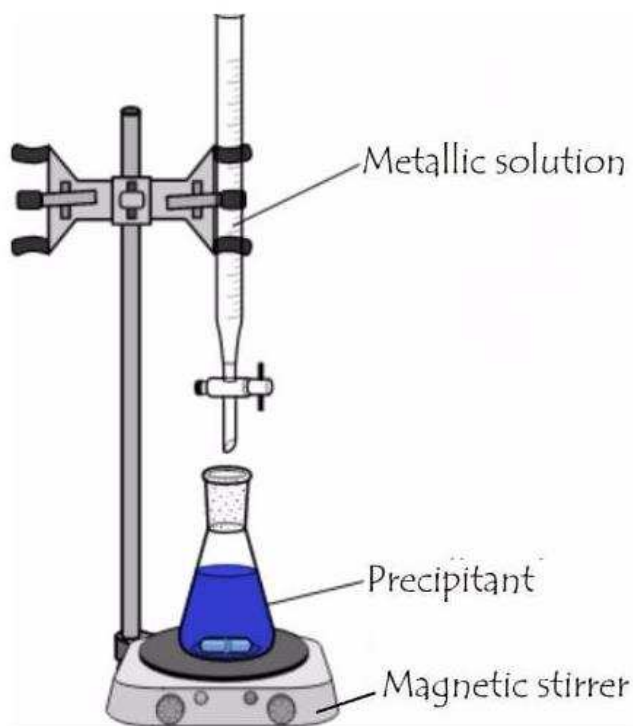


Fig 2.3 Experimental setup of Chemical precipitation method

The unit operations typically required in this technology include neutralization, precipitation, coagulation/flocculation, solids/liquid separation, and dewatering. The effectiveness of a chemical precipitation process is dependent on several factors including the type and concentration of ionic metals present in solution, the precipitant used, the reaction conditions (especially the pH of the solution), and the presence of other constituents that may inhibit the precipitation reaction. The most widely used chemical precipitation process is hydroxide precipitation, in which metal hydroxides are formed by using Calcium hydroxide or Sodium hydroxide as the precipitant.

2.3 Preparation of Cuprous Oxide Nanoparticles

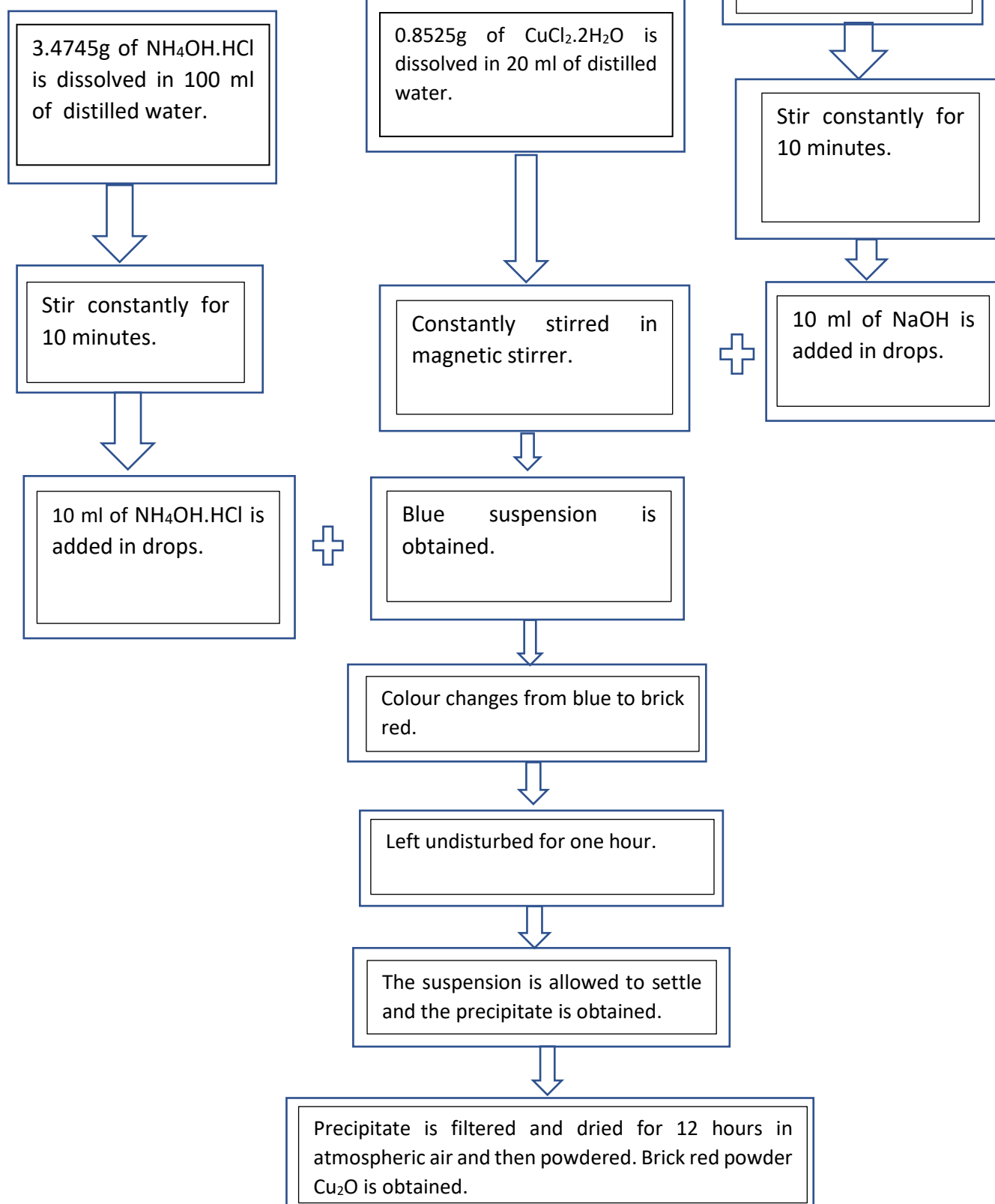
The experiment was done with 0.8525g of cupric chloride dihydrate along with 4g of NaOH and 3.4745g of hydroxyl amine hydrochloride. Each of the substances were dissolved separately in distilled water and solutions of 200ml separately and 20ml separately were prepared. NaOH solution was taken in a burette and was allowed to drip into the cupric chloride dihydrate solution that was at constant stirring. On

completion of the dripping process, the solution mixture NAOH and cupric chloride dihydrate was kept at constant stirring for 15 minutes, blue suspension was obtained. Now the burette again was filled with hydroxyl amine hydrochloride solution and was now allowed to drip into the blue suspension obtained from the previous stirring. On completion of the dripping process, the solution was kept at constant stirring for 15 minutes. And finally brick red suspension was produced. It was left undisturbed for one hour. The suspended particles was filtered and dried for 12 hours in atmospheric air and then powdered using motar and pestle.



Fig 2.4 Pure Cu₂O Nanoparticles

2.4 Flowchart



CHAPTER III

CHAPTER III

MATERIALS AND METHODS

3.1 Chemicals

All the chemicals and reagents used in the present study were of analytical grade and were used as received without further purification. Cupric chloride dihydrate ($\text{CuCl}_2 \cdot 2\text{H}_2\text{O}$, 99.9%, Sigma-Aldrich), Sodium dodecylbenzenesulphonate ($\text{C}_{12}\text{H}_{25}\text{C}_6\text{H}_4\text{SO}_3\text{Na}$, 95%, Loba Chemie), Hydroxylamine hydrochloride ($\text{NH}_2\text{OH} \cdot \text{HCl}$, 98.0%, Loba Chemie), Sodium hydroxide (NaOH , 98%, Loba Chemie), Methanol (CH_3OH , 99%, Merck) and Ethanol ($\text{C}_2\text{H}_5\text{OH}$, 99%, Merck). Double distilled water was used in all the experiments.

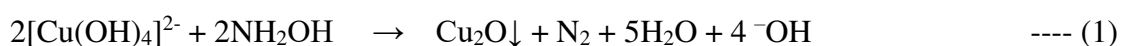
3.2 Experimental Section

3.2.1 Synthesis of SDBS capped Cu_2O nanostructures:

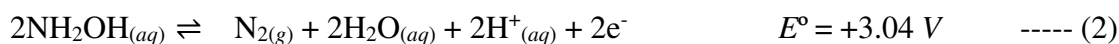
In a typical synthesis, 0.8525g (0.5 M) of cupric chloride dihydrate ($\text{CuCl}_2 \cdot 2\text{H}_2\text{O}$) was dissolved in 10 mL of deionized water at room temperature. Subsequently, 1.7501 g of sodium dodecylbenzenesulphonate was added and subjected to gentle stirring for 30 minutes to ensure complete dissolution. After obtaining a homogenous solution, 10 mL of 1 M NaOH solution was added dropwise under constant stirring to the mixture placed in a water bath set at 305 K (32 °C) while a blue precipitate of $\text{Cu}(\text{OH})_2$ was produced. The resulting solution was stirred for 1 h and then 10 mL of 0.5 M solution of the reducing agent hydroxylamine hydrochloride, was added drop-by-drop as the solution is being stirred vigorously. The colour of the solution turning ochre or brick red gradually after the addition of reducing agent indicates the formation of Cu_2O . The obtained precipitate was left undisturbed for 1 h and then centrifuged at 3000 rpm, washed several times with ethanol and redispersed in methanol for further analysis.

Hydroxylamine as the reducing agent:

The reducing agent hydroxylamine is environmentally benign and involves the formation of by-product nitrogen gas, which liberates during the course of the reaction as shown below,



The redox reactions involved in the above synthesis at alkaline medium are given below:



3.3 Characterization Techniques

The characterization of nanoparticles is a branch of nanometrology that deals with the measurement of the physical and chemical properties of nanoparticles. In general, the characterization techniques can be categorized into two: imaging by microscopy and analysis by spectroscopy. We have chosen spectroscopy methods of characterization. Spectroscopy, which measures the particles' interaction with electromagnetic radiation as a function of wavelength, is useful to determine the concentration, size and shape of the nanoparticles.

3.4 X-ray Diffraction

The powder X-ray diffraction patterns were acquired at room temperature on a PANalytical X'Pert Pro X-ray diffractometer using Cu K α radiation equipped with an X'Celerator detector in the continuous scanning mode. The samples were scanned over the angular range of $2\theta = 10^\circ$ - 80° with a step size of 0.02° and acquisition time of 0.5s per step.

The peak width varies inversely with crystallite size and microstrain and is more pronounced at higher 2θ angles. Therefore, the average crystallite size (L) of the nanostructures can be calculated from the extent of line broadening in the high intense peak using Scherrer equation,

$$L = 0.94 \lambda / \beta_{2\theta} \cos \theta$$

where $\beta_{2\theta}$ is the full width at half maximum (FWHM) of the peak after correcting for instrumental line broadening, θ is the angle of incidence or Bragg Angle, λ ($= 1.5406 \text{ \AA}$) is the wavelength of the X-ray used.

3.4.1 Applications

- XRD is a non-destructive technique.
- To identify the crystalline phases and orientation.
- To determine the structural properties:

Lattice parameters (10-4Å), strain, grain size, epitaxy, phase composition, (Laue) order-disorder transformation and thermal expansion.

- To measure the thickness of thin films and multi-layers.
- To determine the atomic arrangement.

3.5. Optical Absorbance

Ultra violet and visible absorption spectroscopy is the technique by which we measure attenuation of light that passes through a consideration sample or also that are reflected from the sample. Both parts (UV and Vis) of light are energetic enough to excite electrons to higher energy levels.

UV-visible diffuse reflectance spectra (UV-Vis DRS) were recorded for the die-pressed disk samples at ambient temperature using JASCO V-530 UV-visible spectrophotometer equipped with an integrating sphere assembly in the wavelength range of 300-800 nm, where BaSO₄ serves as the reference material.

The absorbance of the sample over the UV-visible region was derived from the recorded reflectance spectra employing Kubelka-Munk function as given below:

$$f(R_{\infty}) = \frac{K}{S} = \frac{(1 - R_{\infty})^2}{2R_{\infty}}$$

where K is the absorption coefficient, S is the scattering coefficient (independent of wavelength for particle dimension > 5 μm) and R_∞ is reflectance of the sample with reference to the standard. From the expression, two extreme conditions could be conceived: (i) when absorption coefficient at a particular wavelength is negligible (K→0), R_∞→1 i.e. reflectivity is maximum and (ii) when scattering at a particular wavelength tends to zero (S→0), R_∞→0 i.e. reflectivity is negligible. In the absorbance spectrum, the intersection point of the tangents drawn to the energy/wavelength axis at the absorption offset and to the linear portion of the absorption edge gives the optical band gap of the sample.

3.5.1 Applications

a) To detect the Chromophore functional group:

To determine the functional group in the material exclusively, it confirms the presence and absence of the Chromosphere in the sample which should be compound. Chromophore is an atom or group which is responsible for the colour of the compound.

b) To determine the unknown compound:

With the help of the UV-Vis spectroscopy, unknown compounds can be determined in the sample. For this purpose, the required compound is compared to spectrum of the reference compound if luckily both the spectrum matches, then the confirmation of unknown compound can be noted.

c) To measure the purity of the sample:

The purity of the substance can be measured by this unique technique. For this purpose, absorption of the reference and the sample under observation is compared and via relative calculations of the absorption intensity, the purity of the sample can be confirmed.

3.6FOURIER TRANSFORM INFRARED (FTIR) SPECTROSCOPY

FTIR stands for Fourier Transform Infrared, the preferred method of infrared spectroscopy. When IR radiation is passed through a sample, some radiation is absorbed by the sample and some passes through (is transmitted). The resulting signal at the detector is a spectrum representing a molecular ‘fingerprint’ of the sample. The usefulness of infrared spectroscopy arises because different chemical structures (molecules) produce different spectral fingerprints.

3.6.1 Principle and Methodology

. The FTIR uses interferometry to record information about a material placed in the IR beam. The Fourier Transform results in spectra that an analyst uses to identify or quantify the material.

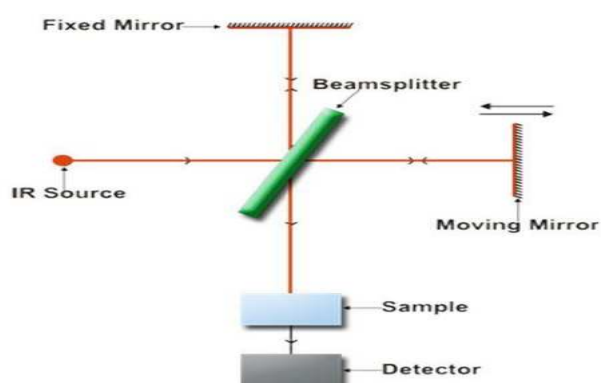


Fig 3.1 Working of FTIR

An FTIR spectrum arises from interferograms being ‘decoded’ into recognizable spectra. Patterns in the spectrum help identify the sample, since molecules exhibit specific IR fingerprints.

3.6.2 Applications

FTIR can be a single purpose tool or a highly flexible research instrument. The total scope of FTIR applications is extensive. Some of the more common applications are:

- Detection and identification of different elements and compounds.
- Quality verification of incoming/outgoing materials.
- Deformulation of polymers, rubbers, and other materials through Thermogravimetric infra-red (TGA-IR) or Gas Chromatography infra-red (GC-IR) analysis.
- Microanalysis of small sections of materials to identify contaminants.
- Analysis of thin films and coatings.
- Monitoring of automotive or smoke stack emissions.
- Used in the field of forensics, medicine, etc.

CHAPTER IV

CHAPTER IV

RESULTS AND DISCUSSION

4.1 Structural Characterization

The phase purity and crystal structure of the as-synthesized samples were analysed from the powder X-ray diffraction patterns recorded between the 2θ range 20-80° and is shown in Fig. 4.1 & 4.2. All the diffraction peaks (Fig. 4.1) can be readily indexed to the cuprite crystal structure (space group: $Pn\bar{3}m$) of Cu_2O having lattice constants $a = b = c = 4.267 \text{ \AA}$ and are in accordance with those reported in literature (JCPDS Card No. 05-0667).

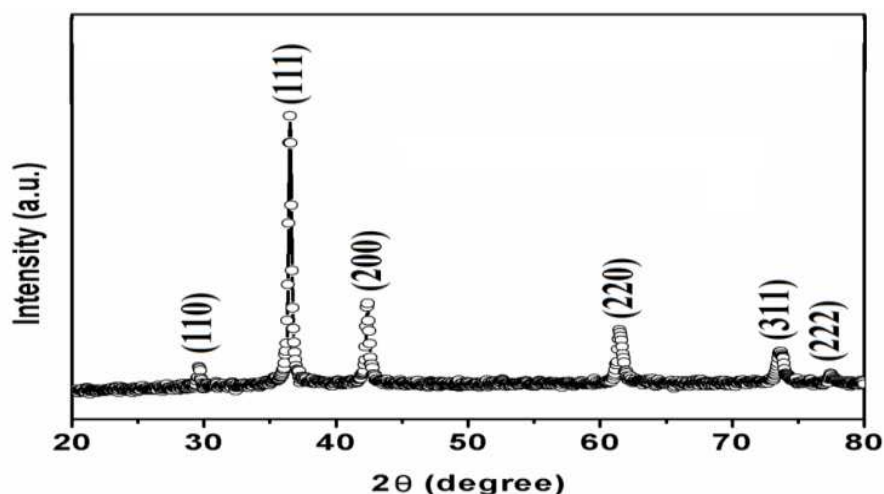


Fig 4.1 Powder X-Ray diffractogram of the as-synthesized Cu_2O nanocrystals

The diffraction peaks with 2θ values 29.6°, 36.5°, 42.4°, 61.4°, 73.6° and 77.5° correspond to the crystal planes (110), (111), (200), (220), (311) and (222) of the cubic phase⁴³ of Cu_2O respectively. Moreover, no distinct peaks of any impurities such as copper or other copper oxides were detected in the diffraction pattern implying the high purity of the sample. The broadening of diffraction peaks could be ascribed to the small crystallite size and the resulting strain in the crystal lattice.

Table 1. Crystallographic parameters of prepared Cu₂O nanostructures prepared with the reducing agents (a) Hydroxylamine (b) L-Ascorbic acid (c) D-Glucose.

2θ (degree)	Crystal plane	d-spacing (Å)	Relative Intensity (%)
29.66°	(110)	3.0113	7.41
36.52°	(111)	2.4601	100.00
42.40°	(200)	2.1318	30.70
61.47°	(220)	1.5082	19.85
73.61°	(311)	1.2867	11.56
77.53°	(222)	1.2312	2.48

4.2 Optical Characterization

4.2.1 Absorption Characteristics:

The absorption characteristics of the Cu₂O nanostructures were investigated by UV-Visible absorption spectroscopy at room temperature which is displayed in Fig. 4.2. The absorption spectrum exhibits broad absorption bands in both UV and visible region displaying the absorption onset at 456, 472 and 571nm for the Cu₂O nanostructures synthesized using hydroxylamine, ascorbic acid and glucose respectively.

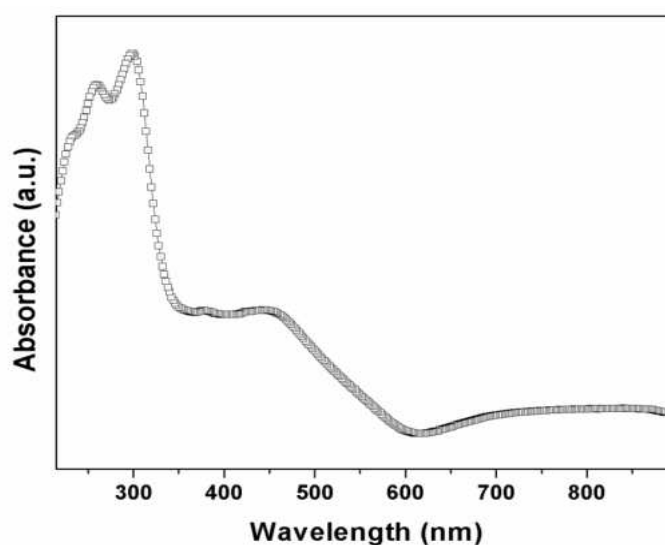


Fig. 4.2 Optical absorption spectrum of Cu₂O nanostructures prepared using hydroxylamine as the reducing agent.

4.2.2 FTIR Spectroscopy

FTIR spectroscopy is a powerful analytical technique for structural characterization based on the absorption of infrared radiation by different functional groups present in the material of interest. It can also be used to differentiate between Cu(I) and Cu(II) present in the sample since vibration due to $\nu\text{Cu(I)-O}$ bond appears around 625 cm^{-1} [24] while $\nu\text{Cu(II)-O}$ bond vibration is observed at 536 and 482 cm^{-1} .

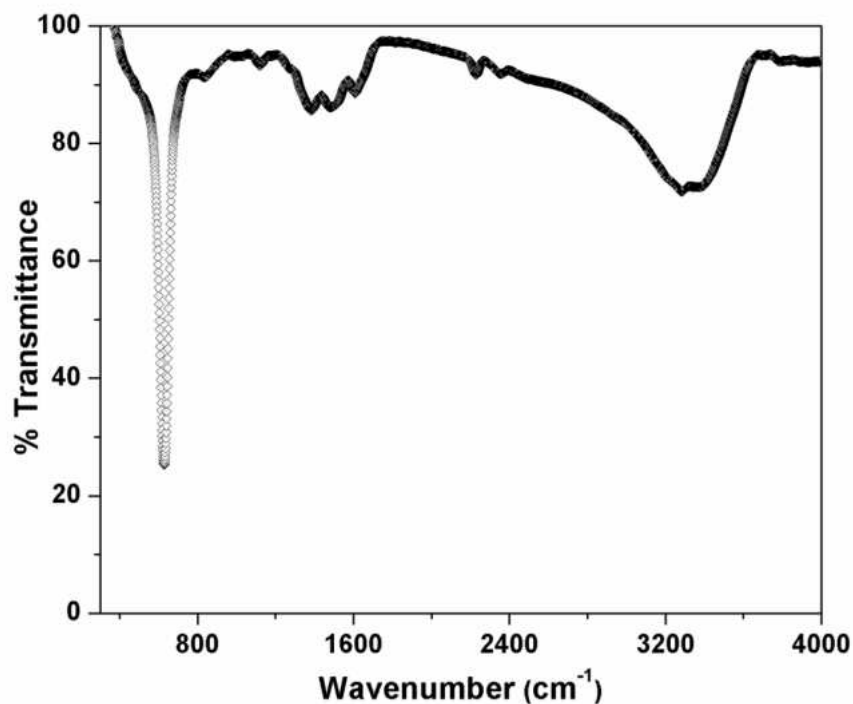


Fig. 4.3 FT-Infrared spectrum of as-prepared Cu₂O nanostructures

The presence of broad absorption band at 634 cm^{-1} due to Cu(I)-O vibration and absence of Cu(II)-O vibrations confirms the presence of copper in the univalent oxidation state.

CHAPTER V

CHAPTER V

CONCLUSION

5.1 Summary

In this investigation , cuprous oxide nanoparticles were prepared by chemical precipitation method. And thus, Cuprous oxide nanoparticles were obtained with minimal impurities.

From the XRD studies , it is found that cuprous oxide nanoparticles exhibit cubic structure as confirmed from the (JCPDS Card No. 05-0667). The XRD peaks of the cuprous oxide nanoparticles at different temperatures were found to be very broad and sharp indicating that the particles are nanocrystalline.

Further, the broad absorption band (peak) at 634 cm^{-1} in the FTIR spectrum confirms the presence of Cu(I)-O bond.

The estimation of UV absorption onset for cuprous oxide nanoparticles was found to be at 456, 472 and 571nm respectively. Broad absorption bands were also absorbed in both UV and visible regions.

This study is an evident proof that the cuprous oxide nanoparticles can be prepared in a simple and cost-effective manner using chemical precipitation method to cater the needs of various applications in future.

5.2 References

- [1] Hui Wang and Hong-Yuan Chen(2002), successfully prepared Cu₂O nanoparticles using microwave irradiation method.
- [2] Suresh Sahadevan ,Kaushik Pal and Zaira Zaman Chowdhury(2017),synthesised Cu₂O nanoparticles using chemical precipitation method.
- [3] V.D.Rajput and A.Fedorenko (2018), determined the effects of Cu₂O nanoparticles on crop plants.
- [4] Amin Asadi and Loke Kok Foong (2020),characterised the stability and dynamic viscosity of Cu₂O water hybrid nanofluids.
- [5] Ali Nazari and Shadi Riahi (2011) determined the effects of Cu₂O nanoparticles on compressive strength of self-compacting concrete.
- [6] Paniz Esfandfar and Aliakbar Saboury (2015) made a spectroscopic study on interaction between Cu₂O nanoparticles and bovine serum albumin.
- [7] Fang wang and Heng deng (2016) synthesized Cu₂O via sol-gel method.
- [8] Zhigang Zang and Jiro Temmyo (2013) synthesized cuprous oxide flims by radical oxidation at low temperature for PV application.
- [9] Ye feng wang and jing hui zeng (2008) determined the hydrothermal synthesis of cuprous oxide microcrystals with controlled morphology.(volume 10, pages 3731-3734)
- [10] HuamingYanga and JingOuyanga(2006) electrochemically synthesized the property of cuprous oxide nanoparticles. (Volume 41, pages 1310-1318)
- [11] FenXu and Xiaohui (2003) synthesized shape controlled sub-micro cuprous oxide octahedra. (volume 6, issue 11, pages 1390-1392)
- [12] KOUTI. Mand MATOURI L. (2010) determined the fabrication of nanosized cuprous oxide using feshling's solution. (volume 17, pages 73 to 78)

A STUDY OF ACOUSTICAL PARAMETERS OF SELECTED EDIBLE OIL

Project report submitted to the Department of Physics

ST. MARY'S COLLEGE (AUTONOMOUS)

THOOTHUKUDI

Affiliated to MANONMANIUM SUNDARANAR UNIVERSITY, TIRUNELVELI

In partial fulfillment of the requirement for the award of

BACHELOR'S DEGREE IN PHYSICS

BY

S. ANNAI THANGA SELVA SAROJENI - 18AUPH03

A. MANI KARTHIGA SAKTHI - 18AUPH27

C. SUBALAKSHMI - 18AUPH43

K. SUBALATHA - 18AUPH45

S. TREFILLA MISSIER - 18AUPH47

Under the Guidance of

DR. S. EUCHRISTA IMMACULATE SYLVIA, M.Sc., M.Phil., Ph.D.,



Department of Physics

ST. MARY'S COLLEGE (AUTONOMOUS)

Reaccredited with "A+" Grade by NAAC

Thoothukudi

2020 – 2021.

CERTIFICATE

This is to certify that this project work entitled, **“A STUDY OF ACOUSTICAL PARAMETERS OF SELECTED EDIBLE OIL”** is submitted to **ST. MARY’S COLLEGE (AUTONOMOUS), THOOTHUKUDI** in partial fulfillment for the award of Bachelor’s degree in Physics and is a record of work done during the year 2020-2021 by the following students.

S. ANNAI THANGA SELVA SAROJENI - 18AUPH03

A. MANI KARTHIGA SAKTHI - 18AUPH27

C. SUBALAKSHMI - 18AUPH43

K. SUBALATHA - 18AUPH45

S. TREFILLA MISSIER - 18AUPH47

S. brevistigmata Cinnamulathyi

GUIDE

Russie 2 da

HEAD OF THE DEPARTMENT

HEAD

Department of Physics,
St. Mary's College (Autonomous),
Thoothukudi - 628 001.

A. Lucas Reception
EXAMINER

EXAMINER

(914) 21

Lucia Rose

PRINCIPAL

St. Mary's College (Autonomous)
Thoothukudi - 628 001.

ACKNOWLEDGEMENT

First, we wish to thank the Lord Almighty for His blessings upon us that lead to the successful completion of our project.

Our special thanks to our principal **Dr. Sr. A.S.J. Lucia Rose M.Sc., M.Phil., Ph.D., PGDCA.,** for providing the necessary facilities in the institution for carrying out our project work.

We register our deep sense of gratitude to our head of the department **Dr. Sr. Jessie Fernando M.Sc., M.Phil., Ph.D.,** for her exemplary guidance, monitoring and encouragement throughout the course of this project.

We would like to express our gratitude to our guide, **Dr. Mrs. S. Euchrista Immaculate Sylvia M.Sc., M.Phil., Ph.D.,** for her guidance and constant support in every stage of our project work.

We sincerely acknowledge the financial assistance funded by DBT, New Delhi for the successful completion of the project work.

We are happy to take this opportunity to sincerely thank all the professors of our department and supportive staff for their constant support.

We are also thankful to our parents and everyone else who directly or indirectly helped us to bring out this project successfully.

CHAPTER**CONTENT****PAGE NO**

I INTRODUCTION

1

II LITERATURE REVIEW

3

III MATERIALS AND METHODS

5

IV OBSERVATIONS, TABULATIONS
AND GRAPHICAL REPRESENTATIONS

14

V RESULT, DISCUSSION
AND CONCLUSION

22

BIBLIOGRAPHY

CHAPTER - I

INTRODUCTION

Quality and Nutrition value of food products are much essential for healthy life of human beings. Processing a food is therefore very much essential to maintain the characteristics of the food with its nutritional content and the processing technique should be free of additives and chemicals. So, technology used for food processing should be given much importance. Many food processing involves various thermal and non thermal technology. The thermal technology has been used to improve physiochemical characteristics and to control food quality and extend life of food products. One of the non-thermal technologies is the ultrasonic methodology which has negligible effect in the nutritional value of food products. The ultrasonic is considered to be a promising and emerging technology that can be used in food processing technology.[5]

Ultrasonics is defined as sound waves with frequency exceeding human hearing limit. The process of studying the molecular interaction from the variation of thermodynamic parameters and their liquid mixtures are very useful to understand the thermodynamic and transport properties associated with heat and fluid flow which gives insight into the molecular process of interaction. Ultrasonic technology is employed in wide range of application such as medicine, biology, agriculture, industry, material science, oceanography. A knowledge of acoustical parameters of food study using ultrasonic interferometer technology will provide useful information for the food processing technology.

Ultrasonics techniques are preferred because it is eco-friendly. This project is designed to study about few acoustical parameters of few edible oil such as Coconut oil, Neem oil, Sunflower oil, Sesame oil and Groundnut oil. The above given oil are chosen because of its innumerable uses.

The uses of Neem oil can boost the immunity of persons to every day microbial infections. The Neem oil is used to prevent urinary infections and is known for its powerful anti fungal and anti microbial property. Neem oil is used to treat skin diseases like eczema, ring worm, scabies and psoriasis. (www.healthline.com)

The importance of Groundnut oil is very much accepted as it lowers the cholesterol level. It prevents the risk of heart attack. The Groundnut oil reduces the cancer causing agent. It is applied on any part of the body to cure joint pain, dry skin, eczema and other skin problems. The Groundnut oil is utilized as a skin smoother, emulsifier and emollient. It is used as a substitute for many oil like almond oil and olive oil. (www.healthline.com)

The Sesame oil is rich in anti-oxidant and thus protects our body from free radical. Anti-oxidant present in Sesame oil acts as a thinner for blood. It helps to heal wounds because it is having anti- oxidant and anti -microbial properties. (www.healthline.com).

The Sunflower oil is known to prevent heart disease. It is used for preventing constipation and lowering "bad" LDL cholesterol. Sunflower oil can be applied directly to the skin for healing wounds, skin injuries, psoriasis, and arthritis; and as a massage oil. In foods, Sunflower oil is used as a cooking oil. (en.wikipedia.org).

Coconut oil may improve the dental health by attacking the harmful bacteria in the mouth. It reduces plaque build-up, tooth decay and fights gum disease. The presence of MCTs in Coconut oil breakdown into ketones, which can be used by braincells for fuels. Coconut oil helps to retain moisture and reduce inflammation. (www.healthline.com).

OBJECTIVES:

Reckoning with the significant reasons for the study of acoustic parameters, the project was carried out with the following objectives.

1. To determine the ultrasonic velocity of liquid of different edible oil using ultrasonic interferometer.
2. To obtain the density of the selected oil.
3. To determine the coefficient of viscosity of the experimental oil using Ostwald's viscometer.
4. To find the values of adiabatic compressibility (β_a), Intermolecular free length (L_f), ultrasonic attenuation(α/f^2), acoustical impedance (Z) and relaxation time(τ) of the oil.

CHAPTER - II

LITERATURE REVIEW:

Mahammad Ali, M.K. and Basharith Ali ,(2014) have studied the ultrasonic velocity for some commonly used edible oil using multi frequency ultrasonic interferometer. They reported that density of these oil and some physical parameters such as ultrasonic velocity and acoustic impedance depends on the % of UFA and SFA contained in the edible oil.

Bhattacharya, (1981) studied the measurement of ultrasonic propagation in Coconut oil in the vicinity of phase transition. He gave a review that ultrasonic propagation in a system consisting Coconut oil and CCl_3 is considered as a function of temperature near T_c in the low region. Hence he reported that the ultrasonicattenuation (α/f^2) of the complex binary mixture of Coconut oil and CCl_3 exhibited strong frequency and temperaturedependence near T.His result satisfies FB theory which connects α/f^2 with v and temperature.

Rav, and Reddy,*et al.*, (1980) gave a review on adulteration in oil and fats by ultrasonic method. He reported that the ultrasonic revealed velocity changed when the oil were recycled. His study revealed that increase in ultrasonic velocity after recycling of oil was attributed to the reduce in SFA % and increase in USFA% .

Clements, MC. DJ, and Povey, *et al.*, (1990) have studied the measurements of ultrasonic characterization of a food emulsion. The ultrasonic velocity and attenuation of salad cream were measured for various oil concentration and mean droplet size over a range of frequencies using ultrasonic pulse echo technique. This study reported that it was used to find the particle size by ultrasonic velocity.

Najmie, M.M.K. and Khalid, K.*et al.*, (2011) have studied the measurement of density and ultrasonic characterization of Palm oil trunk infected by Ganoderma Boninense Disease. This study shows that the ultrasonic velocity in the affected area of the Palm oil was lesser than the healthy areas.

Nikoli Biban, D. and Kegl Breda.*et al.*, (2012) have studied the determination of speed of sound and density of fluids depending on the pressures. This study showed that the parameters such as ultrasonic velocity, bulk modulus and density of liquid fuels were important for predicting the behaviour of fuel injection systems in diesel engine .

Jaafar.*et al.*, (1993) have studied the ultrasonic determination of Palm oil content in michella. This study has employed an ultrasonic technique to determine the oil content in the homogeneous solution of Crude Palm and michella. This study reported that density, acoustic impedance and temperature have an impact on the ultrasonic velocity in the liquids.

Gladwell, N. and Javanaud, C.*et al.*, (1985) have studied the ultrasonic behaviour of edible oil in correlation with Rheology. This study revealed the ratio of volume to shear viscosity decreased with frequency and that the molecular rearrangements require greater degree of co-operation compared with the shear relaxation.

CHAPTER - III

MATERIALS AND METHODS.

The knowledge of thermodynamic and physical properties of certain edible oil can be used for medicinal purposes. Ultrasonic waves are effective means for examining and analyzing several physical properties of the materials. Thus, ultrasonic and viscometric studies offer simple, easy and accurate ways for calculating the physical parameters which throw light on molecular interactions in liquids. Many medicinal applications require quantitative data of the viscosity and density of these liquid extracts.

This project deals with the experimental study of ultrasonic velocity, density and viscosity of the different edible oil at room temperature.

The parameters such as ultrasonic velocity (U), density (ρ) and viscosity (η) and computed parameters such as adiabatic compressibility (β_a), free length (L_f), acoustical impedance (Z) and relaxation time (τ) are studied.

ULTRASONIC INTERFEROMETER

THEORY:

Ultrasonic interferometer is a simple and direct device which yields accurate and consistent data, from which one can determine the velocity of ultrasonic sound in a liquid medium with a high degree of accuracy. A crystal-controlled interferometer (model M-83S) supplied by Mittal enterprises, New Delhi, operating frequencies ranging from 1 to 12 MHz has been used to measure the ultrasonic velocity.

ULTRASONIC DEFINITION:

Ultrasonic sound refers to sound pressure with a frequency greater than the human available range (20Hz to 20KHz). When an ultrasonic wave propagates through a medium, the molecules in that medium vibrate over short distance in a direction parallel to the longitudinal wave. During this vibration, momentum is transferred among molecule. This causes the wave to pass through the medium.

ULTRASONIC INTERFEROMETER:



ULTRASONIC INTERFEROMETER

An ultrasonic interferometer is a simple and direct device to determine the ultrasonic velocity in liquid with a high degree of accuracy. In an ultrasonic interferometer, the ultrasonic waves are produced by the piezo electric methods. At a fixed frequency variable path interferometer, the wavelength of the sound in an experimental liquid medium is measured, and from this one can calculate its velocity through that medium. The ultrasonic cell consists of a double walled brass cell with chromium plated surfaces having a capacity of 10ml. The double wall allows water circulation around the experimental liquid to maintain it at a known constant temperature. The micrometer scale is marked in units of 0.01 mm and has an overall length of 25mm. Ultrasonic waves of known frequency are produced by a quartz crystal which is fixed at the bottom of the cell. There is a movable metallic plate parallel to the quartz plate, which reflects the waves. The waves interfere with their reflections, and if the separation between the plates is exactly an integer multiple of half wave length of sound, standing waves are produced in the liquid medium. Under these circumstances, acoustic resonance occurs. Resonant waves are maximum in amplitude, causing a corresponding maximum in the anode current of the piezoelectric generator.

WORKING PRINCIPLE:



The principle used in the measurement of velocity (U) is based on the accurate determination of the wavelength (λ) in the medium. Ultrasonic waves of known frequency (f) are produced by quartz crystal fixed at the bottom of the cell. These waves are reflected by a movable metallic plate kept parallel to the quartz crystal. If the separation between these two plates is exactly a whole multiple of the sound wave length, standing waves are formed in the medium. This acoustic resonance gives rise to an electrical reaction on the generator driving the quartz crystal and anode current of the generator become a maximum. If the distance is now increased or decreased and the variation is exactly one-half wavelengths or multiple of it, anode current become maximum from the knowledge of wavelength (λ). The velocity (U) can be obtained by the relation

$$\text{Velocity} = \text{wavelength} \times \text{frequency}$$

$$U = \lambda f \text{ (m/s).}$$

ADJUSTMENT OF ULTRASONIC INTERFEROMETER:

For initial adjustment two knobs are provided on high frequency generator, one is marked with "ADJ" to adjust the position of the needle on the ammeter and the knob marked "GAIN" is used to increase the sensitivity of the instrument for greater deflection, if desired. The ammeter is used to notice the number of the maximum deflection while micrometer is moved up or down in liquid.

PROCEDURE:

1. Unscrew the knurled cap of cell and lift it away from double walled construction of the cell. In the middle position of it pour experimental oil and screw the knurled cap. Wipe of the excess liquid overflowing from the cell.
2. Insert the cell in heavy base socket and clamp it with the help of screw provided on its side.
3. Connect the high frequency generator with cell by coaxial cable provided with the instrument. In ultrasonic interferometer frequency selector knob should be positioned at desired frequency (same frequency as that of liquid cell chosen).
4. Move the micrometer slowly in either clockwise or anticlockwise direction till the anode current on the ammeter on the high frequency generator shows a maximum or minimum.
5. Note the reading of micrometer corresponding to the maximum or minimum in micro ammeter. Take about 10 readings of consecutive maximum or minimum and tabulate them.
6. Take average of all differences ($\lambda/2$).
7. Once the wavelength is known the velocity (U) in the oil can be calculated with the help of the relation $U = \lambda f$.

VISCOMETER:



VISCOMETER

A viscometer (also called viscosimeter) measures the apparent viscosity of the liquid for a given flow rate and temperature. For liquids with viscosities which vary with flow conditions, an instrument called a Rheometer is used. Thus, a Rheometer can be considered as a special type of instrument. Viscometers only measure under one flow condition.

In general, either the fluid remains stationary and an object moves through it, or the object is stationary and the fluid moves past it. The drag caused by relative motion of the fluid and a surface is a measure of the viscosity. The flow conditions must have a sufficiently small value of Reynolds number for there to be laminar flow.

OSTWALD'S VISCOMETER:

Ostwald viscometer, also known as U-tube viscometer or capillary viscometer is a device used to measure the viscosity of the liquid with a known density. The method of determining viscosity with this instrument consists of measuring the time for the known volume of the liquid to flow through the capillary under the influence of gravity. Ostwald viscometer is named after the German chemist Wilhelm Ostwald,

MEASUREMENT OF VISCOSITY:

The viscosity of liquid is measured using Ostwald's viscometer. The viscometer is filled with reference (distilled water) and it is held in a controlled water bath. The water in the viscometer is kept undisturbed for the attainment of the experimental temperature. Using a suitable arrangement, the water is sucked above the marked level and then it is allowed to flow freely. The time taken for the flow of water is noted. The water is replaced with a mixture, whose viscosity is to be determined. Proceeding the same, the time taken for flow of liquid mixture at the experimental temperature was determined. Using the time taken for the distilled water and mixture, the viscosity of unknown liquid mixture is determined using the formula,

$$\frac{\eta_s}{\eta_w} = \frac{\rho_s}{\rho_w} \times \frac{t_s}{t_w}$$

Where η_s , ρ_w and t_w are the viscosity, density and time flow of water respectively and η_s , ρ_s and t_s , are the viscosity, density and time flow of unknown liquid mixture respectively. For most products, the viscosity is required to be high at low shear rates to prevent sedimentation or slumping, but to thin down at higher shear rates to facilitate application or processing. The viscosity of liquids is an important property that must be measured precisely in some industries. From Viscosity measurement, we can obtain much useful behavioral and predictive information for various products.

ACOUSTIC PARAMETERS

ULTRASONIC VELOCITY (U):

Ultrasonic velocity is the speed at which ultrasonic sound waves travel through a medium.

Ultrasonic velocity (U) has been calculated from the expression,

$$U = \lambda f \text{ (m/s)}$$

Where,

$\lambda = 2d / N$ = Wavelength of the ultrasonic waves in oil in metre.

N = Number of maxima or minima.

D = Distance between two successive maxima or minima in metre.

f = Frequency in hertz.

MEASUREMENT OF THE DENSITY:

The density measurement was made by specific gravity bottle. The specific gravity bottle was initially rinsed using acetone (cleaning agent). The weight of the specific bottle was measured. Then the weight of the specific gravity bottle with the liquid was measured. From the weight measurement the density of the liquid was calculated.

$$\text{Relative Density} = \frac{\text{weight of the liquid}}{\text{weight of the same volume of water}}$$

$$\text{R.D} = \frac{W_2 - W_0}{W_1 - W_0}$$

$$\rho = \text{R.D} \times \text{Density of water (Kg/m}^3\text{)}$$

where ,

W_0 = weight of the empty S.G bottle in Kg.

W_1 = weight of the S.G bottle with water in Kg.

W_2 = weight of the S.G bottle with liquid in Kg.

VISCOSITY (η):

The viscosity of a fluid is a measure of its resistance to deformation at a given rate. For liquids, it corresponds to the informal concept of "thickness". For example, syrup has a higher viscosity than water. Viscosity (η) of the liquid has been calculated from the expression

$$\eta = \frac{\rho t \times \eta_0}{\rho_0 t_0} \text{ (Ns/m}^2\text{)}$$

where ,

η, η_0 = Viscosity of liquid and water respectively in Ns/m².

ρ, ρ_0 = Density of liquid and water respectively in Kg/m³.

t, t_0 = Time taken for liquid and water respectively in s.

ADIABATIC COMPRESSIBILITY (β_a):

Adiabatic compressibility is, when an element of fluid is compressed, the work done on it heats it up. Adiabatic compressibility (β_a) has been calculated from the expression

$$\beta_a = \frac{1}{\rho U^2} \text{ (m}^2\text{/N)}$$

where,

ρ = Density of the liquid in Kg/m³.

U = Ultrasonic velocity of the liquid in m/s.

INTERMOLECULAR FREE LENGTH(L_f):

Intermolecular free length is the distance between the surfaces of the neighboring molecules. In general, when the ultrasonic velocity increases, the value of the free length decreases. The decrease in intermolecular free length indicates the interaction between the solute and solvent. Free length L_f , has been calculated from the expression.

$$L_f = K_T \beta_a^{1/2} (A^0)$$

$$K_T = (93.875 + 0.345T) \times 10^{-8} \text{ (kgms}^2\text{)}$$

where,

K_T = Jacobson's constant which is a temperature dependent in kgms^2 .

β_a = Adiabatic compressibility in (m^2/N) .

ACOUSTIC IMPEDANCE (Z):

Acoustic impedance is the resistance to sound wave propagation. The denser the material, the more acoustic impedance it has; the more echogenic it is, the whitest it appears on our screen. Acoustic impedance (Z) has been calculated using the expression.

$$Z = \rho U \text{ (Kg/m}^2\text{/s)}$$

where,

U = Velocity of the liquid in m/s.

ρ = Density of the liquid in Kg/m^3 .

RELAXATION TIME (τ):

Relaxation time is the time required for a viscous substance to recover from shearing stress after flow has ceased. Relaxation time (τ) has been calculated using the expression

$$\tau = \frac{4}{3} \beta_a \eta \text{ (s)}$$

where,

η = Viscosity of the liquid in Ns/m^2 .

β_a = Adiabatic compressibility in m^2/N .

ULTRASONIC ATTENUATION (α/f^2):

Attenuation in ultrasound is the reduction in amplitude of the ultrasound beam as a function of distance through the imaging medium. Ultrasonic attenuation has been calculated from the expression,

$$\alpha/f^2 = \frac{8\pi^2\eta}{3\rho U^2} (\text{Np/ms}^2)$$

where,

α/f^2 = Ultrasonic attenuation in Np/ms².

η = Viscosity of the liquid in Ns/m²

ρ = Density of the liquid in Kg/m³.

U = Velocity of the liquid in m/s.

CHAPTER - IV

OBSERVATIONS, TABULATIONS AND GRAPHICAL REPRESENTATIONS:

Table 1: VELOCITY OF DIFFERENT EDIBLE OIL

SAMPLE	ULTRASONIC VELOCITY (U) x 10 ³ (m/s)
COCONUT OIL	1.380
GROUNDNUT OIL	1.440
NEEM OIL	1.440
SUNFLOWER OIL	1.440
SESAME OIL	1.440

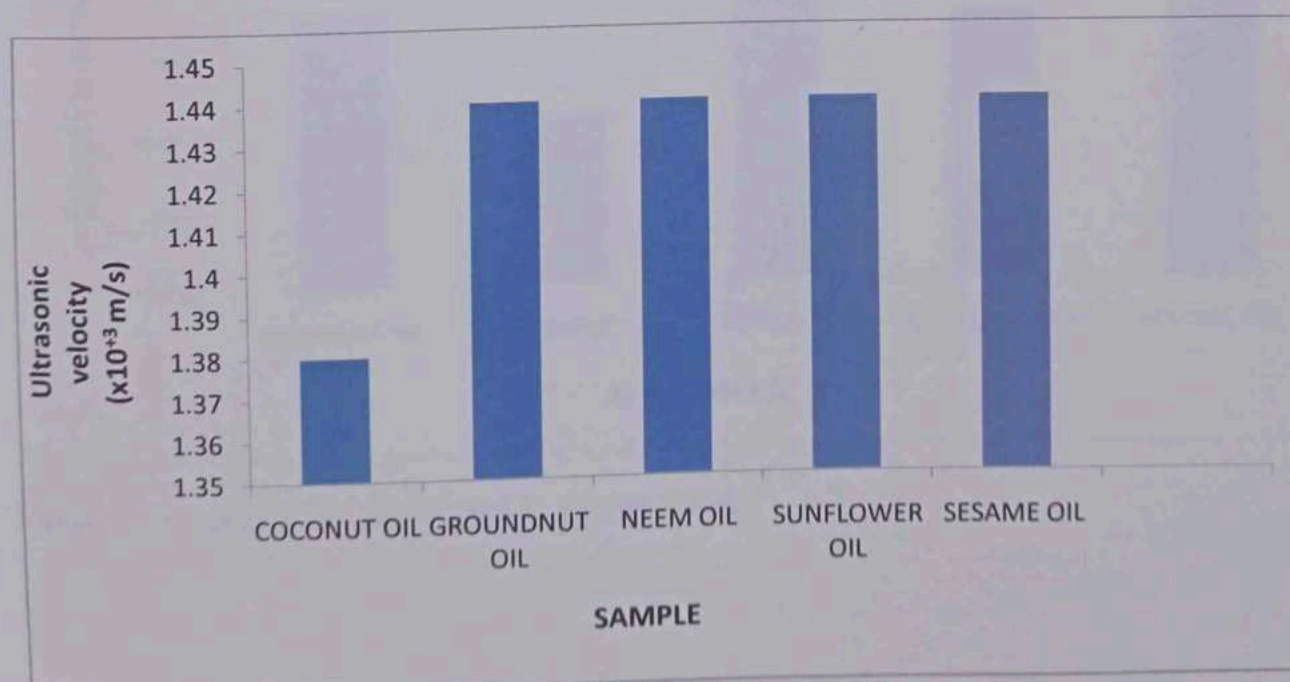


Figure 1: VELOCITY OF DIFFERENT EDIBLE OIL

Table 2: DENSITY OF DIFFERENT EDIBLE OIL

SAMPLE	DENSITY (ρ) $\times 10^3$ (Kg/m ³)
COCONUT OIL	0.9528
GROUNDNUT OIL	0.9462
NEEM OIL	0.9599
SUNFLOWER OIL	0.9527
SESAME OIL	0.9532

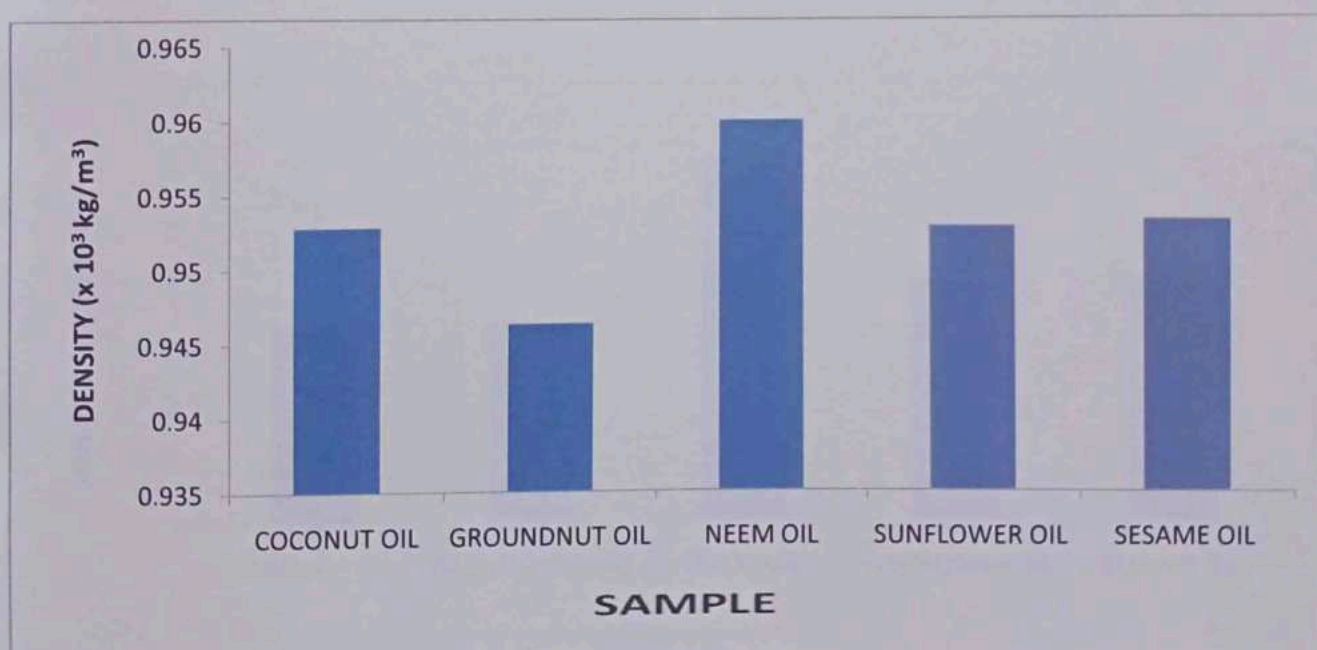


Figure 2: DENSITY OF DIFFERENT EDIBLE OIL

Table 3: VISCOSITY OF DIFFERENT EDIBLE OIL

SAMPLE	VISCOSITY (η) $\times 10^{-2}$ (Ns/m ²)
COCONUT OIL	3.429
GROUNDNUT OIL	3.335
NEEM OIL	6.148
SUNFLOWER OIL	4.048
SESAME OIL	4.120

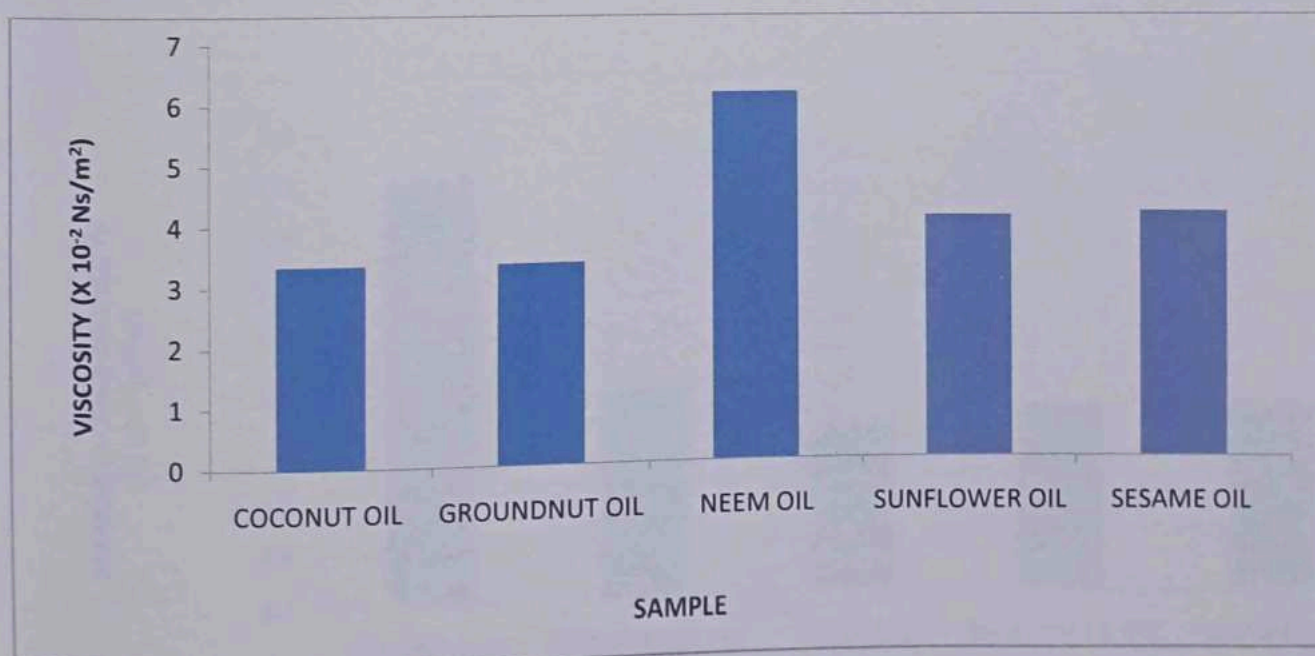


Figure 3: VISCOSITY OF DIFFERENT EDIBLE OIL

Table 4: ADIABATIC COMPRESSIBILITY OF DIFFERENT EDIBLE OIL

SAMPLE	ADIABATIC COMPRESSIBILITY (β_a) $\times 10^{-10}$ (m^2/N)
COCONUT OIL	5.5111
GROUNDNUT OIL	5.0964
NEEM OIL	5.0237
SUNFLOWER OIL	5.0619
SESAME OIL	5.0592

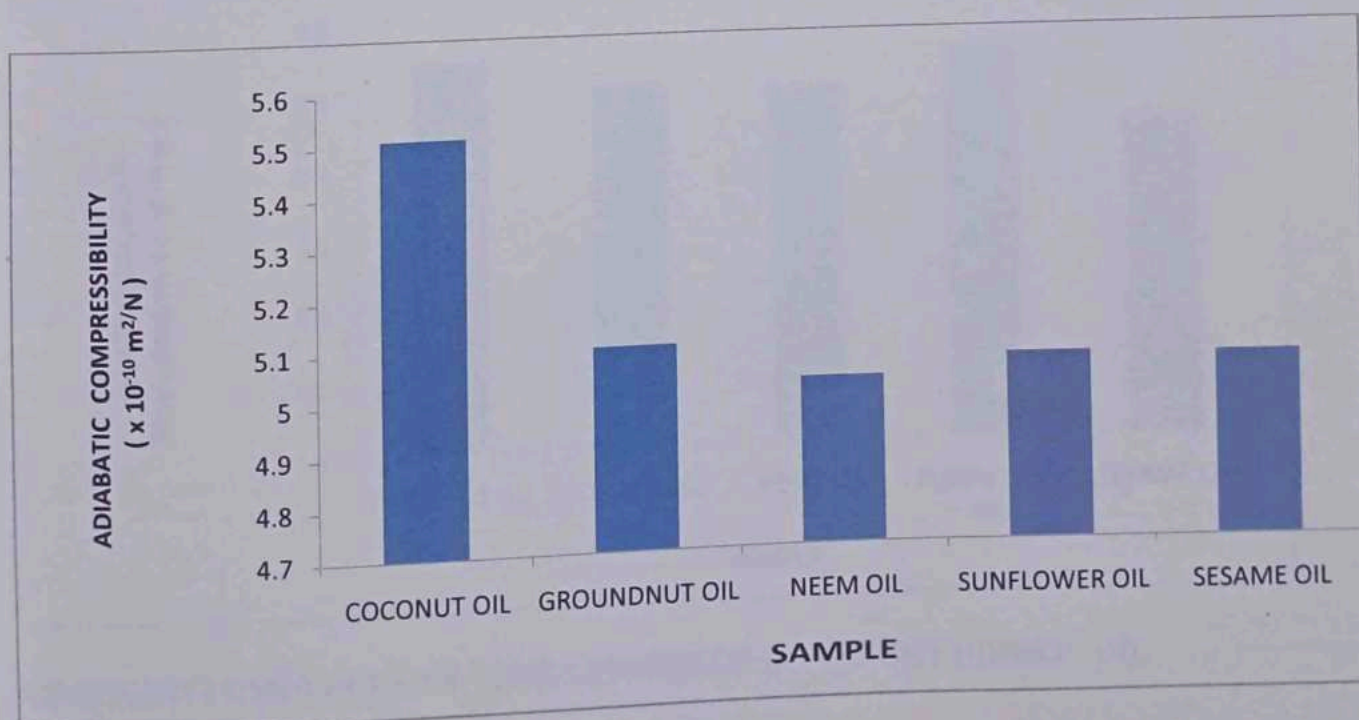


Figure 4: ADIABATIC COMPRESSIBILITY OF DIFFERENT EDIBLE OIL

Table 5: INTERMOLECULAR FREE LENGTH OF DIFFERENT EDIBLE OIL

SAMPLE	INTERMOLECULAR FREE LENGTH (L_f) $\times 10^{-10}$ (m)
COCONUT OIL	0.5514
GROUNDNUT OIL	0.5099
NEEM OIL	0.5027
SUNFLOWER OIL	0.5065
SESAME OIL	0.4501

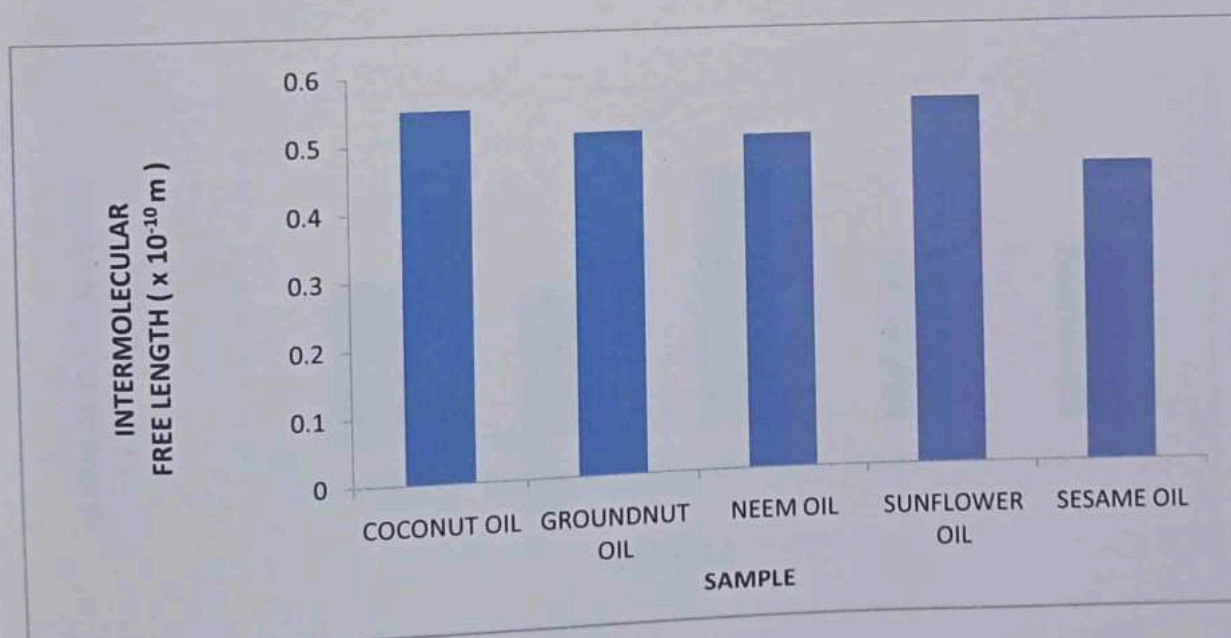


Figure 5: INTERMOLECULAR FREE LENGTH OF DIFFERENT EDIBLE OIL

Table 6: ULTRASONIC ATTENUATION OF DIFFERENT EDIBLE OIL

SAMPLE	ULTRASONIC ATTENUATION $(\alpha/f^2) \times 10^{-11}$ (Np/ms ²)
COCONUT OIL	4.9690
GROUNDNUT OIL	4.4687
NEEM OIL	8.1213
SUNFLOWER OIL	5.3877
SESAME OIL	5.4807

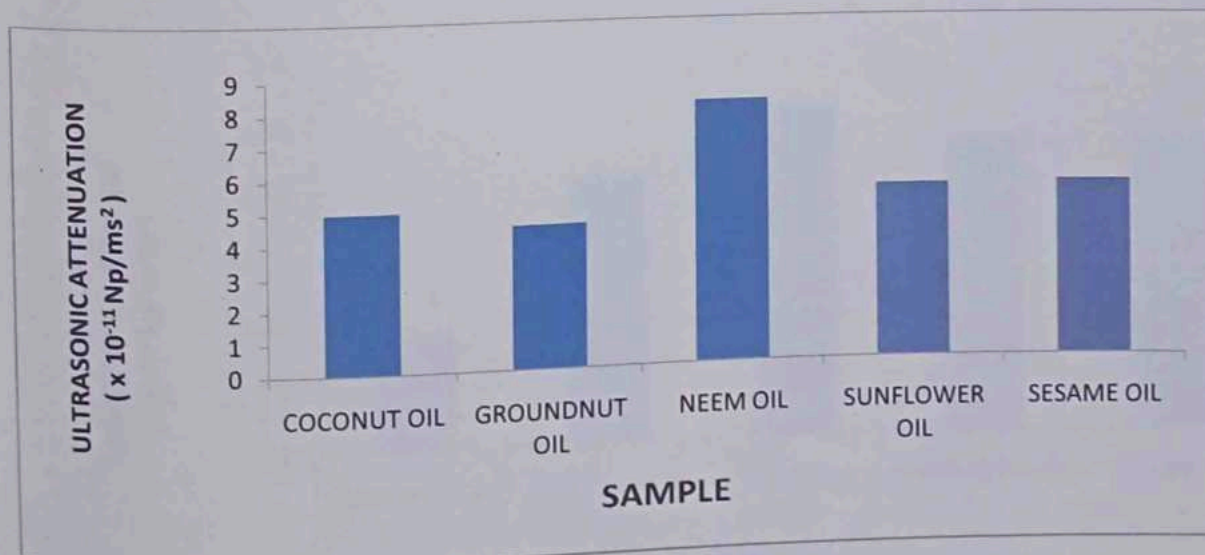


Figure 6: ULTRASONIC ATTENUATION OF DIFFERENT EDIBLE OIL

Table 7: ACOUSTIC IMPEDANCE OF DIFFERENT EDIBLE OIL

SAMPLE	ACOUSTIC IMPEDANCE (Z) x 10 ⁶ (Kg/m ² /s)
COCONUT OIL	1.3149
GROUNDNUT OIL	1.3626
NEEM OIL	1.3823
SUNFLOWER OIL	1.3718
SESAME OIL	1.3726

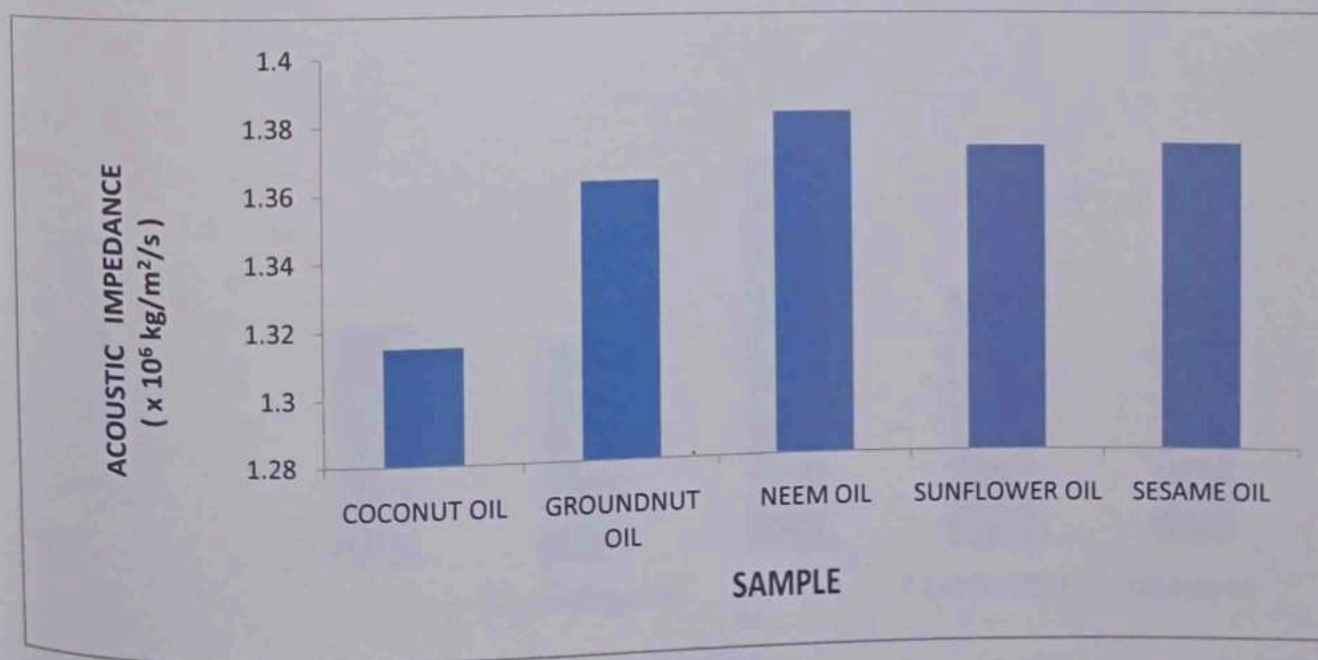


Figure 7: ACOUSTIC IMPEDANCE OF DIFFERENT EDIBLE OIL

Table 8: RELAXATION TIME OF DIFFERENT EDIBLE OIL

SAMPLE	RELAXATION TIME (τ) $\times 10^{-13}$ (s)
COCONUT OIL	2.5199
GROUNDNUT OIL	2.2662
NEEM OIL	4.1185
SUNFLOWER OIL	2.7322
SESAME OIL	2.7794

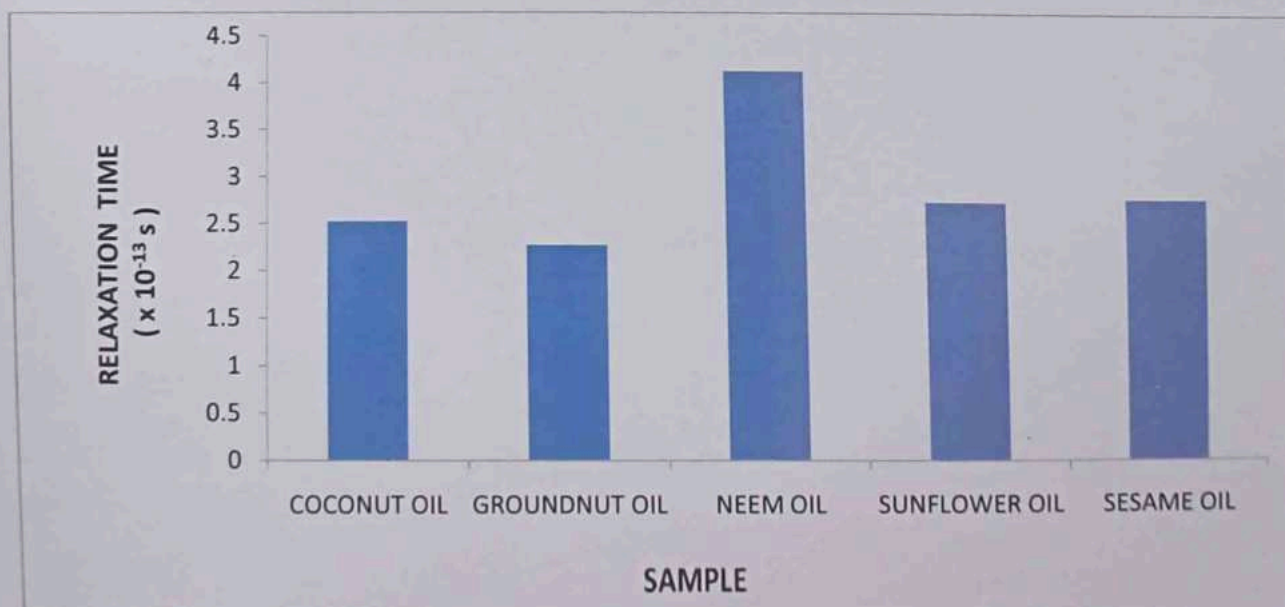


Figure 8: RELAXATION TIME OF DIFFERENT EDIBLE OIL

CHAPTER - V

RESULT,DISCUSSION AND CONCLUSION.

Velocity of 3MHZ ultrasonic wave in pure edible oil, densities and viscosities of the edible oil were measured with pre-calibrated interferometer, density bottle and viscometer respectively to nearest mg in room temperature and are tabulated. The values of derived parameters such as Velocity (U), Density(ρ), Viscosity(η), Adiabatic Compressibility (β_a), Intermolecular Free Length (L_f) and Acoustic Impedance (Z) are calculated using standard relations and are tabulated.

The ultrasonic velocity of Coconut oil is lesser than all the other edible oil. All the other oil were found to have equal values for ultrasonic velocity.

Density value for all the edible oil was found to be equal.

Viscosity of Coconut and Groundnut oil were found to be very nearly equal. The values of viscosity for Sunflower and Sesame oil were also found to be approximately equal in value but higher than Coconut oil and Groundnut oil. Neem oil was found to have the highest viscosity value.

Adiabatic compressibility of all edible oil was almost equal except Coconut oil which was slightly higher.

Intermolecular free length of Groundnut oil, Neem oil and Sunflower oil was calculated and found to be equal in values, but the value of Intermolecular free length of Sesame oil was found to be less and that of Coconut oil was slightly greater than others.

Coconut and Groundnut oil had almost equal values of ultrasonic attenuation. Sunflower and Sesame oil were found to have equal values. Neem oil was found to have highest value among all the above.

The value of acoustic impedance was found to be nearly equal for all the edible oil.

Groundnut oil was found to have the least value for relaxation time and Neem oil the maximum value. Relaxation time was almost the same for Coconut oil, Sunflower oil and Sesame oil.

SAMPLE	ULTRASONIC VELOCITY (U) x 10 ³ (m/s)	DENSITY (ρ) 10 ³ (Kg/m ³)	VISCOSITY (η) x 10 ⁻² (Ns/m ²)	ADIABATIC COMPRESSIBILITY (β _a) x 10 ⁻¹⁰ (m ² /N)	INTERMOLECULAR FREE LENGTH (L _f) x 10 ⁻¹⁰ (m)	ULTRASONIC ATTENUATION (α/ρ ²) x 10 ⁻¹¹ (Np/m s ²)	ACOUSTIC IMPEDANCE (Z)x10 ⁶ (Kg/ m ² /s)	RELAXATION TIME (τ)x 10 ⁻¹³ (s)
COCONUT OIL	1.380	0.9528	3.429	5.5111	0.5514	4.9690	1.3149	2.5199
GROUNDNUT OIL	1.440	0.9462	3.335	5.0964	0.5099	4.4687	1.3626	2.2662
NEEM OIL	1.440	0.9599	6.148	5.0237	0.5027	8.1213	1.3823	4.1185
SUNFLOWER OIL	1.440	0.9527	4.048	5.0619	0.5065	5.3877	1.3718	2.7322
SESAME OIL	1.440	0.9532	4.120	5.0592	0.4501	5.4807	1.3726	2.7794

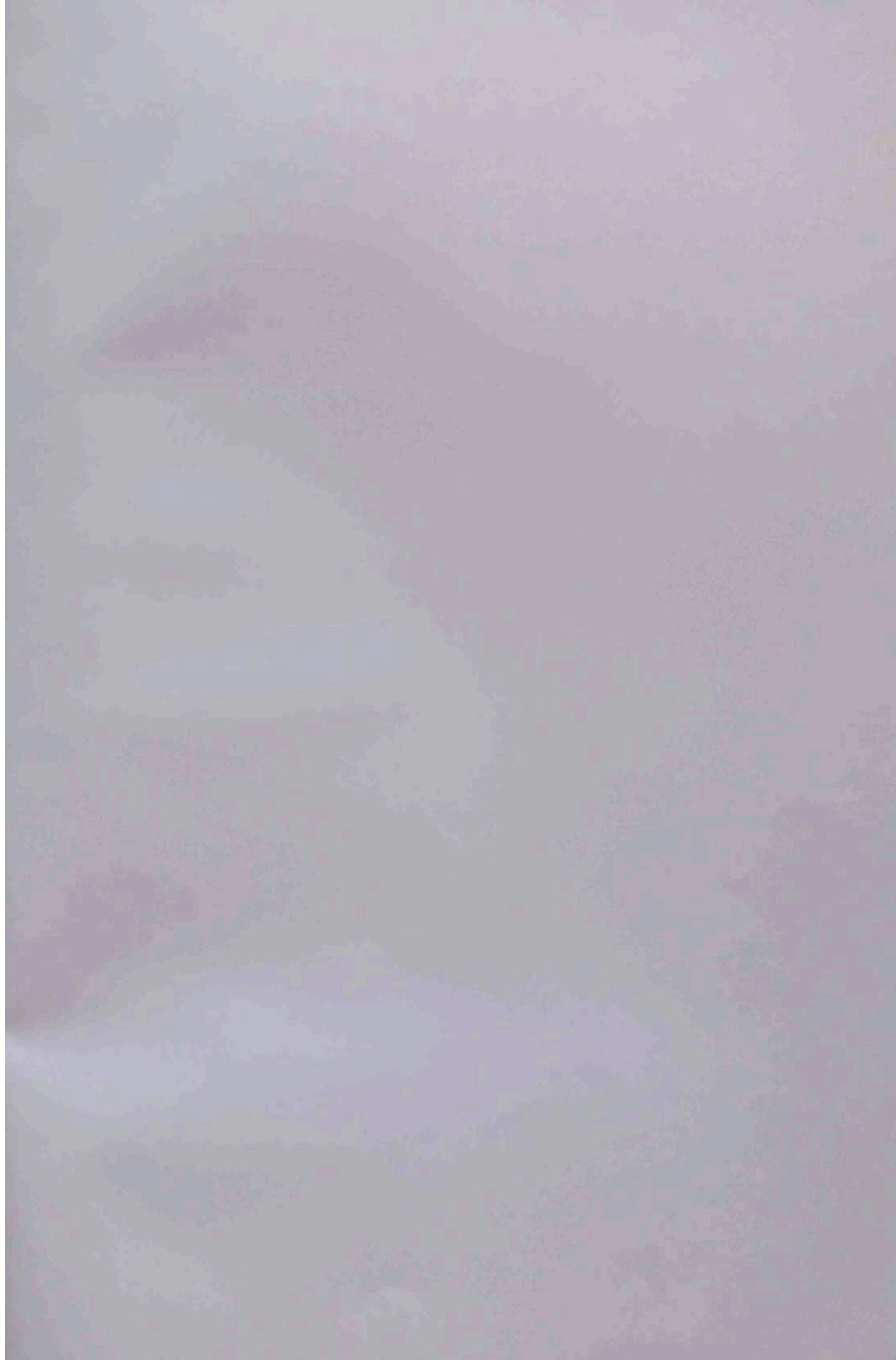
CONCLUSION.

The ultrasonic velocity (U), Density (ρ) and Viscosity (η) have been measured for various edible oil at room temperature 304K. From these data, few acoustic parameters such as Adiabatic Compressibility (β_a), Intermolecular Free Length (L_f), Acoustic Impedance (Z) and Relaxation time (τ) have been computed using standard relations. These variations in ultrasonic velocity and other parameters plays a significant role in understanding the different properties of edible oil and hence can be utilized for medical applications.

BIBLIOGRAPHY

LIST OF REFERENCES

- Bhattacharya. "Ultrasonic propagation in Coconut oil". *Pramana* (1981), Volume 21.
- Gladwell N, Javanaud C, Rahalkar. "Ultrasonic behaviour of edible oil in correlation with Rheology". *Journal of the American oil chemists*, (1985).
- Jaafar R, Shaari A, Kassim , R & NAW, M.N. "Ultrasonic determination of Palm oil content in michella", *Proc seminar on Industrial Physics* (Mass publisher Bangi, Selangor ,Malaysia), (1993).
- Mc Clements DJ, Povey, MJW, Jury. "Ultrasonic characterization of a food Emulsion". *Application of ultrasound for the functional modification of proteins and Sub micron emulsion fabrication*, (1990).
- Mohammed E.A and Mohammed R, Alhajhoj. "Importance and Applications of Ultrasonic Technology to Improve Food Quality", (2018).
- DOI: <http://dx.doi.org/10.5772/intechopen.88523>
- Mohammad Ali SK, Bashrath Ali. "Ultrasonic velocity for commonly used Edible oil". *International journal of science, Environment and Technology*, (2014).
- Najmie M.M.k , Khalid K, Sidek A, Jusoh MA. "Density and Ultrasonic characterization of Palm oil Trunk infected by Ganoderma Boninense disease". *Measurement Science Review*, (2011).
- Nikolic Biban , Kegl Breda, Markovic Sasa D, Miltovic Melanija S. "Determination of speed of sound and velocity of fluids depending on pressures", (2012).
- Rahalkar R.R, Javanand C. "Velocity of sound in vegetable oil". *Journal of American Oil chemists*, (1998).
- Rao, Reddy, LCS and Prabhu, CAR. "Adulteration is oil and fats by ultrasonic method." *International Journal of food science and technology*, (1980).
- Sidek HA.A, Chow S.P, Shaari A.H, Shenin. "Ultrasonic studies of Palm oil and other in vegetable oil", (1996).



SOLAR INVERTER

Project report submitted to St.Mary's College (Autonomous),
Thoothukudi, Affiliated to MANONMANIAM
SUNDARANAR UNIVERSITY, Tirunelveli, in the partial
fulfillment of the requirement for the award of

BACHELOR'S DEGREE IN PHYSICS

BY

R. AKSHAYA PRABA	18AUPH01
J. B. DOSHINI	18AUPH16
R. JOLIN MACHADO	18AUPH22
S. MANIMALA	18AUPH28
K. S. RATHIKA	18AUPH37

Guide and supervisor

Mrs. R. Maria Nevis Jeyaseeli M.Sc., B.Ed., M.Phil.,



DEPARTMENT OF PHYSICS

St. Mary's College (Autonomous), Thoothukudi.

(Re-Accredited with "A+" Graded by NACC)

2020 – 2021

CERTIFICATE

This is to certify that this project work entitled solar inverter is submitted to St. Mary's College (Autonomous), Thoothukudi, in partial fulfillment for the award of Bachelor's degree in Physics and it is a record of work done during the year 2020 – 2021 by the following students:

BY

- | | |
|--------------------|----------|
| 1. AKSHAYA PRABA.R | 18AUPH01 |
| 2. DOSHINI.J.B | 18AUPH16 |
| 3. JOLIN MACHADO.R | 18AUPH22 |
| 4. MANIMALA.S | 18AUPH28 |
| 5. RATHIKA.K.S | 18AUPH37 |

[Signature]
09/04/2021
GUIDE

[Signature]
HEAD OF THE DEPARTMENT
HEAD

Department of Physics,
St. Mary's College (Autonomous),
Thoothukudi - 628 001.

A. Lucas Rexulu
EXAMINER
19/4/21

Lucia Rose
PRINCIPAL
St. Mary's College (Autonomous)
Thoothukudi - 628 001.

ACKNOWLEDGEMENT

Our fervent thanks to God Almighty for guiding us in the completion of our project work successfully.

We express our deep sense of gratitude to our respected principal Dr. Sr. A. S. J. Lucia Rose M.Sc., PGDCA, M.Phil., Ph.D., for permitting us to utilize all the necessary facilities of the institution for carrying out our project work.

We record our sincere thanks for the valuable suggestions made by our Head of the department Dr. Sr. Jessie Fernando M.Sc., M.Phil., Ph.D., in the completion of our project.

We owe our deep gratitude to our guide Mrs. R. Maria Nevis Jeyaseeli M.Sc., B.Ed., M.Phil., who took keen interest on our project work and revitalized us to do our project work successfully.

We are thankful to and fortune enough to get constant encouragement, support and guidance from all the teaching staffs of our department and we would like to extend our sincere esteems to all staff in laboratory for their timely support.

We are also thankful to our parents and one and all who have helped us directly and indirectly to bring out this project successfully.

CONTENT

TITLE	Page number
CHAPTER 1	1
1.1 Aim of the project	2
1.2 Introduction to Energy Resources	3
• NON-RENEWABLE ENERGY	4
• RENEWABLE ENERGY	5
• SOLAR ENERGY	6-10
CHAPTER 2	11
2.1 Literature Review	12-13
CHAPTER 3	14
3.1 Solar Inverter	15
3.2 Types of solar Inverters	16-20
CHAPTER 4	21
4.1 Principle	22
4.2 Hardware requirements	23-30
CHAPTER 5	31
5.1 Block diagram	32
5.2 Circuit diagram	33
5.3 Working of solar inverter	34-35

CHAPTER 6	36
6.1 Tabulation	37
6.2 Graph	38
CHAPTER 7	39
7.1 Advantages	40
7.2 Disadvantages	41
7.3 Applications	42
7.4 Scope for future use	43-44
CHAPTER 8	45
8.1 Conclusion	46
8.2 Bibliography	47

CHAPTER - 1

1.1 AIM OF THIS PROJECT:

- The main aim of this project is to use solar energy for household loads using an inverter. Solar energy is converted to electrical energy by photo-voltaic (PV) cells. This energy is stored in batteries during day time for the utilization purpose whenever required
- .
- A solar inverter converts the direct current (DC) output of a photovoltaic solar panel into a utility frequency alternating current (AC) that can be fed into a commercial electrical grid or used by a local, offline electrical network
- To find the efficiency of the standalone battery backup solar inverter that can be used for easy installation of solar inverters in rural households.

1.2 INTRODUCTION TO ENERGY RESOURCES

Energy is the capacity to do work and is required for life processes. An energy resource is something that can produce heat, power life, move objects, or produce electricity. Matter that stores energy is called a fuel. Human energy consumption has grown steadily throughout human history. Early humans had modest energy requirements, mostly food and fuel for fires to cook and keep warm. In today's society, humans consume as much as 110 times as much energy per person as early humans. Most of the energy we use today come from fossil fuels (stored solar energy).

There are two type of energy sources

- 1) Non-Renewable Energy Sources
- 2) Renewable Energy Sources

NON-RENEWABLE ENERGY SOURCES

Non-renewable energy comes from sources that will run out or will not be replenished in our lifetimes-or even in many, many lifetimes ^[1]. Most non-renewable energy sources are

- **Fossil fuels**

Fossil fuels are formed due to the continuous heating and compressing of organic matter buried beneath the earth's surface. The organic matter mainly comprises of plant and animal remains that have decomposed, heated, and compressed over million of years to form fossil deposits.

The deposits are extracted through drilling or mining and they can be in liquid, gas or solid form. fossil fuels are highly combustible, making them as rich source of energy. Example of fossil fuels include:

- **Crude oil**

Crude oil, also referred to as petroleum oil is the only non-renewable resource that is extracted in liquid form. It is found between the layers of earth's crust or between the rocks and it is retrieved by drilling a vertical well into ground and ocean floor.

- **Natural gas**

Natural gas is a gaseous non-renewable resource that is found to below the earth's crust but near crude oil deposits in the subsurface. Natural gas primarily consists of methane, but may also contain other forms of natural gas such as propane, ethane and butane. Methane is odorless and it is mixed with a special additive to give it an odor for easy detection in case there is gas ovens, stoves and grills.

- **Coal**

Coal is created by compressed organic matter and it contains carbon and hydrocarbon matter ^[2]. It is formed from plant filled swamps that have been covered by sediments for millions of years. Coal is extracted by digging up the ground and taking out the coal solids for processing into energy. The main types of coal are anthracite, lignite, bituminous coal and sub-bituminous coal. Bituminous is found in the United States. It has high heat content and is used in generating energy and in making steel and iron. Anthracite have high heating value and is used in metal industry.

- **Nuclear Energy(uranium)**

Nuclear energy is primarily obtained through the mining and refining of uranium ore, a naturally occurring radioactive element below the earth's surface. Uranium is found in small quantities and miners often gather the uranium deposits for refining and purification. The mineral generates power through a process known as nuclear fusion which creates enough pressure to run turbines and generate nuclear power

RENEWABLE ENERGY SOURCES

Wind, solar, and biomass are three emerging renewable sources of energy. Renewable energy is generally defined as energy that is collected from resources which are naturally replenished on a human timescale, such as sunlight, wind, rain, tides, waves, and geothermal ^[3].

- **Wind power**

Wind power is another renewable energy. The wind's kinetic energy makes turbines spin creates a mechanical movement. Afterwards, a generator transforms this mechanical energy into electricity. There are several types of wind renewable energies onshore wind turbines, offshore wind turbines and even floating wind turbines. But the operating principles are basically the same for all these types of wind –generated energy.

- **Hydro-Electric Power**

Hydroelectric power consists in the transformation of the kinetic energy of the water (from rivers, dams, marine currents or tides) into mechanical energy by turbines

- **Biogas**

Biomass is made up of organic materials from plants or animals that contain stored energy. The combustion of these natural materials produce renewable energy. Some examples of generating energy from biomass are

- ✓ Directly burning the solid biomass like garbage or wood to produce heat.
 - ✓ Converting biomass into biogases such as methane or CO₂ due to bacterial activity that happens in the absence of oxygen
- Using sugar or corn crops to create bio-fuels such as bio-ethanol and biodiesel and mixing them with fossil fuels afterward.

Geothermal Power

The Earth's generates and stores geothermal energy. Radioactive materials decaying inside the Earth are emitting energy. Electricity can be created using directly or indirectly this energy depending on the technology implemented ^[5].

SOLAR ENERGY

Solar energy is quite simply the energy produced directly by the sun and collected elsewhere, normally from the Earth. The process creates heat and electromagnetic radiation. The heat remains in the sun and is instrumental in maintaining the thermonuclear reaction. The electromagnetic radiation (including visible light, infra-red light, and ultra-violet radiation) streams out into space in all directions ^[6].

Only a very small fraction of the total radiation produced reaches the Earth. The radiation that does reach the Earth is the indirect source of

nearly every type of energy used today. The exceptions are geothermal energy, and nuclear fission and fusion. Even fossil fuels owe their origins to the sun; they were once living plants and animals whose life was dependent upon the sun. Much of the world's required energy can be supplied directly by solar power. More still can be provided indirectly.

Due to the nature of solar energy, two components are required to have a functional solar energy Generator. These two components are a collector and a storage unit. The collector simply collects the radiation that falls on it and converts a fraction of it to other forms of energy (either electricity and heat or heat alone). The storage unit is required because of the non-constant nature of solar energy; at certain times only a very small amount of radiation will be received. At night or during heavy cloud cover, for example, the amount of energy produced by the collector will be quite small. The storage unit can hold the excess energy produced during the periods of maximum productivity, and release it when the productivity drops. In practice, a back up power supply is usually added, too, for the situations when the amount of energy required is greater than both what is being produced and what is stored in the container. In 21st century solar energy is expected to become increasingly attractive as a renewable source because of its inexhaustible supply and its non-polluting character. The “photovoltaic effect” is the mechanism by which Silicon solar panels harness the sun's energy and generate electricity ^[5].

SOLAR CONSTANT

Solar constant, total radiation energy received from the sun per unit of time per unit of area on a theoretical surface perpendicular to the sun's rays and at Earth's mean distance from sun. The solar constant is used to quantify the rate at which energy received upon a unit surface such as solar panel. Solar constants are used in various atmospheric and geological

sciences. The relative constant does vary by 0.2% in a cycle that peaks once every eleven years. The first attempt at estimating solar constant was made by Claude Pouillet in 1838 at made by Claude Pouillet in 1838 at kW/m². The constant is rated at a solar minimum of 1.361kW/m² and a solar maximum of 1.362 ^[2].

USES OF SOLAR ENERGY

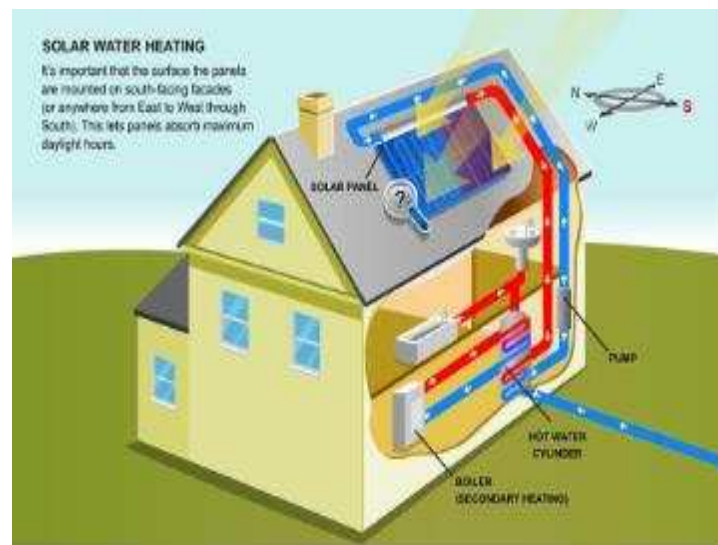
People use energy for many things, but a few general tasks consume most of the energy. These tasks include transportation, heating, cooling, and the generation of electricity. Solar energy can be applied to all four of these tasks with different levels of success.

HEATING

Heating is the business for which solar energy is best suited. Solar heating requires almost no energy transformation, so it has a very high efficiency. Heat energy can be stored in a liquid, such as water, or in a packed bed. A packed bed is a container filled with small objects that can hold heat (such as stones) with air space between them. Heat energy is also often stored in phase-change or heat-of-fusion units. These devices will utilize a chemical that changes phase from solid to liquid at a temperature that can be produced by the solar collector.

The energy of the collector is used to change the chemical to its liquid phase, and is as a result stored in the chemical itself. It can be tapped later by allowing the chemical to revert to its solid form. Solar energy is frequently used in residential homes to heat water. This is an easy application, as the desired end result (hot water) is the storage facility. A hot water tank is filled with hot water during the day, and drained as

needed. This application is a very simple adjustment from the normal fossil fuel water heater.



HEATING APPLICATION OF SOLAR ENERGY

COOLING

Solar energy can be used for other things besides heating. It may seem strange, but one of the most common uses of solar energy today is cooling. Solar cooling is far more expensive than solar heating, so it is almost never seen in private homes. Solar energy is used to cool things by phase changing a liquid to gas through heat, and then forcing the gas into a lower pressure chamber. The temperature of a gas is related to the pressure containing it, and all other things being held equal, the same gas under a lower pressure will have a lower temperature. This cool gas will be used to absorb heat from the area of interest and then be forced into a region of higher pressure where the excess heat will be lost to the outside world. The net effect is that of a pump moving heat from one area into another, and the first is accordingly cooled ^[6].

TRANSPORTATION

Of the main types of energy usage, the least suited to solar power is transportation. While large, relatively slow vehicles like ships could power themselves with large onboard solar panels, small constantly turning vehicles like cars could not. The only possible way a car could be completely solar powered would be through the use of battery that was charged by solar power for a photovoltaic cell is only 32.3%, but at this efficiency, solar electricity is very economical. Most of our other forms of electricity generation are at a lower efficiency than this. Unfortunately, reality still lags behind theory and a 15% efficiency is not usually considered economical by most power companies, even if it is fine for toys and pocket calculators. Hope for bulk solar electricity should not be abandoned, however, for recent scientific advances have created a solar cell with an efficiency of 28.2% efficiency in the laboratory. This type of cell has yet to be field tested. If it maintains its efficiency in the uncontrolled environment of the outside world, and if it does not have a tendency to break down, it will be economical for power companies to build solar power facilities after all. Now, we know that solar panel transfers electrons into DC, and most appliance at home is using AC, why we use inverters ^[3].

CHAPTER – 2

2.1 LITERATURE REVIEW

[Britt; Jeffery s. (tucson.AZ) Wiedeman; Scott (Tucson.AZ) 2012]

They have presented an experimental investigation to study a semiconductor material used in a PV cell and its importance in determining the efficiency of the solar cell at various parameters such as regards to behavior with respect to temperature, weight and as well as other parameters with which it is used and all those contribute to the deciding factor of efficiency of the PV cell. The inventor has conducted many experimental researchers to devise improvised methods and apparatus for forming thin film layers of semiconductor materials. The field of photovoltaic generally relates to multi-layer materials, converts sun light directly into DC Electrical Power. The basic mechanism for this conversion is “The Photovoltaic Effect”. Solar cells are typically configured as a co-operating sandwich of P-Type and N-Type semiconductors, in which the N-Type semi-conductor material (on one side of the sandwich) exhibits an excess of electrons and the P-Type semiconductor material (on the other side of the sandwich) exhibits an excess of holes each of which signifies the absence of an electron.

[Ho; Frank. (Yorba Linda, CA) Yeh; Milton Y (Santa Monica, CA) 1995]

Has worked on in improving the efficiency of Solar Cells. They have found that the efficiency of the solar cell varies from 15% to 22% and innovations are being carried out by changing the combination of semiconductor material in the PV cell and find out improved efficiency. The inventor has analyzed the properties of semiconductor material thoroughly and has come out with a combination of cells- cascaded cell, permits achieving more than overall efficiency of 23%. Up to the present time it has been proposed to use either Germanium or Gallium Arsenide as the substrate for

solar cell in which the principal active junction is formed of N-Type and P-Type Gallium Arsenide. Attempts are continuing at developing solar cells that efficiently use as much of solar spectrum as possible. In order to catch as much as possible photons, the semiconductor used in the solar cell must be designed for a small band gap, since the semiconductor material is otherwise transparent to radiation with photon energy less than the band gap.

[Bareis; Bernard F (Plano, TX) and Goei; E Esmond T. (Dublin, CA) 2004] They have investigated on the concentrating solar energy receivers. In their study they have commented that the solar collectors can be classified into focusing type (concentrating type) and Non – focusing type (non-concentrating type). The inventor has designed the concentrating type solar energy receiver comprising a primary parabolic reflector having a centre and a high reflective surface on a concave side of the reflector and having a fixed axis extending from the concave side of the reflector and passing through a fixed point of the primary parabolic reflector and a conversion module having a reception surface. Non concentrating type solar collecting devices intercept parallel un-concentrated rays of the sun with an array of photovoltaic cells. The output is the direct function of array.

[Zhao; Xiaofeng (Guangdong, CN) 2011] The authors have conducted a study on solar collecting and utilizing device and have concluded that the efficacy of a solar energy conversion system depends on the various parameter such as the quantum of radiation, intensity, direction, the tilt angle of the collector, temperature etc. In case of solar collector and utilizing device the sun tracking and beam focused radiation are of paramount importance. This device consist of paraboloidal mirror, a sun

light collector, a solar storage and conversion device and a solar tracking equipment wherein said sunlight collector compresses a light guide which convert factual into substantially parallel light beam and deflect them in a desired direction and a curved surface condenser mirror which receive the substantially parallel light beams reflected from the light guider and converting them into a solar storage and conversion.

[SB Sadati, M.Yazdani – Asrami and others 2010]

The author worked on evaluation of supplying ruler and residential area using photovoltaic systems in I.R. Iran. They have commented on use of sun's energy has the biggest energy supplies and is clean and annexable source which can be utilize by using appropriate technologies. The total solar radiation received by different regions throughout the year the average energy consumption required effect of temperature voltage – current curve characteristics have been conceder for evolving a photo voltaic system to meet the domestics required, economic analysis has been made for justification of the use age of photovoltaic system.

[Zhao; Xiaofeng (Guangdong, CN) 2007]

They had worked Solar Collectors. The solar device is categorized as a multi-layer heat storage structure and the said heat storage structure corresponds to plurality of curved surface mirrors and as a light receiving hole for receiving the condensed light from the curved surface mirror. The heat structure contains a working fluid to transfer of storing the energy such as groups of melted salts, water steam, smelting raw material and photo electric cell. As compared thermal power generation the solar electric power generation reduces the civil works in the building, avoids pollution,

waste handling and air preheat-pollution treatment with comparative calculation for building a solar thermal power station, it is inferred that it's costs intensive compared to conventional power station. However considering the environmental impact on the space occupation and land usage, his method is more appropriate.

[Coc Oko and S.N Nanchi 2012]

They have worked on Optimum Collector Tilt Angle for low latitudes. There are many factors that affect the solar radiations falling on the earth. Some of the factors that affect the intensity of the extra-terrestrial solar radiation on the earth's horizontal and tilted surfaces are clouds, dusts and shades. In designing the solar equipment, the designer has to pay more attention towards harnessing the isolation to the optimum level for effective performance of the equipment. Determination of the tilt angle at lower latitudes is one such effort for a country like Nigeria.

[Nataraj Pandiarajan, Rama Badran, Rama Prabha and Ranganathan 2012]

They have worked on application of circuit model for energy conversion system. The solar energy is directly converted to electrical energy without any electrical parts by the use of photovoltaic system. PV system is widely utilized to cater power demands of the society in many countries. The efficacy of the PV system depends on the operation of the system components and its performance. The efficiency of the solar system conversion technology stands at about 15 to 25% mainly because of the conversation of DC power to AC power through battery banks. The best way to utilize the PV System energy is to deliver it to the AC mains directly, without battery banks. Studies on the PV system in operation reveal that inverters contribute to 63% failure rate, modules 15% and other components 23% with a failure occurring on an average of every 4 to 5

to 12 years. To reduce the failure rate of the PV systems it is necessary to reduce failure rates of inverters and components of effective performance.

CHAPTER - 3

3.1 SOLAR INVERTER

A solar inverter is similar to a normal electric inverter but uses the energy of the sun (i.e) solar energy. A solar inverter helps in converting the direct current into alternating current with the help of solar power. Direct power is the power which runs in one direction inside the circuit and helps in supplying current when there is no electricity. Direct current are used for small appliances like mobile phones, mp3 players , IPod etc. where there is power stored in form of battery in case of alternating current, it is the power that runs back and forth inside the circuit. The alternate power is generally used for household appliances. A solar inverter helps devices that runs on DC power to run in ac power so that the user makes use of AC power ^[7].

Solar inverters are also called as photovoltaic solar inverters. These devices can help you save lot of money. The small-scale grid one have just two components (i e) the panels and the inverter while the off grid systems are complicated and consists of batteries which allow users to use appliances during the night when the sunlight is not available. The solar panels and batteries that are placed on rooftops attract sun's rays and then converts the sunlight into electricity.

The batteries too grab the extra electricity so that it can then be used to run appliances at night. Solar power inverters have special functions adapted for use with photovoltaic arrays, including maximum power point tracking and anti-islanding protection.

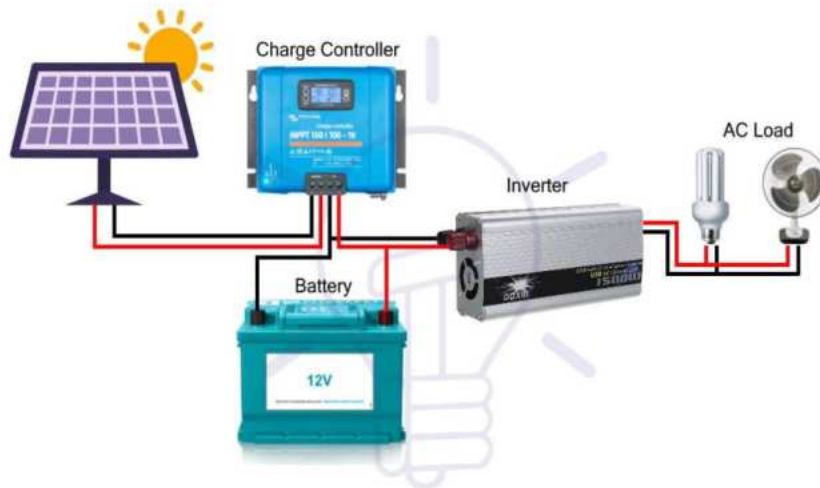
3.2 TYPES OF SOLAR INVERTER

There are several types of solar inverters. Some of them are mentioned below :-

- Stand-Alone Inverters
- Grid Tie Inverters
- Battery Backup Inverters
- String Inverters
- Micro-Inverters
- Central Inverters

STAND –ALONE INVERTERS

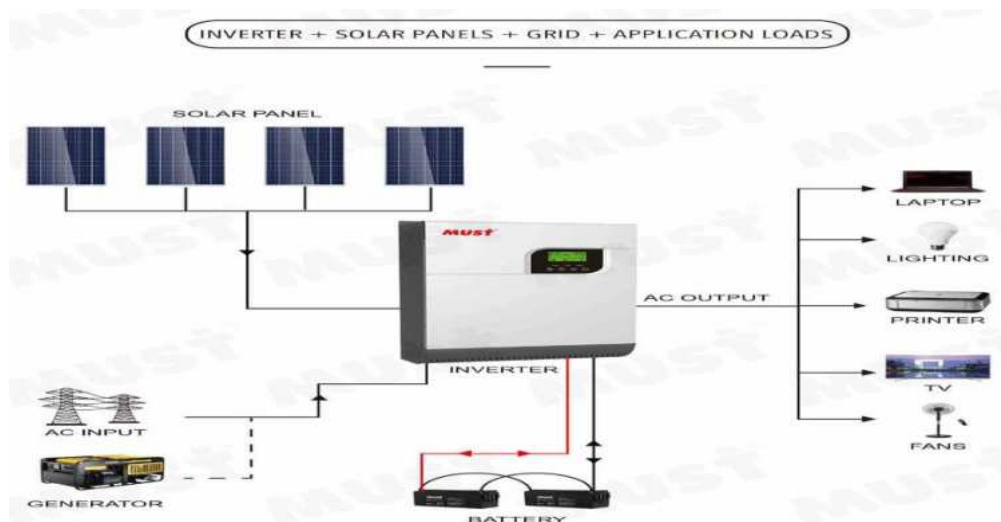
Stand-Alone inverters used in isolated system where the inverter, draws its DC energy from batteries charged by photovoltaic arrays .Many stand-alone inverters also incorporate integral battery charges to replenish the battery from an AC source, when available. Normally these do not interface in any way with the utility grid, and such are not required to have anti-islanding protection ^[8].



Stand-alone Inverter

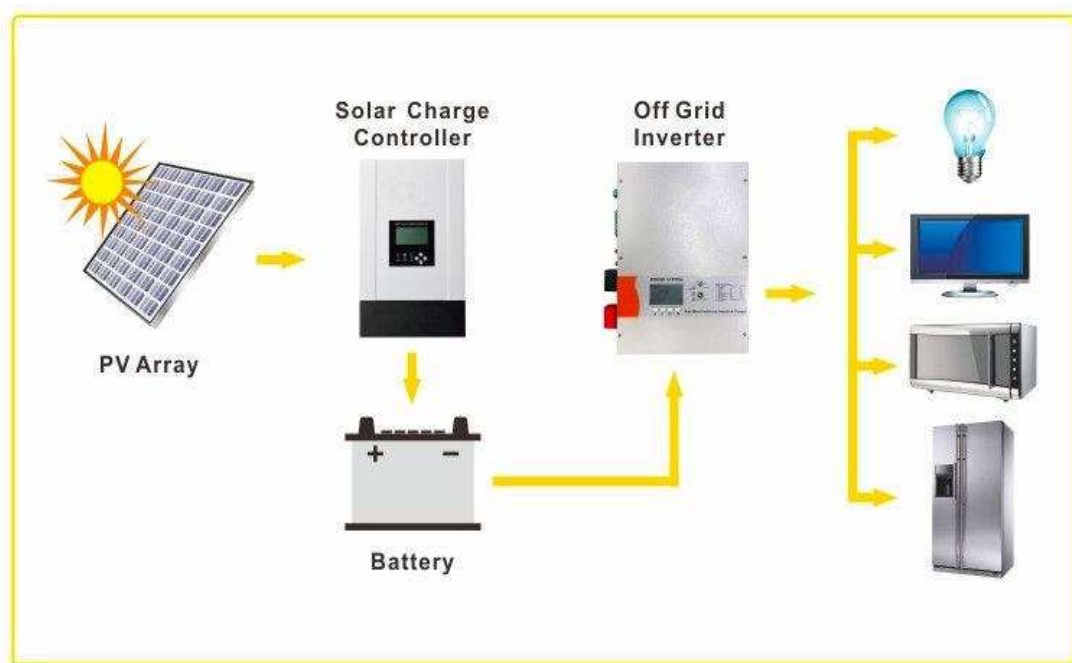
GRID TIE INVERTERS

Grid Tie inverters, which match phase with a utility-supplied sine wave grid tie inverters are designed to shut down automatically upon loss of utility supply, for safety reasons. They do not provide backup power during utility outages.



BATTERY BACKUP INVERTERS

Battery backup inverters are special inverters which are designed to draw energy from, a battery manage the battery charge via an onboard charger and export excess energy to the utility grid. These inverters are capable of supplying AC energy to selected loads during a utility outages and are required to have anti-islanding protection.

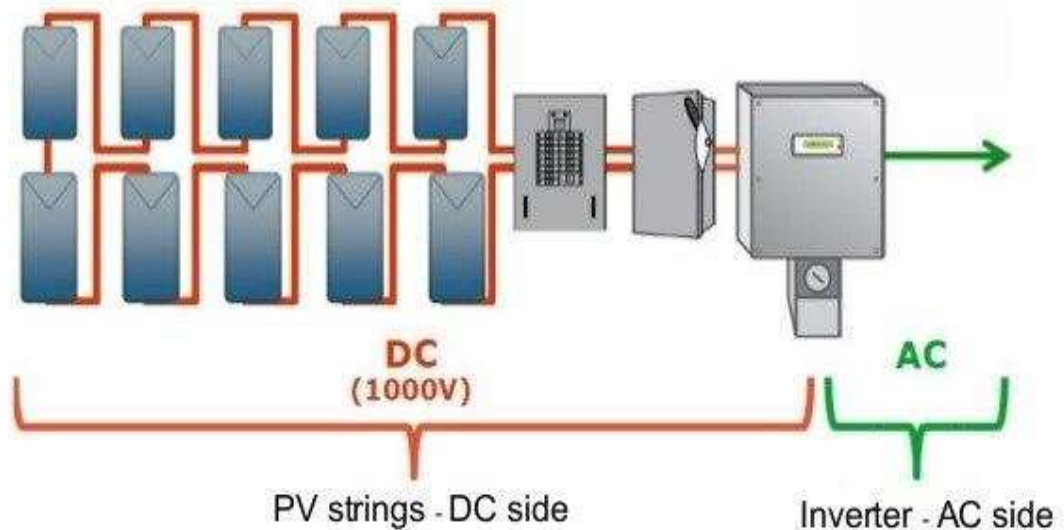


STRING INVERTERS

String Inverters multiplies strings originates from the solar panels are attached to the inverters and the DC electricity produced in them are then transformed into AC current. A solar system located on a roof doesn't require more than one or a maximum of two-string inverters. They are cheaper than other types of inverters and kept in the closer proximity of fuse box and electricity meter. The problem with this type of inverter is that if one panel is obstructed with shading, the remaining panels will be sabotaged too and the efficiency will go down to a significant amount

besides, less scope to expand the solar panels for the future. This type of inverters is the main type of solar inverter at home.

String inverter layout



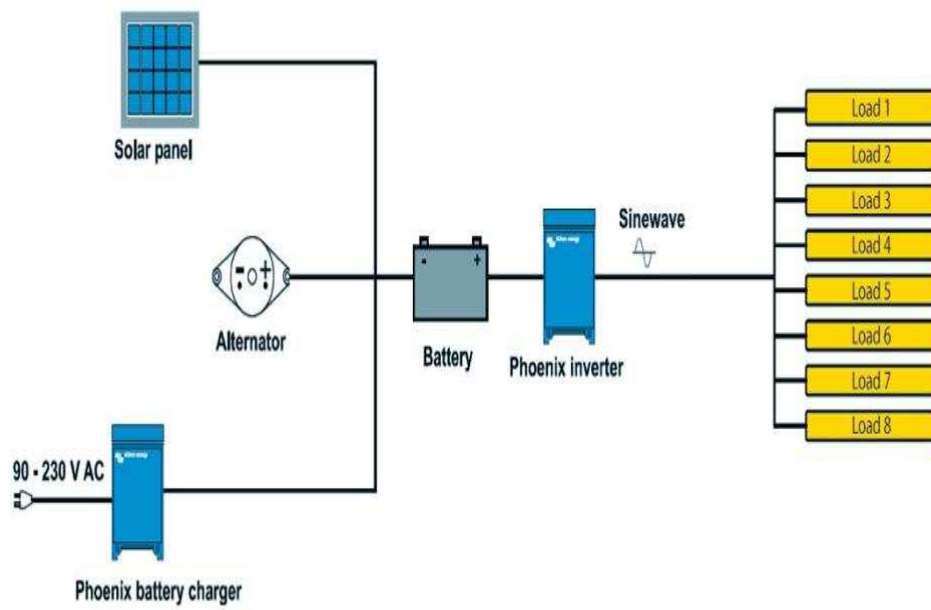
MICRO-INVERTERS

Microinverters installed for each panel to optimize each panel's power in a module-level. so the transformation of the DC current to AC happens in each inverter connected to each panel. Therefore shading on one panel will not impinge upon the other panels, results in less variation or no compromise of the optimum efficiency. Alongside the commercial use, micro inverters are chosen as the best solar inverter for home as well. Although they used to be expensive in the past, their prices have recently gone down to a reasonable level.



CENTRAL INVERTERS

It resembles the string inverters, but instead of putting the strings of panels in the inverter, it joints all of the strings of panels together and inserts it into a combiner box which is kept in a protected territory. Afterwards, the strings are then connected to an inverter which receives the DC electricity from the combiner box and a pad, its installation cost is very less. It is less vulnerable to any physical or natural damage since it's kept in a protected area, which is free from any harsh weather. Since they have more capacity compared with string and micro-inverter, they are mostly used in large scale properties.



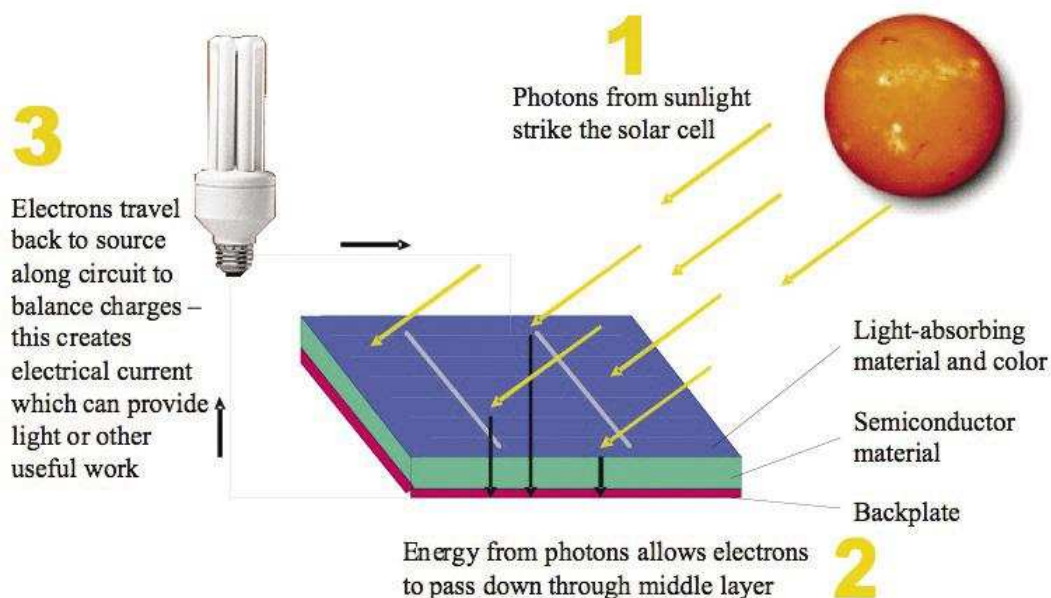
CHAPTER- 4

4.1 PRINCIPLE OF SOLAR INVERTER

A solar inverter or PV inverter converts the direct current output of a photovoltaic (PV) solar panel into utility frequency alternating current, (AC) that can be fed into commercial electrical grid or used by a local, off-grid electrical network. It is critical component in a photovoltaic system allowing the use of ordinary commercial appliances. Solar inverters have special functions adapted for the use with photovoltaic arrays, including maximum power point tracking and anti-islanding protection

PHOTOVOLTAIC EFFECT

The photovoltaic effect is a process that generates voltage or electric current in a photovoltaic cell when it is exposed to sunlight. It is this effect that makes solar panels useful, as it is how the cells within the panel convert sunlight to electrical energy. The photovoltaic effect was first discovered in 1839 by Edmond Becquerel ^[10].



ANTI-ISLANDING PROTECTION

Anti-islanding protection is a way for the inverter sense when there is a problem with the power grid, such as power outage and shut itself off to stop feeding power back to the grids ^[11].

4.2 HARDWARE REQUIREMENTS

1. SOLAR PANEL

A solar panel (also solar module, photovoltaic module or photovoltaic panel) is a packaged, connected assembly of solar cells, also known as photovoltaic cells. The solar panel can be used as a component of a larger photovoltaic system to generate and supply electricity in commercial and residential applications. Because a single solar panel can produce only a limited amount of power, many installations contain several panels. A photovoltaic system typically includes an array of solar panels, an inverter, and sometimes a battery and interconnection wiring. Solar panels use light energy (photons) from the sun to generate electricity through the photovoltaic effect. The structural (load carrying) member of a module can either be the top layer or the back layer. The majority of modules use wafer- based crystalline silicon cells or thin-film cells based on cadmium telluride or silicon. The conducting wires that take the current off the panel may contain silver, copper or other non-magnetic conductive transition metals.

Polycrystalline Solar Panels (Poly-SI)

You can quickly distinguish these panels because this type of solar panels has squares, its angles are not cut, and it has a blue, **speckled look**. They are **made by melting raw silicon**, which is a **faster and cheaper** process than that used for monocrystalline panels.

This leads to a lower final price but also lower **efficiency (around 15%)**, lower space efficiency, and a **shorter lifespan** since they are affected by hot temperatures to a greater degree. However, the differences between mono-and polycrystalline types of solar panels are not so significant and the choice will strongly depend on your specific situation. The first option offers a slightly higher space efficiency at a slightly higher price but power outputs are basically the same.



2. CAPACITORS:

The inverter works by chopping the DC from batteries at a high frequency and passing this chopped current to a small but powerful high-

frequency transformer, to be converted to higher voltage. The high voltage which is rectangular in form and also chopped, need to be rectified and made smooth, so in the next stage, the PWM sine wave former, to work.

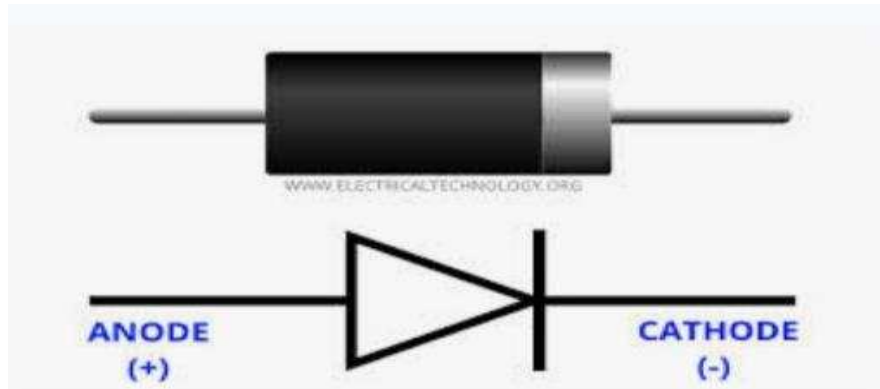
The word “smooth” implies that there need to be some form of energy storage to fill in with energy when the waveform has its peak voltage and to deliver that energy to the next inverter stage when the waveform has its valley.



3. DIODES:

If we were to connect two inverter gates together so that the output of one fed into the input of another, the two inversion functions would “cancel” each other out so that there would be no version from input to final output.

A special logic gate called a buffer is manufactured to perform the same function as two inverters. It’s symbol is simply a triangle, with no inverting “bubble” on the output terminal.



4. VARIABLE RESISTOR:

A variable resistor is a resistor of which the electric resistance value can be adjusted. A variable resistor is in essence an electro-mechanical transducer and normally works by sliding a contact over a resistive element. When a variable resistor is used as a potential divider by using 3 terminal it is called a potentiometer. When only two terminals are used, it functions as a variable resistance and is called a rheostat. Electronically controlled variable resistors exist, which can be controlled electronically instead of by mechanical action. These resistors are called digital potentiometers.



5. MOSFET:

A MOSFET or metal oxide semiconductor field Effect Transistor, unlike a Bipolar Junction Transistor (BJT) is a unipolar device in the sense that it uses only the majority carriers in the conduction.

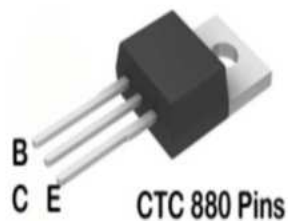
Switching in Electronics:

Semiconductor switching in electronic circuit is one of the important aspects. A semiconductor device like a BJT or a MOSFET are generally operated as switches i.e. they are either in ON state or in OFF



6. CTC880

Pin connection of CTC 880. Its equivalent is D 880

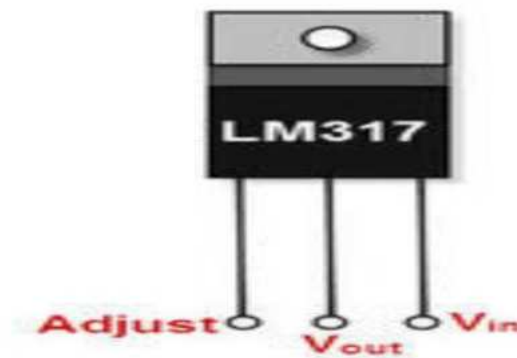


Features:-

- * NPN Low frequency power amplifier
- * DC current gain (hFE) ,typically 60 to 300
- * Continuous collector current is 3A
- * Collector-emitter voltage (VCE) is 60V
- * Emitter Base voltage(VBE) is 7V
- * Available in TO – 220 package

7. TC SEC KA317

It is a three terminal positive adjustable regulator



Features:-

- * Output current in Excess of 1.5A
- * Output adjustable between 1.2V and 37V
- * Internal Thermal overload protection
- * Internal short-circuit current limiting

* Output-Transistor Safe operating Area Corporation

* To – 220package

8. RESISTANCE (1 Kilo Ohm):

One kilo ohm is equal to 1000 ohms, which is the resistance between two points of a conductor with one ampere of a conductor with one ampere of current at one volt. The kilohm is a multiple of the ohm, which is the SI derived unit for electrical resistance. In the metric system, "Kilo" is the prefix for 10 ohm.



9. TRANSFORMER 12-0-12:

12-0-12 5 Amp Centre Tapped Step Down Transformer is a general purpose chassis mounting mains transformer. Transformer has 230V primary winding and centre tapped secondary winding. The transformer is a static electrical device that transfers energy by inductive coupling between its winding circuits.



10. 12V-8AH DC BATTERY(VIRLA):

A valve regulated lead-acid (VRLA) battery, commonly known as a sealed lead-acid (SLA) battery, is a type of lead-acid battery characterized by a limited amount of electrolyte absorbed in a plate separator or formed into a gel; proportioning of the negative and positive plates.



11. MULTIMETER:

A multimeter or multitester is a measuring instrument that can measure multiple electrical properties. A typical multimeter can measure voltage, resistance, and current, in which case it is also known as a volt-ohm-milliammeter. Analog multimeters use a microammeter with a moving pointer to display readings.



12. MULTICORE CONNECTING WIRES:

A multicore cable is a type of electrical cable that combines multiple signals or power feeds into a single jacketed cable. The term is normally only used in relation to a cable that has more cores than commonly encountered.

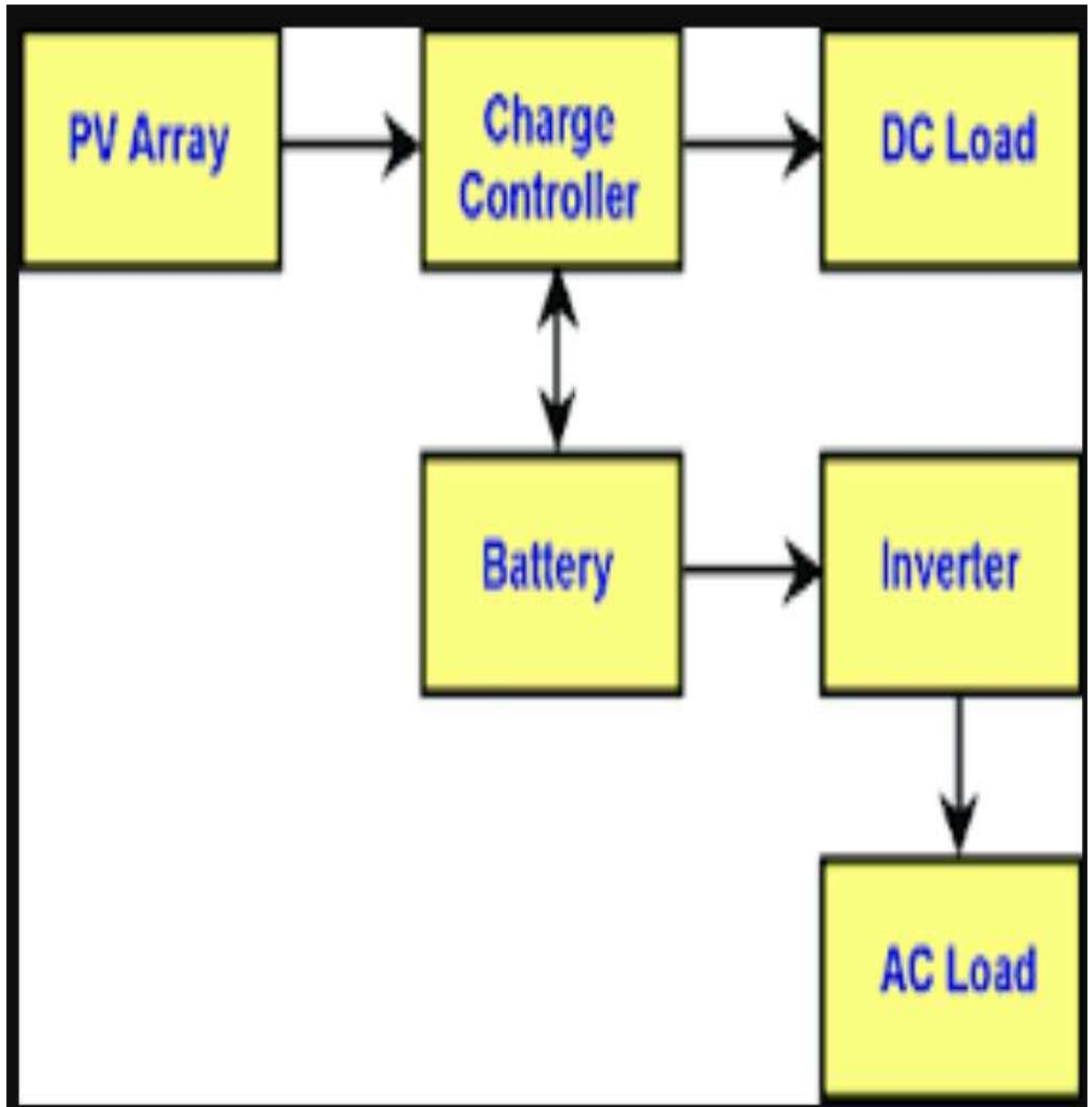


13. THERMAL CONDUCTORS:

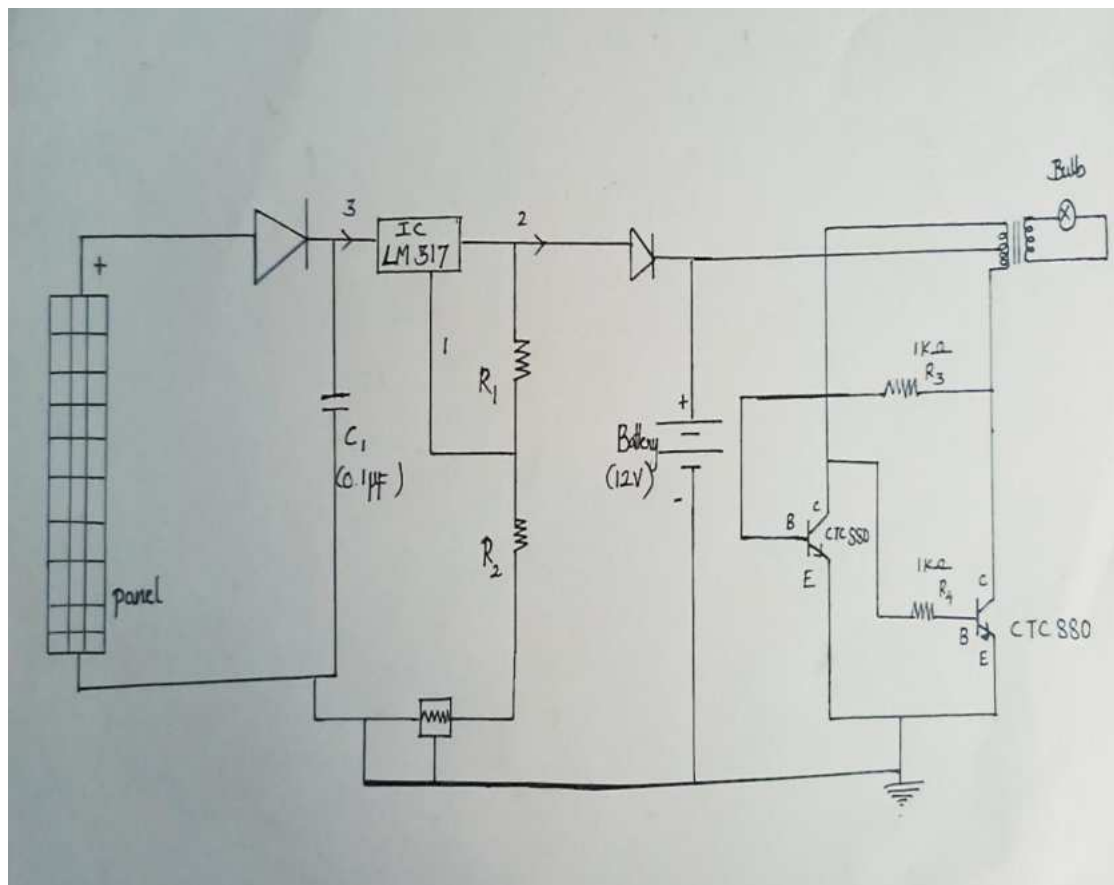
Conduction is the transfer of thermal energy between particles of matter that are touching. Materials that are good conductors of thermal energy are called thermal conductors. Metals are especially good thermal conductors because they have freely moving electrons that can transfer thermal energy quickly and easily.

CHAPTER – 5

5.1 BLOCK DIAGRAM



5.2 CIRCUIT DIAGRAM



5.3 WORKING OF SOLAR INVERTER

A Solar inverter works by taking in the direct current or DC output from our solar panel and transforming it into our alternating output 120V current or AC output. The appliances in our home run on AC, not DC, which is why the solar inverter must change the DC output that is collected by our solar panels.

The sun shines down on our solar panels (photovoltaic (PV) cells) which are made of semiconductor layers of crystalline silicon or gallium arsenide. These layers are combination of both positive and negative layers which are connected by a junction. When the sun shines, semiconductor

layers absorb light and send the energy to the PV cell. This energy runs around and bumps electrons loose and they move between the positive and negative layers producing an electric current known as Direct current (DC).

Once this energy is produced it is stored in a battery during daytime for the operation purposes whenever needed. The purposed system is designed to utilize solar energy for home loads using an inverter. Then the energy is sent to the inverter. when the energy is sent to the inverter, it is in the DC format but our home requires AC. The inverter grabs the energy and runs it through a transformer, which then splits out an AC output. The inverter, in essence, tricks the transformer into thinking that the DC is actually AC, by forcing it to act in a way like AC – the inverter runs the DC through two transistors on and off superfast and feed two varying sides of the transformer. The inverter will step up the voltage from 12 volts to 120 volts, which is the voltage used throughout the grid. This conversion of voltage is what allows a 12 volts DC solar panel to be tied into a 120 volt AC grid ^[12].





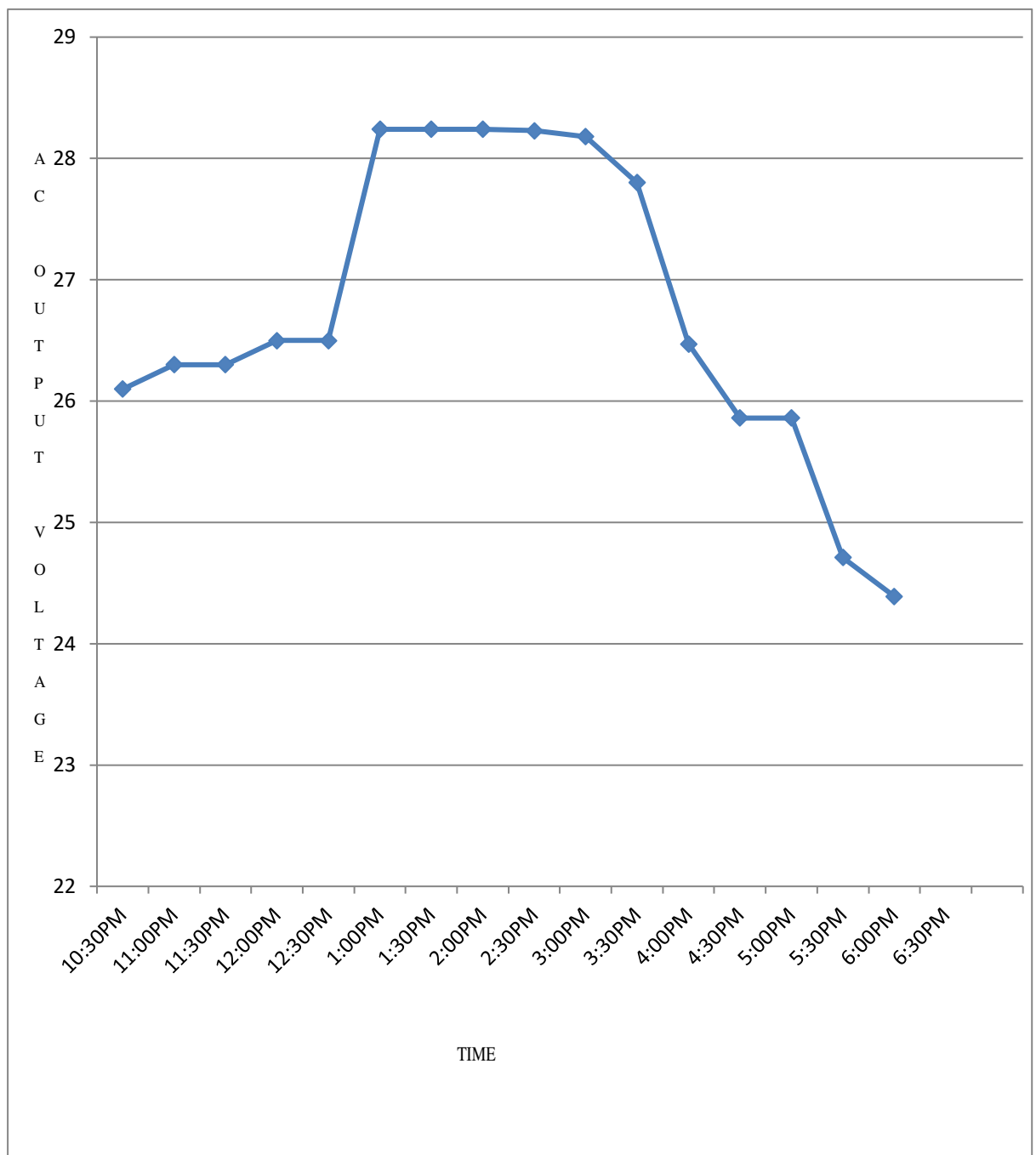


CHAPTER – 6

6.1 TABULATON

TIME	INPUT DC VOLTAGE FROM SOLAR PANEL	OUTPUT AC VOLTAGE FOR LOAD
10:30 AM	18.74	26.1
11:00 AM	19.3	26.3
11:30 AM	19.5	26.3
12:00 PM	20.1	26.5
12:30 PM	20.12	26.5
1:00 PM	20.29	28.24
1:30 PM	20.36	28.24
2:00 PM	20.34	28.24
2:30 PM	20.21	28.23
3:00 PM	20.1	28.18
3:30 PM	19.64	27.8
4:00PM	18.7	26.47
4:30 PM	15.24	25.86
5:00 PM	14.61	25.86
5:30 PM	13.37	24.71
6:00 PM	12.8	24.39
6:30 PM	12	23.9

6.2 GRAPH



Output AC voltages for Load from input DC voltage from panel at different timings on 26/03/2021 are measured, tabulated and graph is drawn. From the graph, it is seen that high voltage is drawn between 1:30 p.m. to 3:00 p.m. and further the voltage falls gradually as the time passes.

CHAPTER – 7

7.1 ADVANTAGES OF SOLAR INVERTER

- Solar energy has constantly helped in decreasing the green house effect and global warming.
- Solar based devices will help in saving money and also energy because many people have started using these devices.
- A Solar inverter helps in changing the DC into AC batteries. This supports people who uses a partial amount electricity [13].
- The synchronous solar inverter helps small home owners and also power companies as they are huge in size.
- The multifunction solar inverters the finest among all and works powerfully. It converts the DC to AC very carefully which is suitable for commercial establishments.
- This inverter is cost effective, low cost than generators, therefore there is a ease of installation.
- Solar inverter provides constant and uninterrupted power supply.
- There is no requirement of electricity and manpower to operate the device.
- As moving parts is not involved, its efficiency is further enhanced. It acts as a power backup solution.
- It is an eco-friendly means of power generation.
- It helps in reduction in consumption from conventional source of energy.
- High efficiency and outstanding energy harvest in a small modular design.
- Central and Micro-inverters can be up to 95% efficient.

7.2 DISADVANTAGES

- Central inverters is difficult to do properly and it's usually the hardest part of designing a solar energy ^[14].
- For central inverter, the output from your whole array can drop significantly, if any one of the panel is shaded.
- Micro-inverters are more expensive.

7.3 APPLICATIONS OF SOLAR INVERTER

- Solar inverters can be used domestic applications. It can be plugs in your houses for your TV, computer and other wired products ^[8].
- Solar inverters can be used for industrial applications.
- Solar inverter helps in DC power utilization.
- HVDC transmission can be done using solar inverters.
- Electric vehicle drives can be run through solar inverters.
- Solar inverters convert low frequency main AC power to a higher frequency used for induction heating ^[13].
- String inverters are most suitable for residential as well as commercial purposes as it covers the ambit of small utility installations that generally falls under 1MW. String inverters are best suitable for homeowners who are looking for lower-cost PV systems or properties with roofs that are uncomplicated and get consistent sunlight through the day.

- Central inverters are generally used for large commercial installations, industrial faculties or utility scale solar farms as central inverters support uniform and consistent production throughout. They are generally not preferred for residential requirements as their much smaller counter part—string inverters are sufficient for fulfilling household energy requirements.
- Micro inverters are best suitable for residential and commercial arrangements wherein the solar panels face different directions, hence combating inefficiencies created due to shading. It is costlier than string inverters but is the perfect solution for installations where there is a disparity in the amount of sunlight received by individual solar panels.
- Off Grid inverters are most suitable for remote or rural areas where the power grid would be impractical and uneconomical.
- Grid-Tie inverters are most suitable for homes and offices in urban areas which have access to power connections and lines to connect to the utility grid. Solar users who do not want to invest in batteries should opt for Grid-Tie inverters.
- Hybrid inverters are ideal for users who want to cut off costs by utilizing energy produced from sunlight during daytime as well as store the same in batteries to support energy usage after sunset. Hybrid solar inverters are a perfect choice for buyers who are encountering frequent power outages, faults and excessive load shedding.

7.4 SOLAR ENERGY AS A FUTURE

Solar power has two big advantages over fossil fuels. The first is in the fact that it is renewable it is never going to run out. The second is its effect on the environment ^[15].

POLLUTION FREE ENERGY

While the burning of fossil fuels introduces many harmful pollutants into the atmosphere and contributes to environmental problems like global warming and acid rain, solar energy is completely nonpolluting. While many acres of land must be destroyed to feed a fossil fuel energy plant its required fuel, the only land that must be destroyed for a solar energy plant is the land that it stands on. Indeed, if a solar energy system were incorporated into every business and dwelling, no land would have to be destroyed in the name of energy. This ability to decentralize solar energy is something that fossil fuel burning cannot match.

REDUCTION IN GREEN HOUSE GASES

Global warming and energy policies have become a hot topic on the international agenda in the last years. Developed countries are trying to reduce their greenhouse gas emissions. For example, the European Union has committed to reduce their greenhouse gas to at least 20% below 1990 levels and to produce no less than 20% of its energy consumption from renewable sources by 2020. In this context, photovoltaic (PV) power generation has an important role to play due to the fact that it is a green source. The only emissions associated with PV power generation are those from the production of its components. After their installation they generate electricity from the solar irradiation without emitting greenhouse gases. In their life time, PV panels produce more energy than that for their

manufacturing. Also, they can be installed in places with no other use, such as roofs and deserts.

CHAPTER – 8

8.1 CONCLUSION

Inverters are 95% efficient. Inverters play significant role in providing alternate current supplies at the times of crucial power requirements. The primary use of solar inverters is to convert direct current to alternating current through an electrical switching process.

Photovoltaic power production is gaining more significance as a renewable energy source due to its many advantages. These advantages include everlasting pollution free energy production scheme, ease of maintenance and direct sunbeam to electricity conversion. However, the high cost of PV installations still forms an obstacle for this technology. Moreover, the PV panel output power fluctuates as the weather conditions such as isolation level and cell temperature. The described design of the system will produce the desired output of the project. The inverter will supply an AC source from DC source. The project described is valuable for the promising potentials it holds within, ranging from the long run economic benefits to the important environmental advantages. This work will mark one of the few attempts for pollution free environment in the field of renewable energy. With increasing improvements in solar cell technology and power electronics, such projects would have more value added and should receive more attention and support.

8.2 BIBLIOGRAPHY

- [1] N.S. Subrahmanyam & A.V.S.S. Sambamurty, Ecology:
Alpha Science International Publications, UK (January 30, 2006), 2nd
edition;
- [2] Anuj kumar Rana & Manoj kumar Rana, Environment and Ecology:
Global vision publications, New Delhi (October 15, 2012)
- [3] MC Dash, Fundamentals of Ecology: Mc Graw Hill Education, India
(June 15, 2009), 3rd edition;
- [4] G.D. Rai, Nonconventional Energy sources: khanna publishers, Delhi
(January 1, 1973)
- [5] Khan.B.H, Non conventional source of Energy: published by
Mc Graw Hill, India; (August 3, 2016), 3rd edition
- [6] M.P. Agarwal, Solar energy: published by S. Chand, Delhi (january
1, 1983)
- [7] Gupta.J.B., Electronics devices and Circuit: published by SK Kataria
& sons-New Delhi: (2012), 1st edition
- [8] Nanda Kyati, Bishwajeet Kumar Pandey and Kaila Karthik, Power
analysis of solar inverter on FPGA: published by LAP LAMBERT
Academic, Germany (November 5, 2015)
- [9] Hadaate Ullah and Golam Moktader Nayeem, Charge controller and

Inverter: published by LAP LAMBERT academic, Germany (February 2,2012)

[10]www.britannica.com

[11]www.siliconsolar.com

[12]www.circuitdigest.com

[13]www.elprocus.com

[14]www.inverter.com

[15]www.irena.org

**SOLVING NEWTON'S EQUATIONS
USING MICROPROCESSOR 8085**

Project report submitted to the Department of Physics

ST.MARY'S COLLEGE (AUTONOMOUS)

THOOTHUKUDI

Affiliated to MANONMANIAM SUNDARANAR UNIVERSITY,

TIRUNELVELI

In partial fulfillment of the requirement for the award of

BACHELOR'S DEGREE IN PHYSICS

BY

M. ANUSHIYA DEVI	-18AUPH06
R. DAFFODIL	-18AUPH13
V. DIVYA	-18AUPH15
V. JAYA DARSENE	-18AUPH20
A. SHALOM ABINAYA	-18AUPH39
S. YUTHITH	-18AUPH49



Under the guidance of

Dr. M. SHEEBA M.Sc., B.Ed., M.Phil. SET, Ph.D.

Department of Physics

ST.MARY'S COLLEGE (AUTONOMOUS)

Reaccredited with A+ Grade by NAAC

Thoothukudi

2020 - 2021

CERTIFICATE

This to certify that the project work entitled "SOLVING NEWTON'S EQUATIONS USING MICROPROCESSOR 8085" is submitted to St. Mary's College (Autonomous), Thoothukudi in partial fulfillment for the award of the Bachelors' Degree in Physics and is a record of work done during the year 2020 – 2021 by the following students.

M. ANUSHIYA DEVI	18AUPH06
R. DAFFODIL	18AUPH13
V. DIVYA	18AUPH15
V. JAYA DARSENE	18AUPH20
A. SHALOM ABINAYA	18AUPH39
S. YUTHITH	18AUPH49

M. Anushiya Devi
GUIDE

Lucia Rose
HEAD OF THE DEPARTMENT
HEAD
Department of Physics,
St. Mary's College (Autonomous),
Thoothukudi - 628 001.

A. Lucas Raul
EXAMINER
19/4/21

Lucia Rose
PRINCIPAL
St. Mary's College (Autonomous),
Thoothukudi - 628 001.

ACKNOWLEDGEMENT

We are extremely grateful to the Lord almighty for the successful completion of our project during the year 2018 -2021.

We wish to express our deep sense of gratitude to Dr.Sr. A.S.J. Lucia Rose, M.Sc, PGDCA, M.Phil, Ph.D, Principal, St. Mary's College, Tuticorin for her benign leadership and constant support which were very much helpful for us in carrying out this project.

With gratitude we record our indebtedness to our respected Head of the department Dr. Sr. Jessie Fernando M.Sc., M.Phil., Ph.D for her constant support in carrying out this project.

We express our sincere gratitude to our guide Dr. M. Sheeba M.Sc., B.Ed., M.Phil, SET, Ph.D for her abundant support which greatly helped in the completion of this project.

We sincerely acknowledge the financial assistance funded by DBT under Star College Scheme, New Delhi for the successful completion of the project work.

We are highly obliged in taking the opportunity to sincerely thank all the professors and supportive staff for their constant support.

Our humblest gratitude to our family members who provided support both directly and indirectly to the successful completion of this project.

CONTENT

- **Certificate**
- **Acknowledgement**

Chapter I – INTRODUCTION	1
1.1 Introduction to Microprocessor in Physics	
1.2 Aim of the project	
Chapter II - LITERATURE REVIEW	2
Chapter III – KINEMATICS AND MICROPROCESSOR 8085	
3.1 Equations of Motion	5
3.2 Microprocessor 8085	8
3.2.1 Evolution of Microprocessor 8085	10
3.2.2 Pin diagram	13
3.2.3 Operating Procedure	15
Chapter IV - PROGRAM AND EXECUTION	
4.1 Statement problem	18
4.2 Manual calculation	18
4.3 Microprocessor 8085 program	21
4.4 Tabulations	24
4.5 Graphs	26
Chapter V – CONCLUSION	28
5.1. Result & Discussion	
5.2 Conclusion	

Chapter I

INTRODUCTION

1.1 Introduction to Microprocessor in Physics

Microprocessors are very large scale integrated circuits. One single chip has an arithmetic and logic unit, a set of registers and control sections, linked internally by pixety. Microprocessor has an evolutionary effect on experimental Physics. Microprocessors are used in a large scale by meteorologists and crystallographers. These people make use of large frame computers. Microprocessor based systems are widely used in industries for measurement, display and monitoring of physical quantities like temperature, pressure, speed, flow, etc. Transducers are used to convert physical quantities into electrical signal. The electrical signal is applied to a converter and the result is displayed in the microprocessor [1].

1.2 Aim of the project

- To choose and solve a statement problem which employs equations of kinematics.
- To write an 8085 Microprocessor program to solve the chosen problem.
- To change the inputs of the program and obtain a tabulation.
- To analyse the tabulation and draw a graph.

Chapter II

LITERATURE REVIEW

Kimasha Borah [2] has given an overview of microprocessor 8085 and its applications. Microprocessor is a program controlled semiconductor device i.e IC which fetches, decodes and executes instructions. Microprocessors have day to day applications in equipments like DVD players, test instruments, smoke alarms and audio and visual components. The display of the the medical devices such as EEG and ECG is based on microprocessor. Due to the wide variety of uses it has revolutionized the human civilization.

Shashank Kumar Singh and et al [3] has studied the applications of microprocessor and microcontroller. The portion of the computer that allows it to do more work than a simple computer is the microprocessor. Modern microprocessor can perform extremely sophisticated operations in areas such as meteorology, aviation, nuclear physics and engineering. Microcontrollers and microprocessors are widely used in embedded systems. Though microcontrollers are preferred over microprocessors for embedded systems due to low power consumption. This work presents the general application of microprocessors and microcontrollers. The impact of the microprocessor, however, goes far deeper than new and improved products. Microprocessors and Microcontrollers provide a new dimension to our society.

Vishwajit Bakrola [4] has presented the development of 8085 microprocessor based system, specifically designed for educational purpose. 8085 is an excellent material for the fundamental of microprocessor based system. The 8085 is in the core of entire system. In

this system, Demultiplexing is achieved with the help of D type latch integrated circuits, which provides separate data lines and address lines. The interfacing of memory is done with the microprocessor to provide necessary instruction to implement on the system. The output port is designed with combinations logic circuit and interfaced with the entire system to gain necessary output.

Manoj Barfa and et al [5] has presented the implementation of 16 bit microprocessor. The central unit of all smart devices are processors, whether they be electronic devices or otherwise. Their smartness comes as a direct result of the decisions and controls that processor makes. The existing commercial microprocessors are provided as black box units; with which users are unable to monitor internal signals and operation process, neither can they modify the original structure.

Priyanka and et al [6] has presented a study on applications of microprocessor .Microprocessors are applicable to a wide range of information processing tasks, ranging from general computing to real-time monitoring systems. The microprocessor facilitates new ways of communication and how to make use of the vast information available online and offline both at home and in workplace. Electric Utilities Company have traditionally used electromechanical (EMR) distance relays for the protection of transmission lines in the past, and many such relays are still in use in power systems today. Microprocessor-based protective relays applications in the power systems protection were investigated. The overall scheme takes up less panel space, the design and wiring is simpler and less costly to implement. Installation and maintenance testing are greatly reduced.

Udhbave Singh and et al [7] has implemented the machine learning algorithm using microprocessor. The aim of the paper is to

provide a better solution for control of railway crossing & prevention of accidents caused due to absence of it. In order to do that we use Microprocessor. Presently human intervention is required in order to control barriers, use of microprocessor reduces human errors & can responsibly avert drastic accidents. Making use of machine Learning algorithms can pave the way for automation leading to ultimate substitution of human workforce. The workforce can then be employed more efficiently making the organization more streamlined & cost effective. It will also decrease the cost incurred by the organization as the number of employees will decrease & employees will be provided with useful tasks increasing overall efficiency.

Chapter III

KINEMATICS AND MICROPROCESSOR 8085

3.1 Equations of motion

In physics, equations of motion (Kinematic equations) are equations that describe the behaviour of a physical system in terms of its motion as a function of time. More specifically, the equations of motion describe the behaviour of a physical system as a set of mathematical functions in terms of dynamic variables.

Kinematics is the science of describing the motion of objects using words, diagrams, numbers, graphs, and equations. Kinematics is a branch of mechanics. The goal of any study of kinematics is to develop sophisticated mental models that serve to describe (and ultimately explain) the motion of real-world objects by using newton's laws of motion. They are as follows,

Newton's laws of motion

Newton's laws of motion are three laws that describe the relationship between the motion of an object and the forces acting on it.

Newton's first law

The first law states that an object at rest will stay at rest, and an object in motion will stay in motion unless acted on by a net external force. Mathematically, this is equivalent to saying that if the net force on an object is zero, then the velocity of the object is constant.

Newton's second law

The second law states that the rate of change of momentum of a body over time is directly proportional to the force applied, and occurs in the same direction as the applied force.

Newton's third law

The law states that every action has an equal and opposite reaction.

Kinematics is simple. It concerns only variables derived from the positions of objects and time. In circumstances of constant acceleration, these simpler equations of motion are usually referred to as the SUVAT equations, arising from the definitions of kinematic quantities:

- Displacement(s)
- Initial velocity (u)
- Final velocity (v)
- Acceleration (a)
- Time (t).

The following equations can be utilized for any motion that can be described as being either a constant velocity motion or a constant acceleration motion. They can never be used over any time period during which the acceleration is changing. Each of the kinematic equations includes four variables. If the values of three of the four variables are known, then the value of the fourth variable can be calculated. In this manner, the kinematic equations provide a useful means of predicting information about an object's motion if other information is known.

The three kinematic equations that describe an object's motion are:

$$\diamond d = u t + \frac{1}{2} a t^2$$

$$\diamond v^2 = u^2 + 2as$$

$$\diamond v = u + at$$

Where,

$s \rightarrow$ Displacement of the object.

$t \rightarrow$ Time for which the object moved.

$a \rightarrow$ Acceleration of the object.

$u \rightarrow$ Initial velocity of the object.

$v \rightarrow$ Final velocity of the object

Displacement (d):

The action of moving something from its place or position. It is defined to be the change in position of an object. It is a vector quantity.

Unit: m.

Acceleration (a):

Acceleration is the rate of change of velocity. Usually, Acceleration means the speed is changing but not always. It is a vector quantity.

Unit: m/s^2

Initial velocity is the velocity at time interval $t=0$. It is the velocity at which the motion starts.

Final velocity (v):

Final velocity is the velocity which the body has at the end of the given time period.

Each of these three equations appropriately describes the mathematical relationship between the parameters of an object's motion. As such, they can be used to predict unknown information about an object's motion if other information is known.

Computer's Central Processing Unit (CPU) built on a single Integrated Circuit (IC) is called a microprocessor. It is a computer processor where the data processing logic and control is included on a single integrated circuit or a small number of integrated circuits.



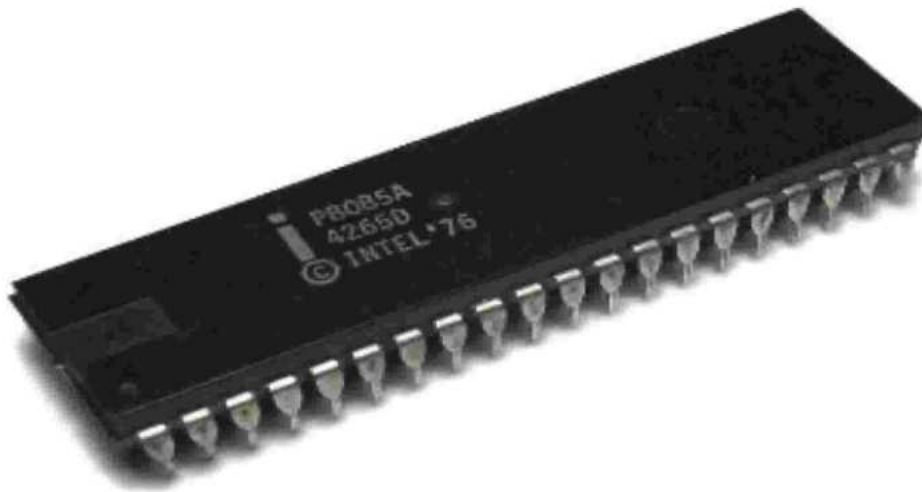


Fig 3.2 Microprocessor 8085 chip

It is a programmable, multipurpose, clock -driven, register-based electronic device that reads binary instructions from a storage device called memory, accepts binary data as input and processes data according to those instructions and provides results as output. The microprocessor contains millions of tiny components like transistors, registers, and diodes that work together.

A microprocessor is designed to perform arithmetic and logic operations that make use of small number holding areas called registers. Generally microprocessor operations include addition, subtraction, comparison of two numbers and fetching numbers from one area to another. The microprocessor follows a sequence to execute the instruction:

- Fetch
- Decode
- Execute

Initially, the instructions are stored in the storage memory of the computer in sequential order. The microprocessor fetches those instructions from the stored area (memory), then decodes it and executes those instructions till STOP instruction is met. Then, it sends the result in binary form to the output port. Between these processes, the register stores the temporary data and ALU (Arithmetic and Logic Unit) performs the computing functions. The evolution, features and working of an 8085 Microprocessor is described briefly,

3.2.1 Evolution

A Microprocessor is a complete computation engine that is fabricated on a single chip.

- The first microprocessor was the INTEL 4004, introduced in 1971. The 4004 is a 4 -bit processor.
- The microprocessor constructed to make it into a home computer was the INTEL 8080, a complete 8-bit computer on one chip, introduced in 1974.
- In 1976, Intel updated the 8080 design with the 8085 by adding two instructions to enable / disable three added interrupt pins and the serial I/O pins.
- In 1978 Intel introduced the 8086, a 16-bit processor which gave rise to the X86 architecture. It did not contain floating point instructions.
- In 1980 the Intel released the 8087. It is the first math co-processor.
- The first microprocessor to make a real splash in the market was the Intel 8088, introduced in 1979 and incorporated into IBM Personal Computer.

- The Personal Computer market moved from the 8088 to the 80286 to the 80386 to the Pentium H to the Pentium HI to the Pentium IV. All of these microprocessors are made by Intel and all of them are improvement on the basic design of the 8088.
- Some second source manufactures also produced CMOS version of the microprocessor 8085-80C85. The 8085 was produced at speeds ranging from 3MHz to 6MHz.

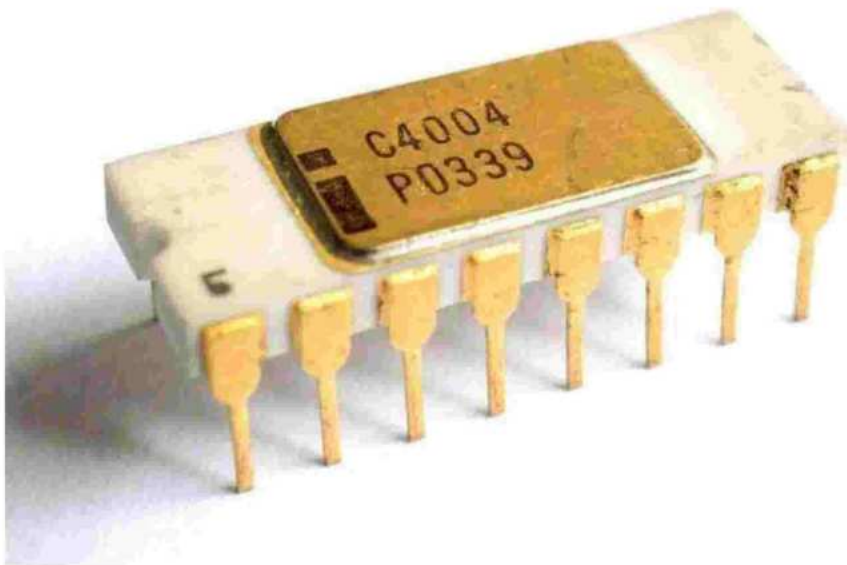
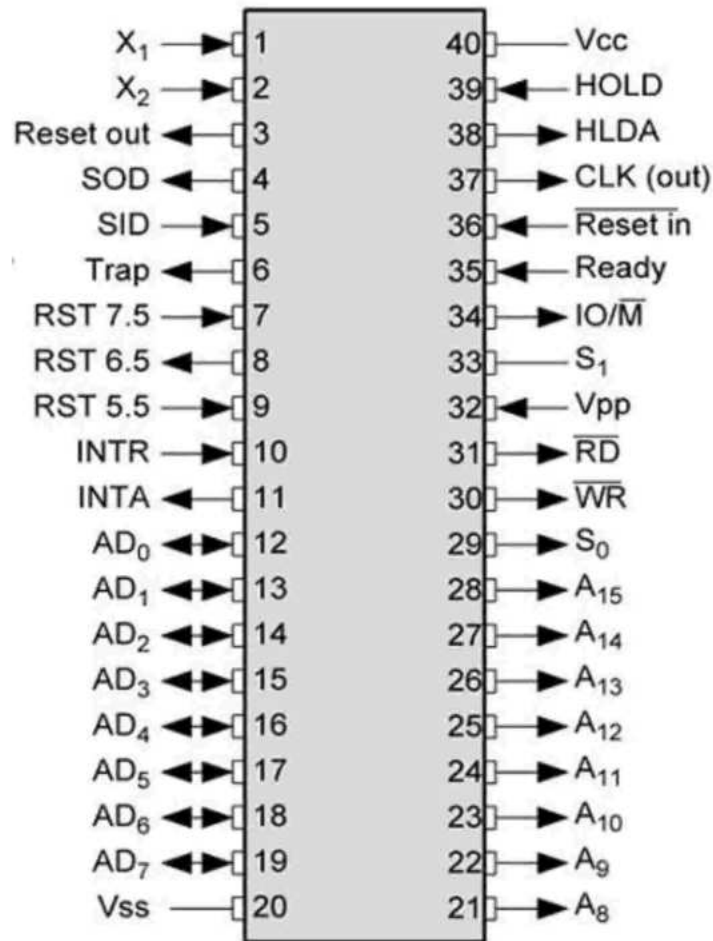


Fig 3.3 Intel 4004

Intel Microprocess				
Name	Year	Transistors	Clock speed	Data width
8080	1974	6,000	2 MHz	8 bits
8085	1976	6,500	5 MHz	8 bits
8086	1978	29,000	5 MHz	16 bits
8088	1979	29,000	5 MHz	8 bits
80286	1982	134,000	6 MHz	16 bits
80386	1985	275,000	16 MHz	32 bits
80486	1989	1,200,000	25 MHz	32 bits
Pentium	1993	3,100,000	60 MHz	32/64 bits
Pentium II	1997	7,500,000	233 MHz	64 bits
Pentium III	1999	9,500,000	450 MHz	64 bits
Pentium IV	2000	42,000,000	1.5 GHz	64 bits
Pentium IV "Prescott"	2004	125,000,000	3.6 GHz	64 bits
Intel Core 2	2006	291 million	3 GHz	64 bits
Pentium Dual Core	2007	167 million	2.93 GHz	64 bits
Intel 64 Nchalem	2009	781 million	3.33 GHz	64 bits

Fig 3.4 Evolution over the years

3.2.2 Pin Diagram



Address Bus: A8 - A15:

These pins carry the higher order of address bus. The address is sent from microprocessor to memory A8 – A15. It carries the least significant 8-bit of memory I/O address.

Data Bus: AD0 - AD7:

Data bus is of 8 bit. It is used to transfer data between microprocessor and memory. AD0 – AD7. It carries the least significant 8-bit address and data bus.

Control Signals:

RD: This signal indicates that the selected IO or memory device is to be read and is ready for accepting data available on the data bus.

WR: This signal indicates that the data on the data bus is to be written into a selected memory.

Status Signals:

IO/M: This signal is used to differentiate IO and Memory operations

S0 & S1: These signals are used to identify the type of current operation.

Power Supply:

VCC: It indicates +5v power supply.

VSS: It indicates ground signal.

Interrupt signals:

TRAP: It is usually used for power failure and emergency shutoff.

RST 7.5: It is a maskable interrupt. It has the second highest priority.

RST 6.5: It is a maskable interrupt. It has the third highest priority.

RST 5.5: It is a maskable interrupt. It has the fourth highest priority.

INTR: It is a general purpose interrupt. It is a maskable interrupt. It has the lowest priority.

Externally Initiated Signals:

INDA: It is an interrupt acknowledgement signal.

RESET IN: This signal is used to reset the microprocessor by setting the program counter to zero.

RESET OUT: This signal is used to reset all the connected devices, when the microprocessor is reset.

READY: This signal indicates that the device is ready to send or receive data.

HOLD: This signal indicates that another master is requesting the use of the address and data buses.

HLDA: It indicates that CPU has received the HOLD request and it will relinquish the bus in next clock.

Serial I/O signals:

SOD: The output SOD is set or reset as specified by the SIM instruction.

SID (Serial Input Dataline): The data on this line is loaded into accumulator whenever a RIM instruction is executed.

Clock Signals:

X1, X2: A crystal (RC, LC, N/W) is connected at these two pins and is used to set frequency of the internal clock generator. This frequency is internally divided by 2.

CLK OUT: This signal is used as the system clock for devices connected with the Microprocessor.[9]

3.2.3 Operating procedures

Generally, a microprocessor performs four different operations: memory read, memory write, input/output read and input/output write. In the memory read operation, data will be read from memory and in the memory write operation, data will be written in the

memory. Data input from input devices are I/O read and data input to output device are I/O write operations. The memory read/write and Input/output read and write operations are performed as part of communication between the microprocessor and memory or Input/output device.

Microprocessors communicate with the memory, and I/O device through address bus, data bus and control bus. For the communication, firstly the microprocessor identifies the peripheral device by proper addressing. Then a sends data provides control signal for synchronization. . Initially, the microprocessor places a 16-bit address and the address bus. Then the external decoder logic circuit decodes the 16-bit address on the address bus and the memory location is identified. Thereafter, the microprocessor sends MEMR control signal which enable the memory IC. After that, the content of the memory location is placed on data bus and also sent to the microprocessor.

The step-by-step procedure of data flow is given below:

- The 16-bit memory address is stored in the program counter. Therefore, the program counter sends the 16-bit address on the address bus. The memory address decodes and identifies the specified memory location.
- The control unit sends the control signal RD in the next clock cycle and the memory IC is enabled RD is active for two clock periods.
- When the memory IC is enabled, the byte from the memory location is placed on the data bus AD-AD2 after that data is transferred is the microprocessor

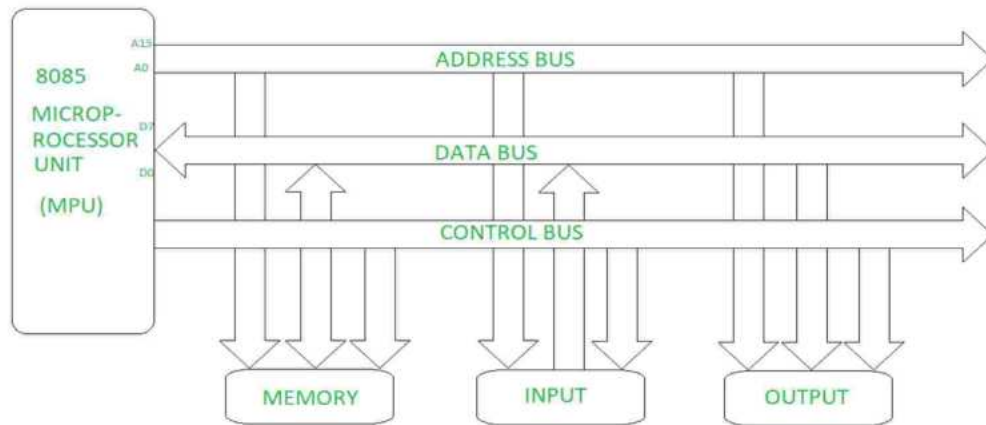


Fig 3.5 Bus organisation of microprocessor 8085

CHAPTER IV

PROBLEM AND EXECUTION

4.1 Statement problem

A Spacecraft is flying in a straight course with velocity 50 km/s. After reaching a particular distance, its velocity becomes 120 km/s.

If the spacecraft fires its rocket for a time period of 10 s,

1. Find the distance travelled by the spacecraft for the given initial velocity and also for $u=75$ km/s and $u=100$ km/s. Plot a graph to show the variation for each of the given initial velocity.
2. If the final velocity 120 km/s is changed in the order of 140 km/s and 160 km/s and the initial velocity is kept constant at $u = 75$ km/s, find the distance for each value of v respectively. Plot a graph to show the variation of 'a' for each value of 'v'.
3. Draw graphs to show the variation of acceleration with the varied Initial and Final velocities.

4.2 Manual calculation

1. To find the value of distance for the given three values of initial velocity (u), **A.** $u=50$ km/s, **B.** $u=75$ km/s, **C.** $u= 100$ km/s.

A. $u=50$ km/s, $v=120$ km/s, $t=10$ s

$$v = u + at$$

$$a = v - u / t$$

$$= 120 - 50 / 10$$

$$\mathbf{a = 7 \text{ km/s}^2}$$

$$\mathbf{v^2 = u^2 + 2as}$$

$$2as = v^2 - u^2$$

$$s = v^2 - u^2 / 2a$$

$$= (120)^2 - (50)^2 / 2(7)$$

$$= 11900 / 14$$

$$\mathbf{s = 850 \text{ km}}$$

B. $u = 75 \text{ km/s}$, $v = 120 \text{ km/s}$, $t = 10 \text{ s}$

$$\mathbf{v = u + at}$$

$$a = v - u / t$$

$$= 120 - 75 / 10$$

$$\mathbf{a = 4.5 \text{ km/s}^2}$$

$$\mathbf{v^2 = u^2 + 2as}$$

$$s = v^2 - u^2 / 2a$$

$$= (120)^2 - (75)^2 / 2(4.5)$$

$$= 14400 - 5625 / 9$$

$$\mathbf{s = 975 \text{ km}}$$

C. $u = 100 \text{ km/s}$, $v = 120 \text{ km/s}$, $t = 10 \text{ s}$

$$\mathbf{v = u + at}$$

$$a = v - u / t$$

$$a = 120 - 100 / 10$$

$$\mathbf{a = 2 \text{ km/s}^2}$$

$$\mathbf{s = v^2 - u^2 / 2as}$$

$$= (120)^2 - (100)^2 / 2(2)$$

$$= 14400 - 10000 / 4$$

$$\mathbf{s = 1100 \text{ km}}$$

2. To find the value of distance for each value of the final velocities, **A.** $v = 120 \text{ km/s}$, **B.** $v = 150 \text{ km/s}$, **C.** $v = 160 \text{ km/s}$.

A. $u = 75 \text{ km/s}$, $v = 120 \text{ km/s}$, $t = 10 \text{ s}$

$$\mathbf{v = u + at}$$

$$a = v - u / t$$

$$= 120 - 75 / 10$$

$$\mathbf{a = 4.5 \text{ km/s}^2}$$

$$\mathbf{v^2 = u^2 + 2as}$$

$$s = v^2 - u^2 / 2a$$

$$= (120)^2 - (75)^2 / 2(4.5)$$

$$\mathbf{s = 975 \text{ km}}$$

B. $u = 75 \text{ km/s}$, $v = 150 \text{ km/s}$, $t = 10 \text{ s}$

$$\mathbf{v = u + at}$$

$$a = v - u / t$$

$$= 140-75/10$$

$$\mathbf{a=6.5 \text{ km/s}^2}$$

$$\mathbf{v^2=u^2+2as}$$

$$s=v^2-u^2/2a$$

$$= (140)^2-(75)^2/2(6.5)$$

$$\mathbf{s=1075 \text{ km}}$$

C. $u= 75 \text{ km/s}$, $v= 160 \text{ km/s}$, $t= 10 \text{ s}$

$$\mathbf{v = u + at}$$

$$a = v-u/t$$

$$= 160-75/10$$

$$\mathbf{a = 8.5km/s^2}$$

$$\mathbf{v^2= u^2+2as}$$

$$s = v^2-u^2/2a$$

$$= (160)^2-(75)^2/2(8.5)$$

$$\mathbf{s=1175 \text{ km}}$$

4.3 Microprocessor 8085 program

3500= u, 3501= v, 3502= t

LXI SP, 4000H

LXI H, 3500H

MOV B, A

INX 3500H

MOV A, M
SUB B
MOV L, A
MVI H, 00H
LDA 3502H
MOV C, A
MVI B, 00H
CALL DIV
XCHG
DAD H
PUSH H
LDA 3500H
CALL SQU
LDA 3501H
CALL SQU
POP H
POP D
MOV A, L
SUB E
MOV L, A
MOV A, H
SBB D

MOV H, A
POP B
CALL DIV
POP H
SHLD 3503H
HLT

 DIV
 LXI D, 0000H
LOOP 1 MOV A, L
 SUB C
 MOV L, A
 MOV A, H
 SBB B
 MOV H, A
 JC LOOP 2
 INX D
 JMP LOOP 1
LOOP 2 DAD B
 PUSH D
 RET

MUL

MOV C, A

MVI B, 00H

MOV E, C

MOV D, B

LXI H, 0000H

DAD B

LOOP 1 DCX D

MOV A, E

ORA D

JNZ LOOP 1

PUSH H

RET

4.4 Tabulations

Table 4.1: Final Velocity is kept constant, Initial Velocity is varied

Initial velocity	Final velocity	Time period	Distance
50	120	10	850
75	120	10	975
100	120	10	1100

Table 4.2: Initial velocity is kept constant and Final velocity is varied

Initial velocity	Final velocity	Time period	Distance
75	120	10	975
75	150	10	1075
75	160	10	1175

Table 4.3: Acceleration as Initial velocity is varied

Initial velocity	Acceleration
50	7
75	4.5
100	2

Table 4.4: Acceleration as Final velocity is varied

Final velocity	Acceleration
120	4.5
150	6.5
160	8.5

4.5 Graphs

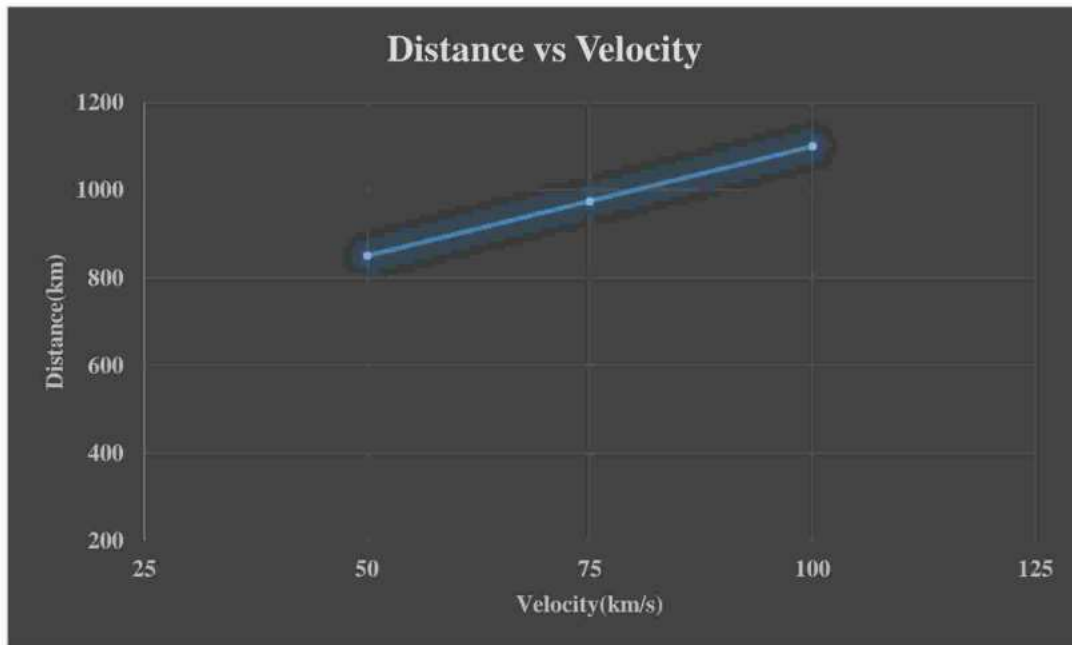


Fig 4.1: Variation of Distance with varied Initial Velocity

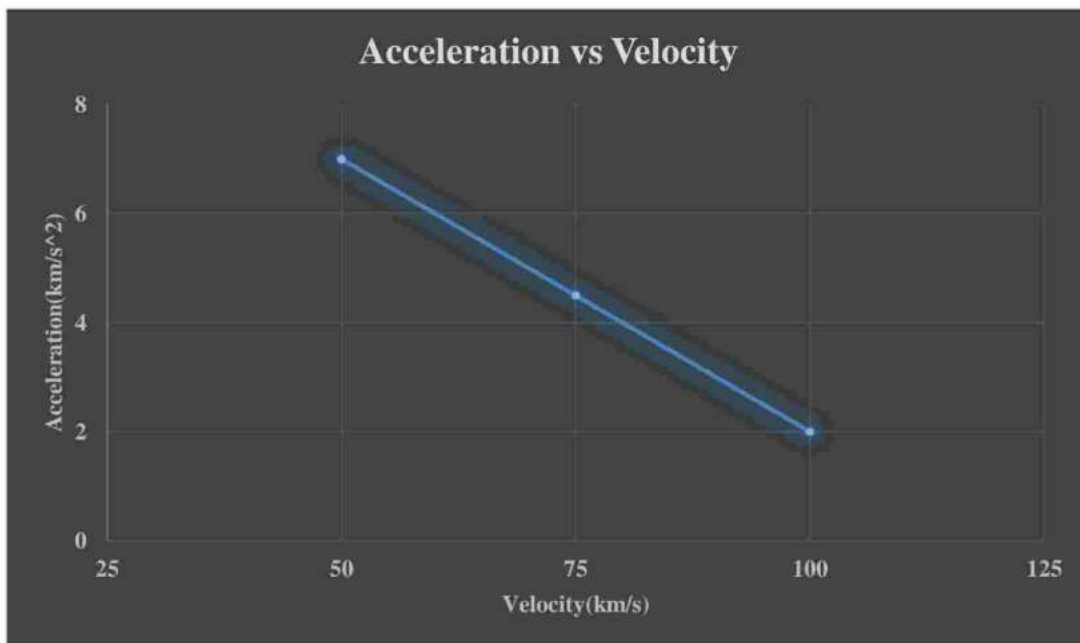


Fig 4.2: Variation of Acceleration with varied Initial Velocity

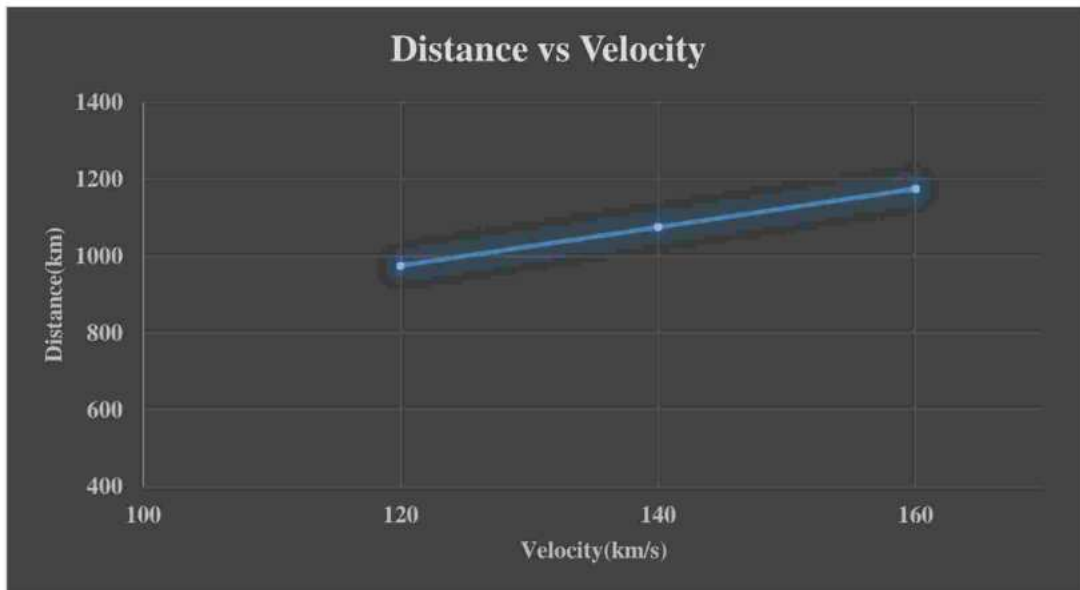


Fig 4.3: Variation of Distance with varied Final Velocity

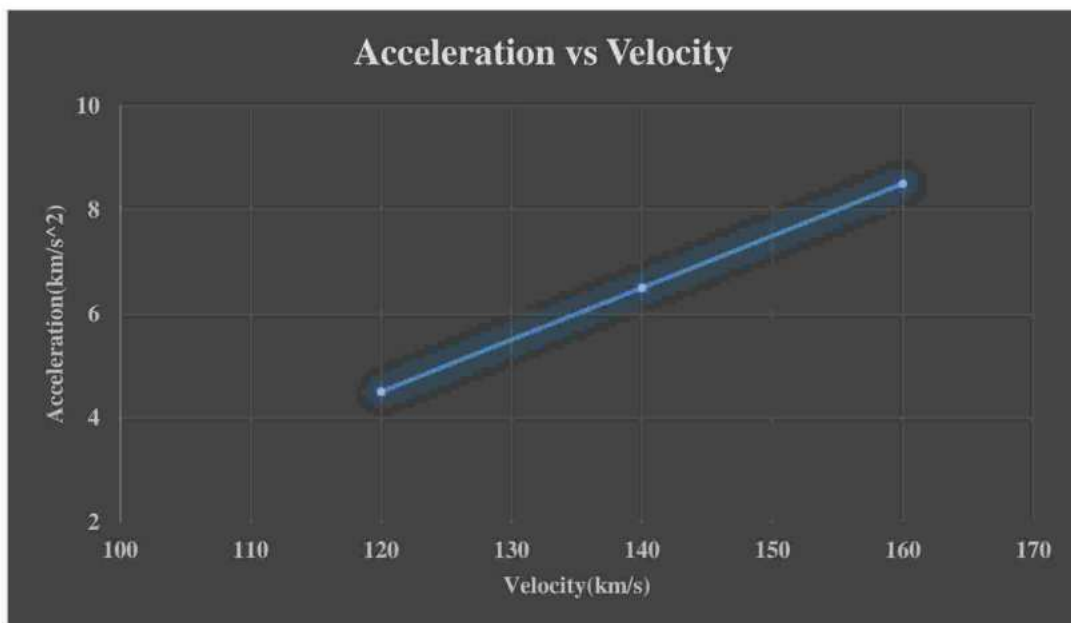


Fig 4.4: Variation of Acceleration with varied Final Velocity

Chapter V

CONCLUSION

5.1 Result & Discussion

The Microprocessor 8085 program for solving a kinematic equation word problem is executed and the outputs are obtained in hexadecimal format. Graphs are plotted that show the variation of distance and acceleration with respect to changes in initial and final velocities respectively. It can be seen that the acceleration due to gravity decreases as the initial velocity increases and increases when the final velocity is increased. As for distance, it can be seen increasing when either initial or final velocities are increased.

5.2 Conclusion

Many mathematical and physical equations can be solved by using microprocessor programs just like it has helped to solve kinematic equations and has provided us outputs to draw a certain result. In conclusion, a Microprocessor program is the basis of very advanced Engineering and AI (Artificial Intelligence) in every field, whether in physical or mathematical field and so on. With the help of Microprocessor programs, complex mechanisms are made easy. Thus Microprocessor paves the way for the Modern world.

Bibliography

- [1] www.europhysicsnews.org, www.msuniv.ac.in.
- [2] Kimasha Borah, Overview of microprocessor 8085 and its applications, IOSR Journal of Electronics and Communication Engineering, 2015, 10, 9-14.
- [3] Shashank Kumar Singh and et al, Applications of microprocessor and microcontroller, International Journal for Scientific Research and Development, 2015, 3, 1183-1187.
- [4] Vishwajit Bakrola, Development of 8085 microprocessor based output, International Journal of Engineering Development and Research, 2014, 2, 2524-2527.
- [5] Manoj Barfa and Deepak Sharma, Implementation of 16 bit microprocessor, International Journal of Innovative Research in Technology, 4, 409-414.
- [6] Priyanka. P and Rajesh. K.M, Study on applications of microprocessor and microcontroller, International Journal of Innovative Research in Technology, 2018, 5, 396-400.
- [7] Udbhav Singh and Shripad. G. Desai, Study on implementation of machine learning algorithm using microprocessor, International Journal of Innovative Research in Technology, 2020, 7, 217-219.
- [8] Soumitra Kumar Mandal, Microprocessors and Microcontrollers (Architecture, programming and interfacing using 8085, 8086 and 8051)
- [9] www.tutorialspoint.com, www.slideshare.net.

DETECTION OF OBJECT DISTANCE USING ARDUINO UNO

Project work submitted to St.Mary's College (Autonomous), Thoothukudi, affiliated to Manonmaniam Sundaranar University, Tirunelveli in partial fulfilment of the

Requirement for the award of the BACHELOR'S DEGREE IN PHYSICS

By

M. BHAVANI	18AUPH09
J. CHRISTY CHITRA	18AUPH12
J. MAHALAKSHMI	18AUPH26
K. ROXINA	18AUPH38
T. VIJAYA LAKSHMI	18AUPH48

GUIDE AND SUPERVISOR

Dr. M. SHEEBA M.Sc., B.Ed., M.Phil., SET., Ph.D.,



**DEPARTMENT OF PHYSICS
ST.MARY'S COLLEGE (AUTONOMOUS)**

(Re- accredited with 'A+' Grade by NAAC)

THOOTHUKUDI-628001

2020- 2021

CERTIFICATE

This is to certify that the project work entitled "DETECTION OF OBJECT DISTANCE USING ARDUINO UNO" is submitted to ST. MARY'S COLLEGE(AUTONOMOUS) THOOTHUKUDI in partial fulfilment for the award of Bachelor's Degree in Physics and is a record of work done during the year 2018-2021 by the following students.

M. Bhavani	18AUPH09
J. Christy Chithra	18AUPH12
J. Mahalakshmi	18AUPH26
K. Roxina	18AUPH38
T. Vijaya lakshmi	18AUPH48

M. Shree

GUIDE

Resmi Jale

HEAD OF THE DEPARTMENT

HEAD

Department of Physics,
St. Mary's College (Autonomous),
Thoothukudi - 628 001.

A. Lucas
EXAMINER
19/4/21

Lucia Rose
PRINCIPAL
St. Mary's College (Autonomous)
Thoothukudi - 628 001.

ACKNOWLEDGEMENT

First and foremost, we thank the almighty for drizzling his enduring blessings throughout this project.

Secondly we stretch out our amiable gratitude to Dr.Sr.A.S.J.Lucia Rose, Principal, St.Mary's College, Tuticorin for rendering us an opportunity to work in this project.

We stretch out our heart filled thankfulness to our head of the department, Dr.Sr.Jessie M.Sc, M.Phil, Ph.D for her support to complete this project.

We extend our ardent gratitude to our guide Dr.M.Sheeba M.Sc, B.Ed, M.Phil, SET, Ph,D for outpouring her treasured ideas and for her untiring guidance to bring out this project a successful one.

We do render our heartfilled gratitude for the financial assistance funded by DBT under Star College Scheme, New Delhi, for the successful completion of this project.

We put forth our respectful gratitude to all professors and supportive staffs for their untiring effort.

Conclusively, I spread out my wholesome gratitude to our family and friends for the immense support rendered in completing the project.

ABSTRACT

Recent COVID-19 pandemic gave us huge loss of lives. On account of this pandemic all the countries in the world initiated many rules and regulations keep ourselves hygienic, washing hands, wearing mask, maintaining physical and social distancing. It is really a challenge to maintain physical distancing in public places. Now, we are in the situation of helping our affected world by introducing some devices which will help to detect and maintain the physical distance.

In our project we have introduced a device to detect the physical distancing with the help of radar software using sensor and arduino ATmega328P. It detects the objects or humans upto a distance of 40 cm. We have made a small sample working model of physical distancing this idea can be used in a larger manner so that it can be installed in public places.

In Chapter I, we have discussed about the main aim of this project and also we have given an introduction to the basics of electronics.

In Chapter II, we have given the literature review using arduino.

In Chapter III, we have given a brief note on the components that we have used in our project.

In Chapter IV, we have discussed the setup, construction, working, coding for arduino and the coding for radar processing.

In Chapter V, we have jotted down the applications and the conclusion our project.

CONTENTS

Certificate

Acknowledgement

Abstract

CHAPTER I – INTRODUCTION

1.1 Electronics

1.2 Arduino

1.3 Aim of the project

CHAPTER II – LITERATURE REVIEW

CHAPTER III – DESCRIPTION OF COMPONENTS AND

SOFTWARE

3.1 Ultrasonic sensor

3.2 Buzzer

3.3 Jumper wire

3.4 Arduino

3.5 Servo motor

3.6 Bread board

3.7 Radar software

CHAPTER IV- CONSTRUCTION AND WORKING

4.1 Introduction

4.2 Construction

4.3 Working

4.4 Pin configuration

4.5 Coding for arduino uno

4.6 Coding for radar processing

CHAPTER V- CONCLUSION

5.1 Conclusion

BIBLIOGRAPHY

CHAPTER –I

INTRODUCTION

1.1 Electronics

The name Electronics comes from an electron, which is a very small, invisible quantity of electricity present in all materials.

Today electronics plays a key role in the rapidly expanding horizon of science and technology. Global communication of information, digital computers, data processing at incredible speeds, robots, control of machines and processes, control of energy, management of environment, detection of targets, remote sensing, fast medical diagnostics are the gifts of electronics.

Primarily electronics is a subject dealing with devices where the generation and the flow of electrons are controlled. Circuits, subsystems and systems are instrumented using these electronic devices for carrying out different operations. The science and the engineering of electronics are less than 100 years old. Developments of electronics have been very fast, particular over the past 3 decades, and the industrial and commercial applications have fortunately kept pace with these development.

Flow of electrons through conductors causes an electrical current. It is really the discoveries of electrons through vacuum, gases and solids which gave birth to electronics and opened entirely new and unlimited avenues in all field of science and technology.

1.2 Arduino uno

Arduino was born at the Ivrea Interaction Design Institute as an easy tool for fast prototyping, aimed at students without a background in electronics and programming. As soon as it reached a wider community, the Arduino board started changing to adapt to new needs and challenges, differentiating its offer from simple 8-bit boards to products for IoT applications, wearable, 3D printing, and embedded environments.

All Arduino boards are completely open-source, empowering users to build them independently and eventually adapt them to their particular needs.

The Arduino software is easy-to-use for beginners, yet flexible enough for advanced users. It runs on Mac, Windows, and Linux. Teachers and students use it to build low cost scientific instruments, to prove chemistry and physics principles, or to get started with programming and robotics. Designers and architects build interactive prototypes, musicians and artists use it for installations and to experiment with new musical instruments.



Fig 1.1: Arduino Uno

1.3 Aim of the Project

The project aims at bringing a thirst for Physics in this modern era. In this project we have brought about the basic usage of arduino uno. This project gives a deep sense of awareness about the recent life killer “CORONA”. The project aims at playing a dual role, by being a benchmark in the growing field of Physics and to serve as a tool for creating awareness against the deadly virus “corona”. In this project “distance measurement” is the foundation of the project. The setup acts as a source and measures the distance and detects the objects at a range of 40 cm. The setup works on the principle of arduino uno which is coded using arduino IDE. The radar is programmed using the radar software. If the source is placed in a crowded surrounding, the setup detects the objects which are closer than 40 cm and helps in maintaining social distance. Thus the project meets the need of today’s world.

CHAPTER –II

LITERATURE REVIEW

Arduino has greater academic applications. Kuldeep Singh Kaswan and etal[1] investigated, the roles of Arduino among microcontroller boards. They have identified the different types of Arduino boards and its applications from the literature work done.

Anas[2] has studied a system for measuring, monitoring and estimation of some environment's parameters like temperature, humidity, and volume of CO₂. The system was developed using Arduino Uno microcontroller and its platforms. It has high level scalability and is cost-effective, which makes it suitable for other environment monitoring applications. His paper contains elaborate explanations of the overall system architecture as well as hardware and software requirements of the system. Viability of the system has also been demonstrated through presentation of some results obtained

Alessio and etal[3] have designed to develop distance measurement system using ultrasonic waves and interfaced with arduino. We know that human audible range is 20 Hz to 20 kHz. We can utilize these frequency range waves through ultrasonic sensor HC-SR04. The advantages of this sensor when interfaced with arduino which is a control and sensing system, a proper distance measurement can be made with new techniques. This distance measurement system can be widely used as range meters and as proximity detectors in industries. The hardware part of ultrasonic sensor is interfaced with arduino. This method of measurement is efficient way to measure small distances precisely.

CHAPTER-III

DESCRIPTION OF COMPONENTS AND SOFTWARE

3.1 Ultrasonic sensor

An ultrasonic sensor can convert electrical energy into acoustic waves and vice versa.



Fig 3.1: Ultrasonic sensor

3.1.1 HC-SR04 Sensor Features

- Operating voltage: +5V
- Theoretical Measuring Distance: 2cm to 450cm
- Practical Measuring Distance: 2cm to 80cm
- Accuracy: 3mm
- Measuring angle covered: $<15^\circ$
- Operating Current: $<15\text{mA}$
- Operating Frequency: 40Hz

3.1.2 Applications

- Used to avoid and detect obstacles with robots like biped robot, obstacle avoider robot, path finding robot etc.
- Used to measure the distance within a wide range of 2cm to 400cm
- Can be used to map the objects surrounding the sensor by rotating it
- Depth of certain places like wells, pits etc can be measured since the waves can penetrate through water.

If we need to measure the specific distance from the sensor, this can be calculated based on the formula:

Distance= Speed* Time. The speed of sound waves is 343 m/s. So,

Total Distance= (343 * Time of height(Echo) pulse)/2

Total distance is divided by 2 because signal travels from HC-SR04 to object and returns to the module HC-SR-04. To prevent the disruption of the ultrasonic signals coming from the sensor, it's important to keep the face of the ultrasonic transducer clear of any obstructions.

Common obstructions include:

- Dirt
- Snow
- Ice
- Other Condensation

For this particular use case, the manufacturing companies offer Self Cleaning sensors. Ultrasonic Sensors are best used in the non-contact detection of:

- Presence
- Level
- Position
- Distance

Non-contact sensors are also referred to as proximity sensors. Ultrasonic sensors are independent of:

- Light
- Smoke
- Dust
- Color

Ultrasonic sensors are superior to infrared sensors because they aren't affected by smoke or black materials, however, soft materials which don't reflect the sonar (ultrasonic) waves very well may cause issues. It's not a perfect system, but it's reliable

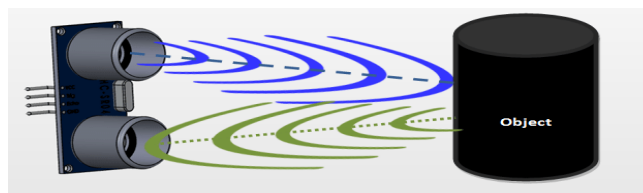


Fig 3.2: Sensing the distance

3.2. Buzzer

A buzzer or beeper is an audio signaling device, which may be mechanical, electromechanical, or piezoelectric (piezo for short). Typical uses of buzzers and beepers include alarm devices, timers, and confirmation of user input such as a mouse click or keystroke. A buzzer is a device that provides an audio signal in a circuit when a voltage is applied to it. It comes in many different forms which include mechanical, electromechanical, and piezoelectric. A switch is an electronic component that has the function of allowing and preventing current flow when used in a circuit. They are of different types such as piezo buzzers that use oscillating voltage, electromechanical buzzers that use self-oscillations as in a horn, electro-acoustic buzzers that convert electrical signals into sound vibrations, and more.

3.2.1. Working Principle

The buzzer is a sounding device that can convert audio signals into sound signals. It is usually powered by DC voltage. It is widely used in alarms, computers, printers and other electronic products as sound devices. The buzzer is mainly divided into piezoelectric buzzer and electromagnetic buzzer, represented by the letter "H" or "HA" in the circuit. According to different designs and uses, the buzzer can emit various sounds such as music, siren, buzzer, alarm, and electric bell.

3.2.2. Types

- Piezoelectric buzzers.
- Magnetic buzzers.

- Electromagnetic buzzers.
- Mechanical buzzers.
- Electromechanical buzzers

3.2.2.1. Piezo buzzer

The piezoelectric buzzer uses the piezoelectric effect of the piezoelectric ceramics and uses the pulse current to drive the vibration of the metal plate to generate sound. Piezoelectric buzzer is mainly composed of multi-resonator, piezoelectric plate, impedance matcher, resonance box, housing, etc. The multi-resonator consists of transistors or integrated circuits. When the power supply is switched on (1.5~15V DC operating voltage), the multi-resonator oscillates and outputs 1.5~2.5 kHz audio signal. The impedance matcher pushes the piezoelectric plate to generate sound. The piezoelectric plate is made of lead zirconate titanate or lead magnesium niobate piezoelectric ceramic, and silver electrodes are plated on both sides of the ceramic sheet. After being polarized and aged, the silver electrodes are bonded together with brass or stainless steel sheets.

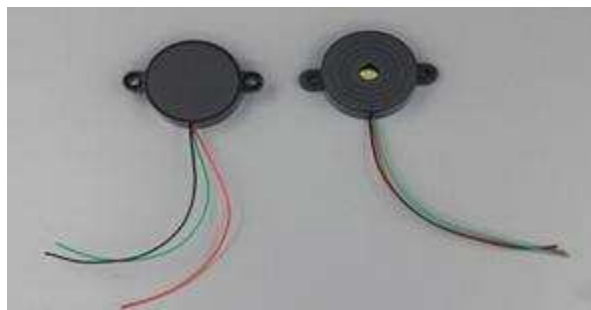


Fig 3.3: Piezo buzzer

3.2.2.2. Electromagnetic buzzer

Electromagnetic buzzer is composed of oscillator, solenoid coil, magnet, vibration diaphragm, housing, etc. When the power supply is switched on, the audio signal current generated by the oscillator passes through the solenoid coil, which generates a magnetic field. The vibration diaphragm periodically vibrates and sounds under the interaction of the solenoid coil and the magnet. The frequency of the general electromagnetic buzzer is 2-4 kHz.



Fig 3.4: Electromagnetic buzzer

3.2.2.3. Mechanical buzzer

The mechanical buzzer is a special sub-category of the electromagnetic buzzer, which consists of an oscillator, an electromagnetic coil, a magnet, a casing and etc. Under the interaction of the electromagnetic coil and the magnet, the diaphragm on the outer casing is periodically bridged to emit sound.



Fig 3.5: Mechanical buzzer

3.2.2.4. Electromechanical buzzer

Electromechanical buzzers use a bare metal disc and an electromagnet. A magnetic field is generated when a voltage is applied causing the magnet to move and the metal disc to vibrate. This generates an audible sound.



Fig 3.6: Electromechanical buzzer

3.2.2.5. Magnetic buzzer

A magnetic buzzer is a current driven device, but the power source is typically a voltage. The current through the coil is determined by the applied voltage and the impedance of the coil. A piezo buzzer differs from a magnetic buzzer in that it is driven by a voltage rather than a current.



Fig 3.7: Magnetic buzzer

3.2.3. Buzzer Features and Specifications

- Rated Voltage: 6V DC
- Operating Voltage: 4-8V DC
- Rated current: <30mA
- Sound Type: Continuous Beep
- Resonant Frequency: ~2300 Hz
- Small and neat sealed package
- Breadboard and Perf board friendly

3.2.4. Applications of Buzzer

- Alarming Circuits, where the user has to be alarmed about something
- Communication equipments.
- Automobile electronics
- Portable equipments, due to its compact size.

3.3. Jumper wire

A jump wire (also known as jumper wire, or jumper) is an electrical wire, or group of them in a cable, with a connector or pin at each end which is normally used to interconnect the components of a breadboard or other prototype or test circuit, internally or with other equipment or components, without soldering. Individual jump wires are fitted by inserting their "end connectors" into the slots provided in a breadboard, the header connector of a circuit board, or a piece of test equipment. Jumper wires typically come in three versions:

- Male-to-Male
- Male-to-Female
- Female-to-Female

The difference between each is in the end point of the wire. Male ends have a pin protruding and can plug into things, while female ends do not and are used to plug things into. Male-to-male jumper wires are the most common and what you likely will use most often. When connecting two ports on a breadboard, a male-to-male wire is what we will need.

3.3.1. Female to Female

These are 20cm long jumper wires terminated with female-to-female socket. Use these to jumper from any male header on any board. Multiple jumpers can be connected next to one another on a 0.1" header. They work great with breadboards, Arduinos, and really any 0.1" pitch prototyping board. Wires are the connecting parts of a circuit. Jumper wires are small wire ducts that can be used to connect components to each other on

bread boards or elsewhere. The female and female heads of this product, with plastic heads, can provide easier connection without need to soldering.



Fig 3.8: Female to Female

3.3.2. Male to Male

These Male-to-Male Jumper Wires are very handy for making wire harnesses or jumpering between headers on PCB's. These jumper wires come in a 'strip of 40 (4 pieces of each of ten colors). The sockets on either end have 0.1" spacing and fit cleanly next to each other on standard-pitch 0.1" (2.54mm) header. They are in a 'ribbon strip' instead of individual wires and can always be pulled to make individual jumpers, or keep them together to make neatly organized wire harnesses. For best results, when plugging these in a line, have the sides with the 'silver latch bit' sticking out since that side is a tiny bit wider than 0.1"



Fig 3.9: Male to Male

3.3.3. Male to Female

These are Jumper wire male to female, used in connecting female header pin of any development board (like Arduino) to other development board having male connector.



Fig3.10: Male to Male

Features

- Easy to plug
- Appropriate length for jumping
- Length: 20cm
- Color: Red, yellow, green, white, black
- Jumpers are made from 26 AWG wires
- Material: Plastic

3.4 Arduino

The Arduino Uno is a microcontroller board based on the ATmega328 (datasheet). It has 14 digital input/output pins (of which 6 can be used as PWM outputs), 6 analog inputs, a 16 MHz ceramic resonator, a USB connection, a power jack, an ICSP header, and a reset button. Arduino is an open-source electronics platform based on easy-to-use hardware and software. Arduino boards are able to read inputs and turn it into an output.

Arduino board designs use a variety of microprocessors and controllers. The boards are equipped with sets of digital and analog input/output (I/O) pins that may be interfaced to various expansion boards (Shields) or Breadboards (other circuits on them).

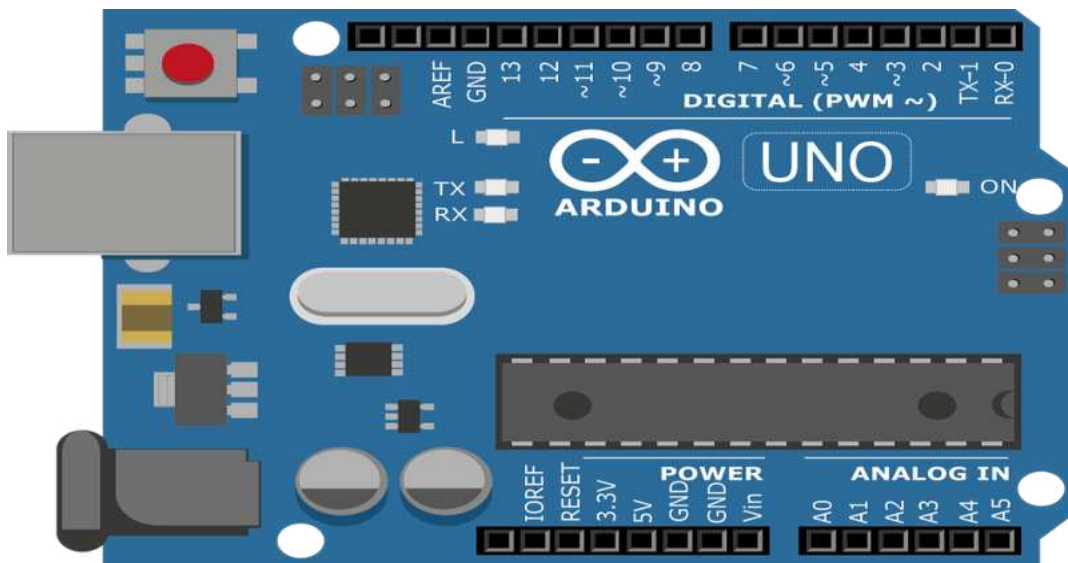


Fig 3.11: Arduino board

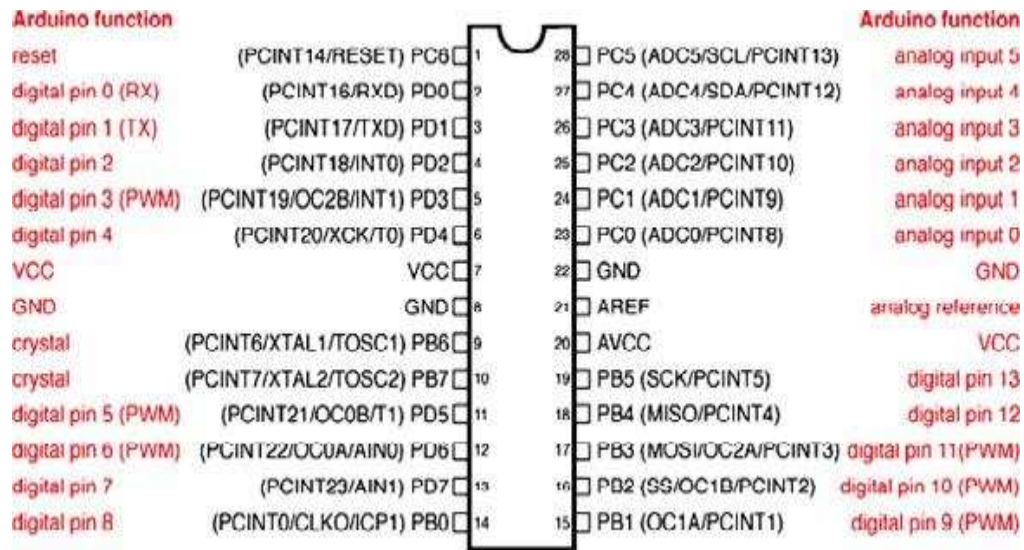


Fig 3.12: Arduino uno pin mapping

3.4.3 Function of the pins

- **Powerpin(Vin,3.3V,5V, GND)**

V in: Input voltage to arduino when using an external power source.

5V: Regulated power supply used to power Microprocessor

3.3V: Supply generated by on board voltage regulator (50 mA).

GND: Ground pins.

- **Reset pin**

Resets the arduino.

- **Analog pins(A0-A5):**

Used to provide analog input in the range of 0-5 V.

- **Input / Output pins (0-13)**

Can be used as input or output

- **Serial pins (0 R(x),1T(x)**

Used to receive and transmit TTL serial data.

- **External Interrupts (2, 3)**

To trigger an interrupt.

- **PWM (3,5,6,9,11)**

Provides 8-bit PWM output.

- **SPI (10(S S), 11(MOSI),12(MISO)and13(SCK)**

Used for SPI communication.

- **Inbuilt LED(13)**

To turn on the inbuilt LED.

- **TWI (A4(SDA),A5(SCA):**

Used for TWI communication.

- **AREF**

To provide reference voltage for input voltage.

3.5 Servo motor

A servo motor is a simple electric motor, controlled with the help of servo mechanism. If the motor as a controlled device, associated with servomechanism is DC motor, then it is commonly known as a DC Servo Motor. If AC operates the controlled motor, it is known as a AC Servo Motor.



Fig 3.13: Servo motor

3.5.1 Principle

Servo motor works on the PWM (Pulse Width Modulation) principle, which means its angle of rotation is controlled by the duration of pulse applied to its control PIN. Basically, servo motor is made up of DC motor which is controlled by a variable resistor (potentiometer) and some gears.

3.5.2 Types of servo motors

Servo motors can be of different types on the basis of their applications. The most important amongst them are AC servo motor, DC servo motor, brushless DC servo motor, positional rotation servo motor, continuous rotation servo motor, and linear servo motor.



3.14: Types of servo motor

3.5.3 Applications

- Machine Tool (Metal Cutting)
- Machine Tool (Metal Forming)
- Antenna Positioning
- Packaging
- Woodworking
- Textiles
- Printing

3.6. Bread board

A breadboard is a solderless device for temporary prototype with electronic and test circuit designs. Most electronic components in electronic circuits can be interconnected by inserting their leads or terminals into the holes and then making connections through wires where appropriate. The breadboard has strips of metal underneath the board and connect the holes on the top of the board. The top and bottom rows of holes are connected horizontally and split in the middle while the remaining holes are connected vertically.

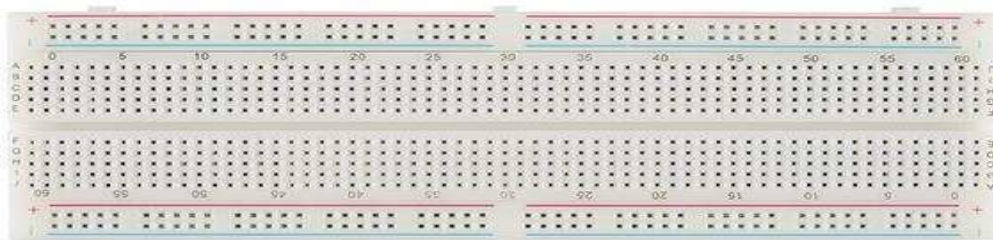


Fig 3.15: Breadboard

In figure 3.21 all holes in the selected row are connected together, so the holes in the selected column. The set of connected holes can be called a node:

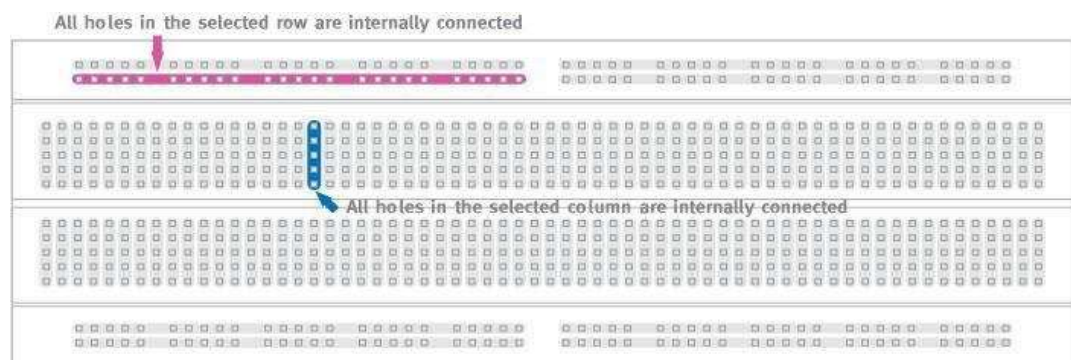


Fig 3.16: Holes in breadboard

The term breadboard comes from the early days of electronics, when people would literally drive nails or screws into wooden boards on which they cut bread in order to connect their circuits. Luckily, since we probably do not want to ruin all our cutting boards for the sake of an electronics project, today there are better options.



Fig 3.17: Breadboard

Inside a breadboard

The inside of the breadboard has rows of metal chips that can fit into the leads.



Fig 3.18: Metal chips

When we press a component's lead into a breadboard hole, one of these clips grabs onto it.



Fig 3.19: Components in metal clips

Some breadboards are actually made of transparent plastic, so we can see the clips inside.



Fig 3.20: Transparent breadboard

3.6.1 Types of breadboard based on sizes

3.6.1.1. Mini Breadboard

Mini breadboard is the smallest type of solderless electronic board on this one. Mini breadboard is used to make a mini circuit that does not require large amounts of electronic components. The number of connection holes owned by the mini breadboard is approximately 170 points. The connection point is used as the connection point of the electronic components.

3.6.1.2. Medium Breadboard

Medium breadboard is also called breadboard half breadboard. This is because the number of connection holes is half of the number of holes owned by the largest type. The connection point owned by this one breadboard is approximately 400.

3.6.1.3. Large Breadboard

For the third type of breadboard this is the largest type. If we want to make a large number of electronic component connections, then we can

use a large breadboard. The number of points owned is as many as 830 points.

3.6.2 Types of breadboard

- Solder less type
- Solder type

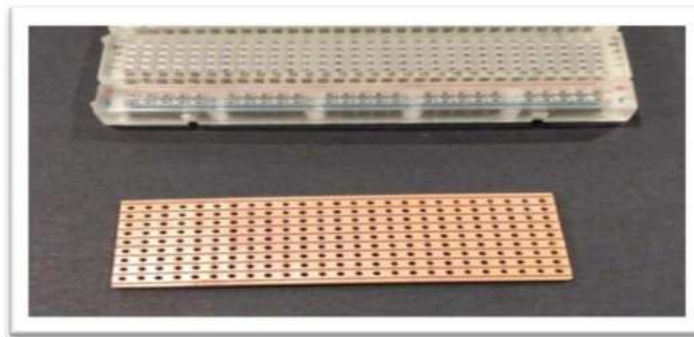


Fig 3.21: Solder and Solderless breadboard

Breadboard Type 1: Solder less

The first types of breadboards is the solder less breadboard. This kind of breadboard is the most common type of breadboard used for prototyping and testing electronic circuits without having to solder components. They are available in a variety of sizes, shapes, and ratings.



Fig 3.22: Solder less breadboard

The circuits that are built on solderless breadboards are temporary and are mainly used to test the functionality of a circuit before finalising its design onto a Printed Circuit Board (PCB). Solder less breadboards are composed with rows and columns of holes big enough to accept most wire gauges and component leads. If a component lead does not fit into the hole, a wire can be soldered onto the lead that will fit in the hole.

Breadboard Type 2: Solder

While solder less breadboards are temporary in nature, solder breadboards provide a more permanent setup for our electronic circuits. Solder less breadboards can get quite annoying as things can come loose with slight movement. A solder breadboard provides a more robust setup.

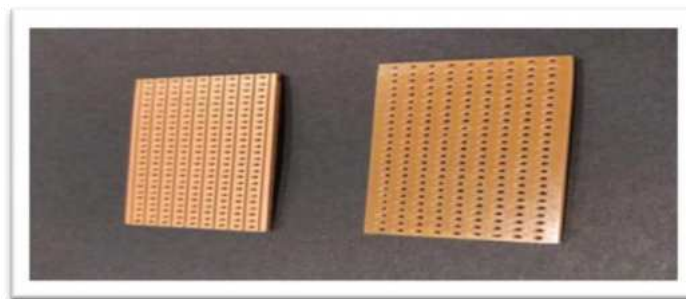


Fig 3.23: Solder breadboard

It consists of holes for components (much like a solder less breadboard) but with copper tracing. We will need a soldering iron to solder these components to the solder breadboard which will create an electrical connection with the copper tracing. Solder breadboards also come in a variety of shapes and sizes depending on our needs.

3.7 RADAR

A software- defined radar is a versatile radar system, where most of the processing, like signal generation, filtering, up-and down conversion etc is performed by a software.

In our project we have used the radar processing to display the name of our college and the distance of the target from the sensor in cm. We have made this possible by a program. We have coded the radar in such a way that it displays the distance.

In fig 3.24, the green lines indicates the calibration of the radar .Once when the object is detected the lines turn red indicating that there is a object within the range which is detected by the ultrasonic sensor.

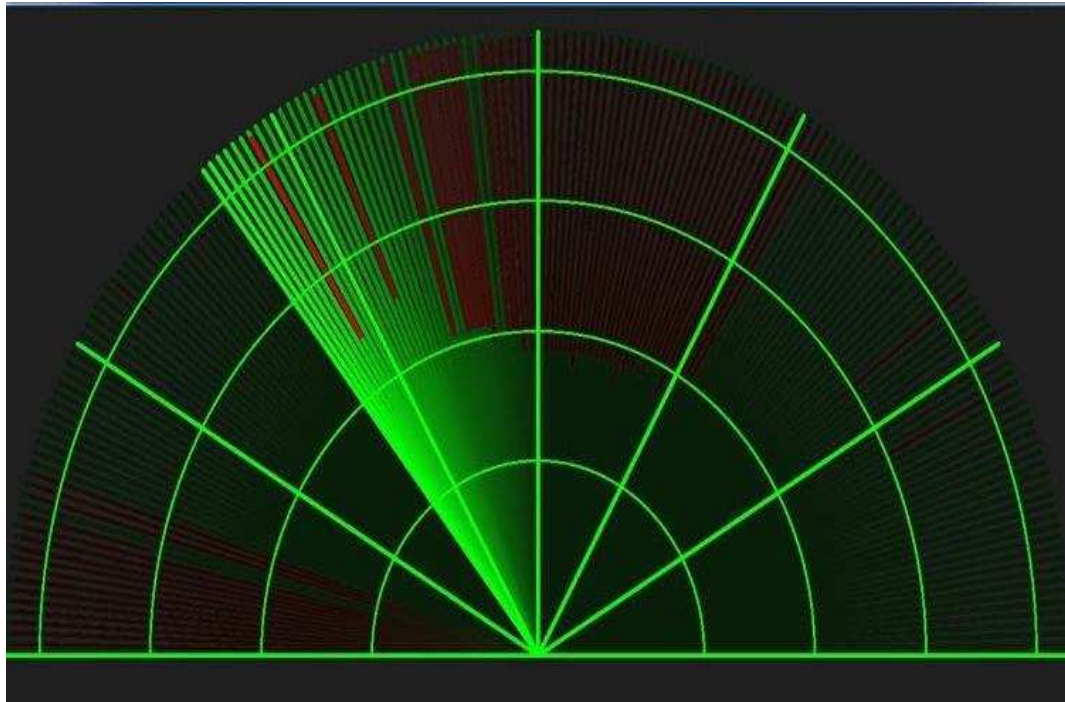


Fig 3.24: Radar

CHAPTER- IV

CONSTRUCTION AND WORKING

4.1 Introduction

Starting with the ultrasonic sensor, it has four pins; arduino has sets of pins namely the power pin set (8 pins), analog input pin set (6 pins), uno pin set (2-13 pins). It has a reset pin at the end of the arduino pin. Arduino board is built up with microprocessors and microcontrollers. Near the reset pin we have the power supply pin. A buzzer is fitted to a bread board. The entire set up is fixed in the bread board.

4.2 Construction

- ❖ The first pin of the sensor is connected to the ground pin (GND) of the power pin set.
- ❖ The second pin of the sensor is connected to the 6th pin of the uno pin set.
- ❖ The third pin of the sensor is connected to the 7th pin of the uno pin set.
- ❖ The fourth pin of the sensor is connected to the 5V pin of the power pin set.
- ❖ The buzzer is fixed to the bread board.
- ❖ One end of the buzzer is connected to the ground of the bread board
- ❖ The other end of the buzzer is connected to the 9th pin of the uno pin set.

- ❖ The 5V pin and the ground (GND) of the power pin set is connected to the ground of the buzzer.
- ❖ The servo motor has two wires twisted and is connected to the main supply of the set up.
- ❖ Three pins from the ground of the buzzer is connected to the main supply pin.

4.3 Working

The set up works on the principle of arduino uno. The power supply is taken from the laptop and it is connected to the power supply slot of the arduino pin. Once connected the ultrasonic sensor begins to detect the objects within a range of 40 cm. If the object is too close to the sensor, the buzzer begins to give a mild buzzer sound. This works with help of the arduino uno coding. Further, the radar application is made to run in the laptop and now the radar software works. The radar shows spikes of green entitled as “RADAR SYSTEM-ST.MARYS COLLEGE”. The objects detected within a range of 40 cms is depicted in red spikes and the distance of the detected object is displayed in the “DISTANCE” column. Thus the ultrasonic sensor detects the distance of a target.

4.4 Pin configuration

HC-SR04 Ultrasonic Sensor:

- VCC to Arduino 5V
- GND to Arduino GND

- Echo to Arduino pin 12
- Trig to Arduino pin 13

LCD Display :

- VSS to Arduino GND
- VCC to Arduino 5V
- VEE to Arduino GND
- RS to Arduino pin 11
- R/W to Arduino pin 10
- E to Arduino pin 9
- DB4 to Arduino pin 2
- DB5 to Arduino pin 3
- DB6 to Arduino pin 4
- DB7 to Arduino pin 5
- LED+ to Arduino 5V
- LED- to Arduino GND

4.5 Coding for arduino uno

// program to run arduino to perform the task of detection

```
#include <LiquidCrystal.h>
```

```
#define trigger 18
```

```
#define echo 19
```

```
LiquidCrystal lcd(2,3,4,5,6,7);
```

```
float time=0,distance=0;
```

```
void setup()
```

```
{  
  
  lcd.begin(16,2);  
  
  pinMode(trigger,OUTPUT);  
  
  pinMode(echo,INPUT);  
  
  lcd.print(" Ultra sonic");  
  
  lcd.setCursor(0,1);  
  
  lcd.print("Distance Meter");  
  
  delay(2000);  
  
  lcd.clear();  
  
  lcd.print(" st.marys college ");  
  
  delay(2000);  
  
}  
  
void loop()  
  
{  
  
  lcd.clear();  
  
  digitalWrite(trigger,LOW);  
  
  delayMicroseconds(2);  
  
  digitalWrite(trigger,HIGH);  
  
  delayMicroseconds(10);
```

```
digitalWrite(trigger,LOW);

delayMicroseconds(2);

time=pulseIn(echo,HIGH);

distance=time*340/20000;

lcd.clear();

lcd.print("Distance:");

lcd.print(distance);

lcd.print("cm");

lcd.setCursor(0,1);

lcd.print("Distance:");

lcd.print(distance/100);

lcd.print("m");

delay(1000);

}
```

4.6 Coding for radar processing

//program to run the radar software

```
import processing.serial.*;

import java.awt.event.KeyEvent;

import java.io.IOException;

Serial myPort;

// defubes variables

String angle="";

String distance="";

String data="";

String noObject;

float pixsDistance;

int iAngle, iDistance;

int index1=0;

int index2=0;

PFont orcFont;

void setup()

{
```

```
size (1366,700);  
  
smooth();  
  
myPort = new Serial(this,"COM5", 9600);  
  
myPort.bufferUntil('.');
```

So actually it reads this: angle,distance.

```
}  
  
void draw()  
{  
  
  fill(98,245,31);  
  
  // simulating motion blur and slow fade of the moving line  
  
  noStroke();  
  
  fill(0,4);  
  
  rect(0, 0, width, height-height*0.065);  
  
  fill(98,245,31); // green color  
  
  // calls the functions for drawing the radar  
  
  drawRadar();  
  
  drawLine();  
  
  drawObject();  
  
  drawText();  
}
```



```
}

void serialEvent (Serial myPort)

{

    // reads the data from the Serial Port up to the character '.' and puts it into
    the String variable "data".

    data = myPort.readStringUntil('.');

    data = data.substring(0,data.length()-1);

    index1 = data.indexOf(",");

    angle= data.substring(0, index1);

    distance= data.substring(index1+1, data.length());

    // converts the String variables into Integer

    iAngle = int(angle);

    iDistance = int(distance);

}

void drawRadar()

{

    pushMatrix();

    translate(width/2,height-height*0.074);

    noFill();
```

```
strokeWeight(2);

stroke(98,245,31);

// draws the arc lines

arc(0,0,(width-width*0.0625),(width-width*0.0625),PI,TWO_PI);

arc(0,0,(width-width*0.27),(width-width*0.27),PI,TWO_PI);

arc(0,0,(width-width*0.479),(width-width*0.479),PI,TWO_PI);

arc(0,0,(width-width*0.687),(width-width*0.687),PI,TWO_PI);

// draws the angle lines

line(-width/2,0,width/2,0);

line(0,0,(-width/2)*cos(radians(30)),(-width/2)*sin(radians(30)));

line(0,0,(-width/2)*cos(radians(60)),(-width/2)*sin(radians(60)));

line(0,0,(-width/2)*cos(radians(90)),(-width/2)*sin(radians(90)));

line(0,0,(-width/2)*cos(radians(120)),(-width/2)*sin(radians(120)));

line(0,0,(-width/2)*cos(radians(150)),(-width/2)*sin(radians(150)));

line((-width/2)*cos(radians(30)),0,width/2,0);

popMatrix();

}

void drawObject() {

  pushMatrix();
```

```
translate(width/2,height-height*0.074);

strokeWeight(9);

stroke(255,10,10); // red color

pixsDistance = iDistance*((height-height*0.1666)*0.025);

// limiting the range to 40 cms

if(iDistance<40)

{

    // draws the object according to the angle and the distance

    line(pixsDistance*cos(radians(iAngle)),-
pixsDistance*sin(radians(iAngle)),(width-
width*0.505)*cos(radians(iAngle)),-(width-
width*0.505)*sin(radians(iAngle)));

}

popMatrix();

}

void drawLine() {

    pushMatrix();

    strokeWeight(9);

    stroke(30,250,60);

    translate(width/2,height-height*0.074);
```

```
    line(0,0,(height-height*0.12)*cos(radians(iAngle)),-(height-
height*0.12)*sin(radians(iAngle)));

    popMatrix();

}

void drawText()

{

    pushMatrix();

    if(iDistance<40) {

        noObject = "Keep Distance";

    }

    else {

        //noObject = "In Range";

    }

    fill(0,0,0);

    noStroke();

    rect(0, height-height*0.0648, width, height);

    fill(98,245,31);

    textSize(25);

    text("10cm",width-width*0.3854,height-height*0.0833);
```

```
text("20cm",width-width*0.281,height-height*0.0833);

text("30cm",width-width*0.177,height-height*0.0833);

text("40cm",width-width*0.0729,height-height*0.0833);

textSize(40);

text("*St Marys College* ", width-width*0.98, height-height*0.0277);

text("Angle: " + iAngle + " °", width-width*0.555, height-height*0.0277);

text("Distance: ", width-width*0.36, height-height*0.0277);

text("ST.MARY'S COLLEGE", width-width*0.65, height-height*0.95);

if(iDistance<40)

{

    text("          " + iDistance + " cm", width-width*0.225, height-
height*0.0277);

}

textSize(25);

fill(98,245,60);

translate((width-width*0.4994)+width/2*cos(radians(30)),(height-
height*0.0907)-width/2*sin(radians(30)));

rotate(-radians(-60));

text("30°",0,0);

resetMatrix();
```

```
    translate((width-width*0.503)+width/2*cos(radians(60)),(height-  
height*0.0888)-width/2*sin(radians(60)));  
  
    rotate(-radians(-30));  
  
    text("60°",0,0);  
  
    resetMatrix();  
  
    translate((width-width*0.507)+width/2*cos(radians(90)),(height-  
height*0.0833)-width/2*sin(radians(90)));  
  
    rotate(radians(0));  
  
    text("90°",0,0);  
  
    resetMatrix();  
  
    translate(width-width*0.513+width/2*cos(radians(120)),(height-  
height*0.07129)-width/2*sin(radians(120)));  
  
    rotate(radians(-30));  
  
    text("120°",0,0);  
  
    resetMatrix();  
  
    translate((width-width*0.5104)+width/2*cos(radians(150)),(height-  
height*0.0574)-width/2*sin(radians(150)));  
  
    rotate(radians(-60));  
  
    text("150°",0,0);  
  
    popMatrix();}
```

CHAPTER -V

CONCLUSION

Thus this object detecting device can detect the objects or person upto a distance of 40 cm. This is very useful during recent pandemic Covid-19 issue to maintain physical distancing. Our project can detect very small distance and we can use the large modified form of this project to detect long distance. So it can be used in many places like markets, ration shops, super markets, bustands etc. One of the main applications is that it maintains physical distancing during this covid-19 period. By this device we can identify the number of objects which are at the limited distance of 40 cm so we can easily find out the people who are not maintaining physical distancing. Therefore this device will be very useful for present situation mainly during this pandemic.

**GREEN SYNTHESIS OF ZINC OXIDE NANOPARTICLES
AN ECO-FRIENDLY APPROACH**

Project work submitted to St. Mary's College (Autonomous),
Thoothukudi, affiliated to Manonmaniam Sundaranar University,
Tirunelveli in partial fulfilment of requirements for an award of,

BACHELOR'S DEGREE IN PHYSICS

BY

C. Ani Rexlin	-	8AUPH02
A. Bevinsha	-	18AUPH08
S. Gifty Kiruba Rani	-	18AUPH17
K. Koushika	-	18AUPH24
A. Meekaney	-	18AUPH29
S. Shanmuga Priya	-	18AUPH40

Guidance and supervision by
DR. SR. JESSIE FERNANDO



DEPARTMENT OF PHYSICS

St. Mary's College (Autonomous), Thoothukudi-1
(Re-Accredited with "A+" grade)

2020-2021

CERTIFICATE

This is to certify that this project work entitled, "GREEN SYNTHESIS OF ZINC OXIDE NANOPARTICLES - AN ECO-FRIENDLY APPROACH" is submitted to ST. MARY'S COLLEGE (AUTONOMOUS), THOOTHUKUDI in partial fulfilment for the award of Bachelor's Degree in Physics and is a record work done during the year 2020-2021 by the following students.

C. ANI REXLIN	-	18AUPH02
A. BEVINSHA	-	18AUPH08
S. GIFTY KIRUBA RANI	-	18AUPH17
K. KOUSHIKA	-	18AUPH24
A. MECKANCY	-	18AUPH29
S. SHANMUGA PRIYA	-	18AUPH40

Dessu 2 do
GUIDE

Dessu 2 do
HEAD OF THE DEPARTMENT
HEAD

Department of Physics,
St. Mary's College (Autonomous),
Thoothukudi - 628 001.

S. Eusebia Ammaculige
EXAMINER 15/4/21.

Lucia Rose
PRINCIPAL
St. Mary's College (Autonomous),
Thoothukudi - 628 001.

DECLARATION

We hereby declare that the project entitled, **“GREEN SYNTHESIS OF ZINC OXIDE NANOPARTICLES - AN ECO-FRIENDLY APPROACH”** submitted to **St. Mary's College (Autonomous), Thoothukudi**, affiliated to Manonmaniam Sundaranar University, for the Bachelor's Degree of Science in Physics is our original work and that, it has not previously formed the basis for the award of any Degree, Diploma or similar title.

Ani Rexlin .C -18AUPH02

Bevinsha. A -18AUPH08

Gifty Kiruba Rani. S -18AUPH17

Koushika. K -18AUPH24

Meckancy. A -18AUPH29

Shanmuga Priya. S -18AUPH40

Station: Thoothukudi

Date :

ACKNOWLEDGEMENT

In the development of this project, thanks must flow outward as the sparks fly upward. Invaluable guidance without which, this project would not have seen the light of this day. A large number of people have devoted their time, energy and talent at our disposal and we salute them all.

First of all, we would like to thank God Almighty for His sunny disposition and skill in pulling everything together. We are infinitely indebted to our College Principal **Dr. Sr. A.S.J. LUCIA ROSE M.Sc., M.Phil., Ph.D., PGDCA** for providing this opportunity and we are extremely thankful for all the help encouragement and invaluable moral support provided to us throughout the project work.

We owe our special gratitude to **Dr. Sr. JESSIE FERNANDO**, Head of the department of Physics and our project guide for her inspiring guidance, encouragement and scholarly suggestion which helped us to complete this work successfully.

We profusely thank **Prof. Mrs. P. PADMAVATHI**, Assistant Professor of Physics (SSC) for her assistance and support throughout this project.

We would like to extend our gratitude to department of Physics, St. Mary's college (Autonomous), Thoothukudi for providing us with Hot air oven and muffle furnace used for the preparation of nanoparticles.

And also, we thank **Mr. VINCENT, St. JOESPH'S COLLEGE, TRICHY** for carrying out the characterization studies and providing us with the result promptly.

We wish to accord our sincere gratitude to our non-teaching staff members who helped us to carry out our project work in the lab smoothly.

“Remembrance is the sweetest flower in the garden of thoughts”.

We also thank our parents and friends from the depth of our hearts for their profound encouragement and timely help.

CHAPTER	CONTENTS	PAGE NO
I	INTRODUCTION	
1.1	Introduction	2
1.2	Nanoscience and Nanotechnology	3
1.3	Nanoscale	4
1.4	Types of Nanoparticles	4
1.5	Shape of Nanoparticles	6
1.6	Concepts of nano world	7
1.7	Review of literature	7
1.8	Aim of the Present Work	13
1.9	Material Importance	13
1.10	Image of ZnO Particles	15
II	PREPARATION OF PURE ZnO NANOPARTICLES	
2.1	Introduction	17
2.2	Chemical Approach	17
2.3	Green approach for NPs synthesis	17
2.4	Co-Precipitation Method	18
2.5	Material Preparation	20
2.6	Flow Chart	22

III CHARACTERIZATION TECHNIQUES

3.1	Introduction	24
3.2	X-Ray Spectroscopy	24
3.3	Scanning Electron Microscopy	28
3.4	Energy Dispersive X-Ray Spectroscopy	33

IV RESULT AND DISCUSSION

4.1	Characterization using XRD	36
4.2	Characterization using SEM	43
4.3	Characterization using EDAX	44

V SUMMARY AND CONCLUSION

5.1	Summary and Conclusion	46
5.2	Bibliography	47
5.3	Images	52
5.4	Tables	52

CHAPTER-1

INTRODUCTION

1.1 INTRODUCTION:

As a rapidly growing sector in materials science, nano technology and nano science deal with materials that have particles within a size range of 1 to 100 nm and a high surface-to-volume ratio [1]. In general form, these particles are termed as nanoparticles (NPs) which exhibit highly controllable physical, chemical and biological properties in the atomic and sub- atomic levels. However, these unique features create opportunities to use them in different sectors such as electronics, optoelectronics, agriculture, communications, and bio medicine [2,3]. In recent years, several NPs are showing their effectiveness in different sectors of technology, among which zinc oxide(ZnO) NPs have gained much more importance in the recent years due to their attractive and outstanding properties such as high chemical stability, high photostability, high electro chemical coupling coefficient and a wide range of radiation absorption[4]. Again, ZnO NPs are also recognized as n-type multifunctional semiconductor materials that have a wide band gap of 3.37eV and excite on binding energy up to 60 MeV even at room temperature[1]. Nowadays, ZnO NPs are predominantly used as antimicrobial agents, delivering systems vaccines and anti- cancer systems, photo catalyst, bio sensors, energy generators and bio-imaging materials [5–7]. Among themselves, the photo catalytic application of ZnO NPs are significant. Several fabrication techniques are used to produce ZnO NPs such as thermal hydrolysis techniques, hydro thermal processing, sol-gel method, vapor condensation method, spray pyrolysis and thermo chemical techniques [8]. Nevertheless, recently a new synthesis method has been introduced and that is called biosynthesis scheme in which the NPs are prepared by using biological materials

having significant reducing and stabilizing features. Moreover, NPs with variable size and shape can be achieved through this process. Researchers proposed several possible plant extracts and fungal bio masses that were used in the green synthesis of ZnO NPs such as Aloe Barbadensis Miller (Aloe Vera) leaf extract [9], Poncirus trifoliata leaf extract [10], Parthenium hysterophorus L. (Carrot grass) leaf extract [11], Aspergillus aeneus [12], Calotropis procera latex [13], Sedumal fredii I lance[14], Physalis alkekengi L.[15],etc. However, the smaller particle size of ZnO NPs was observed by using Poncirus trifoliata leaf extract (8.48–32.51nm), while for others, the results were satisfactory [16]. In addition, another potential element for the preparation of ZnO NPs through the bio synthesis method is considered to be a leaf extract of Papaya leaf. The present study focusses on the preparation of ZnO NPs by bio synthesis method. In bio synthesis method, Papaya leaf extract is used, which is used for medicinal purposes. The Zinc Oxide nanoparticles are known to be one of the multifunctional inorganic nanoparticles and Zinc Oxide crystallites have been synthesized by simple and eco-friendly method.

1.2 NANOTECHNOLOGY AND NANOSCIENCE:

Nanotechnology is science, engineering, and technology used to study materials at the nanoscale, which is about 1 to 100 nano meters. Nanoscience and nanotechnology are the study and application of extremely small things and can be used across all the other science fields, such as chemistry, biology, physics, materials science, and engineering. Nanoscience and nanotechnology involve the ability to see and to control individual atoms and molecules.

Today's scientists and engineers are finding a wide variety of ways to deliberately make materials at the nanoscale to take advantage of their enhanced properties such as higher strength, lighter weight, increased

control of light spectrum, and greater chemical reactivity than their larger-scale counterparts [17].

1.3 NANOSCALE:

A nanometre is one-billionth of a meter. Nanomaterials have at least two dimensions that are between 1 and 100 nanometres in size. On this scale, interatomic (coulombic) forces become large, and must be considered when undertaking studies to characterize, experiment, and model the behaviours of nanomaterials. Nanomaterials (NMs) are functional materials consisting of particles with at least one dimension below 100 nanometres (nm)

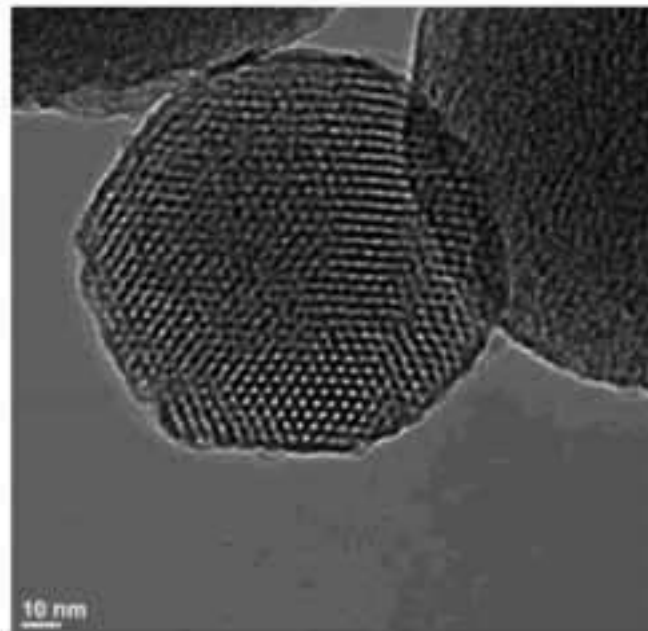


Fig 1.1

1.4 TYPES OF NANOPARTICS:

- **Natural nanomaterials**—A nanomaterial made by nature through (bio)geochemical or mechanical processes, without direct or indirect connection to a human activity or anthropogenic process.

- **Incidental nanomaterials**—A nanomaterial unintentionally produced as a result of any form of direct or indirect human influence or anthropogenic process.
- **Engineered nanomaterials**—A nanomaterial conceived, designed, and intentionally produced by humans. Nanoparticles are being produced in any number of processes, and they are at large in the environment.
- **Anthropogenic nanomaterials**—Both incidental and engineered nanomaterials.



Fig 1.2

- **Nano minerals** are defined as minerals that only exist in the size range of approximately one to a few tens of nanometres in at least one dimension. Well-known examples include most clays and metal oxides (with ferrihydrite, an iron oxyhydroxide, as a type example).
- **Mineral nanoparticles** are defined as minerals that have nano-dimensions, but these are minerals that can also exist in larger sizes.

- **Amorphous nanoparticles** are the same, except without atomic structural order.
- **Thin Films and Coatings** also occur on the nanoscale. These may be on the order from a few nanometres to a hundred nanometres in thickness, and may either be natural or engineered. Surface films and coatings commonly have compositions and structures that are not directly related to their underlying substrates. Thin films can be characterized by AFM imaging, and by a variety of analytical methods such as Auger Electron Spectroscopy, X-ray photoelectron spectroscopy, and Time-of-Flight SIMS.
- **Natural nanoparticles** are ubiquitous in the Earth system. They have many sources; volcanic activity, cosmic dust, aeolian particles derived from weathering and wind erosion, chemical precipitation in many environments, biomineralization, and biomass combustion. Nanoparticles are important constituents of the atmosphere, oceans, soils, and in biota (produce or ingested by organisms).

1.5 SHAPES OF NANOPARTICLES:

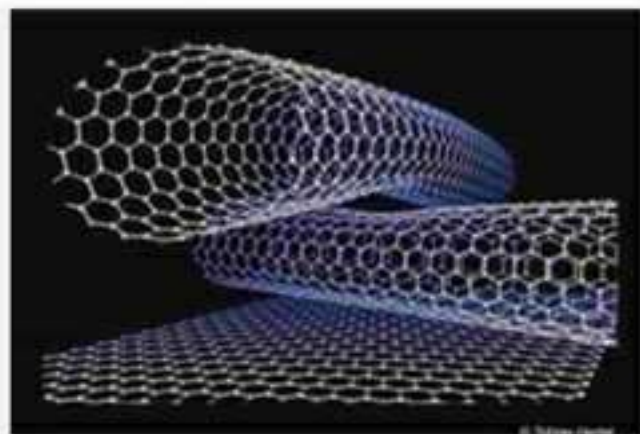


Fig 1.3

Nanoparticles "are as small as ~1 nm and may range up to several tens of nanometres in at least one dimension".

- Nanosheets or nanofilms have one dimension in this size range; (e.g., clay minerals)
- Nanorods have two dimensions in this size range
- Nanoparticles have three dimensions in this size range
- Nanotubes are nanoscale materials that have a tube-like structure; e.g., carbon nanotubes in the accompanying figure.

1.6 CONCEPTS OF NANO WORLD:

The nanoscience revolution requires a fundamentally new understanding of the properties of matter at the nanoscale. Here are some contexts and concepts that require special consideration when dealing with the nanoscale compared with micro- or mesoscale

- Quantum effects are dominant on the nanoscale
- Properties of matter change as a function of particle size on the nanoscale.
- "Mineral nanoparticles also behave differently than larger micro- and macroscopic crystals of the same mineral. Surface areas become quite large with respect to volume at the nanoscale.
- Consequently, surface energies become quite large with respect to Gibbs Free Energy.
- Classical theory of nucleation and growth of crystals (one atom at a time into an ordered crystal structure) is not entirely accurate.
- Control of Grain Size on Solubility on the Nanoscale:
- The contribution of nanoparticles to global bio/geochemical cycling is rarely considered [18].

1.7 REVIEW OF LITERATURE:

Kumari et al., (2015) studied the influence of nitrogen doping on structural and optical properties of ZnO nano particles. Un-doped and N

doped ZnO nano particles were synthesized by using chemical precipitation method. The prepared samples were differentiated through X-Ray Diffraction technique (XRD), Transmission Electron Microscopy (TEM) equipped with Energy Dispersive X-ray (EDAX) spectroscopy, UV-visible spectroscopy, Fourier Transform Infrared (FTIR) and came to a conclusion that the formation of impurity free wurtzite phase for undoped and N doped samples was uncertain through XRD analysis. The crystallite size was found increasing with increase in N doping concentration [19].

Rochman et al., (2017) explained the synthesis of ZnO nanoparticles made by Sol-Gel method. The parameters used in this process are variations in pH, in increasing order, of 7 to 12, in steps of 1 by using two principal reactions method to produce compound oxide, such as hydrolysis and condensation by considering Sodium hydroxide as an agent. Research reveals that greater the pH of the sol-gel will increase the agglomeration of particle and vice-versa [20].

Sutradhar et al., (2016) study used green synthesis of zinc oxide nanoparticles (ZnO) by thermal method and under microwave irradiation using the aqueous extract of tomatoes as non-toxic and also nature-friendly reducing material. They concluded that microwave-assisted green chemistry has been used for the preparation of ZnO NPs. A facile approach has been reported using tomato extract, acting as reducing agent for the synthesis of ZnO NPs of well-defined dimensions in huge amount. This eliminated the need of toxic chemicals for the production of nanoparticles. The synthesis has been done by thermal process as well as under microwave irradiation using different power and the synthesized nanoparticles were successfully used to prepare nanocomposites for photovoltaic applications[21].

Ahmed et al., (2017) depicts the Structural, optical, and

magnetic properties of Mn-doped ZnO samples deals with the microstructure, optical, and magnetic properties of Zn, Mn powder samples with $x = 0.02\text{--}0.08$ synthesized by a solid-state reaction method. X-ray diffraction showed that the cell characteristics between a and c , increased with the increase in Mn content, which showed that Mn ions substitute into the lattice of ZnO. It states that Mn-doped ZnO nano-powders have been successfully prepared by a solid-state reaction route. XRD studies showed the incorporation of Mn into the ZnO lattice. The structural, optical and magnetic investigations showed that FM observed at room temperature is an intrinsic property of the ZnO: Mn powder samples due to VO and defects, and it does not originate from any secondary magnetic phase or cluster formation[22].

Thaweesaeng et al.,(2013) explained that Pure ZnO and Cu -doped ZnO nano-powders (1, 2, 3, 4 and 5 wt % Cu) were synthesized by co-precipitation method without further post-heat treatment .It reveals that's synthesized ZnO and Cu-doped ZnO nano powders have been successfully prepared using co-precipitation technique. The XRD results confirmed that the crystal structure of all not synthesized samples is hexagonal wurtzite with a average crystallite sizes is approximately 25-27 nm corresponding to inter-planar spacing, lattice constant and micro-strain of as-synthesized powders [23].

Khalil et al., (2014) reported that ZnO nanoparticles were obtained by thermal decomposition of a binuclear zinc curcumin complex as single source precursor. Research explained that low heat energy was applied to degrade the organic moiety. Nanoparticles with a size ranging from 117 ± 4 nm were obtained from an easily prepared organic moiety consisting metal complex precursor. Such a type of precursors has potential for synthesizing metal oxide nanoparticles [24].

Sutradhar et al.,(2015) conducted research on the synthesis of zinc oxide (ZnO) nanoparticles and its composite with natural graphite (NG) powder for application in solar cells working. ZnO nanoparticles were prepared using green tea leaf extract as non-toxic and eco-friendly reducing material under microwave irradiation. A facile approach has been reported using green tea leaf extract, acting as reducing agent for the synthesis of ZnO nanoparticles of well-defined dimensions in bulk amount. Excellent reproducibility of these nanoparticles, without using any additional capping agent or stabilizer, will have a huge advantage as compared with microbial extraction, and biotechnology [25].

Matinise et al., (2017) conducted experiments to develop a better and reliable process for the bio-fabrication of Zinc oxide nanoparticles through green method using *Moringa Oleifera* extract as an effective chelating agent and concluded, Zinc oxide nanoparticles with particle size ranging from 12.27 and 30.51 nm have been successfully synthesized naturally by *Moringa-oleifera* extract and characterized using different methods. The XRD and EDS studies have shown that an annealing at about 500°C in air is required for the synthesis of pure wurtzite ZnO phase. This was stated via the XRD investigations highlighting on the polycrystalline nature of the nanoparticles[26].

Sindhura et al.,(2013) explained the biogenic zinc nanoparticles were synthesized using the leaves of *Parthenium hysterophorus* by green synthesis method. UV–VIS absorption spectroscopy was used to monitor the quantitative formation of zinc nanoparticles. The properties of the synthesized zinc nanoparticles were studied using scanning electron microscopy and nanoparticle analyzer. Zinc nanoparticles were seen to be spherical in shape with size ranged between 16-108.5 nm. They came to a conclusion that the zinc nanoparticles were synthesized using *Parthenium hysterophorus* leaf extract by green synthesis

method. Zinc nanoparticles coupled with microbial activity promises potential applications in agriculture where zinc is one of the essential micronutrients which is need to be supplied to the crop plants [27].

Alias et al., (2010) concluded that ZnO nanoparticles were processed at different pH values by the sol-gel process and centrifuged at 3000 rpm within 30 minutes. The ZnO powders agglomerate when synthesized in acidic and neutral conditions (pH 6 and 7). They stated that Fine powders were obtained when the pH of the sols was increased to 9. The maximum crystallite size of the ZnO powder was obtained at pH 9. The particles sizes of the ZnO synthesized ranged between pH 6 and 11 were in the range of 36.65–49.98 nm. Ultraviolet-visible studies (UV-vis) also revealed that ZnO processed ranging from pH 8 to 11 has good optical properties with band gap energy (E_g) between 3.14 and 3.25 eV[28].

Sangeetha et al.,(2011) reported on the production of nanostructure zinc oxide particles by both chemical and biological process. Highly stable and spherical zinc oxide nanoparticles are produced by using zinc nitrate and Aloevera leaf extract and stated that greater than 95% conversion to nanoparticles has been achieved with aloe leaf broth concentration greater than 25%. Structural, morphological and optical properties of the synthesized nanoparticles have been characterized by using UV-Vis spectrophotometer, FTIR, Photoluminescence, SEM, TEM and XRD analysis. SEM and TEM analysis shows that the zinc oxide nanoparticles prepared were poly dispersed and the average size ranged between 25 to 40 nm. The particles obtained have been found to be predominantly spherical and the particle size could be controlled by varying the concentrations of leaf broth solution [29].

Rao et al.,(2016) stated that study has been to use a biologically mediated, low temperature approach for the synthesis of zinc oxide nanoflowers. "Green" methods have a number of advantages over conventional approaches; these include the use of environmentally benign reactants and its economic feasibility. The cell free extract of *Chlamydomonas reinhardtii*, a fresh water microalga was used to synthesize the nanoflowers. The nanoflowers were composed of individual nanorods that assembled to form flower-like structures. The nanorods measured 330 nm in length and these nanorods self-assembled to form porous nanosheets that were found to measure 55–80 nm. Particle size analysis revealed that the larger porous nanoflowers approximately measured 4 μ m. Powder X-ray diffraction studies revealed that the zinc oxide nanoflowers had a hexagonal wurtzite crystal structure. Fourier transform infrared spectroscopy analysis suggested that algal biomolecules were responsible for the synthesis and stabilization of zinc oxide nanostructures. These nanoflowers demonstrate enhanced photocatalytic activity against methyl orange (MO) under natural sunlight [30].

Pulit-Prociak et al.,(2016) study presents a method for functionalization of textile materials using fabric dyes modified with silver or zinc oxide nanoparticles. Embedding of these nanoparticles into the structure of other materials makes that the final product is characterized by antimicrobial properties. Indigo and commercially available dye was involved in studies. It is worth to note that silver nanoparticles were obtained in-situ in the reaction of preparing indigo dye and in the process of preparing commercial dye baths. Such a method allows reducing technological steps. The modified dyes were used for dyeing of cotton fibers. The antimicrobial properties of final textile materials were studied. *Saccharomyces cerevisiae* strain was

used in microbiological test and concluded that the results confirmed biocidal activity of prepared materials [31].

1.8 AIM OF THE PRESENT WORK:

The aim of the present work is:

- To synthesize ZnO nanoparticles
- To determine the structure and size of the pure ZnO nanoparticles using X-Ray Diffraction analysis, SEM and EDAX.

1.9 MATERIAL IMPORTANCE:

1.9.1 ZINC OXIDE:

Zinc oxide (ZnO) is a common inorganic compound with a large number of uses. It is insoluble in water but soluble in dilute acids and bases. Its melting point is extremely high—1975 °C, where it also decomposes. Zinc compounds were probably used by early humans, in processed and unprocessed forms, as a paint or medicinal ointment, but their composition is uncertain. Since ZnO nanoparticles are a relatively new material, there is concern over the potential hazards they can cause. Because they are very tiny, nanoparticles generally can travel throughout the body, and have been shown in animal studies to penetrate the placenta blood-brain barrier, individual cells, and their nuclei. Tissues can absorb them easily due to their size which makes it difficult to detect them. However, human skin is an effective barrier to ZnO nanoparticles, for example when used as a sunscreen, unless abrasions occur. ZnO nanoparticles may enter the system from accidental ingestion of small quantities when putting on sunscreen [32].

1.9.2 USAGE:

The main usage of zinc oxide (zinc white) was in paints and as an

additive to ointments. Zinc white was accepted as a pigment in oil paintings by 1834 but it did not mix well with oil. This problem was solved by optimizing the synthesis of ZnO. In 1845, Le Claire in Paris was producing the oil paint on a large scale, and by 1850, zinc white was being manufactured throughout Europe. The success of zinc white paint was due to its advantages over the traditional white lead: zinc white is essentially permanent in sunlight, it is not blackened by sulphur-bearing air, it is non-toxic and more economical. Because zinc white is so "clean" it is valuable for making tints with other colours, but it makes a rather brittle dry film when unmixed with other colours. For example, during the late 1890s and early 1900s, some artists used zinc white as a ground for their oil paintings. All those paintings developed cracks over the years.

In recent times, most zinc oxide was used in the rubber industry to resist corrosion. In the 1970s, the second largest application of ZnO was photocopying. High-quality ZnO produced by the "French process" was added to photocopying paper as a filler. This application was soon displaced by titanium [23].

1.9.3 APPLICATIONS OF PAPAYA LEAF:

1. DENGUE FEVER:

- One of the most prominent medicinal benefits of papaya leaf is it's potential to treat certain symptoms associated with Dengue fever.
- Papaya leaves extract significantly increased blood platelet levels.
- Studies have found that papaya leaf extract can improve blood platelet levels in people with Dengue fever.

2.PROMOTE BALANCED BLOOD SUGAR:

- Papaya leaves extract to have potent antioxidant and blood sugar – lowering effects. This is attributed to papaya leaf's ability to protect insulin-producing cells in the pancreas from the damage and premature death.

3.DIGESTIVE FUNCTION:

- Papaya leaf contain fibre a nutrient that supports healthy digestive function and a unique compound called papain.
- Papain is used for its ability to break down large proteins into smaller, easier to digest proteins and amino acid.

4. SUPPORT HAIR GROWTH:

- Papaya leaf masks and juices are often used to improve hair growth and scalp health, but evidence to support it' s efficiency for these purpose is extremely limited.
- Papaya leaf contains several compounds with antioxidant properties, such as flavonoids and vitamin E.

5. ANTICANCER PROPERTIES:

- Papaya leaf extract has demonstrated a powerful ability to inhibit the growth of prostate and breast cancer cells in test-tube studies, but neither animal nor human experiments have replicated these results [34].

1.10 IMAGE OF ZnO PARTICLES:



Fig 1.4

CHAPTER-2

PREPARATION OF PURE ZnO NANOPARTICLES

2.1 INTRODUCTION:

There are few methods to synthesis nanoparticles. Slow evaporation, hydro thermal, co-precipitation, sol-gel process are some of them. Here we used the co-precipitation method to prepare ZnO nanoparticles.

2.2 CHEMICAL APPROACH:

In the chemical approach, the main components are the metallic precursors, stabilizing agents and reducing agents (inorganic and organic both). Reducing agents such as sodium citrate, ascorbate, sodium borohydride (NaBH_4), elemental hydrogen, polyol process, tollens reagent, N,N-dimethylformamide (DMF) and poly(ethylene glycol)-block copolymers are used [35].

2.3 GREEN APPROACH FOR SYNTHESIS OF ZnO NPs:

Traditional methods are used from past many years but researches have proved that the green methods are more effective for the generation of NPs with the advantage of less chances of failure, low cost and ease of characterization [36]. Physical and chemical approaches of synthesizing NPs have posed several stresses on environment due to their toxic metabolites. Plant-based synthesis of NPs is certainly not a troublesome procedure, a metal salt is synthesized with plant extract and the response is completed in minutes to couple of hours at typical room temperature. This strategy has attracted much more attention amid the most recent decade particularly for silver (Ag) and gold (Au) NPs, which are more secure as contrasted with other metallic NPs. Generation of NPs from green techniques can be scaled up effortlessly and they are fiscally smart too. In light of their exceptional properties the greenly orchestrated NPs are currently favoured over the traditionally delivered NPs. Use of more chemicals, which are harmful and toxic for human health and

environment, could increase the particle reactivity and toxicity and might cause unwanted adverse effects on health because of their lack of assurance and uncertainty of composition [37]. Green methods of synthesis are significantly attractive because of their potential to reduce the toxicity of NPs. Accordingly, the use of vitamins, amino acids, plants extracts is being greatly popularized nowadays [38].

2.4 CO-PRECIIPITATION METHOD:

2.4.1 CO-PRECIIPITATION:

Co-precipitation method refers to obtain a uniform composition in two or more cations homogeneous solution through precipitation reaction, which is one of important methods for the synthesis of composites containing two or more kinds of metal elements. The coprecipitation technique is probably the simplest and convenient chemical pathway to synthesize nanoparticles. Co-precipitation reactions involve the simultaneous occurrence of nucleation, growth, coarsening, and/or agglomeration processes.

Co-precipitation reactions exhibit the following characteristics:

- The products are generally insoluble species formed under conditions of high [supersaturation](#).
- Nucleation is a key step, and a large number of small particles will be formed.
- Secondary processes, such as [Ostwald ripening](#) and aggregation, dramatically affect the size, morphology, and properties of the products.
- The supersaturation conditions necessary to induce precipitation are usually the result of a chemical reaction.

Typical Co-Precipitation Synthesis Methods:

Metals formed from aqueous solutions, by reduction from nonaqueous solutions, electrochemical reduction, and decomposition of metal organic precursors. Oxides formed from aqueous and nonaqueous solutions. Metal chalcogenides formed by reactions of molecular precursors. Microwave sonication-assisted coprecipitation.

2.4.2 ADVANTAGES:

Coprecipitation method has the advantages of directly obtaining homogeneous nanomaterials with small size and size distribution through various chemical reactions in the solution.

- Simple and rapid preparation.
- Easy control of particle size and composition.
- Various possibilities to modify the particle surface state and overall homogeneity.
- Low temperature.
- Energy efficient.
- Does not involve use of organic solvent.

2.4.3 DISADVANTAGES:

- Not applicable to uncharged species.
- Trace impurities may also get precipitated with the product.
- Time consuming.
- Batch-to-batch reproducibility problems.
- This method does not work well if the reactants have very different precipitation rates [39].

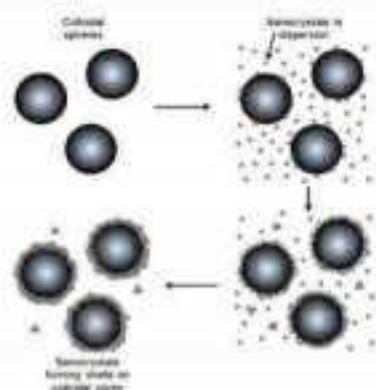


Fig 2.1

2.5 MATERIAL PREPARATION:

In the present work, pure ZnO nanoparticles are prepared by Co-precipitation method. This method is simplest and convenient pathway to synthesize nanoparticles.

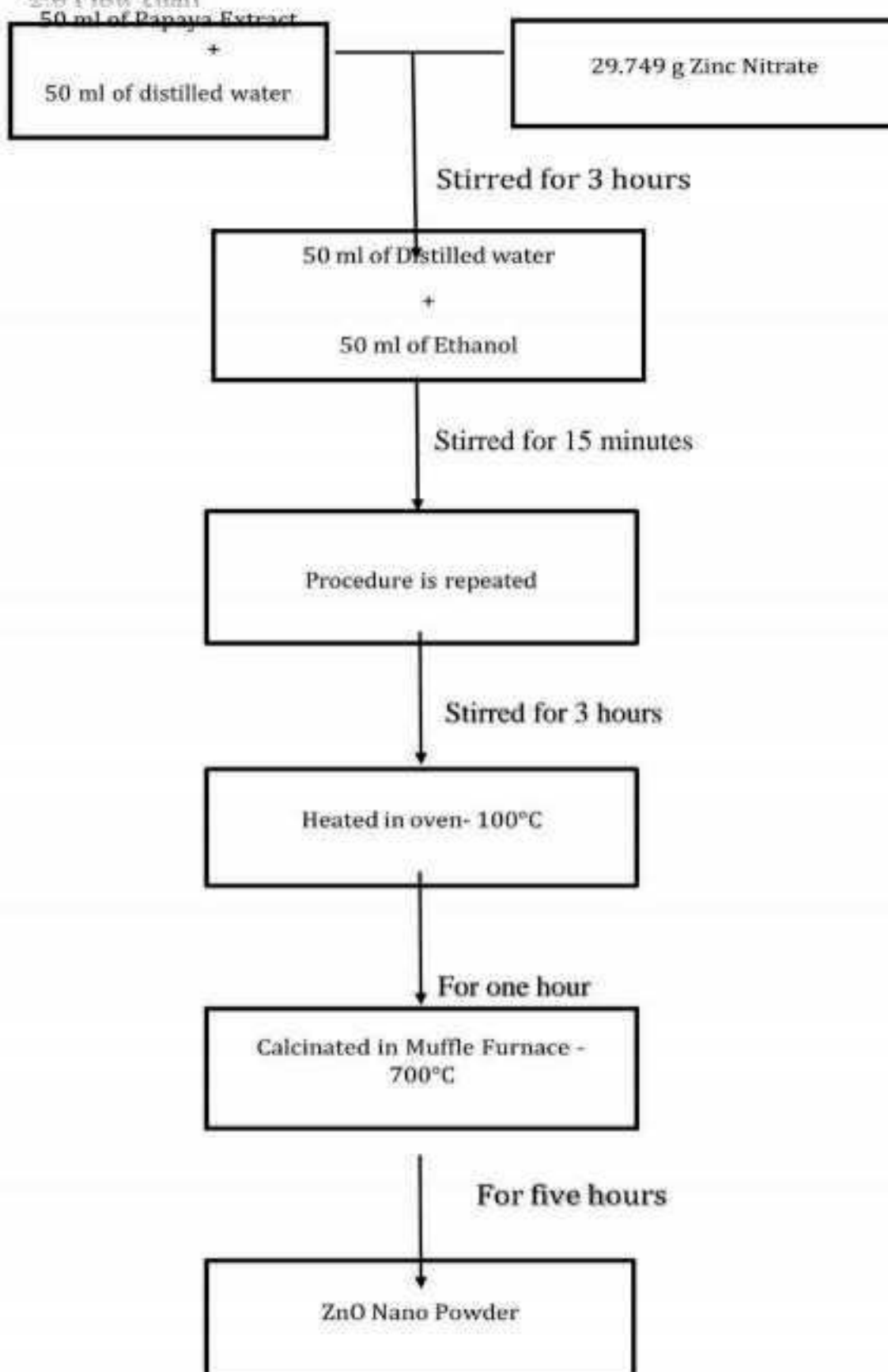
2.5.1 SYNTHESIS OF PURE ZINC OXIDE NANOPARTICLES:

29.474g of Zinc Nitrate is dissolved in 50ml extract of papaya leaf mixed with distilled water. The beaker is washed well with acetone. The mixture is poured in the beaker, kept in magnetic stirrer and stirred thoroughly for 3 hours. 50ml of ethanol and 50ml of distilled water is added and again stirred for 15 minutes. The beaker is kept undisturbed for hours. The green coloured liquid changes into dark yellow colour. The clear liquid is poured out and 50 ml of ethanol and 50 ml of distilled water is added and again stirred for 3 hours. Now, the dark yellow coloured liquid changes into pale yellow colour. The procedure is repeated for 5 times. The liquid thus obtained is a clear liquid. The sample is filtered and heated in hot air oven at 100°C for 1 hour. The dried sample is placed in muffle furnace at 700°C for 5 hours. The precipitate thus obtained is finely powdered. Thus the Nano Particles of Zinc Oxide is obtained.



Fig 2.2

2.6 Flow chart



CHAPTER-3

CHARACTERIZATION

3.1 INTRODUCTION:

After the synthesis of NPs it is must to ponder the morphology and other conformational subtle elements by utilizing different spectroscopic strategies. The most widely utilized systems are: UV-vis absorption spectroscopy, X-ray diffraction (XRD), Fourier transmission infrared (FTIR) spectroscopy, dynamic light scattering (DLS), energy dispersive X-ray examination (EDAX), scanning electron microscopy (SEM), transmission electron microscopy (TEM) and so on.

3.2 XRD SPECTROSCOPY:

X-ray diffractograms of nano-materials give an abundance of data from phase creation to crystallite estimate, from cross section strain to crystallographic introduction, XRD is non-contact and non-destructive, which makes it ideal for in situ studies [40].

Other techniques for characterization of NPs are EDS and DLS, the energy dispersive spectroscopy (EDS) is used to separate the characteristic X-rays of different elements into an energy spectrum, is used for detection of elemental composition of metal NPs. Dynamic light scattering analysis of incident photons is used to determine the surface charge and the hydrodynamic radius of the NPs.

3.2.1 X-RAY DIFFRACTION (XRD):

X-ray diffraction is based on constructive interference of monochromatic X-rays and a crystalline sample. These X-rays are generated by a cathode ray tube, filtered to produce monochromatic radiation, collimated to concentrate, and directed toward the sample. The interaction of incident rays with the sample produces constructive

interference (and a diffracted ray) when condition satisfy Bragg's law,

$$n\lambda = 2d \sin\theta$$

where,

n is the order of the diffracted beam

λ is the wavelength of the incident X-ray beam.

d is the distance between adjacent planes of atom (the d-spacing).

θ is the angle of incident of the x-ray beam.

When a crystal is bombarded with X-rays of a fixed wavelength (similar to spacing of the atomic-scale crystal lattice planes) and at certain incident angles, intense reflected X-rays are produced when the wavelengths of the scattered X-rays interfere constructively. In order for the waves to interfere constructively, the differences in the travel path must be equal to integer multiples of the wavelength. When this constructive interference occurs, a diffracted beam of X-rays will leave the crystal at an angle equal to that of the incident beam.

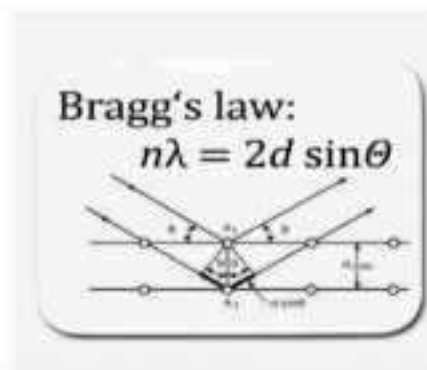


Fig 3.1

A similar process occurs upon scattering neutron waves from the nuclei or by a coherent spin interaction with an unpaired electron. These re-emitted wave fields interfere with each other either constructively or destructively (overlapping waves either add up together to produce

stronger peaks or are subtracted from each other to some degree), producing a diffraction pattern on a detector or film. The resulting wave interference pattern is the basis of diffraction analysis.

3.2.2 INSTRUMENTATION AND CHARACTERIZATION: X-RAY POWDER DIFFRACTION ANALYSIS:

X-ray powder diffraction (XRD) is a rapid analytical technique primarily used for phase identification of a crystalline material and can provide information on unit cell dimensions. The analysed material is finely ground, homogenized, and average bulk composition is determined.

PRINCIPLE:

Max von Laue, in 1912, discovered that crystalline substances act as three-dimensional diffraction gratings for X-ray wavelengths similar to the spacing of planes in a crystal lattice. X-ray diffraction is now a common technique for the study of crystal structures and atomic spacing.

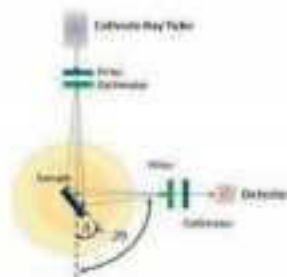


Fig 3.2

X-ray diffraction is based on constructive interference of monochromatic X-rays and a crystalline sample. These X-rays are generated by a cathode ray tube, filtered to produce monochromatic radiation, collimated to concentrate, and directed toward the sample. The interaction of the incident rays with the sample produces constructive

interference (and a diffracted ray) when conditions satisfy [Bragg's Law](#) ($n\lambda=2d \sin \theta$). This law relates the wavelength of electromagnetic radiation to the diffraction angle processed and counted. By scanning the sample through a range of 2θ angles, all possible diffraction directions of the lattice should be attained due to the random orientation of the powdered material. Conversion of the diffraction peaks to d-spacings allows identification of the mineral because each mineral has a set of unique d-spacings. Typically, this is achieved by comparison of d-spacings with standard reference patterns.

3.2.3 X-RAY DIFFRACTOMETER:

A diffractometer is a [measuring instrument](#) for analysing the structure of a material from the [scattering](#) pattern produced when a beam of [radiation](#) or particles (such as [X-rays](#) or [neutrons](#)) interacts with it.

X-ray diffractometers consist of three basic elements: an X-ray tube, a sample holder, and an X-ray detector. X-rays are generated in a cathode ray tube by heating a filament to produce electrons, accelerating the electrons toward a target by applying a voltage, and bombarding the target material with electrons [41].



fig 3.3

3.3.1 SCANNING ELECTRON MICROSCOPE: ELECTRONBEAM AND ELECTRON COLUMN:

Electrons are emitted from the filament of an electron source and subsequently collimated into a beam. The electron beam travels through the electron column, which consists of a set of lenses that focus the beam onto the sample surface. Electron microscope lenses can be electrostatic or magnetic, depending on whether they use an electrostatic field or a magnetic field to focus the electron beam. To better understand how these lenses work, let's take a step back and look at how electrons can be deflected in an electrostatic field.

DEFLECTORS:

Electrons are negatively charged particles and travel through the electron column at high energy and high speed. One way to deflect these particles is to let them travel through an electric field generated by two plates at potential $+U$ and $-U$. Under the influence of the electric field, the electron is deflected at an angle that depends on the electron energy, the electric field applied in between the plates, and the length of the plates. The faster, or the more energetic the electron, the smaller the deflection angle. The higher the electric field and the longer the plates, the bigger the deflection angle. A device consisting of two plates at different potential is called a deflector.

To get an electrostatic lens, one could think of mirroring the effect of a deflector, such that the outer electrons traveling off the optical axis can be focused on the same point. whenever there is a lens effect, the energy of the beam changes, meaning that the electrons either accelerate or decelerate. This can be done simply by having an aperture on different potential around the beam.

ELECTROSTATIC LENSES:

Electrostatic lenses consist of metallic plates connected to high voltage with an aperture that the electron beam travels through. Single-aperture lenses consist of a single metallic plate at high voltage and can often be found in electron sources. The single-aperture lenses can either terminate an accelerating field or be followed by an accelerating field. In the first case, the lens is positive, meaning that the beam converges into a crossover, while in the second case, the lens is negative, meaning that the beam diverges

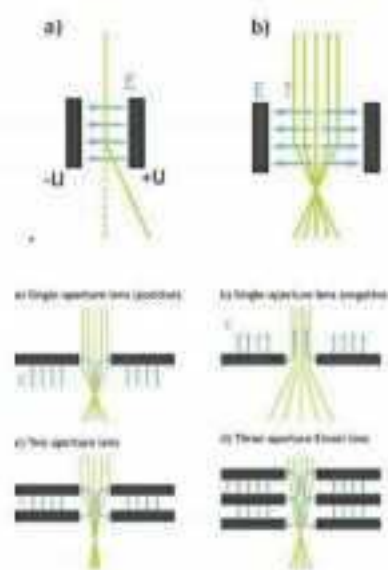


Fig 3.5

A two-aperture lens consists of two metallic plates at different potential with aligned apertures. In an accelerating two-aperture lens, the electric field is placed in between the two plates points at the top plate. The electrons that enter this lens will feel a strong field that pushes them closer to the optical axis. As they travel through the second plate, the electrons feel an opposite force that pushes them towards the aperture. As a total effect, this is a positive lens and the beam is focused in a plane below the second plate.

A three-aperture Einzel lens consists of three plates with aligned apertures, that can either have the same diameter, or a different one. Einzel lenses are commonly used in electron optics for the advantage of having an equal beam potential at the entrance and exit of the lens. The three electrodes generate three lenses: the first and the third are positive, where the electric field lines point towards the plates, and the second is negative. The total lens is positive and the beam is focused on a plane below the third lens.

MAGNETIC LENSES:

Magnetic lenses use the Lorentz force, that is proportional to the electron charge and velocity, to deflect electrons. Magnetic lenses consist of a metallic body (called the ferromagnetic circuit) that ends with two pole pieces. The magnetic field is given by a coil positioned at the top of the ferromagnetic circuit. The strength of the lens can be altered by varying the magnetic field B . This is done by modifying the geometry of the pole piece, namely the distance between the pole pieces, and the current flowing into the coils (excitation).

THE SEM ELECTRON COLUMN:

The electron column consists of the electron source, where the electrons are emitted, and a set of lenses. The electrons are condensed into a beam by the condenser lenses and then focused onto the sample surface by the final lens, also called the objective lens, as shown. The source tilt and the scanning of the beam at the sample is done by coils at the source and right above the final lens. All SEMs have an electron column with electrostatic lenses and magnetic lenses [42].

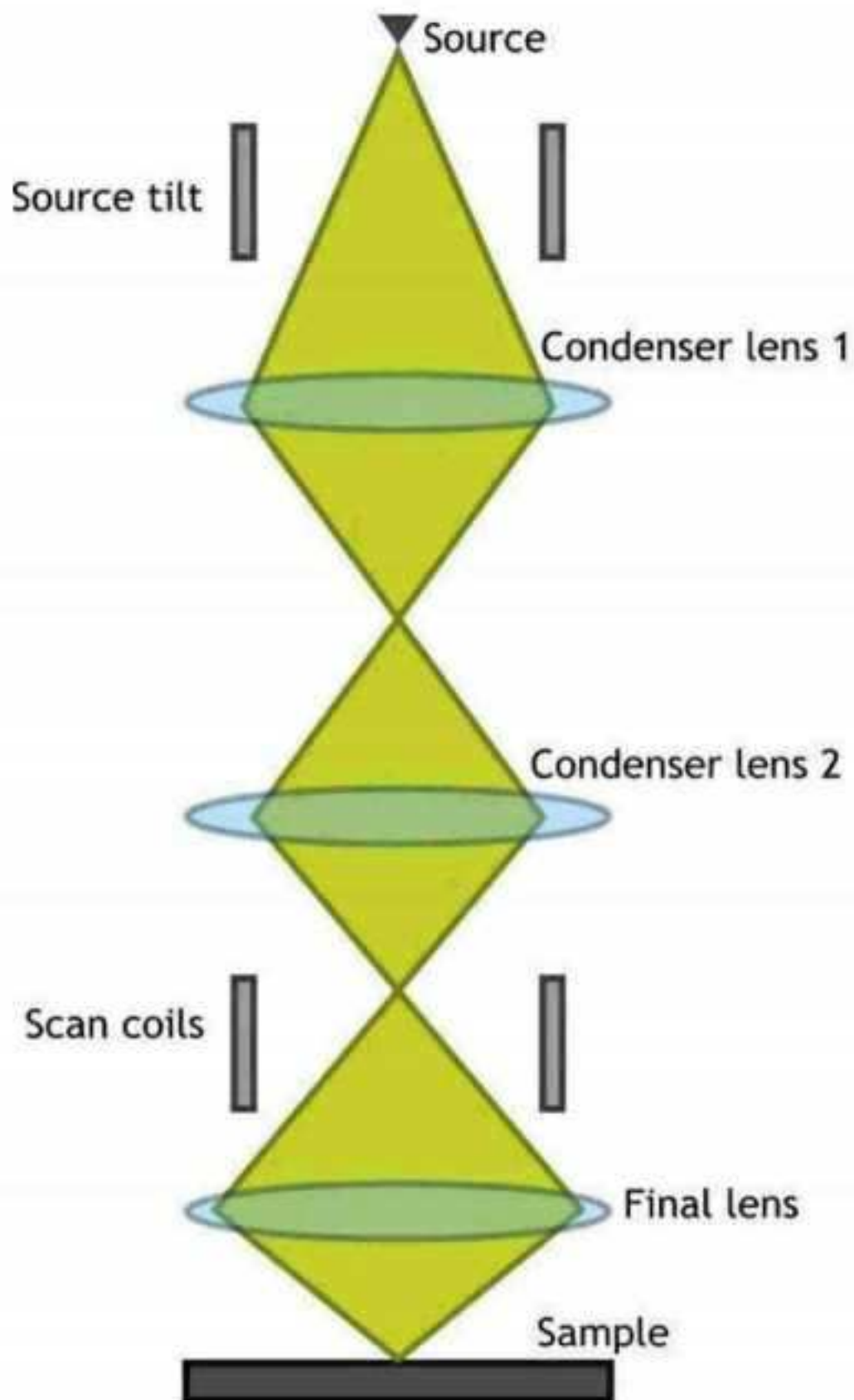


Fig 3.6

3.4 ENERGY DISPERSIVE X- RAY SPECTROSCOPY:

Energy-dispersive X-ray spectroscopy (EDX) is a surface analytical technique where an electron beam hits the sample, exciting an electron in an inner shell, causing its ejection and the formation of an electron hole in the electronic structure of the element.

EDS analysis is also called energy dispersive X-ray analysis or energy dispersive X-ray microanalysis. It is an analytical technique used for the elemental analysis or chemical characterization of a sample. It relies on an interaction of some source of X-ray excitation and a sample. Its characterization capabilities are due in large part to the fundamental principle that each element has a unique atomic structure allowing a unique set of peaks on its X-ray emission spectrum. The results of EDS analysis for the cracked surface of a BOF slag particle after autoclave treatment is shown below. It can be seen that Ca is the dominant element in the sample, although chloride is also found in the sample.

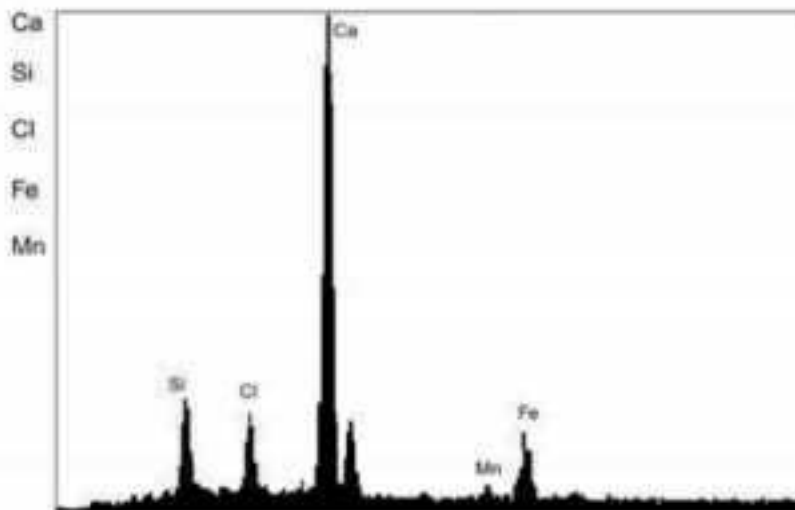


fig 3.7

Energy-dispersive X-ray spectroscopy (EDS, EDX, or XEDS) is an analytical technique used for the elemental analysis or chemical characterization of a sample. It relies on the investigation of the

interaction of some source of X-ray excitation and a sample. Its characterization capabilities are due in large part to the fundamental principle that each element has a unique atomic structure allowing unique sets of peaks on its X-ray spectrum. To stimulate the emission of characteristic X-rays from a specimen, a high energy beam of charged particles such as electrons or protons or a beam of X-rays is focused into the sample being studied. At rest, an atom within the sample contains ground state (or unexcited) electrons in discrete energy levels or electron shells bound to the nucleus. The incident beam may excite an electron in an inner shell, ejecting it from the shell while creating an electron hole where the electron was. An electron from an outer, higher-energy shell then fills the hole, and the difference in energy between the higher-energy shell and the lower-energy shell may be released in the form of an X-ray. The number and energy of the X-rays emitted from a specimen can be measured by an energy-dispersive spectrometer. As the energy of the X-rays is characteristic of the difference in energy between the two shells, and of the atomic structure of the element from which they were emitted, this allows the elemental composition of the specimen to be measured [43].

CHAPTER-4

RESULT AND DISCUSSION

4.1 CHARACTERIZATION USING XRD:

The structural characterization of the pure zinc oxide nanoparticles is carried out by XRD method. The X-ray diffraction experiments are carried out with a XPERT-PRO Diffraction system using the $\text{CuK}\alpha$ radiation of wavelength 1.5406\AA . The type of the scan used is continuous and ranging from 10° to 80° . The average grain size is calculated using the Debye Scherrer formula,

$$D = \frac{K\lambda}{Q \cos \theta}$$

Where,

- D is the mean size of the ordered (crystalline) domains, which may be smaller or equal to the grain size or the particle size. (nm)
- K is the dimensionless shape factor, with a value close to unity (0.9)
- λ is the wavelength of the X-Ray radiation [$\lambda = 1.5406\text{\AA}$]
- β is the line broadening at half the maximum intensity (FWHM)
- θ is the angle of diffraction. (degree)

Fig(4.1) shows the XRD pattern for Zinc oxide nanoparticles prepared using Carica Papaya leaf extract as bio-reductant. The powder XRD pattern for the pure ZnO nanoparticles with the high intensity peak observed at $2\theta = 36.17^\circ$. The absence of impurity peaks reveals that ZnO nanoparticles exhibit high crystalline quality.

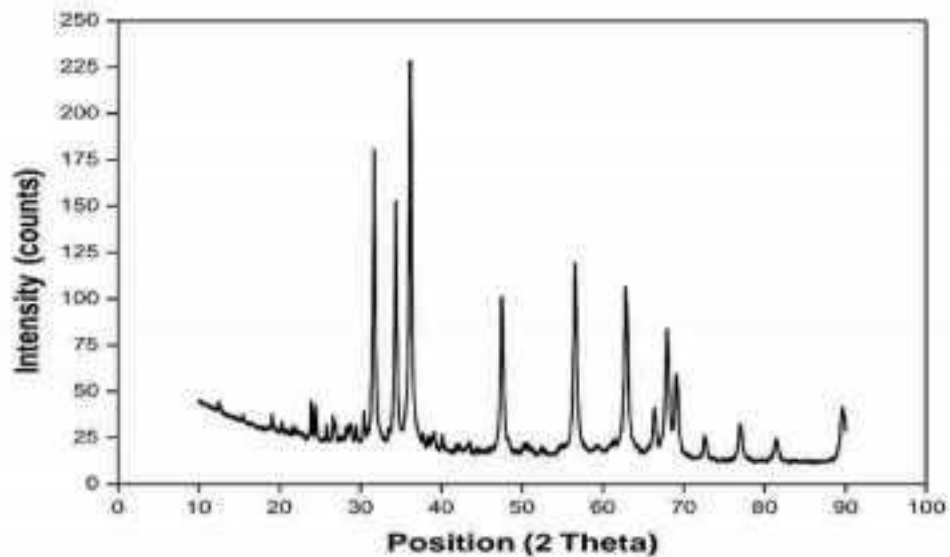


Fig 4.1

Calculation:

$$K=0.9 \quad \lambda = 1.5406 \times 10^{-10} \text{ m}$$

$$D = \frac{K\lambda}{Q \cos \theta}$$

$$1. \quad 2\theta = 19.0996 \quad \theta = 9.5498 \quad \beta = 0.1701$$

$$D = \frac{0.9 \times 1.5406 \times 10^{-10}}{0.1701 \times \cos(9.5498) \times 3.14}$$

$$= 47.38399 \times 10^{-9} \text{ m}$$

$$D = 47.38399 \text{ nm}$$

$$2. \quad 2\theta = 23.9497 \quad \theta = 11.9749 \quad \beta = 0.1684$$

$$D = \frac{0.9 \times 1.5406 \times 10^{-10}}{0.1684 \times \cos(11.9749) \times 3.14}$$

$$= 48.249015 \times 10^{-9} \text{ m}$$

$$D = 48.249015 \text{ nm}$$

$$3. \quad 2\Theta=24.4482 \quad \Theta=12.2241 \quad \beta=0.1677$$

$$D = \frac{0.9 \times 1.5406 \times 10^{-10}}{0.1677 \times \cos(12.2241) \times 3.14}$$

$$= 48.49560 \times 10^{-9} \text{m}$$

$$D = 48.49560 \text{ nm}$$

$$4. \quad 2\Theta=26.6459 \quad \Theta=13.3230 \quad \beta=0.1525$$

$$D = \frac{0.9 \times 1.5406 \times 10^{-10}}{0.1525 \times \cos(13.3230) \times 3.14}$$

$$= 53.56166 \times 10^{-9} \text{m}$$

$$D = 53.56166 \text{ nm}$$

$$5. \quad 2\Theta=29.5561 \quad \Theta=14.7781 \quad \beta=0.9758$$

$$D = \frac{0.9 \times 1.5406 \times 10^{-10}}{0.9758 \times \cos(14.7781) \times 3.14}$$

$$= 8.424 \times 10^{-9} \text{m}$$

$$D = 8.424 \text{ nm}$$

$$6. \quad 2\Theta=30.4089 \quad \Theta=15.2045 \quad \beta=0.1534$$

$$D = \frac{0.9 \times 1.5406 \times 10^{-10}}{0.1534 \times \cos(15.2045) \times 3.14}$$

$$= 52.69766 \times 10^{-9} \text{m}$$

$$D = 52.69766 \text{ nm}$$

$$7. \quad 2\Theta=31.6851 \quad \Theta=15.84255 \quad \beta=0.2126$$

$$D = \frac{0.9 \times 1.5406 \times 10^{-10}}{0.2126 \times \cos(15.84255) \times 3.14}$$

$$= 38.86242 \times 10^{-9} \text{m}$$

$$D = 38.86242 \text{ nm}$$

$$8. \quad 2\Theta=34.3485 \quad \Theta=17.1743 \quad \beta=0.2098$$

$$D = \frac{0.9 \times 1.5406 \times 10^{-10}}{0.2098 \times \cos(17.1743) \times 3.14}$$

$$= 39.6521 \times 10^{-9} \text{m}$$

$$D = 39.6521 \text{ nm}$$

$$9. \quad 2\Theta=36.1725 \quad \Theta=18.0862 \quad \beta=0.2224$$

$$D = \frac{0.9 \times 1.5406 \times 10^{-10}}{0.2224 \times \cos(18.0862) \times 3.14}$$

$$= 37.59740 \times 10^{-9} \text{m}$$

$$D = 37.59740 \text{ nm}$$

$$10. \quad 2\Theta=39.1063 \quad \Theta=19.5531 \quad \beta=1.0241$$

$$D = \frac{0.9 \times 1.5406 \times 10^{-10}}{1.0241 \times \cos(19.5531) \times 3.14}$$

$$= 82.30580 \times 10^{-9} \text{m}$$

$$D = 82.30580 \text{ nm}$$

$$11. \quad 2\Theta=40.1090 \quad \Theta=20.0545 \quad \beta=0.2189$$

$$D = \frac{0.9 \times 1.5406 \times 10^{-10}}{0.2189 \times \cos(20.0545) \times 3.14}$$

$$= 38.65321 \times 10^{-9} \text{m}$$

$$D = 38.65321 \text{ nm}$$

$$12. \quad 2\Theta=47.4670 \quad \Theta=23.7335 \quad \beta=0.2576$$

$$D = \frac{0.9 \times 1.5406 \times 10^{-10}}{0.2576 \times \cos(23.7335) \times 3.14}$$

$$= 33.70519 \times 10^{-9} \text{m}$$

$$D = 33.70519 \text{ nm}$$

$$13. \quad 2\Theta=56.5168 \quad \Theta=28.2584 \quad \beta=0.2703$$

$$D = \frac{0.9 \times 1.5 / 406 \times 10^{-10}}{0.2703 \times \cos(28.2584) \times 3.14}$$

$$= 33.38423 \times 10^{-9} \text{m}$$

$$D = 33.38423 \text{ nm}$$

$$14. \quad 2\Theta=60.8552 \quad \Theta=30.4276 \quad \beta=5.0995$$

$$D = \frac{0.9 \times 1.5406 \times 10^{-10}}{0.1701 \times \cos(9.5498) \times 3.14}$$

$$= 18.076089 \times 10^{-9} \text{m}$$

$$D = 18.076089 \text{ nm}$$

$$15. \quad 2\Theta=62.7940 \quad \Theta=31.397 \quad \beta=0.2798$$

$$D = \frac{0.9 \times 1.5406 \times 10^{-10}}{0.2798 \times \cos(31.397) \times 3.14}$$

$$= 33.2800751 \times 10^{-9} \text{m}$$

$$D = 33.2800751 \text{ nm}$$

$$16. \quad 2\Theta=66.3136 \quad \Theta=33.1568 \quad \beta=0.2933$$

$$D = \frac{0.9 \times 1.5406 \times 10^{-10}}{0.2933 \times \cos(33.1568) \times 3.14}$$

$$= 32.370243 \times 10^{-9} \text{m}$$

$$D = 32.370243 \text{ nm}$$

$$17. \quad 2\Theta=67.8800 \quad \Theta=33.94 \quad \beta=0.2976$$

$$D = \frac{0.9 \times 1.5406 \times 10^{-10}}{0.2976 \times \cos(33.94) \times 3.14}$$

$$= 32.192376 \times 10^{-9} \text{m}$$

$$D = 32.192376 \text{ nm}$$

$$18. \quad 2\Theta=69.0166 \quad \Theta=34.5083 \quad \beta=0.3141$$

$$D = \frac{0.9 \times 1.5406 \times 10^{-10}}{0.3141 \times \cos(34.5083) \times 3.14}$$

$$= 30.70838 \times 10^{-9} \text{m}$$

$$D = 30.70838 \text{ nm}$$

$$19. \quad 2\Theta=72.5233 \quad \Theta=36.2616 \quad \beta=0.3739$$

$$D = \frac{0.9 \times 1.5406 \times 10^{-10}}{0.3739 \times \cos(36.2616) \times 3.14}$$

$$= 26.3633768 \times 10^{-9} \text{m}$$

$$D = 26.36337 \text{ nm}$$

$$20. \quad 2\Theta=76.9079 \quad \Theta=38.453 \quad \beta=0.4229$$

$$D = \frac{0.9 \times 1.5406 \times 10^{-10}}{0.4229 \times \cos(38.453) \times 3.14}$$

$$= 23.999935 \times 10^{-9} \text{m}$$

$$D = 23.9999 \text{ nm}$$

$$21. \quad 2\Theta=81.3475 \quad \Theta=40.673 \quad \beta=0.4858$$

$$D = \frac{0.9 \times 1.5406 \times 10^{-10}}{0.4858 \times \cos(40.673) \times 3.14}$$

$$= 21.572260 \times 10^{-9} \text{m}$$

$$D = 21.57226 \text{ nm}$$

$$22. \quad 2\Theta=89.5679 \quad \Theta=44.783 \quad \beta=0.4168$$

$$D = \frac{0.9 \times 1.5406 \times 10^{-10}}{0.4168 \times \cos(44.783) \times 3.14}$$

$$= 26.867294 \times 10^{-9} \text{m}$$

$$D = 26.86729 \text{ nm}$$

PEAK HEIGHT(cts)	Position 2 θ (DEGREE)	MEAN θ (DEGREE)	FWHM β	PARTICLE SIZE D(nm)
377.50	19.0996	9.5498	0.1701	47.3840
986.34	23.9497	11.9749	0.1684	48.2490
737.93	24.4482	12.2241	0.1677	48.4956
740.09	26.6459	13.3230	0.1525	53.5616
1513.15	29.5561	14.7781	0.9758	8.4241
589.07	30.4089	15.2045	0.1534	52.6976
23417.70	31.6851	15.8425	0.2126	38.8624
16776.48	34.3485	17.1743	0.2098	39.6521
37959.10	36.1725	18.0863	0.2224	37.5974
264.96	39.1063	19.5532	1.0241	8.2305
254.38	40.1090	20.0545	0.2189	38.6532
7565.16	47.4670	23.7335	0.2576	33.7052
11069.03	56.5168	28.2584	0.2703	33.3842
88.32	60.8552	30.4276	5.0995	18.0761
9111.64	62.7940	31.397	0.2798	33.2801
1162.43	66.3136	33.1568	0.2933	32.3702
5633.37	67.8800	33.94	0.2976	32.1924
2646.56	69.0166	34.5083	0.3141	30.7084
351.82	72.5233	36.2616	0.3739	26.3634
670.98	76.9079	38.453	0.4229	23.9999
319.27	81.3475	40.673	0.4858	21.5726
1355.11	89.5679	44.783	0.4168	26.8672

The average size of zinc oxide nanoparticle is **33.3785 nm**.

4.2 CHARACTERIZATION USING SEM:

Fig. 4.2 shows the SEM image for Zinc oxide nanoparticles prepared using Carica Papaya leaf extract as bio-reductant. The morphology of the prepared ZnO nano powder was investigated by Scanning electron microscopy (SEM). As shown in Fig.(4.2), the average size of ZnO nanoparticles was estimated to be around 70 - 100nm. The SEM photograph shows that the powder was homogeneous and agglomerated.

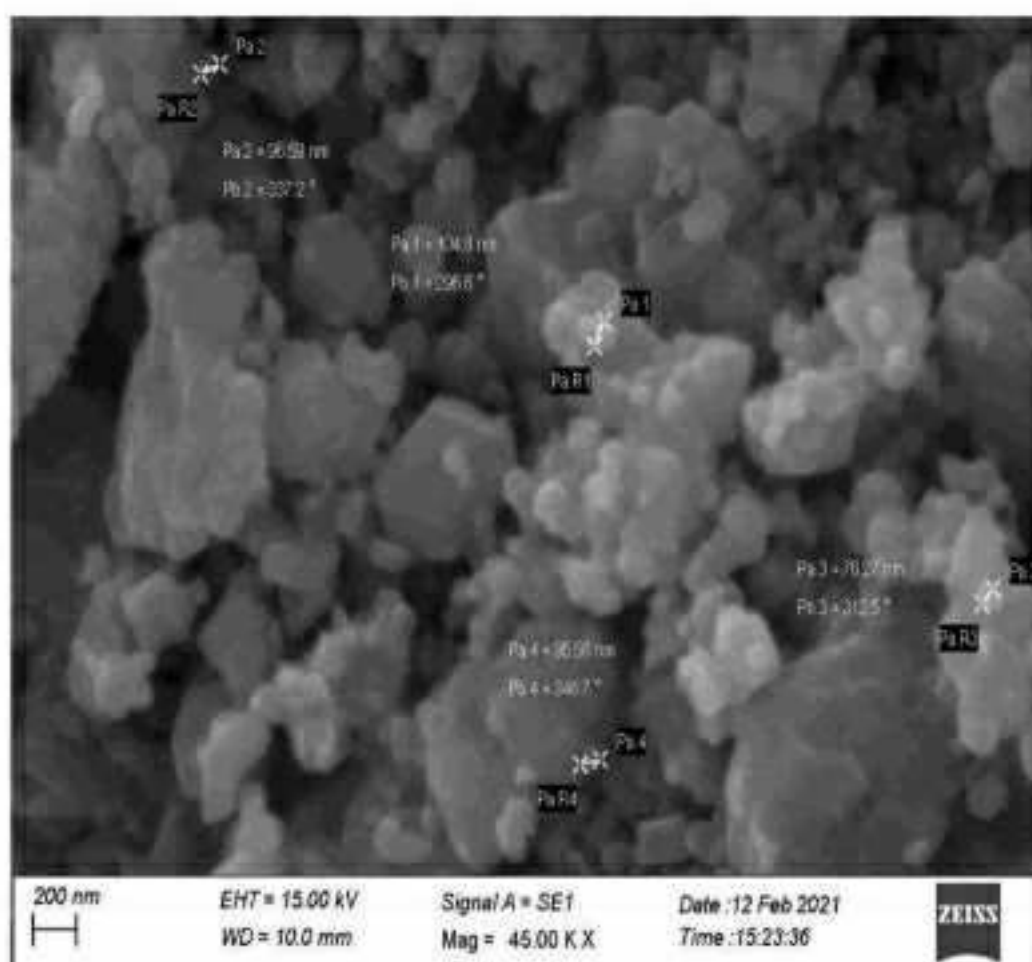
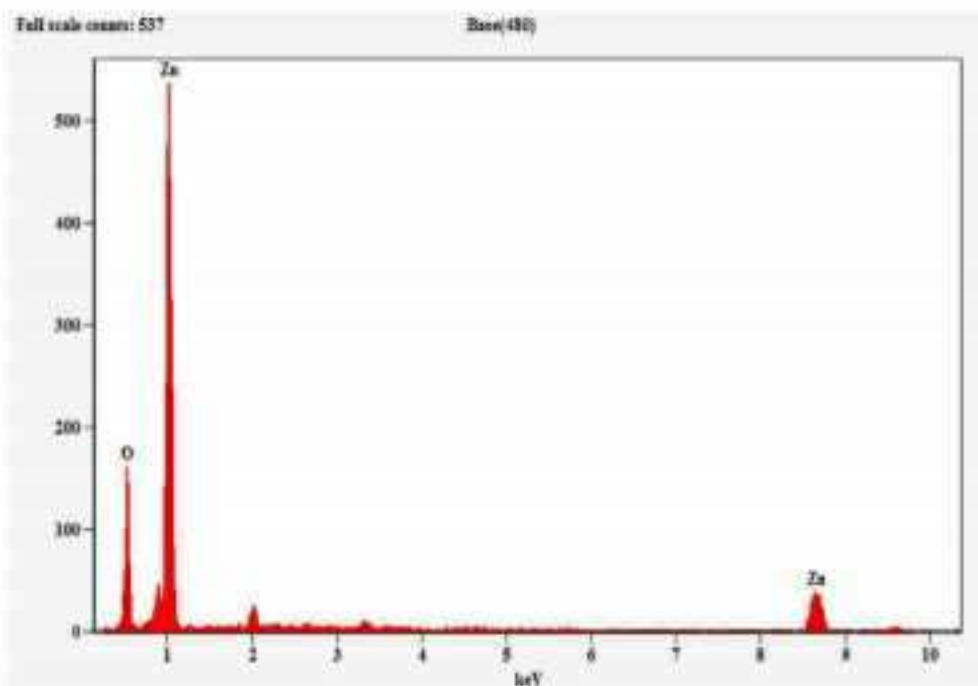


Fig. (4.2) Scanning Electron Microscope (SEM) image of ZnO nanoparticles

4.3 CHARACTERIZATION USING EDAX:

Fig(4.3) shows the EDAX spectrum for Zinc oxide nanoparticles prepared using Carica Papaya leaf extract as bioreductant. EDAX spectrum shows three peaks which are identified as zinc and oxygen. Hence it can be seen that pure ZnO nanoparticles can be prepared using Carica Papaya leaf extract as bioreductant.



Fig(4.3) Energy Dispersive X-ray analysis(EDAX) of ZnO nanoparticles

CHAPTER-5

SUMMARY AND CONCLUSION

5.1 SUMMARY AND CONCLUSION:

Nano sized pure ZnO nanoparticles were synthesized using Carica Papaya leaf extract as reducing agent. XRD, SEM and EDX analysis confirmed that the formation of nanoparticles of pure ZnO. From XRD pattern the average grain size of the ZnO nanoparticles are found to be around 33.3785nm. Compositional analysis using EDAX was performed for the sample and is in very good agreement indicating atomic percentage of Zn and O. From SEM image it is noted that the particles are held together because of weak physical forces.

5.2BIBILOGRAPHY

[1] Chung Y T et al, (2015) Synthesis of minimal-size ZnO nano particles through sol-gel method: Taguchi design optimization Mater. Des. vol 87 pg.780–7

[2] Khan S A et al, (2018) Green synthesis of ZnO and Cu-doped ZnO nano particles from leaf extracts of *Abutilon indicum*, *Clerodendrum infortunatum*, *Clerodendrum inerme* and investigation of their biological and photocatalytic activities Mater. Sci. Eng. C vol 82 pg 46–59

[3] Kairyte K, Kadys A and Luksiene, Z (2013) Anti bacterial and anti fungal activity of photo activated ZnO nano particles in suspension J. Photochem Photobiol B Biol.vol 128 pg 78–84

[4] Kolodziejczak-Radzimska A and Jesionowski T, (2014) Zinc oxide- from synthesis to application: a review Materials (Basel) vol 7 pg 2833–81

[5] Reddy K M et al, (2007) Selective toxicity of zinc oxide nano particles to prokaryotic and eukaryotic systems Appl. Phys. Lett. vol 90 pg10–13.

[6] Yan X and Xu G, (2009) Effect of sintering atmosphere on the electrical and optical properties of $(\text{ZnO})_{1-x}(\text{MnO}_2)_x$ NTCR ceramics Phys. B Condens Matter vol 404 pg 2377–81

[7] Talebian N, Amininezhad S M and Douadi M, (2013) Controllable synthesis of ZnO nano particles and their morphology-dependent antibacterial and optical properties J. Photochem Photobiol B Biol. vol 120 pg 66–73

[8] Rekha K et al, (2010) Structural, optical, photocatalytic and antibacterial activity of zinc oxide and manganese doped zinc oxide nano particles Phys. B Condens Matter vol 405 pg 3180–5

[9] Sangeetha G, Rajeshwari S and Venckatesh R, (2011) Green

synthesis of zinc oxide nano particles by aloe barbadensis miller leaf extract: structure and optical properties Mater. Res. Bull. vol 46 Pg 2560–6

[10] Nagajyothi P C et al, (2013) Green route bio synthesis: characterization and catalytic activity of ZnO nanoparticles Mater. Lett. vol 108 Pg 160–3

[11] Rajiv P, Rajeshwari S and Venckatesh R, (2013) Bio-fabrication of zinc oxide nanoparticles using leaf extract of Parthenium hysterophorus L. and its size-dependent anti fungal activity against plant fungal pathogens Spectrochim Acta—Part A Mol Biomol Spectrosc vol 112 pg 384–7

[12] Shamim A, Mahmood T and Abid M B, (2019) Biogenic synthesis of zinc oxide (ZnO) nano particles using a fungus (Aspargillus niger) and Their Characterization Int. J. Chem. vol 11 Pg 119

[13] Vidya C et al, (2013) Green synthesis of ZnO nanoparticles by Calotropis Gigantea Int J Curr Eng Technol vol 28 pg 2012–4

[14] Qu J, Luo C and Hou J, (2011) Synthesis of ZnO nanoparticles from Zn-hyper accumulator (Sedum alfredii Hance) plants Micro Nano Lett. vol 6 Pg 174-6

[15] Qu J et al, (2011) Zinc accumulation and synthesis of ZnO nanoparticles using Physalis alkekengi L Environ. Pollut. vol 159 pg 1783–8

[16] Parthasarathy G et al, (2016) Green synthesis of zinc oxide nano particles- review paper World J. Pharm. Pharm Sci. vol 5 pg 922–31

[17] <https://telanganatoday.com/what-is-nanotechnology-and-itsapplication>

[18] https://serc.carleton.edu/msu_nanotech/nano_intro.html

[19] Kumari, R., Sahai, A., & Goswami, N. (2015). Effect of nitrogen doping on structural and optical properties of ZnO

nanoparticles. Progress in Natural Science: Materials International, vol 25(4), pg 300-309.

[20] Rochman, N. T., & Akwalia, P. R. (2017, May). Fabrication and characterization of Zinc Oxide (ZnO) nanoparticle by sol-gel method. In Journal of Physics: Conference Series (Vol. 853, No. 1, p. 012041). IOP Publishing.

[21] sutradhar, P., & Saha, M. (2016). Green synthesis of zinc oxide nanoparticles using tomato (*Lycopersicon esculentum*) extract and its photovoltaic application. Journal of Experimental Nanoscience, vol 11(5), pg 314-327.

[22] Ahmed, S. A. (2017). Structural, optical, and magnetic properties of Mn-doped ZnO samples. Results in physics, vol 7, pg 604-610.

[23] Thaweesaeng, N., Supankit, S., Techidheera, W., & Pecharapa, W. (2013). Structure properties of as-synthesized Cu-doped ZnO nanopowder synthesized by co-precipitation method. Energy Procedia, vol 34, pg 682-688.

[24] Khalil, M. I., Al-Qunaibit, M. M., Al-Zahem, A. M., & Labis, J. P. (2014). Synthesis and characterization of ZnO nanoparticles by Thermal decomposition of a curcumin zinc complex. Arabian Journal of Chemistry, vol 7(6), pg 1178-1184.

[25] Sutradhar, P., & Saha, M. (2015). Synthesis of zinc oxide nanoparticles using tea leaf extract and its application for solar cell. Bulletin of Materials Science, vol 38(3), pg 653-657.

[26] Matinise, N., Fuku, X. G., Kaviyarasu, K., Mayedwa, N., & Maaza, M. (2017). ZnO nanoparticles via *Moringa oleifera* green synthesis: physical properties & mechanism of formation. Applied Surface Science, pg 406, 339-347.

[27] Sindhura KS, Prasad TNVKV, Selvam PP, Hussain OM

(2013) Synthesis, characterization and evaluation of effect of phyto-genic zinc nanoparticles on soil exoenzymes. *Apply Nanoscience* vol 1 pg 1-9.

[28] Alias, S. S., Ismail, A. B., & Mohamad, A. A. (2010). Effect of pH on ZnO nanoparticle properties synthesized by sol-gel centrifugation. *Journal of Alloys and Compounds*, vol 499(2), pg 231-237.

[29] Sangeetha, G., Rajeshwari, S., & Venckatesh, R. (2011). Green synthesis of zinc oxide nanoparticles by aloe barbadensis miller leaf extract: Structure and optical properties. *Materials Research Bulletin*, vol 46(12), pg 2560-2566.

[30] Rao, M. D., & Gautam, P. (2016). Synthesis and characterization of ZnO nano flowers using *Chlamydomonas reinhardtii* A green approach. *Environmental Progress & Sustainable Energy*, vol 35(4), pg 1020-1026.

[31]. Pulit-Prociak, J., Chwastowski, J., Kucharski, A., & Banach, M. (2016). Functionalization of textiles with silver and zinc oxide nanoparticles. *Applied Surface Science*, vol 385, pg 543-553.

[32] https://en.m.wikipedia.org/wiki/Zinc_oxide

[33]<https://nanoscalereslett.springeropen.com/articles/10.1186/s11671-018-2532-3>

[34] Ansely Hill,RD,LD on April 15,2020 - medically reviewed by Miho Hatanaka, RDN, L,D.

[35] Zhang X-F, Liu Z-G, Shen W,et al,(2016) Silver nanoparticles: synthesis, characterization, properties, applications, and therapeutic approaches. *IJMS*. vol 17 pg 1534.

[36] Abdelghany TM, Al-Rajhi AMH, AlAbboud MA,et al, (2018) Recent advances in green synthesis of silver nanoparticles and their applications: about future directions. A review. *Bionanoscience*. vol 8 Pg 5–16.

[37] Hussain I, Singh NB, Singh A, et al.(2018) Green synthesis of nanoparticles and its potential application. *Biotechnology Lett.* Pg 38 545–560.

[38] Baruwati B, Polshettiwar V, Varma RS. Glutathione. (2009) promoted expeditious green synthesis of silver nanoparticles in water using microwaves. *Green Chem.* Pg11926–930.

[39] <https://www.sciencedirect.com/topics/materialsscience/coprecipitation>

[40] Anandalakshmi K, Venugobal J, Ramasamy V,(2019) Characterization of silver nanoparticles by green synthesis method using *Pedaliumpurex* leaf extract and their antibacterial activity. *Apply Nanoscience*. vol 6 pg 399–408.

[41] https://serc.carleton.edu/research_education/geochemsheets/techniques/XRD.html

[42] <https://www.thermofisher.com/in/en/home/materials-science/learning-center/applications/scanning-electron-microscope-sem-electron-column>.

[43] <https://www.thermofisher.com/blog/microscopy/edx-analysis-with-sem-how-does-it-work>

5.3 IMAGES:

1.1 Nanoscale of Nano particles

1.2 Constituents of solid sediments

1.3 Shapes of Nanoparticles

1.4 Image of ZnO nano powder

2.1 Formation of nanocrystals

2.2 Synthesis of ZnO nanoparticles

3.1 X-Ray diffraction

3.2 X-Ray powder diffraction analysis

3.3 X-Ray Diffractometer

3.4 Scanning Electron Microscope(BSE,SE)

3.5 Electrostatic lenses

3.6 Scanning Electron Microscope(SEM)

3.7 Result of EDS analysis for the cracked surface of BOF slag particle

4.1 XRD pattern for ZnO nanoparticles from carica papaya leaf

4.2 Sem image for ZnO nanoparticles

4.3 EDAX of ZnO nanoparticles

5.4 TABLE

4.1 Calculation of size of ZnO nanoparticles from XRD pattern